# Differential Metallothionein Isoform Expression as Biomarkers of Cadmium Exposure in Human Urothelium

Rhiannon McNeill

Doctor of Philosophy

University of York

Biology

June 2017

# Abstract

The metallothionein (MT) superfamily consists of 11 genes whose proteins bind to and sequester metals within cells. Although the presence of so many isoforms raises the possibility of differing metal specificities and functions, they have rarely been discriminated in the literature. This thesis investigated the expression and inducibility of MT isoforms in normal human urothelium with the aim of determining whether specific MT isoforms represent discriminatory biomarkers of cadmium exposure, which has been increasingly linked to the development of urothelial cancer (UC) in recent years. Specialised techniques already established were used for the cell, tissue and organ culture of normal human urothelium. These cultures were exposed to cadmium concentrations reflective of *in vivo* human exposure and analysed using isoform-specific primers and antibodies. The results revealed the extent of differential expression of the MT isoforms, including preferential metal activation; for example, zinc could highly induce MT-1G transcript expression but could only cause minimal transcript induction of MT-1M. This demonstrates the importance of distinguishing between all known isoforms when determining MT expression. The discriminatory approach used in this thesis allowed the identification of two MT-1 isoforms, MT-1A and MT-1M, whose protein induction was highly specific to cadmium exposure. Although isoform transcript induction was observed to be transient, the protein expression of MT-1A persisted for at least 6 weeks post exposure, consistent with a metal sequestration role. Investigation using spectroscopic techniques additionally suggested that cadmium could penetrate the protective urothelial barrier and enter the underlying urothelial cells, where it may be sequestered by MT within these long-lived cells, thus serving as a long-term source for chronic exposure. Overall the results suggest that MT-1 isoforms may be useful as urothelial biomarkers of cadmium exposure, potentially allowing the identification of individuals ‘at risk’ of developing UC and additionally, stratifying a subset of cadmium-induced UC.

# Abbreviations

**ABS –** Adult Bovine Serum

**ARE –** Antioxidant Response Element

**AUM –** Asymmetric Unit Membrane

**BASQ –** Basal-squamous-like

**BLAST –** Basic Logical Alignment and Search Tool

**bp –** Base Pair(s)

**BPE –** Bovine Pituitary Extract

**BSA –** Bovine Serum Albumin

**$Ca^{2+}$ -** Calcium Ion

**$CdCl_2$ –** Cadmium Chloride

**cDNA –** Complementary Deoxyribonucleic Acid

**CK –** Cytokeratin

**CLDN -** Claudin

**$CO_2$ –** Carbon Dioxide

**CT –** Cholera Toxin

**DAB -** Diaminobenzidine

**DEPC –** Diethyl Pyrocarbonate

**$dH_2O$ –** DEPC-treated Water

**DMEM –** Dulbecco's Modified Eagle's Serum

**DMSO –** Dimethyl Sulphoxide

**DNA –** Deoxyribonucleic Acid

**DNMT –** DNA Methyltransferase

**dNTP –** Deoxynucleotide Triphosphate

**DTT –** Dithiothrietol

**EDTA-** Ethylenediaminetetra-acetic Acid

**EGF –** Epidermal Growth Factor

**EGFR –** Epidermal Growth Factor Receptor

**FBS –** Foetal Bovine Serum

**GAPDH -** Glyceraldehyde 3-phoshate Dehydrogenase

**GRE –** Glucocorticoid Response Element

**$H_2O$ -** Water

**H&E –** Haemotoxylin and Eosin

**HIF –** Hypoxia Inducible Factor

**HRP –** Horseradish Peroxidase

**IL –** Interleukin

**ISUP –** Internation Society of Urological Pathology

**kb –** Kilobase

**kDa –** Kilodalton

**KSFM –** Keratinocyte Serum-Free Medium

**KSFMc –** Keratinocyte Serum-Free Medium (Complete)

**M –** Molar

**MAPK –** Mitogen-Activated Protein Kinase

**MBP –** Methyl-Binding Proteins

**MES -** Morpholino-ethanesulfonic acid

**mg –** Milligrams

**MI –** Muscle Invasive

**mL –** Millilitres

**mM –** Millimolars

**MOPS -** Morpholino-propanesulfonic acid

**mRNA –** Messenger Ribonucleic Acid

**MT –** Metallothionein

**$N_2$ –** Nitrogen

**NAC –** N-acetyltransferase

**ng –** Nanograms

**NGC –** Non-Genotoxic Carcinogen

**NHU –** Normal Human Urothelial

**nM –** Nanomolar

**nm –** Nanometres

**NMI –** Non-mucle invasive

**$O_2$ –** Oxygen

**°C** – Degrees Centigrade

**P# –** Passage Number

**PBS –** Phosphate Buffered Saline

**PCR –** Polymerase Chain Reaction

**PI –** Proteinase Inhibitor

**PPAR –** Peroxisome Proliferator-Activated Receptor

**PVDF -** Polyvinylidine Fluoride

**PWM** – Positional Weight Matrices

**ROS –** Reactive Oxygen Species

**RNA –** Ribonucleic Acid

**rpm –** Rotations Per Minute

**RPMI -** Roswell Park Memorial Institute

**RT –** Reverse Transcriptase

**SDS –** Sodium Dodecyl Sulphate

**SDS – PAGE –** SDS – polyacrylamide gel electrophoresis

**SF -** Sulforaphane

**TBE –** Tris-Borate-EDTA

**TBS –** Tris Buffered Saline

**TER –** Transepithelial Electrical Resistance

**TF** – Transcription Factor

**TFBS –** Transcription Factor Binding Sites

**TI –** Trypsin Inhibitor

**TJ –** Tight Junction

**Tm –** Melting Temperature

**TNM –** Tumour-Node-Metastasis

**TURBT –** Transurethral Resection of Bladder Tumour

**TV –** Trypsin Versene

**UPK –** Uroplakin

**v/v –** Volume/Volume

**WHO –** World Health Organisation

**w/v –** Weight/Volume

**ZnT –** Zinc Transporter

**ZO –** Zona Occludens

**µg** – Micrograms

**µL –** Microlitres

**µM -** Micromolar

**µm -** Micrometres

# List of Contents

# List of Tables

# List of Figures

# Acknowledgements

First and foremost, my thanks must go to my supervisor Prof. Jenny Southgate. Her steadfast dedication to science and unwavering commitment to her students meant that I was never without support or guidance, and for that I am most grateful. I would also like to thank the rest of the JBU for their help and friendship, which made my time in the laboratory thoroughly enjoyable.

I would also like to thank the other important contributors to my research. This includes my Thesis Advisory Panel members, Prof. Norman Maitland and Prof. Dimitris Lagos, who oversaw and guided my research from the beginning. I would also like to thank Prof. James Catto for the many research discussions we had and his valued insight. I additionally need to express my gratitude for the help and technical expertise offered to myself by Prof. Mark Hodson, without which an important aspect of this research could not have been conducted. I must thank my generous funders too, Yorkshire Cancer Research, without whom none of this work would have been possible.

Lastly, I have to express my heartfelt thanks to my family (including the animal variety) and friends, without whom I would not be where I am today. In particular I would like to thank my special PhD ladies, who got me through thick and thin, and were there for me every day. I also have to give a special thanks to my partner in crime (well, science), whose unwavering support and faith in me has allowed me to reach this moment.

# Declaration

I, Rhiannon McNeill, declare that this thesis is a presentation of original work and I am the sole author. This work has not previously been presented for an award at this, or any other, University. All sources are acknowledged as References.

# Chapter 1: Introduction

## 1.1 The Urothelium

### 1.1.2 Structure and Organisation

The transitional epithelial lining of the mammalian urinary bladder is known as the urothelium (Hicks, 1975). This specialised epithelium also lines the rest of the urinary tract, including the renal pelvis and ureters, and functions to protect the underlying tissues. The urothelium has a stratified organisation and comprises 3 distinct cell zones; basal, intermediate and superficial cells (Jost et al., 1989; see Figure 1). Superficial cells are generally thought of as possessing a highly differentiated phenotype, whereas intermediate and basal cells are associated with a less-differentiated phenotype (Varley et al., 2004). A basement membrane separates the urothelium from the underlying supportive stromal tissue, whose function is to maintain normal urothelial growth, differentiation and maturation (Howlett et al., 1986).

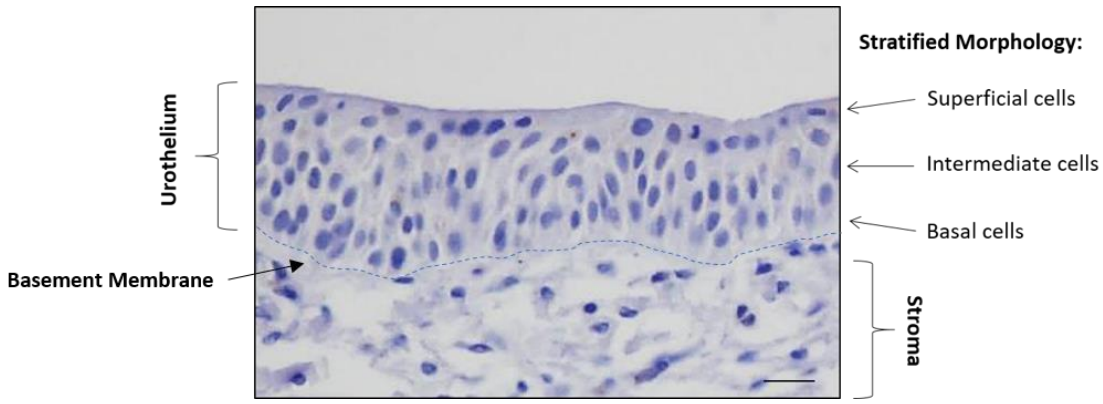


***Figure 1: Illustrated image of the urothelium. The image shows haemotoxylin and eosin staining of a section of ureter, demonstrating the urothelium. The superficial, intermediate and basal cell layers are annotated, along with the underlying basement membrane and stromal tissue. Scale bar: 25 µm.***

Normal urothelium is generally considered to have a low turnover rate and remain in a largely quiescent state, with the average urothelial cell reportedly undergoing mitosis only 1 - 2 times per year (Marceau, 1990). It is also thought that a small fraction of cycling cells exists within the urothelium in order to satisfy any minor renewal requirements.

However, quiescent cells are capable of re-entering the cell cycle and proliferating rapidly when required, for example upon injury. Evidence has suggested that these cells regulate their proliferation and migration via an epidermal growth factor receptor (EGFR)-mediated autocrine signalling loop in order to close gaps (Varley et al., 2004), supporting the observation that the urothelium possesses a high regenerative capacity (Hicks, 1975; Jost, 1986).

The existence of progenitor cells that are responsible for homeostasis of the human urothelium has not been confirmed, but it has been hypothesised that two distinct progenitor cell populations are responsible for generation of basal/intermediate cells and superficial cells separately (Castillo-Martin et al., 2010). Indeed, tracking of urothelial cells using age-related mitochondrial DNA changes demonstrated clonal units spanning all cell layers. These clonal cells had the same lineage and included several basal cells, leading to the proposal these basal cells may be urothelial stem cells; although it was acknowledged that a definitive stem cell marker would be needed for confirmation (Gaisa et al., 2011). This is supported by another study that observed the presence of a subpopulation of basal cells, characterised by cytokeratin (CK) 14 expression, that possessed regenerative properties and could give rise to all cell types of the urothelium (Papafotiou et al., 2016).

Alternatively, it has been proposed that cells from all layers of the urothelium are able to enter the cell cycle and proliferate (Hicks, 1975). Upon injury of the urothelium by uropathogenic *Escherichia coli* (UPEC), proliferation was observed to occur within both the superficial and intermediate cell zones, and approximately double the number of intermediate urothelial cells proliferated compared to basal (Colopy et al., 2014). Additionally, injury has been found to increase transcription of the proliferation-associated SRY-Box 9 (SOX9) gene in all three urothelial cell zones, coinciding with urothelial repair (Ling et al., 2011). It has been suggested that the type of injury to the urothelium may also play a role in determining which cellular zone proliferates in response, suggesting that the urothelium is not solely populated from a basal stem cell population (Balsara and Li, 2017). A recent study has demonstrated that both basal and suprabasal normal human urothelial cells are capable of proliferation *in vitro*, despite their origin in the urothelium *in vivo* (Wezel et al., 2014). Further, both cell groups could be stimulated to differentiate and recapitulate a functional urothelium consisting of all urothelial cell types. These results suggest that urothelial cell differentiation is determined by cellular localisation or niche, rather than being pre-programmed from specific stem or

progenitor cell populations, and are further supported by the lack of a clear anatomical stem cell niche within the urothelium (Balsara and Li, 2017).

### 1.1.3 Barrier Function

One of the main functions of the urothelium is to accommodate changes in urine volume for storage, whilst maintaining a low pressure in the bladder. To achieve this, during bladder filling the urothelium 'unfolds' and superficial cells are thought to alter their morphology in order to accommodate increased urine volume, returning to their cuboidal morphology upon bladder emptying (Minsky and Chlapowski, 1978). Other important functions of the urothelium include control of permeability, cell-cell communication and immune response (Lazzeri, 2006). The urothelium is also essential for the protection and defence of the underlying tissue from exposure to urine and pathogens (Zeidel, 1996; Negrete et al., 1996; Dozmorov et al., 2007). The urinary tract is one of the main excretory routes for the body, and thus a number of potentially harmful compounds are contained within the urine (Caldwell et al., 1995). These compounds are filtered out of the blood via the kidneys and become concentrated in the urine, which is retained in the bladder until such a time that it may be excreted (Krause et al., 2015). Consequently, the urothelium can be exposed to toxic substances at high concentrations for prolonged time periods (National Research Council US Subcommittee on Biologic Markers in Urinary Toxicology, 1995). Thus, it is essential that the urothelium acts as a barrier to prevent these toxins from re-entering the body.

The urothelium is thought to form one of the tightest epithelial barriers in the body (reviewed by Kreft et al., 2010), preventing any trans- or para-cellular passage of toxic constituents from the urine into underlying tissue. The urothelium achieves this tight barrier via the expression of specific differentiation-associated features comprising asymmetric unit membranes (AUM) plaques and tight junctions (TJ), with TJs primarily responsible for barrier tightness and acting as a 'seal' between cells (Farquhar and Palade, 1963) . AUM plaques exist on the apical surface of the superficial layer of cells, covering around 70 - 90 % of the apical cell membrane. These plaques are composed of integral membrane proteins termed uroplakins (UPK), of which there are four major UPK proteins and one minor (reviewed by Wu et al., 2009). As AUM plaques exist only on superficial urothelial cells they can therefore be used as biomarkers of differentiation and are indicative of a functioning urothelial barrier (Sun et al., 1999). Tight junctions exist on the most apical part of the lateral membrane of superficial cells and develop during

urothelial cell differentiation (Varley et al., 2006). They consist of proteins including occludins and claudins, a number of which are expressed prior to differentiation, but re-localise during the process. These proteins differ in their kinetics for relocalisation, with some proteins relocating before others, which appears to reflect the differentiation progression stages *in situ*. Claudin 3 and zona occludens (ZO)-1 protein expression have been identified as the last proteins to localise to their final position at the terminal junctions of superficial cells (the 'kissing point'), and their expression here is therefore particularly linked with development of a functional barrier (Smith et al., 2015). However, both ZO-1 and ZO-2 are thought to be critical to tight junction development, having been implicated in the timing and positioning of claudin polymerisation at tight junction strands (Umeda et al., 2006). Urothelial barrier function can be measured using transepithelial electrical resistance (TER) in accordance with Ohm's Law. TER is a measure of ionic permeability and accounts for both trans- and paracellular pathways, but particularly transcellular solute movement. A reading >500Ω.cm$^2$ is arbitrarily taken as the cut-off for a 'tight' epithelial barrier, whereas a reading <500Ω.cm$^2$ is suggestive of a 'leaky' epithelia, where urine constituents may reach underlying tissues and cause conditions such as vesical ischemia (Frömter and Diamond, 1972; Hohlbrugger, 1996).

### 1.1.4 *In Vitro* Models of Human Urothelium

Prior to the use of human-derived urothelial cells, animal models were regularly used to investigate the urothelium. Although these proved useful in understanding basic physiology and the development of cancer (Cohen et al., 1983; Owens, Wei, & Smart, 1999), there are inherent species differences which mean that animal models are not ideal for studying human bladder carcinogenesis (reviewed by Crallan et al., 2006). Researchers therefore began to establish human urothelial cell lines. A number of human urothelial cancer cell lines exist which can be used to study tumour cell behaviour, as compared by Masters et al. (1986) and Nickerson et al. (2016). To understand the initial events leading to carcinogenesis, normal human urothelial cell lines have also been developed from normal human urothelium. However, a number of these cell lines have been genetically modified to become immortalised; for example, the UROtsa cell line was immortalised using a SV40 large T-antigen construct (Petzoldt et al., 1995), which disables both the p53 and Rb tumour suppressor proteins (Kao et al., 1993). Therefore, although immortalised cell lines are readily available and useful for maintaining long-term culture, they are no longer genetically 'normal'. This presents a problem in that the

early genetic changes responsible for initiating carcinogenesis may already be altered due to the process of immortalisation, and regular cellular processes, such as growth suppressing feedback loops, already altered. For example, immortalisation of normal human urothelial cells with human telomerase reverse transcriptase (hTERT) results in compromised differentiation ability and functional capacity, possibly due to inhibited p16 expression (Georgopoulos et al., 2011). To investigate early carcinogenic events it is therefore important to use urothelial cells that have not been genetically manipulated, and that reflect *in vivo* cells as closely as possible (reviewed by Crallan et al., 2006).

For this thesis, finite normal human urothelial (NHU) cell lines were utilised. NHU cells are non-immortalised, *ex vivo* cells that are obtained via isolation from surgical biopsies and grown in culture (Southgate et al., 1994). Once in culture, the cells adopt a proliferative phenotype and can be serially passaged with a finite lifespan of between 20-30 population doublings (Chapman et al., 2006). Cultures are grown in low calcium, keratinocyte serum-free medium (KSFM) completed with bovine pituitary extract and epidermal growth factor, and supplemented with cholera toxin (Southgate et al., 1994; Southgate et al., 2002). Proliferating NHU cells lack protein markers associated with differentiation, but express markers associated with basal and intermediate cells such as cytokeratin (CK) 5 (Southgate et al., 1994). Stratification of NHU cells can be induced by raising the exogenous calcium concentration, whereupon the cells begin to form layers 3-4 cells thick and decrease proliferation; however, this is not sufficient to induce terminal differentiation as shown by the absence of CK20 and AUM plaques (Southgate et al., 1994) and the absence of a functional barrier (Cross et al., 2005).

NHU cells can be stimulated to differentiate by the addition of adult bovine serum and increasing the exogenous calcium concentration to physiological conditions, resulting in inhibition of proliferation and formation of a cell sheet with a ‘tight’ urothelial barrier. (Cross et al., 2005). This “biomimetic” model is comprised of 3-7 cell layers, including superficial ‘umbrella’ cells (so-called due to their ability to contract and expand; section 1.1.3), and subsequently displays differentiation-associated protein markers such as CK20 and claudin (CLDN) 7 (Cross et al., 2005).

### 1.1.5 Organ Culture

Although the use of NHU cells is preferable to the use of genetically altered, immortalised cell lines, the *in vitro* approach is still limited. The environment these cells are cultured in is artificial and not truly reflective of physiological conditions, with usually only a

single cell type present meaning cell architecture is lost. Intercellular signalling also tends to be impaired due to cell densities typically being lower than 1 % of a tissue environment (Hartung and Daston, 2009). A possible way to overcome these problems is the use of organ culture, which involves removing organ tissue from the human body and growing it *in vitro* (Carrel, 1937). Organ cultures can be maintained for extended periods of time, as long as the correct media, substrate and environment are provided (Resau et al., 1991). Another benefit of using an organ culture approach includes retention of tissue architecture and representation of pathological features. As tissue is used it also means that multiple cell types are present, resulting in cell-cell interactions and preservation of cell morphology and function (Ozaki and Karaki, 2002). Organ cultures are particularly suited for use in carcinogenic studies where *in vivo* study is not ethically possible, and involve exposing human tissue to a relevant dose of carcinogen and determining subsequent morphologic and molecular changes. A protocol for maintaining 3-dimensional organotypic cultures of ureter has previously been developed (Scriven et al., 1997; Varley and Southgate, 2011). Ureter organ culture allows the urothelium to be studied under conditions which are more reflective of *in vivo* conditions, and also enables communication between urothelial cells and the underlying stroma. The use of organ culture in the study of urothelium therefore provides a novel insight into the consequences of human exposure to carcinogens that *in vitro* work alone could not provide. However, the disadvantages of using this approach are that cell numbers cannot be expanded, and replication of results can be problematic due to inherent heterogeneity.

## 1.2 Urothelial Cancer

### 1.2.1 Grading and Staging of Tumours

Around 90-95 % of bladder cancers are urothelial carcinomas, with the remaining 5-10 % presenting mostly as squamous cell carcinomas or adenocarcinomas (Montironi et al., 2016). Urothelial tumours are classified by both staging and grading, using different classification systems. The staging of a tumour refers to the depth of invasion, and urothelial cancer is most often staged using the Tumour-Node-Metastasis (TNM) system (Sobin et al., 2009). Grading of tumours is used to evaluate cytologic and/or growth pattern characteristics, and is classified using the World Health Organisation/International Society of Urological Pathology criteria (Eble et al., 2004).

Graphical representation of the staging and grading systems is depicted below (Knowles and Hurst, 2015).

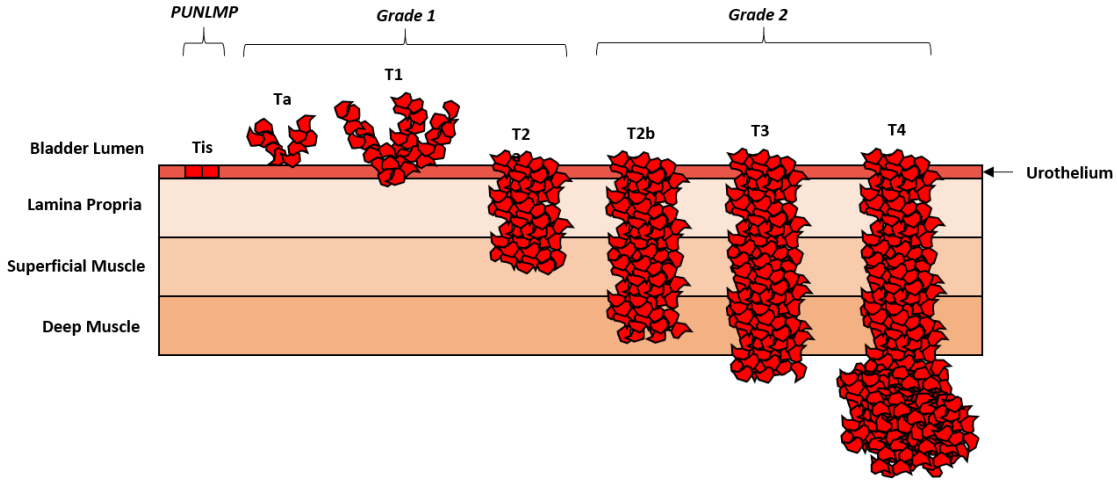


***Figure 2: Urothelial cancer staging and grading. Staging of bladder tumours is performed using the Tumour-Node-Metastasis (TNM) system depending on the depth of invasion.*** *Each T-stage is shown above and tumour-depth indicated. Grading of bladder tumours is performed according to the World Health Organisation (WHO)/International Society of Urological Pathology (ISUP) 2004 criteria, and based on cytologic and/or growth pattern characteristics. PUNLMP = Papillary Urothelial Neoplasm of Low Malignant Potential. Figure adapted from Knowles & Hurst (2015).*

### 1.2.2 Classification of Urothelial Cancer

#### *1.2.2.1 The Two-Pathway Model*

Urothelial carcinomas are currently segregated into two groups based on their level of invasiveness and unique molecular profile, as summarised in Figure 3A. Tumours are classified as either non-muscle invasive (NMI; includes Tis, Ta and T1) or muscle-invasive disease (MI; includes T2, T3 and T4). These groups are associated with specific genetic signatures representing the different molecular pathways of urothelial cancer, and demonstrate distinct histopathological phenotypes and clinical behaviour (Cordon-Cardo, 2008). The majority of bladder cancer diagnoses are NMI (~75 %) and 5-year survival is ~90 %; however, these tumours frequently recur (70 %) and around 10-15 % progress to an invasive form (Prout et al., 1992). High frequency of recurrence is one of the main reasons why bladder cancer has the highest lifetime treatment costs of all cancers (Sievert

et al., 2009). MI bladder cancer presents less often (~20 %) but has a poor prognosis, with 5-year survival <50 % (Cheng et al., 1999). Furthermore, ~50 % patients will go on to develop metastasis (Knowles and Hurst, 2015).

One of the most frequently mutated genes associated with the development of NMI bladder cancer is fibroblast growth factor receptor-3 (FGFR3), with up to 80 % of Ta tumours demonstrating activating point mutations in this gene (Billerey et al., 2001). The PI3-kinase (PI3KCA) gene has also been reported mutated in up to 10 % of NMI tumours, and a subset of tumours can harbour mutations in both FGFR3 and PI3KCA (López-Knowles et al., 2006). The other gene mutation commonly associated with NMI bladder cancer is that of human RAS, presenting in ~18 % NMI disease (Prior et al., 2012; Knowles and Hurst, 2015). By contrast to PI3KCA, RAS mutation appears mutually exclusive with FGFR3 alterations; mutations in one or the other gene are present in >82 % of NMI bladder cancers (Jebar et al., 2005). In addition to these gain-of-function mutations associated with NMI disease, deletions in chromosome 9 are also common (Gibas et al., 1984; Smeets et al., 1987) resulting in the loss of genes such as the postulated tumour suppressor Tuberous Sclerosis-1 (TSC1; Hornigold et al., 1999). Chromosome 9 deletions have also been reported in histologically normal urothelial samples, suggesting that these alterations may be an early event in the development of carcinogenesis (Stoehr et al., 2005). Interestingly, in the small subset of MI tumours presenting with FGFR3 mutations, a high deletion frequency of the chromosome 9 gene cyclin-dependent kinase inhibitor (CDKN) 2A has also been observed (Rebouissou et al., 2012). CDKN2A codes for the tumour suppressor p16, and thus this observation may identify a possible pathway of progression for NMI tumours to MI disease.

In contrast to NMI bladder cancer, the mutations most commonly seen in MI disease are loss-of-function. Moreover, these defective mutations usually occur in tumour suppressor genes, and almost every MI tumour presents with mutations in G1 cell cycle checkpoint genes. The tumour suppressor genes most frequently associated with the development of MI bladder cancer are Tumour Protein-53 (TP53), Retinoblastoma (Rb) and Phosphatase and Tensin Homologue (PTEN; reviewed by Castillo-Martin et al., 2010). The mutation of such genes allows an accumulation of genetic abnormalities, due to the development of genetic instability and anti-apoptotic effects preventing normal cellular function. TP53 in particular is responsible for controlling apoptosis-regulatory genes, along with DNA damage recognition and response. Unusually, loss of TP53 appears to occur as an early event in urothelial cancer (Harney et al., 1995), whereas in other cancer types it is usually

associated with late carcinogenesis (Fearon and Vogelstein, 1990; Rivlin et al., 2011). Indeed, in urothelial cancer it has been reported that TP53 mutations can be correlated with tumour stage and grade, as well as with patient outcome (Sarkis et al., 1993). The Rb protein acts as a cell cycle regulator, and mutations in this gene can result in undetectable protein levels which have been correlated with poor patient outcome and aggressive clinical disease behaviour (Cordon-Cardo et al., 1992; Cordon-Cardo et al., 1997). Mutation of the tumour suppressor PTEN has also been identified as an independent prognostic factor for overall patient survival (Puzio-Kuter et al., 2009). Moreover, in advanced MI bladder cancer, a synergistic tumour suppressor relationship between PTEN and TP53 has been found in relation to inactivation of the senescence pathway (Cully et al., 2006; Puzio-Kuter et al., 2009).

To summarise, the evidence suggests that oncogenic gene activation drives cellular growth resulting in the proliferative-type lesions associated with NMI disease. In contrast, the malignant tumours associated with MI disease arise due to the loss of tumour suppressor genes. However, there appears to be some cross-over between the pathways, with a small number of cases with oncogenic activation also losing tumour suppressor function and progressing to a more malignant, invasive disease.

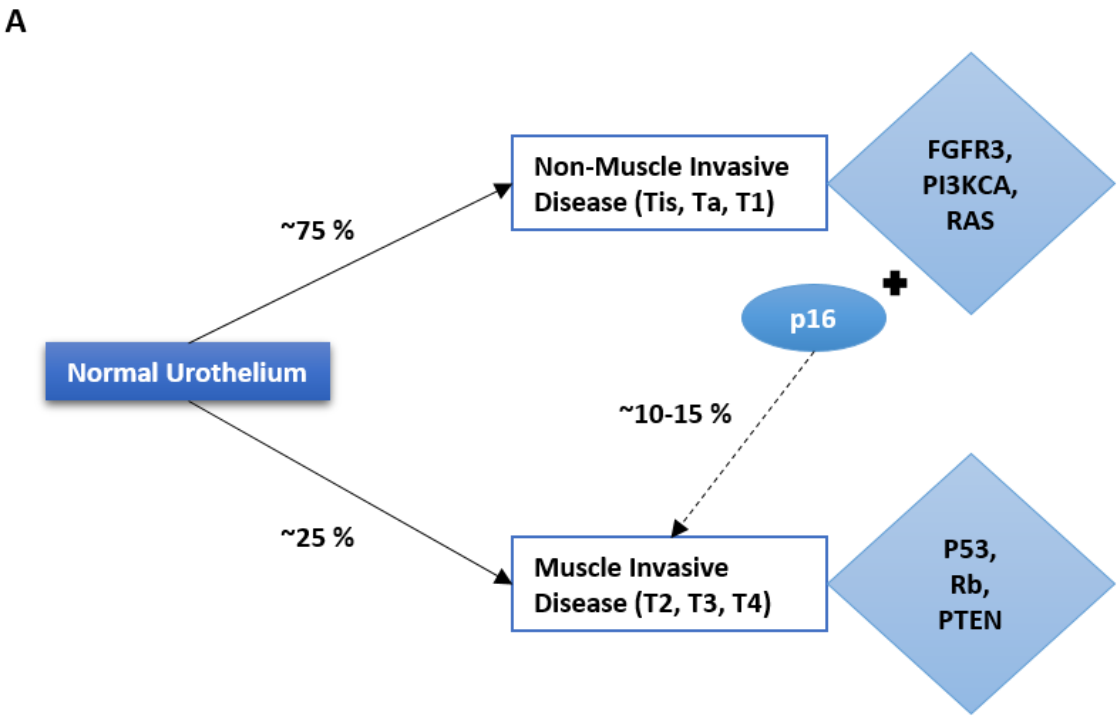

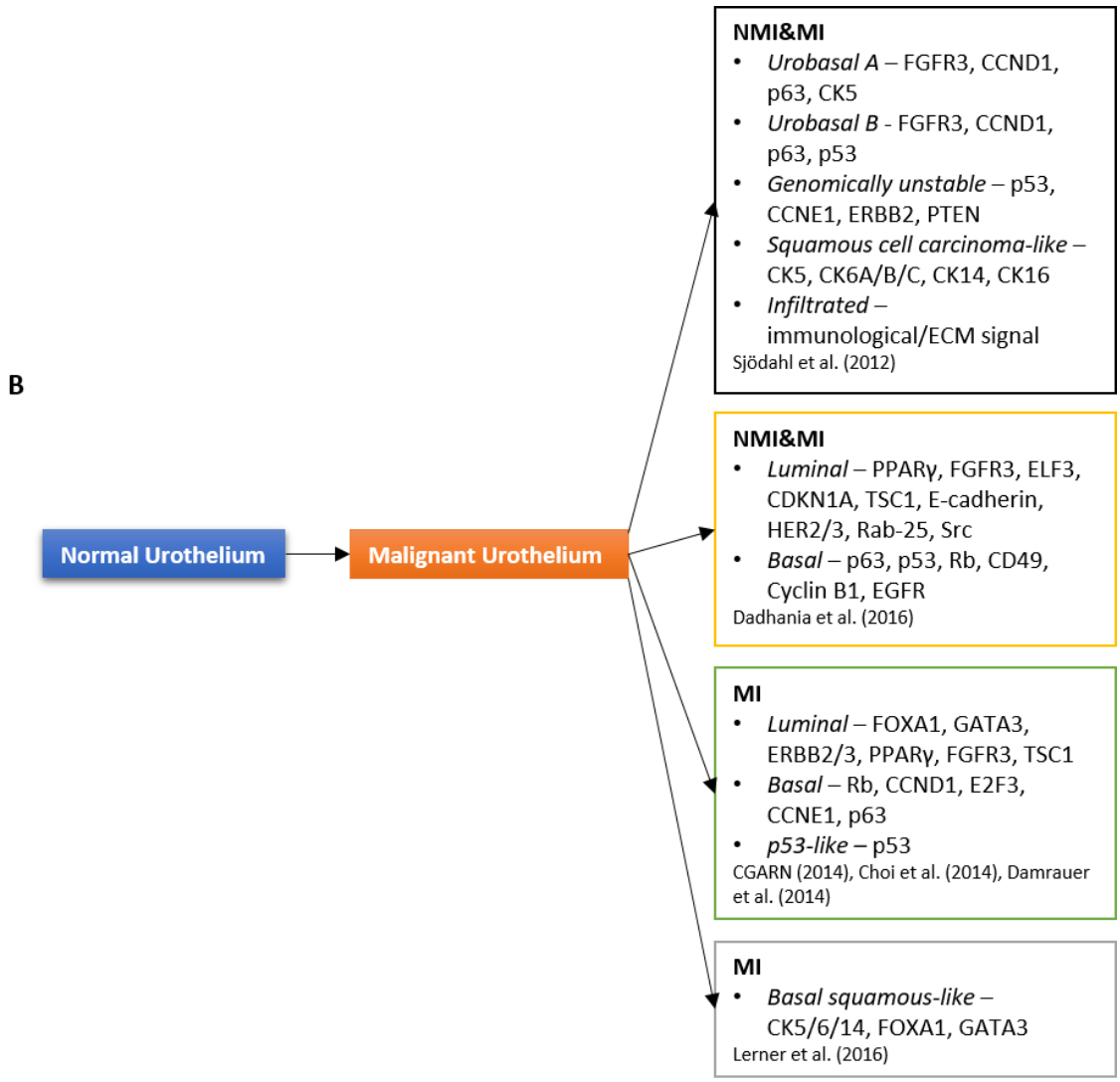


***Figure 3: Summary of current and proposed models for the classification of urothelial cancer.*** *(A) The currently used two-pathway classification model. The model is based on level of invasiveness and genetic profile. ~75 % tumours present as non-muscle invasive (NMI) disease (grades Tis, Ta and T1), whereas ~25 % tumours present as muscle-invasive (MI) disease (grades T2, T3 and T4). The most commonly mutated genes associated with NMI disease are FGFR3, PI3KCA and RAS; MI disease is associated with mutations in the p53, Rb and PTEN genes. ~10-15 % NMI disease will progress to an invasive form, and it is hypothesised that this may be associated with loss of p16 expression. Figure adapted from Castillo-Martin et al. (2010) and Knowles and Hurst (2015). (B) Proposed novel methods of classifying urothelial cancer based on molecular subtypes. Recent genetic studies addressing the heterogeneity in clinical tumour behaviour have reported distinct molecular subtypes of urothelial cancer, although a consensus has not yet been reached. CCND1=cyclin D1; CCNE=cyclin E1; ERBB2=receptor tyrosine- protein kinase erbB2; ECM=extracellular matrix; ELF3=ETS-related transcription factor 3; CDKN1A=cyclin dependent kinase 1A; HER2/3=human epidermal growth factor receptor 2/3; CD49=cluster of differentiation 49; FOXA1=forkhead box protein A1;*

*GATA3=GATA binding protein 3; E2F3=E2F transcription factor 3; CGARN=Cancer Genome Atlas Research Network.*

### *1.2.2.2 Novel Methods of Classification*

Although the literature has prescribed to the two-pathway model of bladder carcinogenesis for some time, there is a vast degree of heterogeneity in clinical tumour behaviour. Genetic studies are now beginning to address this issue and question the usefulness of grouping all urothelial tumours into only two groups (Figure 3B). One of the first studies to investigate novel classification methods analysed transcript expression in a number of tumours from all grades and stages, and identified 5 major subgroups; urobasal A, urobasal B, genomically unstable, squamous cell carcinoma-like and infiltrated. Each subtype showed distinct clinical outcomes and differential expression of a number of gene families (such as cell-cycle and cytokeratins; Sjödahl et al., 2012). Not long after, the Cancer Genome Atlas Research Network (2014) completed an in-depth study of the genetic background of bladder cancer, which also produced several new insights. As a result of this study and two others, three transcriptional subtypes of MI bladder cancer have been defined, all of which demonstrate similarities with breast cancer subtypes (Choi et al., 2014; Damrauer et al., 2014). The two major subtypes are that of 'basal' and 'luminal', which were characterised by features such as p63 activation and FGFR3 mutations respectively. A third subset was also identified and termed 'p53-like', which was observed to be inherently resistant to treatment with chemotherapy (Choi et al., 2014). Recently, a clinical study was performed with the aim of validating the use of luminal and basal subtypes. The results supported the use of these subtypes due to the distinct molecular signatures and clinical behaviour observed. Moreover, they also found that the expression of just two markers (GATA3 and keratin 5/6) was sufficient to identify the subtype with >90 % accuracy (Dadhania et al., 2016). Despite these advances, discussions on how best to classify tumours are still ongoing. New molecular insights have been provided due to improved Omics technology; for example, the potential prognostic value of STAG2 mutations (reviewed by van der Heijden and van Rhijn, 2014), and these novel insights need to be taken into consideration when evaluating classification methods. Currently, the 2-pathway model is still used to define bladder cancer, although a recent consensus was reached to recognise the existence of a subgroup of tumours termed 'Basal-Squamous-like' (BASQ; Lerner et al., 2016). Further large collaborative studies such as those performed by Biton et al., (2014) and Rebouissou et

al., (2014) are needed in order to reach general consensus on the best way to classify bladder cancer, whilst still accounting for heterogeneity of tumour behaviour and novel genetic alterations (e.g. the discovery of mutated PPAR-γ by Biton et al., 2014).

### 1.2.3 Epidemiology and Statistics

Europe has one of the highest incidence rates of bladder cancer in the world, with an estimated 39 986 men diagnosed in Western Europe alone in 2012; most cases of which arise from malignancy in the urothelium. Moreover, mortality rates in affected European men were by far the highest observed worldwide (Antoni et al., 2016). Urinary bladder cancer has the 4$^{th}$ highest incidence rate in males in the United States, and an estimated 58 950 new cases were predicted for 2016 (Siegel et al., 2016). Incidence rates tend to be lower in women, although sex differences appear to vary greatly between countries, with some showing an increasing trend in women (thought to be due to an increase in female smoking rates; Antoni et al., 2016). Not only does bladder cancer rank as the 5$^{th}$ most common cancer in males in Western countries (Ferlay et al., 2010), but it is one of the most costly cancers to treat (Sangar et al., 2005). As discussed earlier (section 1.2.2.1) it is thought that the high treatment costs are due to the recurrent nature of urothelial cancer, especially the NMI form, which often requires lifelong monitoring as well as multiple treatments (Botteman et al., 2003; Sievert et al., 2009). On average, bladder cancer treatment costs the U.K. health economy £ 55.39 million per year. Furthermore, individual patient treatment costs are estimated at around £ 8349.2 per year compared to £ 7294.2 for prostate cancer (another costly malignancy). Despite the discrepancy in treatment costs between cancer types, it has been calculated that around 5-fold more money in the U.K. is invested in prostate cancer research than urothelial, with prostate cancer research receiving yearly >£20 million compared to the <£5 million received by bladder cancer research (Sangar et al., 2005).

### 1.2.4 Causes of Urothelial Carcinogenesis

#### *1.2.4.1 Genotoxic Carcinogens*

A genotoxic carcinogen is a chemical that causes carcinogenesis by directly altering the genetic material of a cell (Hayashi, 1992). The most well-known genotoxic carcinogen causing urothelial cancer is tobacco smoke (Burger et al., 2013). Ever-smokers are predicted to have 2.5 times more risk than non-smokers of developing the disease (Cumberbatch et al., 2016), while ex-smokers are estimated to have double the risk

(Brennan et al., 2000). In fact, tobacco smoke is thought to be responsible for half of all bladder cancer diagnoses (Freedman et al., 2011; Agudo et al., 2012; Park et al., 2014), and in some populations it is thought to cause up to 40 % of all bladder cancer deaths (Park et al., 2014). The specific causative agents found in cigarettes are thought to primarily be chemical carcinogens (aromatic amines, polycyclic aromatic hydrocarbons and N-nitroso compounds) and reactive oxygen species (Janković and Radosavljević, 2007). However, non-mutagenic (see section 1.2.4.2, below) heavy metals have also been found present in tobacco, the possible health effects of which have not been sufficiently emphasised in the past (reviewed by Chiba and Masironi, 1992).

Other causes of bladder cancer may include urinary tract infections such as chronic cystitis (Vermeulen et al., 2015) and *Schistosoma haematobium*, the latter of which is thought to cause the disease via chronic irritation and/or altered metabolism resulting in elevated urinary levels of carcinogenic metabolites (International Agency for Research on Cancer, 1994). Although generally not regarded as a heritable cancer, certain genetic factors have also been identified as risk factors for disease development. For example, specific polymorphisms in the N-acetyltransferase (NAC) 1 and 2 genes can impair detoxification of aromatic amines, leading to elevated production of urinary carcinogenic metabolites and consequently an increased risk of developing bladder cancer (Hein et al., 2000). Lastly, dietary factors can also influence the probability of bladder carcinogenesis. High intake of fats, meats and soy have all been found to increase the risk of bladder cancer, whereas fruit and vegetables appear to decrease the risk; however most of these studies demonstrating this are based on correlation, and to date no study has investigated daily food intake and bladder cancer risk (reviewed by Janković and Radosavljević, 2007).

#### *1.2.4.2 Non-Genotoxic Carcinogens*

Non-genotoxic carcinogens (NGC) are substances that can cause the development of cancer without directly altering the genetic material of a cell (Hayashi, 1992).
Currently, the most well-known group of toxicants that exert carcinogenic effects via secondary mechanisms is that of the heavy metals, which are introduced later in this chapter (section 1.3).

### 1.2.5 Cellular Origin of Urothelial Carcinoma

Cancer ‘stem’ cells, or tumour-initiating cells, are cells with the ability to self-renew, initiate tumours, and give rise to a more differentiated progeny (Suraneni and Badeaux,

2013). The existence of bladder cancer 'stem' cells has not been confirmed, but there are studies that indicate their existence. In a murine model of urothelial carcinogenesis CK14-expressing urothelial basal cells were fluorescently labelled and increased in number before the development of neoplasms, 50 % of which then continued to demonstrate fluorescence (Papafotiou et al., 2016). This led the authors to believe that these CK14-expressing cells were cells of tumour origin, rather than an acquired property of carcinogenesis. Another lineage-tracing study using murine models found that basal urothelial cells gave rise to MI tumours, whereas superficial/intermediate cells gave rise to papillary, NMI tumours (Van Batavia et al., 2014). In humans there has also been evidence indicating the existence of different urothelial cancer stem cell types, that give rise to different subsets of tumour. Marker combinations that corresponded to different urothelial differentiation states could stratify bladder carcinomas into clinically relevant subgroups, identifying a tumour subset with basal tumour-initiating cells which was found to have the worst patient outcome (Volkmer et al., 2012). Findings such as these support the hypothesis that there may be distinct progenitor cells for the cell types of the urothelium, which could act as cells of origin for bladder cancer resulting in the development of different tumour subtypes. However the existence of either urothelial progenitor or stem cells has not been confirmed, with contrasting studies suggesting that urothelial cell phenotype is plastic not hierarchical (Wezel et al., 2014), and thus the exact cellular origin of urothelial carcinoma remains unknown.

### 1.2.6 Clinical Management of Urothelial Cancer

#### *1.2.6.1 Diagnosis*

Haematuria is the most common presenting symptom of urothelial cancer, and diagnoses are confirmed using a combination of cystoscopy, biopsy and/or urine cytology (Metts et al., 2000). Urine cytology is non-invasive and specific for urothelial cancer, but has moderately low sensitivity and cannot be used in isolation (Bassi et al., 2005). In order to reduce the frequency of cystoscopy, which is highly-invasive and can negatively impact patient life quality (Stav et al., 2004), various other urinary markers have been investigated (Yutkin et al., 2010). However due to poor sensitivity and/or expense none have yet been introduced into the standard routine of care, and thus cystoscopy and cytology currently remain the most important tools for diagnosis (Cheung et al., 2013). More recently, the use of Photodynamic Diagnosis (PDD)/Blue-light cystoscopy has been

adopted for the detection of inconspicuous urothelial cancers. This approach involves the instillation of 5-aminolevulinic acid or hexaminolevulinate (blue dye) into the bladder, where it is only absorbed by dysplastic tissue and emits a red colour under a blue reference light (Kriegmair et al., 1994; Burger et al., 2009). PDD/blue-light cystoscopy has been recommended for initial diagnosis, especially in patients with positive urine cytology but negative cystoscopy, and for post-treatment monitoring of patients with CIS or multifocal tumours (Witjes et al., 2010). However, despite the method appearing able to detect more urothelial tumours than normal cystoscopy (Mowatt et al., 2011), there is as yet no evidence confirming that PDD can prevent progression or improve survival of urothelial cancer patients.

#### *1.2.6.2 Treatment*

The first-line treatment for NMI bladder cancer is usually transurethral resection of the bladder tumour (TURBT), where the malignant tissue is physically removed. Surgery is often followed by an adjuvant course of chemo- or immunotherapy in order to delay disease recurrence. Therapeutic agents such as Mitomycin C or Bacillus Calmette-Guerin are instilled directly into the bladder either alone or in various combinations (Babjuk et al., 2013). For MI bladder cancer, a radical cystectomy (complete removal of the bladder and nearby tissue) is the current gold-standard treatment, although radiotherapy is also frequently used (Cheung et al., 2013). Ideally, patients will also receive platinum-based neo-adjuvant chemotherapy (for example using cisplatin) either before or after cystectomy (Vale, 2003).

#### *1.2.6.3 Treatment Resistance*

Despite urothelial tumours generally being chemo-sensitive (response to front-line chemotherapeutic treatment is 50-70 %), patients who suffer a recurrence after initial treatment have a very poor prognosis (Yafi et al., 2011). Up to 70 % of NMI tumours will reoccur, which may not affect life expectancy, but necessitates life-long monitoring and surveillance of the patient which is both costly and detrimental to life-quality (Cookson et al., 1997). MI tumours can also still reoccur post-surgery and up to 50 % of patients will develop metastasis (Raghavan et al., 1990). Combination therapy with cisplatin is the standard treatment for metastatic disease, however tumours are characteristically chemo-resistant and progression-free survival varies from 7 – 9 months (Drayton and Catto, 2012). Additionally, it has been reported that no matter which combination of chemotherapeutics is used, median survival is at best 14 months for patients presenting

with MI disease (von der Maase et al., 2005). A deeper understanding of treatment-resistance is needed in order to develop new treatments that can circumnavigate resistance mechanisms, and thereby prolong the survival of patients diagnosed with MI disease.

## 1.3 Heavy Metal Exposure

### 1.3.1 Examples and Sources of Heavy Metals

Heavy metals are naturally-occurring metallic elements that have a relatively high atomic weight and density compared to water (Fergusson, 1990). Examples include nickel, arsenic, lead, cadmium and chromium. Heavy metals are also considered trace elements due to existing in trace concentrations in various environmental substances (Kabata-Pendia, 2001). Their bioavailability in the environment can be influenced by a number of factors such as temperature and sequestration (Hamelink et al., 1994), and biological factors such as physiological adaptation can also play a role (Verkleji, 1993). Although heavy metals are naturally-occurring and usually reside within the earth's crust, in recent years increasing anthropological activities have resulted in environmental contamination and human exposure, either via habitation or occupation. Such anthropological activities include mining, smelting, coal-burning, and petroleum combustion among others (reviewed by Tchounwou et al., 2012). Certain heavy metals such as iron and zinc are also essential nutrients and are required for a number of biological functions, with a lack of these metals resulting in deficiency and disease (World Health Organisation, 1996).

### 1.3.2 Exposure and Correlation with Carcinogenesis

Five of the heavy metals (chromium, cadmium, mercury, arsenic and lead) show high levels of toxicity and remain a public concern. Moreover, they are classified as either 'known' or 'probable' carcinogens by the International Agency for Research on Cancer (International Agency for Research on Cancer, 1993) and are thought to exert their carcinogenic effects in a non-genotoxic manner (see section 1.2.4.2; Tchounwou et al., 2012). The ability of metal compounds to cause cancer in exposed workers has been documented for some time, with the first studies dating back to the 19$^{th}$ century (Salnikow and Zhitkovich, 2008). As mentioned above (section 1.3.1), human exposure to such carcinogens has increased over recent years due to anthropological activity and increased usage of heavy metals in industrial processes. It is currently estimated that up to 5.3 % of cancer deaths in Britain is due to occupational exposure to carcinogens and specifically,

occupational exposure to heavy metals has been heavily implicated in the development of lung, sinonasal, stomach and bladder cancers (Rushton et al., 2012).

As previously mentioned (section 1.1.3) the urothelium provides a barrier against toxins from the urine re-entering the body. However, as urine is concentrated and stored in the bladder before excretion, this can result in chronic long-term exposure of the urothelium to toxins such as heavy metals. Therefore, the urothelium in particular can be affected by exposure to the same. The vast number of studies documenting a link between urothelial cancer and exposure to heavy metals reflects this, with one study identifying occupational exposure as the second main carcinogenic risk for urothelial cancer after smoking (Ouzzane et al., 2014). Another study demonstrated excess mortality for bladder cancer in populations living in close vicinity to coal-burning industries, with a relative risk (RR) ratio of 1.18 at a 95 % confidence interval (CI; García-Pérez et al., 2009). This observation was supported by a later study from the same authors which also found increased bladder cancer mortality (RR = 1.11, 95 % CI) in populations living in the vicinity of installations for the production of cement, lime, plaster and magnesium oxide (García-Pérez et al., 2015). Carcinogenic risk was especially high when living in the vicinity of cement installations which are known for their release of hazardous air pollutant emissions, which often contain heavy metals. Occupationally, metal-workers have specifically been identified as having a statistically significant higher risk of developing urothelial cancer even after adjustment for smoking; a risk that increased with cumulative exposure to metal-working fluids (Colt et al., 2014). Other occupations that have been identified as high-risk for the development of urothelial cancer include bus/truck driving, road and asphalt making, working in refinery and petrochemicals, plastic/metal manufacturing, welding and pipeline building; all of which are likely to involve heavy metal exposure (Aminian et al., 2014).

### 1.3.3 General Mechanisms of Heavy Metal-Carcinogenesis

Despite being classified as carcinogenic, exactly how the heavy metals exert their effects remains elusive. DNA adducts are usually a key initiating event in organically-induced carcinogenesis, however heavy metals are only weakly mutagenic and cannot bind to DNA (Arita et al., 2012a). It has been suggested that increased production of reactive oxygen species (ROS) could be the primary mechanism of metal-induced carcinogenesis, however this contrasts with evidence that the majority of metals have little or no carcinogenic ability (Salnikow and Zhitkovich, 2008).

In recent years there has been increasing evidence that heavy metals may exert their carcinogenic effects by altering the epigenetic state of a cell, influencing DNA methylation and/or posttranslational histone modifications (Salnikow and Zhitkovich, 2008). Further, changes in micro RNA expression have now also been identified after exposure to heavy metals (Michailidi et al., 2015). Dysregulation of such epigenetic mechanisms has now been found in a multitude of malignancies, particularly in prostate, colorectal, colon and breast cancers, and is thought to play a key role in carcinogenesis (Kanwal and Gupta, 2012).

Chronic arsenic exposure has been shown to alter the expression of DNA methyltransferase (DNMT) and methyl binding proteins (MBD) in prostate epithelial cells, with increased expression of MBD1 and decreased expression of DNMT3a observed. Exposure was also found to cause changes in histone modification levels and expression of histone modifying genes (Treas et al., 2012). However, another study in mice found that arsenic exposure did not affect DNA methylation, but did alter demethylation of histone 3 at lysine 9 (H3K9me2) causing decreased expression of the tumour suppressor p16 (Suzuki and Nohara, 2012). Nickel has also been observed to alter histone modification levels, with increased expression of H3K4me3 and decreased expression of H3K9me2 found in peripheral blood mononuclear cells of workers identified as occupationally exposed to the metal (Arita et al., 2012b). A potential mechanism for the nickel-induced alteration of histone modifications was demonstrated by Chen et al. (2010), who found that nickel ions can replace iron in the structure of the histone demethylase Jumonji Domain-Containing protein 1A (JMJD1A) resulting in inhibition of its activity. However, the specific mechanisms by which nickel and other heavy metals may alter the epigenetic code are still unclear, and whether these changes are sufficient to cause carcinogenesis remains to be seen.

Heavy metals can affect a number of cellular pathways and thus altered epigenetics may not be the only contributor to the development of exposure-related carcinogenesis. Nickel exposure has been observed to activate a specific gene signature in human osteosarcoma and mice embryo fibroblast cells which is similar to that of hypoxia, resulting in stabilisation of the hypoxia-inducible factor (HIF)-α proteins and induction of HIF-1-dependent transcription (Salnikow et al., 1999; Salnikow et al., 2003b; Salnikow et al., 2003a; Maxwell and Salnikow, 2004). Activation of the hypoxia-signalling pathway may lead to nickel-induced carcinogenesis through a number of mechanisms, such as upregulation of growth factors and altered cell growth/metabolism. Meanwhile, lead has

been purported to induce carcinogenesis via increased mitogenesis. A 40-fold increase in mitogenic index was observed in the kidney of rats who were given a single injection of lead acetate (Choie and Richter, 1972), supported by a further study in rats where a 45-fold increase in hyperproliferation was found in lead-exposed renal cortices (Calabrese and Baldwin, 1992). More recently, it has also been suggested that lead can inhibit DNA damage repair, possibly by interfering with important machinery such as DNA and RNA polymerases (reviewed by Silbergeld, 2003). Despite the elucidation of a number of potential mechanisms of heavy-metal induced carcinogenesis the precise molecular mechanisms remain unclear, and it is likely that each heavy metal exerts its effects via a combination of molecular alterations that may be unique to the metal in question. Further large-scale genomic studies are needed to increase understanding of the mechanisms involved and determine the relative contributions of each, with the ultimate aim of developing targeted therapies that may be effective in treating this type of cancer.

## 1.4 Cadmium Exposure

### 1.4.1 Sources of Exposure

Cadmium is a toxic transition metal, and as mentioned in section 1.3.2, has been classified as a known carcinogen by the IARC (International Agency for Research on Cancer, 1993). Previously, cadmium exposure was very rare; however, anthropological activity has seen its release into the environment resulting in wide spread contamination of the biosphere (Agency for Toxic Substances and Disease Registry, 1999). Such anthropological activities include battery production, electroplating, smelting, soldering and burning of fossil fuels, among others (International Agency for Research on Cancer, 1993). Once it has entered the environment, cadmium can be transported and spread in a number of ways. Soluble forms can be transported easily by water and accumulate in aquatic organisms (Keil et al., 2011), with high levels of cadmium having been recorded in seafood (Feki-Tounsi and Hamza-Chaffai, 2014). Cadmium can also be transported for long distances in the atmosphere as either a particle or vapour, before deposition onto either soil or water. Lastly, cadmium can also bind strongly to organic matter and become immobilised in soil, where it is then taken up by plants and crops (Keil et al., 2011). This may explain why smoking is a prominent source of cadmium in the general population (Adams et al., 2011). Tobacco leaves that grow in contaminated environments can end up accumulating cadmium from the surrounding soil, and blood cadmium levels of

smokers have been reported as approximately double that of non-smokers (Agency for Toxic Substances and Disease Registry, 1999).

### 1.4.2 Types of Exposure

The main routes of exposure to cadmium are through ingestion of contaminated food or water, and through inhalation of particles. Dermal contact is of minimal concern, as only 0.05 % of cadmium is able to penetrate the skin's protective barrier (Agency for Toxic Substances and Disease Registry, 1999). However, dietary intake of contaminated food can range from 10 µg/day up to hundreds of micrograms, depending upon environmental contamination conditions (Nordberg, 2003). Ingestion of contaminated water barely contributes to dietary intake, as most cadmium concentrations are 5-fold less than the maximum limit of 5 µg/L (World Health Organisation, 2010; European Commission Council, 1998). Inhalation is by far the most concerning route of entry, as it is estimated that 100 % of cadmium that reaches the alveoli is absorbed into the blood (Satarug and Moore, 2004). This is a major problem for cigarette smokers, as well as occupations in contaminated workplaces, where the major route of exposure is inhalation and between 5-35 % of inhaled cadmium is into adsorbed into the body (Feki-Tounsi and Hamza-Chaffai, 2014). Recent studies have suggested that exposure to contaminated dust specifically is the main route of entry for cadmium into the body. Moreover, significantly higher levels of cadmium have been found in dust from industrial and urban population areas compared to rural (Mohmand et al., 2015), further suggesting that certain industrial occupations may result in exposure to cadmium.

One of the major problems with cadmium exposure is that the human body has limited capability to respond to such a threat. Once ions have entered the body they tend to accumulate in an almost irreversible manner (Feki-Tounsi and Hamza-Chaffai, 2014). The body is unable to metabolise cadmium to a less toxic species (Waalkes, 2003), and although the main elimination route is via the urine, the rate of excretion is very low (Agency for Toxic Substances and Disease Registry, 1999). In fact, it is thought that free cadmium eliminated via the urine may represent less than 0.01 % of the total body burden at that time (Goering et al., 1994). Moreover, cadmium has a long biological half-life of approximately 13.8 years (Suwazono et al., 2009) adding to its cumulative nature. It is generally thought that the long-term presence of cadmium in the body is attributable to metal-binding proteins which act to sequester and thereby detoxify the ions, which is explored in-depth in section 1.5.4.

### 1.4.3 Implication in Urothelial Carcinogenesis

As mentioned in section 1.3.2, exposure to heavy metals has been linked to the development of urothelial cancer in a number of studies (García-Pérez et al., 2009; Rushton et al., 2012; Aminian et al., 2014; Colt et al., 2014; Ouzzane et al., 2014; García-Pérez et al., 2015). Cadmium specifically has also been linked to urothelial carcinogenesis in a number of cases. One study observed that the median cadmium concentration in urine from urothelial cancer patients was 1.8 µg/L, compared to 0.8 µg/L in control cases (Wolf et al., 2009). Another study looked at blood cadmium concentrations from a cohort of bladder cancer patients compared to control. After adjustment for occupation and smoking, they found an increased risk of bladder cancer development for those with increased exposure to cadmium (Kellen et al., 2007). A similar result was obtained by Feki-Tounsi et al. (2013), who also measured blood cadmium concentration and found that concentrations from urothelial cancer patients were twice that of control cases. This link between elevated cadmium in bodily fluids and increased risk of urothelial carcinogenesis has now been repeatedly observed, more recently by Chang et al. (2016) who showed that patients with urothelial carcinoma had higher concentrations of urinary cadmium compared to control. Measurement of cadmium in bodily fluids has proved popular for studying the correlation between cadmium exposure and risk of urothelial carcinogenesis. However, one study performed metal quantification on urothelial tumours and adjacent tissues instead (Feki-Tounsi et al., 2014). Even with a change in source material, increased cadmium concentrations were still found in tissue from urothelial cancer patients compared to control. Interestingly, the elevated levels of cadmium were not observed in the tumour itself; rather, in the 'normal' tissue adjacent to the tumour. The authors suggest this may imply that such carcinogenic metals are able to affect surrounding cellular mechanisms and prime an oncogenic pathway (Feki-Tounsi et al., 2014), perhaps as part of a field effect (Jones et al., 2005).

The link between cadmium exposure and carcinogenesis has also been studied *in vitro* using various cell lines. The normal human prostate epithelial cell line RWPE-1 was chronically exposed to 10 µM cadmium chloride ($CdCl_2$) for 8 weeks. After exposure cells exhibited a loss of contact inhibition, and upon inoculation into mice formed highly invasive adenocarcinomas which were occasionally metastatic (Achanzar et al., 2001). However, RWPE-1 cells have not only undergone immortalisation, but are also already able to form colonies *in vitro* (Rhim et al., 1994), and thus it could be argued that they already have neoplastic properties and thus may not be suitable for investigating

malignant transformation. Another study used the TLR1215 rat liver cell line and found that continuous exposure to 2.5 μM $CdCl_2$ for 10 weeks was sufficient to induce a fibroblastic morphology, as well as a cell proliferation index twice that of controls (Takiguchi et al., 2003). The cells also displayed enhanced invasiveness and significantly elevated growth in serum-depleted medium, suggesting that cell growth had become independent of growth factors (a hallmark of tumorigenic/malignant cells). The human bronchial epithelial cell line 16HBE has additionally been transformed by chronic exposure to cadmium.These cells exhibited overlapping growth and significantly increased colony-formation, which was observed to be dose-dependent. Upon inoculation into nude mice tumours began to form after 2 weeks, and pathological examination revealed the tumours to be poorly differentiated (associated with poor prognosis, as explored in section 1.2.2; Lei et al., 2008).

Few studies have so far investigated the carcinogenic effect of cadmium on human urothelial cells, and these have tended to use immortalised cell lines. Sens et al. (2004) used the UROtsa cell line (previously established by immortalisation of normal human urothelial cells using an SV40 large T-antigen gene construct; Petzoldt et al., 1995), exposing the cells to 1 M $CdCl_2$ for a prolonged time period and then selecting cells that were capable of forming colonies in soft agar. These cells were also able to form tumours when transplanted into nude mice, and the tumours were observed to have epithelial-like features that are consistent with transitional cell carcinoma of the bladder. However, it should be noted that the concentration used in this study is particularly high compared to other studies and to reported *in vivo* exposure (Aimola et al., 2012). Also, although immortalised cell lines are useful for long-term treatment, the major flaw of these cells is that they are no longer genetically 'normal' and a number of signalling pathways are already altered (as mentioned in section 1.1.4). Therefore, in order to understand how cadmium exposure may cause early molecular changes in the cell, primary cells should ideally be utilised (Feki-Tounsi and Hamza-Chaffai, 2014).

### 1.4.4 Mechanisms of Cadmium-Induced Carcinogenesis

As stated earlier (section 1.3.2) cadmium is a non-genotoxic carcinogen, with a low affinity for DNA-binding and only weak mutagenic properties (Pilger and Rüdiger, 2006). Thus, how cadmium exerts its carcinogenic effects remains poorly understood. A multitude of studies have been conducted in order to investigate this, implicating a vast array of potential mechanisms, some of which are explored below.

### *1.4.4.1 Epigenetics*

One of the ways that cadmium exposure is thought to induce carcinogenesis is by altering the epigenetic state of cells (Salnikow and Zhitkovich, 2008; as mentioned in section 1.3.3). As explored earlier (section 1.4.3) experiments using the rat liver cell line TLR1215 revealed that acute exposure to cadmium resulted in significantly decreased DNA methyltransferase (DNMT) activity and reduced global DNA methylation. Conversely, the study observed that chronic exposure resulted in significantly increased DNA methylation and DNMT activity, as well as cellular transformation (Takiguchi et al., 2003). These findings indicate that length of exposure may have distinct effects on the cell, and emphasises the importance of mimicking *in vivo* chronic exposure as closely as possible when using *in vitro* methods. Benbrahim-Tallaa et al. (2007) also found significant changes to the DNA methylome in cadmium-transformed cells using the normal prostate epithelial cell line RWPE-1 (see section 1.4.3). Once transformed by chronic exposure these cells exhibited increased DNMT activity, which was associated with overexpression of DNMT3b. The authors also found reduced expression of the tumour suppressor genes RASSF1A and p16 in transformed cells, and discovered that the promoters of these genes were hypermethylated. Severson et al. (2012) also found hundreds of abnormal DNA methylation events in cadmium-transformed cells, some of which occurred in an agglomerative fashion, further suggesting that DNA methylation is an important target of cadmium-induced cellular changes.

Post-translational histone modifications are also thought to be affected by cadmium exposure, with a recent study in the bronchial epithelial cell line BEAS-2B showing that exposure resulted in elevated global levels of H3K4me3 and H3K9me2 (Xiao et al., 2015). Cadmium exposure has also been reported to cause reduced H3 acetylation and decreased H3K27me1 protein expression in human breast cancer cells (Choi et al., 2008) and mouse embryonic stem cells (Gadhia et al., 2012) respectively. One of the few studies looking at cadmium-induced epigenetic changes in urothelial cells found that cadmium-induced malignant transformation of the UROtsa cell line also resulted in increased H3K4me3, as well as H3K9me3 and H3K27me3 levels. Interestingly, investigation of a specific gene promoter showed that transformation had resulted in the establishment of a bivalent chromatin domain, preparing the gene for rapid transcriptional activation (Somji et al., 2011b).

### *1.4.4.2 Zinc Substitution*

Another potential mechanism of cadmium-induced carcinogenesis is thought to be through cadmium substitution for zinc. These two metallic elements have highly similar properties, meaning that cadmium can substitute for zinc relatively easily in biological systems (Chaney, 2010). However, substitution can destabilise the functional sites of zinc-containing proteins, changing the character and/or rendering them non-functional (Tang et al., 2014). This is especially a problem for zinc-finger proteins as their activities are dependent upon zinc-binding, and cadmium substitution in zinc-finger transcription factors can result in lowered affinity for DNA-binding (Malgieri et al., 2011). Although the effect of cadmium substitution in zinc proteins has been extensively studied in plants (Tang et al., 2014) the effect of substitution, and possible carcinogenic consequences, has been less extensively studied in humans. However, substitution has been investigated in the tumour suppressor protein p53 in human breast cancer cells (MCF-7). The authors found that exposure to cadmium disrupted native p53 conformation, inhibited its ability to bind DNA and decreased transcriptional activity of a downstream reporter gene. They also observed that exposure to cadmium impaired p53 induction in response to DNA damage-inducing agents (Méplan et al., 1999). These results suggest that cadmium may be able to replace zinc in p53 and disrupt its function. The authors later went on to perform a similar experiment but added extracellular zinc after cadmium-induced denaturation of p53. They found that the addition of zinc at physiological concentrations resulted in renaturation and reactivation of p53, suggesting that cadmium exposure caused p53 zinc depletion and that addition of extracellular zinc rescued p53 activity (Méplan et al., 2000).

A secondary problem of cadmium substituting for zinc is that there may be a resultant excess of labile zinc in the cell. Not only can excess zinc in the cell be toxic, but changes in intracellular zinc levels are also associated with tumour growth and progression. This may be because zinc is a cofactor of many proteins involved in carcinogenesis, influencing processes such as cell proliferation and metastasis (Jeong and Eide, 2013). To investigate the effect of cadmium on cellular zinc homeostasis the expression of Zinc Transporter-1 (ZnT-1) has previously been analysed, as it is a key regulator of free zinc and responsible for zinc efflux from the cell (McMahon and Cousins, 1998). The human hepatic cell line HepG2 was exposed to low doses of cadmium (0.1 and 10 µM) which resulted in elevated expression of the ZnT-1 protein, as well as increased localisation at the cell membrane (Urani et al., 2010). This indicated increased cellular zinc levels and therefore a need to increase efflux, supporting the hypothesis that cadmium exposure may

alter zinc homeostasis. After these observations, the authors of the study went on to directly quantify intracellular zinc levels post-exposure to cadmium. The zinc-specific probe Zinquin was utilised and it was found that intracellular labile zinc concentrations increased by 93 % when the cells were exposed to cadmium, indicative of a large displacement of zinc from the proteome (Urani et al., 2015). These results suggest that cadmium can displace zinc from proteins in the cell resulting in increased intracellular labile zinc, which the cell may attempt to counteract by increasing expression of zinc effluxors such as ZnT-1.

#### *1.4.4.3 Miscellaneous*

A number of other potential mechanisms of cadmium-induced carcinogenesis are summarised in the table below, along with respective references and the primary findings (Table 1). With regards to cadmium carcinogenicity in urothelial cells, studies have mainly focused on altered gene expression in immortalised cell lines and have identified 3 gene families of interest: Secreted Protein, Acidic, and Rich in Cysteine (SPARC); Keratin (KRT); and Metallothionein (MT; Feki-Tounsi and Hamza-Chaffai, 2014). These families are summarised in Table 2. Currently, the relationship between KRT and MT expression and urothelial carcinoma is correlational, with their expression primarily used as prognostic factors (Karantza, 2011, and Yamasaki et al., 2006, respectively). In contrast, SPARC expression is thought to play a direct role in the development of urothelial carcinogenesis, with a loss of expression resulting in increased carcinogen-induced inflammation, accumulation of ROS, increased cellular proliferation and increased activation of NF-κB and AP-1 (Said et al., 2013) (Said, 2016)

***Table 1: Summary of other main mechanisms implicated in cadmium-induced carcinogenesis.***

*Each mechanism is accompanied by several findings in the area and the respective references.*

| Mechanism | Main Findings | References |
|---|---|---|
| **Aberrant Gene Expression** | ↑ c-fos, c-jun, c-myc; ↓ p16, RASSF1A; ↑ ACTB, HSP90AA1, HSPA5, HSPA8; ↑ Snail1, MET, TGF-βR, Rac, cdc42 | (Garrett et al., 2002; Benbrahim-Tallaa et al., 2007; Kwon et al., 2013; Urani et al., 2015) |
| **Inhibition of DNA Repair** | ↓ repair of visible light-induced DNA lesions; ↓ repair of oxidative DNA damage, ↓ DNA glycosylase and endonuclease; ↓ nucleotide excision repair; ↓ expression DNA repair genes | (Dally and Hartwig, 1997, Potts et al., 2001; Mukherjee et al., 2004; Zhou et al., 2012) |
| **Inhibition of Apoptosis** | ↓ caspase activity and DNA fragmentation; ↓ benzopyrene-induced apoptosis and AP-1 activation, ↑ ERK | (Gunawardana et al., 2006; Mukherjee et al., 2008) |

***Table 2: Summary of the main gene families altered in cadmium-induced urothelial carcinogenesis.*** *The main observations are summarised along with the respective studies.*

| Gene Family | Main Findings | References |
|---|---|---|
| **SPARC** | ↓ in $CdCl_2$-transformed UROtsa cells and subsequent tumours | (Larson et al., 2010), (Slusser-Nore et al., 2016) |
| **KRT** | ↑ KRT6a in $CdCl_2$-transformed UROtsa cells exposed to insulin and epidermal growth factor; ↑ KRT6, 16, 17 in $CdCl_2$-transformed UROtsa cells and areas of squamous differentiation in subsequent tumours | (Somji et al., 2008; Somji et al., 2011a) |
| **MT** | ↑ MT-1/2 protein due to ↑ MT-1X gene in urothelial cancer; ↑ MT-3 in urothelial cancer cells; | (Somji et al., 2001; Sens et al., 2000) |

## 1.5 The Metallothionein Proteins

The metallothioneins (MTs) are a family of low-molecular weight (~6 kDa), cysteine-rich proteins that are capable of binding to a range of metals, including cadmium (Kägi and Schäffer, 1988). They were first discovered in 1957 as a cadmium-binding protein in equine kidney (Margoshes and Vallee, 1957) and went on to receive much attention due to their unique metal-binding ability and elusive function(s). As mentioned in Table 2, they have also been implicated in cadmium-induced urothelial carcinogenesis, which will be explored in-depth in section 1.5.6.

### 1.5.1 3-Dimensional (3-D) Structure and Conformation

As mentioned above, MTs are capable of binding to a range of metals, and this binding is essential for their 3-dimensional conformation and structure (Figure 4; originally depicted by Babula et al., 2012). Once bound to metal ions, the MT protein forms a molecule with two separate globular domains; a C-terminal α-domain, and an N-terminal β-domain, linked by a short but highly flexible bridging region (Coyle et al., 2002;

Penkowa et al., 2006; Nielsen et al., 2007; Pedersen, Larsen, Stoltenberg, & Penkowa, 2009). Each MT protein is 61-68 amino acids in length, one-third of which is cysteine residues that form metal thiolate clusters in a series of motifs as follows; Cys-X-Cys, Cys-X-Cys-Cys, Cys-X-X-Cys (where X is any amino acid other than cysteine; Kägi and Kojima, 1987). Up to 4 divalent (or 6 monovalent) metal ions can be bound by the 11 cysteine residues of the α-domain, whereas only 3 bivalent (6 monovalent) ions can be bound by the β-domain, due to the domain containing only 9 cysteine residues (Nielsen et al., 2007; Coyle et al., 2002). The metal-binding property of MT confers molecular stability to the protein, with the metal linkages stabilising the secondary structure, and the rate of degradation dependent upon the metal ions within the complex. If the metal is lost the protein structure is rendered disordered, becoming susceptible to proteolysis and consequently being rapidly degraded (Klaassen et al., 1994).

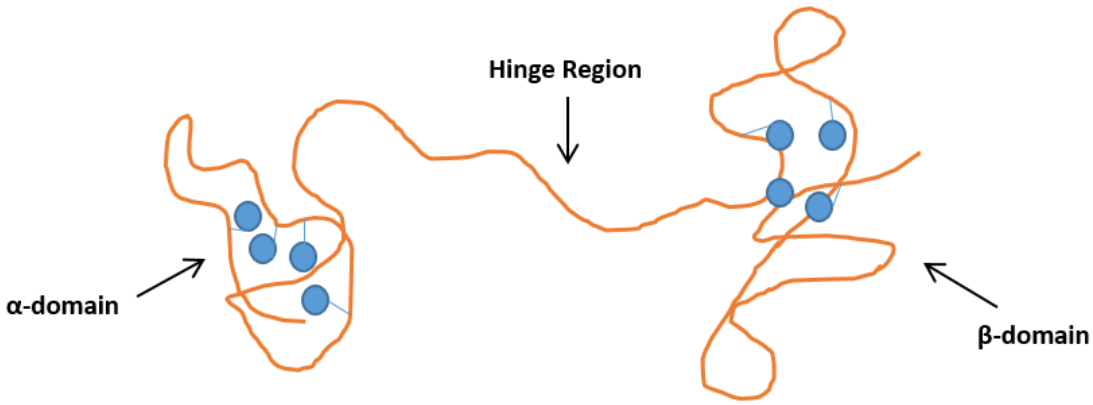


***Figure 4: Schematic diagram showing MT protein structure.*** *The image depicts the 3-dimensional structure of a MT protein bound to metal ions (blue). The different globular domains (α and β) are labelled, separated by a flexible hinge region.*

### 1.5.2 MT Gene Superfamily

The human MT gene superfamily (Figure 5) consists of 11 functional isoforms that are divided into four different subfamilies (MT-1 to MT-4), and five pseudogenes that are thought to originate from duplication and loss-of-function mutations of the parent MT-1 gene (Binz and Kägi, 1997; Sigel et al., 2009; Kimura and Kambe, 2016). Eight of the functional MT gene isoforms are in the MT-1 subfamily; MT-1A, 1B, 1E, 1F, 1G, 1H, 1M and 1X. However, the other MT subfamilies consist of only one gene each; MT-2 (MT-2A), MT-3 and MT-4 (Serén et al., 2014). MT-1 and MT-2 are the most studied

subfamilies to date and are thought to be expressed in a variety of tissues throughout the body (Babula et al., 2012). MT-2 in particular is thought to be the most widely expressed isoform, accounting for up to 50 % total MT expression in humans (Sigel et al., 2009; Raudenska et al., 2013). MT-1 isoforms are thought to be inducible by a variety of factors (Miles et al., 2000; Thirumoorthy et al., 2007; Capdevila et al., 2012). However, MT-3 and MT-4 are non-inducible and demonstrate tissue-specific expression; MT-3 is confined to neuronal tissue, and MT-4 to squamous epithelia (Palmiter et al., 1992; Quaife et al., 1994).

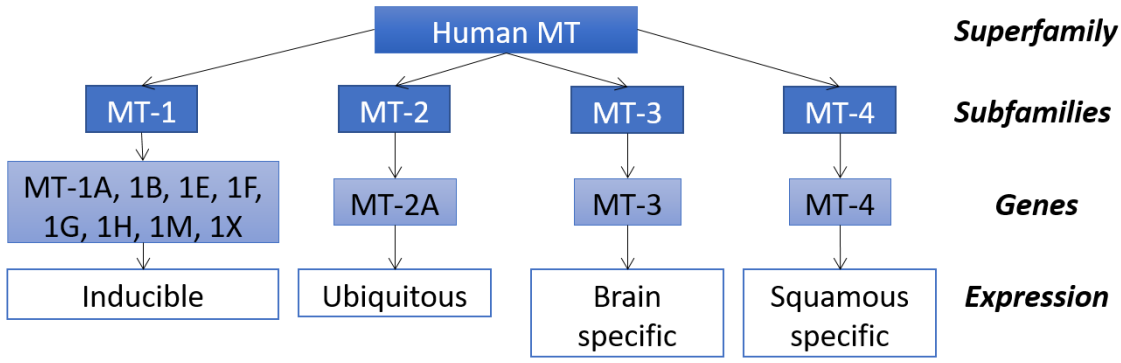


***Figure 5: Diagram of the MT gene superfamily.*** *The superfamily consists of 11 functional isoforms divided into 4 subfamilies; MT-1, MT-2, MT-3 and MT-4. MT-1 consists of 8 isoforms whereas the other subfamilies only consist of one. Each subfamily has distinct expression patterns, and MT-1 and MT-2 are the best studied. Isoforms: genes coding for highly homologous yet distinct proteins.*

### *1.5.2.1 MT Gene Duplication Events*

The MT genes are clustered together at a single locus on chromosome 16 (16q13), which is known for its intra-chromosomal duplication events (Karin et al., 1984; West et al., 1990; Martin et al., 2004). This, and the fact that multiple MT gene isoforms exist in humans, led to studies investigating the evolutionary history of the MT family. A number of phylogenetic studies have been performed in recent years with a view to understanding how multiple isoforms have been produced, and moreover, maintained. Moleirinho et al. (2011) used a combination of phylogenetic, transcriptional and polymorphic analyses in order to explore the diversification of the MT family. They found that the 4 subfamilies arose from a single duplication event prior to the radiation of mammals. However, a second duplication event then occurred in the primate lineage, whereby the MT-1 gene

expanded and formed the 8 active isoforms currently identified in humans. Another study performed phylogenetic, synteny, reconciliation, selection pressure and functional analyses on all active MT isoforms. The reconciliation analyses supported previous studies, revealing a high turnover of gene duplication and loss events. The study also found that there were significant variances in selection pressure during MT gene evolution, and that evolution was primarily in the form of 'purifying selection'; whereby genes are duplicated and maintain related but distinct functions. Interestingly, the results also indicate there was increased selection pressure in the MT-1 and MT-2 subfamilies, which is concordant with the number of isoforms present in the MT-1 subfamily. Lastly, the results showed that there is a higher number of conserved amino acids in the α-domain of the MT structure, suggesting that this domain is quite structurally constrained. However, high variability was observed in the amino acid sequence of the β-domain, which is thought to be the domain most involved in functional divergence of the MTs (Serén et al., 2014). These results support the hypothesis that the MT isoforms may have overlapping but distinct functions, as explored later (section 1.5.5.4).

### 1.5.3 MT Gene Transcriptional Regulation

Investigation of the upstream region of mouse MT-1 revealed a number of imperfect repeats which were named 'metal response elements' (MREs), and such regulatory elements were also identified in other MT genes (Stuart et al., 1985). DNA binding assays were performed using MREs as probes, resulting in the discovery of a zinc-dependent MRE-binding protein now known as MRE-binding transcription factor-1 (MTF-1). MTF-1 was identified as the primary inducer of MT genes and thus co-ordinating the heavy metal response (Palmiter, 1994). MTF-1 is constitutively expressed, having been observed present at both the mRNA and protein levels in various cell lines, and its expression is not influenced by heavy metal exposure (Radtke et al., 1993; Otsuka et al., 2000). However, MTF-1 can be activated by cellular zinc levels increasing, although it requires a higher concentration than other zinc-finger proteins to become saturated (Radtke et al., 1995). Once activated, MTF-1 then binds to the MREs in the MT promoter and induces transcription (Radtke et al., 1993). However, with regards to cadmium exposure, it is currently unclear whether zinc or cadmium by themselves can activate MTF-1. As mentioned earlier (section 1.4.4.2) the two metal ions are structurally similar, and thus cadmium could substitute for zinc in the MTF-1 structure (Chaney, 2010). However, it is also possible that cadmium exposure results in increased intracellular zinc

due to zinc substitution (see section 1.4.4.2), meaning labile zinc is then able to bind and activate MTF-1.

Despite much being known about MTF-1, questions still remain about its metal specificity, as it is currently unclear whether all metals require MTF-1 to induce MT transcription (Miles et al., 2000). Initial studies suggested that MTF-1 was essential for cadmium-induced MT gene transcription, with MTF-1-null cells failing to induce MT expression upon both zinc and cadmium treatment (Heuchel et al., 1994). However, contrasting studies have suggested that cadmium induction of MT is independent of MTF-1. IMR-32 neuroblastoma cells lack functional MTF-1 and yet cadmium was still able to induce MT-1 transcription through an MRE-dependent mechanism. In contrast all other heavy metals tested, including zinc and arsenic, failed to induce transcription (Chu et al., 1999). This suggests that cadmium can induce MT expression via its own unique pathway, which is independent of MTF-1 yet still requires MREs, supporting the hypothesis that other MRE-binding TFs exist. One such factor has already been identified, termed MRE-binding protein (MREBP), which was discovered to bind MREs upstream of the MT-2A gene (Koizumi et al., 1992). However, the role of MREBP remains unclear. Further studies are needed in order to clarify whether MTF-1 is essential for cadmium-induced MT expression, and if not, what other TFs (such as MREBP) and mechanisms may be involved in this potentially novel induction.

### 1.5.4 Proposed Functions of MT

Over the years MT has been suggested to play a role in a number of functions, and thus appears to be a multi-purpose protein. The most well-defined roles are summarised in Table 3, and functions especially pertinent to this research are explored in detail.

***Table 3: Summary of the different proposed functions of metallothionein.*** *Each function is accompanied by respective references.*

| Function | References |
|---|---|
| **Reactive oxygen species scavenger** | (Ruttkay-Nedecky et al., 2013; Penkowa et al., 2006; Lazo et al., 1995) |
| **Regulation of cell cycle progression, differentiation and proliferation** | (Cai et al., 2014; Schulkens et al., 2014; Yap et al., 2009; Liu et al., 2009; Ioachim et al., 2001; Jin et al., 2002; Cherian and Apostolova, 2000) |
| **Angiogenesis** | (Wierzowiecka et al., 2016; Schulkens et al., 2014; Lee et al., 2004; Penkowa et al., 2000) |
| **Immune Responses** | (Ugajin et al., 2015; Mita et al., 2008; Penkowa et al., 2006; Kimura et al., 2001) |
| **Zinc Homeostasis/Regulation of Zinc-Containing Proteins** | See section 1.5.4.1 |
| **Metal Detoxification/Sequestration** | See section 1.5.4.2 |

### *1.5.4.1 Zinc Homeostasis/Regulation of Zinc-Containing Proteins*

MT is the most prominent binder of zinc in the body, and 5-20 % total cellular zinc is bound to MT in the cytoplasm (Kägi and Kojima, 1987; Sigel et al., 2009). It is therefore logical that MT may play a role in zinc homeostasis, and which is supported by the observation of a close relationship between tissue MT expression and zinc content (Bremner, 1987). Numerous studies have attempted to determine the importance of MTs in controlling intracellular zinc. For example, Dalton et al. (1996) found that transgenic mice overexpressing MT-1 were more resistant to zinc deficiency, and they postulated that this may be due to an increased pool of zinc bound to MT. Another study used pregnant transgenic mice constitutively expressing MT-1 and fed them a zinc-deprived

diet. They found that in these mice, only 5.8 % embryos had morphological defects, compared to 21.3 % in control mice (Lee et al., 2003). Both these studies suggest that MT may be an important source of intracellular zinc. However, another study found that although MT-null, zinc-deprived mice had abnormal kidney development and maturation, MT-null-only mice appeared to live normally (Kelly et al., 1996). This questions the role of MT as an essential source of zinc under normal physiological conditions, and instead infers that MT may act as a reservoir for zinc that is only used under zinc-deprived conditions (Miles et al., 2000).

MTs are thought to work in cooperation with zinc transporters (ZnTs) in order to maintain cellular zinc homeostasis, and are implicated in both the maintenance mechanisms of zinc 'buffering' and zinc 'mumbling' (Kimura and Kambe, 2016). Buffering allows the zinc cytosol concentration to remain within the picomolar range under normal conditions, whereas muffling occurs under non-steady state conditions where transient changes in zinc cytosolic concentrations are carefully modulated (Colvin et al., 2010; Krezel and Maret, 2006). It has been shown that when cellular zinc levels become too high, transcription of MT is induced along with concordant induction of several ZnTs, possibly by a common transcription factor such MTF-1 (Günther et al., 2012). Their cooperative expression then aids the reduction of zinc levels until a normal level is once again reached, probably via ZnT efflux and MT binding of zinc (Tomoki Kimura, Itoh, & Andrews, 2009; Otsuka, 2001; Langmade et al., 2000; Guo et al., 2010). This suggests that MT and ZnT may act synergistically to counteract abnormal cellular zinc levels and maintain homeostasis (Kimura and Kambe, 2016).

As part of its role in zinc homeostasis it is thought that MT can also act as a zinc buffer, donating zinc to target proteins in times of need (Krezel and Maret, 2008; Costello et al., 2011). Transfer of zinc occurs via ligand exchange in zinc mediated protein-protein interactions, known as the 'associate mechanism' (Costello et al., 2011; Maret and Li, 2009; Maret, 2011). The donation of zinc to apo-enzymes results in their reactivation; for example, zinc-saturated MT (Zn-MT) is thought to be the primary zinc-donator for the zinc-requiring enzyme apo-carbonic anhydrase (Pinter and Stillman, 2015). Zinc-finger-containing transcription factors are also thought to be a target of Zn-MT, with the complex translocating into the nucleus under times of cellular stress and promoting activation of zinc-finger transcription factors by zinc donation (Sigel et al., 2009). By contrast, it has also been reported that apo-MT can extract zinc from certain transcription factors and inhibit their activity. For example, apo-MT has been observed to extract zinc

from the transcription factors Sp1 and TFIIIA rendering them unable to bind to DNA (Zeng et al., 1991a; Zeng et al., 1991b). Thus, it appears that MT can act as a chaperone for zinc proteins/enzymes, acting to modulate their actions via both the donation and removal of zinc ions.

#### *1.5.4.2 Metal Detoxification/Sequestration*

As stated earlier, MT was originally identified as a cadmium-binding protein (Margoshes and Vallee, 1957). Due to further extensive *in vitro* and *in vivo* studies it is now widely recognised to play an essential role in metal detoxification, due to its high affinity for binding and sequestering metal ions. Sequestration means that the toxic ions are no longer free to bind other proteins and/or alter physiological processes within the cell (Miles et al., 2000; Capdevila et al., 2012; Babula et al., 2012). Studies supporting this role have shown that exposure to various metals results in significant increases of MT levels in a number of tissues, and that the protein appears to accumulate in cell lines that have undergone metal exposure (Cherian and Goyer, 1978; Kägi et al., 1979; Kobayashi and Kimura, 1980). It has also been shown that increased MT expression (due to 'priming' via repeated low-dose metal exposure) can increase a cell's tolerance to toxic doses, presumably due to MT's ability to sequester the metal ions (Goering and Klaassen, 1984). Indeed, cell lines that have developed resistance to cadmium exposure demonstrate very high MT expression, and this resistance crosses over to other heavy metal exposure (e.g. copper; Durnam and Palmiter, 1984).

Once sequestered it is unclear how and where the metal-MT complex is stored, and for what duration. As mentioned in section 1.5.1, metal-bound MT protein is much more resistant to degradation, and the rate of degradation depends upon the metal ions within the structure (Klaassen et al., 1994). For example, Cd-MT has been observed much more resistant to proteolysis than Zn-MT, and therefore has a longer half-life (Coyle et al., 2002; Sigel et al., 2009). This is because MT preferentially binds cadmium over zinc (Kägi and Kojima, 1987), and the difference in binding affinity/degradation rate supports MT's function as a detoxifier of toxic metals yet regulator of essential ones. Indeed, a recent study has suggested that cadmium and zinc bind to MT via separate pathways. The authors observed that zinc appears to form beaded structures in a non-cooperative manner when binding to MT, whereas cadmium forms a four-metal domain cluster via a cooperative mechanism. The authors suggest these metal-specific pathways are reflective of MT's multiple roles as both a zinc donator and metal detoxifier; the MT protein

terminally binds zinc so that the metal can be donated to proteins, whereas MT binds cadmium in a manner that sequesters and detoxifies it (Irvine et al., 2016).

Interestingly, it has been suggested in the literature that metal-MT may be sequestered within the cell in structures termed 'inclusion bodies' (IBs). For example, lead-poisoning has been observed to cause the production of protein-lead complexes which appear within the cell as IBs. Lead was highly concentrated within these organelles, which were often nuclear, and it was unclear whether they were permanent structures or degraded with the cessation of exposure (Choie & Richter, 1972; Goyer et al., 1970). MT has been implicated as the protein in these structures, with one study showing that MT-null cells could not form IBs upon lead-exposure (Qu et al., 2002). Moreover, renal lead-containing IBs from lead-exposed mice were discovered to have MT protein associated with the outside portion of these bodies (Waalkes et al., 2004).

More recent studies have also seen the production of these IBs after arsenic exposure. Originally mislabelled as 'micronuclei', they were observed in urothelial cells from human populations exposed to arsenic-contaminated drinking water in India (Basu et al., 2002). One study repeatedly exposed mice to arsenic in order to further characterise these 'micronuclei', and found that the structures were both eosinophilic and negative for DNA/chromosomal staining; suggesting that the bodies were not micronuclei. The IBs appeared as soon as 6 hours post-exposure, and with high doses could be observed in all cell layers as both intranuclear and intracytoplasmic structures (Dodmane et al., 2014). IBs have also been identified in exfoliated superficial urothelial cells from patients with acute promyelocytic leukaemia undergoing arsenic-based chemotherapy. There were multiple bodies per cell of various sizes, which were identifiable using light microscopy. Moreover, these IBs could still be observed up to 7 months post-chemotherapy. The authors postulated that the metal-containing IBs act as a cellular depot and remained intact until the superficial urothelial cells were sloughed off (Wedel et al., 2013). Although the exfoliated cells analysed in this study showed signs of autolysis, control exfoliated cells did not demonstrate these IBs, suggesting that their presence was due to arsenic exposure and not as a result of cellular damage. However, it should be noted that the authors did not confirm the urothelial origin of these exfoliated cells, and exfoliated renal cells have also been reported in urine (Zhou et al., 2011). Despite this, if further studies can confirm the presence of MT protein in urothelial inclusion bodies, this would further support the sequestration role of MT as a detoxifying mechanism.

### 1.5.5 Metallothionein Isoforms

The individual characteristics of the different MT isoforms have not been extensively studied due to high isoform homology and the assumption of shared function. However, there has been accumulating evidence in recent years that the isoforms are distinct in a number of ways, and in the following sections these differences are explored.

#### *1.5.5.1 Structural Differences*

As explored earlier (section 1.5.2), the MT gene family is diverse and contains a number of homologous isoforms. The MT-1 and MT-2 subfamilies are the most similar, differing by only a single negative charge (Kägi et al., 1979). However, the differences between these subfamilies and the MT-3 and MT-4 subfamilies are more distinct, reflective of their duplicative origin. For example, MT-3 has an additional 8 amino acid sequence that marks it as unique (Palmiter et al., 1992). At the individual isoform level, the structural differences become finer. The MT-1 subfamily genes in particular are extremely homologous and also have similar charges; however, the isoforms appear to have small structural differences and can differ in their post-translation modifications (Miles et al., 2000). Moreover, the isoforms also differ at their N-terminal tryptic peptide, which can be used to differentiate between all 11 functional isoforms (Mehus et al., 2014).

#### *1.5.5.2 MT Isoform Expression and Degradation*

Basal expression of the MT isoforms appears to vary depending on the tissue of origin (Capdevila et al., 2012). For example, MT-2A has been observed constitutively expressed in HepG2 cells under basal conditions, whereas the MT-1F and 1G isoforms are not expressed at all (Jahroudi et al., 1990). In contrast, the MT-1F and 1G isoforms are constitutively expressed in human umbilical vein epithelial cells (HUVEC) under basal conditions, with expression levels higher than those of MT-2A (Conway et al., 2010). It has also been observed that protein translation efficiency can vary depending on the isoform. Mehus et al. (2014) found that MT mRNA expression did not always correlate one-to-one with protein expression, and that varied depending on the specific isoform transcript. For example, the MT-1E isoform represented 30-50 % all MT transcripts expressed, yet only 10-18 % total MT protein. Upon calculation, its protein:mRNA ratio was 4-6 fold lower than the other two isoforms studied (MT-1X and MT-2A), further highlighting fundamental differences between the isoforms. Lastly, it has been hypothesised that there may be separate degradation pathways for the different isoforms,

with some proving more resistant to proteolysis and thereby remaining in the cell for longer (Miles et al., 2000).

These differences in degradation-resistance have been demonstrated in rat liver cells, where MT-1 and MT-2 were observed to degrade at different rates. The biological half-life of Zn-MT-1 was 12.2 hours, whereas the half-life for Zn-MT-2 was 21.9 hours, suggesting that MT-2 is more resistant to proteolysis in these cells (Lehman-McKeeman et al., 1988; Klaassen and Lehman-McKeeman, 1989). Moreover, characterisation of MT degradation products in rat liver has identified different domains from MT-1 and MT-2 present, suggesting that there may be differences in the stability of the metal-binding domains of the two (Saito and Hunziker, 1996).

#### *1.5.5.3 Specific Induction Patterns*

Although the primary inducer of MT transcription is thought to be metal ions a variety of other factors have also been implicated. These include ROS, cytokines, hormones, hypoxia and cellular stress (Bremner, 1987; Futakawa et al., 2006; Kikuchi et al., 1993; Richards et al., 1984; Tanji et al., 2003; Conway et al., 2010). Of note, it is suggested that ROS induce MT expression via antioxidant response elements (AREs) in the promoter, and hormones via the glucocorticoid receptor elements (GREs); however, not all MT promoters are thought to contain these elements (Dalton et al., 1996; Karin et al., 1984b; Miles et al., 2000). The idea that isoforms may contain different elements in their promoter is supported by the observation that MT isoforms can be differentially induced depending upon the factor they are exposed to. For example, glucocorticoids appear able to induce expression of MT-2A, but not MT-1A or 1F (Richards et al., 1984; Varshney et al., 1986).

Furthermore, the isoforms appear to show metal specificity, with different metals inducing distinct isoforms. In HeLa cells it was observed that copper exposure could cause induction of all the MT-1 subfamily, except for MT-1A; however, MT-1A could be significantly induced by both zinc and cadmium exposure. It was also found that zinc, cadmium and copper seemed to preferentially induce MT-1X and MT-2A, causing a much higher induction of these isoforms compared to others (Miura and Koizumi, 2007). Moreover, experiments in the fruit fly *Drosophila melanogaster* have indicated that metal specific induction of isoforms is co-ordinated by MTF-1. Using genomic mapping it was shown that MTF-1 bound different DNA sites depending on the metal stressor, leading the authors to conclude that different MT isoforms preferentially protect against

different insults (Sims et al., 2012). Another group studying *D.melanogaster* also reported exposure-specific results, and suggested that the spatial arrangement of MTF-1 binding sites in isoform gene promoters may be responsible for differential induction (Selvaraj et al., 2005).

The MT isoforms not only differ in their inducers, but it has also been reported that they differ in the timing of their induction. For example, cadmium exposure of HepG2 cells revealed that MT-1G isoform transcript expression was significantly induced after one hour; however, MT-1F was not significantly transcribed until after four hours induction (Sadhu and Gedamu, 1988). To account for the isoform-specific variations in expression it has been suggested that the MT family may be regulated by a family of TFs that are specific to MREs in the promoters, rather than just MTF-1 alone (Searle, 1990; explored earlier in section 1.5.3).

#### *1.5.5.4 Differential Functions*

It is now a commonly held belief that the MT isoforms may serve different functions (Miles et al., 2000; Coyle et al., 2002; Sigel et al., 2009; Capdevila et al., 2012; Brazão-Silva et al., 2015; Kimura and Kambe, 2016). Much of the evidence contributing to this belief has been summarised in the above sections (1.5.1 – 1.5.4), which demonstrate the vast array of differences between the isoforms. It possible that these differences are simply a result of duplication of function, however, there is now strong evolutionary data suggesting that these gene duplications have been selected for and maintained. The recent study by Serén et al. (2014) showed that the MT family had undergone changes in selection pressure, especially in the MT-1 subfamily, resulting in high turnover of gene duplication and loss; yet some gene duplications were maintained. The authors also observed high variability in the amino acid sequence of the β-domain which is involved in functional divergence. These evolutionary studies support the hypothesis that the MT isoforms may have overlapping yet distinct functions.

However, deciphering the different functions of the isoforms is problematic, as it is difficult to study the isoforms in isolation. This is due to their high levels of homology, minimal basal synthesis levels and complicated expression patterns (Capdevila et al., 2012). Isoform expression is particularly hard to study at the protein level due to the high similarity, whereas transcript expression is easier due to sufficient divergence at the 5' and 3' untranslated regions (Mehus et al., 2014). As explored earlier however (section 1.5.5.2) transcript levels do not always reflect protein levels, and therefore it is important

to attempt to differentiate between the isoforms at the protein level. MT protein expression has generally been investigated using antibodies, which has proved useful to obtain basic knowledge but is limited by the reagents available. Currently, there are no validated commercially available antibodies that can distinguish between MT-1 and MT-2 subfamilies, let alone between the isoforms of MT-1 (Jasani and Schmid, 1997). Mass-spectrometry techniques have been employed to some success, however these methods are timely and expensive (Wang et al., 2007; Mehus et al., 2014). The development and validation of isoform-specific MT antibodies is sorely needed, so that initial results investigating transcript expression can be supported and potentially novel isoform-specific functions determined.

### 1.5.6 MT Expression in Cadmium-Induced Urothelial Carcinogenesis

#### *1.5.6.1 Cadmium-Induced MT Expression*

Cadmium has been demonstrated to be the most potent inducer of MT (Kim et al., 2008), with numerous studies confirming MT induction by cadmium exposure *in vitro* (Durnam and Palmiter, 1984; Karin et al., 1984b; Varshney et al., 1986; Kikuchi et al., 1993; Potts et al., 2001; Forti et al., 2010; Fabbri et al., 2012; Mehus et al., 2014; Irvine et al., 2016). Increased MT expression has also been seen *in vivo* in humans that have been occupationally or environmentally exposed to the metal. In male Polish battery-production workers, a significant 2.5-fold increase in general MT transcript expression was found in the blood of workers identified as having been exposed to ambient cadmium (Ganguly et al., 1996). More recently, an association between blood cadmium levels and MT transcript expression was found in humans living in cadmium-contaminated areas of Thailand. The authors produced some distinction between isoforms, looking at MT-1A, MT-2A and MT-3 transcripts separately. They found that MT-1A expression was significantly associated with blood cadmium levels, whereas MT-2A expression was associated with smoking status, and there was no association between MT-3 expression and blood cadmium (Boonprasert et al., 2012). These results emphasise the importance of distinguishing between the isoforms, as only MT-1A was identified as being induced by environmental cadmium exposure in this study.

As mentioned earlier, MT isoform expression appears cell- and tissue-specific (section 1.5.5.2). Therefore, to identify cadmium-induced isoforms relevant to the bladder it is essential that normal human urothelial tissue/cells are used. Few studies have been conducted looking at MT expression in urothelium, with or without cadmium exposure.

However, one study used the immortalised urothelial cell line UROtsa to look at MT isoform and transcript expression in cadmium-transformed cells. They found increased transcript expression of all three MT isoforms studied; MT-1E, MT-1X and MT-2A. They also found increased MT protein expression using the pan-specific E9 antibody, which identifies both MT-1 and MT-2 subfamilies (Zhou et al., 2006a). This study clearly seems to indicate that cadmium exposure induces MT expression in the urothelium; however, only three isoforms were studied at the transcript level and only general MT-1/2 expression at the protein level. Moreover, the urothelial cells used were an immortalised cell line and thus were already genetically altered from normal human urothelium (see section 1.1.4). Further studies using primary samples to determine expression of all MT isoforms would aid the understanding of how *in vivo* cadmium exposure can alter MT expression in the bladder.

#### *1.5.6.2 MT Expression in Urothelial Cancer*

Altered MT expression has been observed in a number of different cancers, including lung, hepatic, breast, colorectal and urothelial carcinomas (Pedersen et al., 2009). In urothelial cancer, high expression of MT-1 and MT-2 has been associated with advanced tumour grade and stage, worse overall survival, reduced disease-free survival and decreased disease-free progression (Siu et al., 1998; Sens et al., 2000; Ioachim et al., 2001; Somji et al., 2001; Saga et al., 2002; Yamasaki et al., 2006; Zhou et al., 2006a; Wülfing et al., 2007; Hinkel et al., 2008). Specifically, it was found that the 5 year survival rate for patients with low MT-1/2 expression was 72 %, whereas for patients with high MT-1/2 expression it was only 32 % (Hinkel et al., 2008). It was also observed that only 37.5 % superficial tumours demonstrated MT-1/2 expression, whereas 65.2 % invasive tumours showed expression (Yamasaki et al., 2006). Originally, MT-3 was also thought to be highly expressed in bladder tumours, with negative expression at both the transcript and protein level in normal bladder tissue (Sens et al., 2000). However, this has only been found by one research group, and the results are in direct contrast to the general consensus that MT-3 expression is restricted to neural tissue (Palmiter et al., 1992).

Again, the problem with these studies is a lack of discrimination between the MT isoforms. Most of the studies conducted looking at MT expression in urothelial cancer only analysed protein expression using the pan-specific MT-1/2 E9 antibody, meaning the isoform(s) responsible for increased MT protein abundance remain unknown. However, one study using the E9 antibody also went on to determine isoform-specific

transcript expression in normal and malignant bladder tissue, having detected over-expression of MT-1/2 protein expression in all high-grade tumour samples. They found that MT-2A transcript was expressed in both normal and malignant tissue, but that the MT-1E transcript was expressed inconsistently. They also observed that MT-1X transcript expression was highly over-expressed in bladder cancer tissue compared to normal tissue. However, in contrast to MT-1/2 protein expression, MT-1X transcript levels did not vary with tumour grade (Somji et al., 2001). The data emphasises the importance of analysing MT isoform expression, so that individual isoforms responsible for gross protein changes may be identified and subtle changes in transcript expression identified.

#### *1.5.6.3 MT Expression in Cadmium-Induced Urothelial Carcinogenesis*

Studies directly investigating MT expression in cadmium-induced urothelial carcinogenesis are rare, most likely due to difficulty in gaining access to patient samples that have been strongly linked to cadmium exposure. To overcome this, one group have developed an *in vitro* cell culture model using cadmium-exposed malignantly-transformed UROtsa cells, to determine factors such as MT expression. Upon inoculation into nude mice these cells were capable of forming tumours, and the authors went on to analyse MT protein expression in these heterotransplants. They observed high MT-1/2 protein expression similar to that observed in high-grade bladder tumours, with the highest expression observed in less-differentiated areas of the tumour. Interestingly, the authors also found expression of MT-3 transcript and protein which had not been present in the transformed cell cultures prior to inoculation, leading to the suggestion that MT-3 expression may be a consequence of tumour-formation. To identify the MT isoforms responsible for high expression of MT-1/2 protein in the heterotransplants, transcript expression in the malignantly-transformed UROtsa cell cultures was analysed. Significantly increased levels of MT-1E, 1X and 2A transcripts were observed in the cadmium-exposed, malignantly-transformed cells, suggesting that these isoforms may be responsible for the increased MT-1/2 protein expression. However, the other MT isoforms were not analysed, and thus may also play a role in the increased protein abundance (Zhou et al., 2006a; Zhou et al., 2006b).

To date, there has been only one *in vivo* study looking at MT expression and cadmium concentrations in urothelial carcinoma (mentioned briefly earlier in section 1.4.3). Wolf et al. (2009) took urinary samples from control and bladder cancer patients and analysed

them for MT-bound cadmium, using a combination of mass-spectrometry approaches. The authors found that urinary cadmium was predominantly bound to the MT fraction, and that the median concentration of MT-bound cadmium was significantly higher in bladder cancer patients; 1.8 µg/L compared to 0.8 µg/L in the control group. This is the first study showing such a correlation between MT, cadmium and urothelial cancer. However, it is unclear how many of the urothelial carcinoma samples may have been linked to cadmium exposure, as no account was made for smoking and/or occupation. This could explain why there was a high amount of data variance in the cancer cohort, as some patients were probably never exposed to cadmium and thus may have had much lower cadmium concentrations. In order to further investigate the correlation between MT expression and cadmium-induced urothelial cancer a more in-depth study is needed, with sufficient patient details to stratify cases into exposed and control patient cohorts.

### 1.5.7 MT Expression in Cadmium-Induced Urothelial Carcinogenesis – Cause or Consequence?

#### *1.5.7.1 Cause – Potential Mechanisms of Carcinogenesis*

A number of the proposed normal functions of MT could potentially contribute to carcinogenesis, such as its role in proliferation, angiogenesis and ROS scavenging (section 1.5.4). It is for this reason that MT expression is often seen as a 'double-edged sword'; on the one hand, it functions to protect the cell, but by the same mechanisms can also facilitate malignant events (Hart et al., 2001; Sigel et al., 2009; Pedersen et al., 2009; Capdevila et al., 2012). For example, it has been shown that MT can contribute to cell survival by increasing resistance to ROS-induced apoptosis, which becomes a problem when the cell in question has acquired neoplastic properties (Eneman et al., 2000). Resistance to apoptosis, along with increased cellular proliferation (also mediated by MT; Ioachim et al., 2001) can result in the survival and expansion of deleterious cells which would otherwise be removed from the body. It has additionally been shown that cadmium exposure can result in inhibition of DNA repair (Potts et al., 2001), which coupled with increased cellular protection via cadmium-induced MT expression, increases the probability of cells with dangerous mutations proliferating and passing on these defects to their progeny (Hart et al., 2001). The ability to counteract ROS could also play a role in chemotherapy resistance, and high levels of MT expression have been correlated with treatment resistance in bladder cancer (Satoh et al., 1993; Wülfing et al., 2007). Specifically, after radical surgery and adjuvant chemotherapy, 100 % patients with high

tumour MT expression progressed within 9 months. By contrast, even after 5 years only 65 % patients with low MT expression had progressed (Yamasaki et al., 2006). MT has not only been suggested to indirectly inhibit chemotherapy due to ROS scavenging and upregulation of pro-survival mechanisms, but also via direct sequestration of platinum-based chemotherapeutic agents such as cisplatin (Hagrman et al., 2003).

The ability of MT to sequester carcinogenic metals is also a potential contributor to the development of carcinogenesis. Although sequestration is an efficient detoxification method in the short-term, it also means that the metal ions remain in the body for prolonged periods of time. MT-cadmium complexes may have a slow rate of degradation (section 1.5.4.2) but at some point the protein is lost, meaning that the cadmium ions are freed, before again being bound by MT protein. MT therefore appears to play a key role in the systemic cycling of cadmium, which may result in repeated release of carcinogenic ions over time (Sandbichler and Höckner, 2016). This imperfect system of cadmium chelation supports the hypothesis that cadmium detoxification is a property of MT rather than its evolutionary function, and that its ability to bind cadmium is actually just a result of its ability to regulate zinc (Vašák and Meloni, 2011; Capdevila et al., 2012). Despite these data, a putative role for MT expression in urothelial carcinogenesis has not been confirmed. The consequences of cadmium-induced MT expression remain to be elucidated, with questions surrounding a potential switch from cytoprotective mechanisms to pro-carcinogenic, and whether once a tumour is established MT expression only contributes to carcinogenesis rather than initiating it.

#### *1.5.7.2 Consequence – MT as a Potential Biomarker of Cadmium Exposure*

As discussed earlier (section 1.5.6.1), cadmium appears to be a potent inducer of MT expression. It has therefore been suggested that MT may be a useful biomarker of cadmium exposure. MT expression is already used in a number of organisms as a means of monitoring environmental contamination and remediation. Waterborne cadmium-contamination is often monitored using aquatic organisms such as fish, where MT protein can accumulate in organs such as the gills (Smaoui-Damak et al., 2009; Shariati et al., 2011). Invertebrate organisms are commonly used for monitoring soil-contamination, with earthworms especially proving useful indicators. The MT concentration in their coelomic fluid has proved a particularly sensitive biomarker and has been recommended for use in the monitoring and assessment of polluted soil (Calisi et al., 2014).

MT has also been suggested as biomarker of human exposure to occupational and environmental cadmium. MT expression in peripheral blood lymphocytes (PBLs) has been suggested as a sensitive marker of exposure, where one study showed a significant increase in PBL MT-1/2 transcript in workers occupationally exposed to ambient cadmium (Ganguly et al., 1996). The use of MT as a biomarker has been further supported by *in vitro* studies demonstrating that culturing PBLs with cadmium resulted in dose-dependent increases in MT-1/2 transcript (Yamada and Koizumi, 2001). A recent study attempted some differentiation between the PBL MT isoforms in workers exposed to cadmium. Using MT-1A, 1E, 1F and 1X transcript analysis they found that MT-1E, 1F and 1X transcript expression increased with blood cadmium levels, whereas MT-1A transcript expression increased with urinary cadmium levels (Chang et al., 2009). Correlation between PBL MT expression and cadmium-exposed individuals was supported by a further study looking at populations residing in cadmium-contaminated areas in Thailand. The authors found that PBL MT-1A and MT-2A transcript expression was significantly elevated in exposed individuals and correlated with blood and urinary cadmium levels (Boonprasert et al., 2012). Due to the findings of studies such as these it has been suggested that PBL MT-1/2 isoforms may be a useful biomarker of cadmium exposure and internal dose, and may therefore have a role in monitoring occupational exposure (Chang et al., 2009).

However, a potential flaw of using PBLs to monitor human cadmium exposure is that it involves obtaining blood samples, when other bodily fluids such as urine are more easily obtained and readily available. It has also been suggested that blood cadmium levels are only reflective of recent exposure, whereas urinary cadmium reflects cumulative exposure over time and overall body burden (Agency for Toxic Substances and Disease Registry, 2008). This supports the hypothesis that cadmium may accumulate in the bladder, and thus urinary MT expression may prove a more useful biomarker of long-term exposure than PBL MT. This hypothesis has been investigated by a number of different research groups looking at occupationally exposed workers, with concurring results. Urinary metallothionein levels have been found to be elevated in cadmium-exposed worker groups and correlated with cadmium concentrations in the liver, kidney, blood and urine (Tohyama et al., 1981; Shaikh and Tohyama, 1984; Shaikh et al., 1990; Nakajima et al., 2005; Chen et al., 2006). Moreover, elevated MT levels were observed in the urine from an environmentally-exposed patient for up to 14 years after cessation of

exposure, and correlated with urinary cadmium levels which also remained elevated (Tang et al., 1999).

The ability to detect elevated MT expression post-exposure supports MT as a potential biomarker, as exposure of an individual may no longer be current. However, the longevity of MT expression would need further investigation, as it is important to establish how recent exposure would have to be for MT expression to remain elevated. Another flaw with the biomarker studies previously performed is that there is no discrimination between the urinary MT isoforms induced by cadmium exposure. As examined earlier (section 1.5.5.3), MT isoform induction appears highly specific, and thus it would be important to identify a urinary isoform specific to cadmium exposure. Otherwise, elevated general MT expression could be a result of secondary exposure events such as increased ROS, which could also be caused by a number of other factors e.g. infection (Wang et al., 2004; Mita et al., 2008).

A biomarker of exposure to cadmium would be useful for several reasons. Monitoring worker exposure to occupationally-based cadmium would be useful in preventing toxicity from the same, as well as preventing long-term effects such as osteoporosis and potential carcinogenesis (see section 1.4.3; Roels et al., 1999; Jarup et al., 1998). Furthermore, a biomarker could be used to identify patients whose urothelial cancer may be linked to cadmium exposure. Molecular analysis of these cancers could potentially prove useful for further elucidation of the mechanisms of cadmium-induced carcinogenesis, and thus how to target treatment. Additionally, as MT expression has been linked to chemotherapy resistance (section 1.5.7.1), its expression in tumours could potentially inform clinicians that frequent monitoring of these patients for recurrence is required post-treatment.

## 1.6 Thesis Aims and Objectives.

### 1.6.1 Aims

To investigate the MT response of normal human urothelium to cadmium exposure, assessing individual MT isoforms as potential biomarkers of exposure.

### 1.6.2 Objectives

- To characterise basal and heavy metal-inducible MT isoform expression in normal human urothelium.
- To determine whether cadmium can cross an intact urothelial barrier.
- To investigate the specificity and longevity of MT isoform induction.
- To observe whether *in vitro* MT induction can be translated to *ex vivo* ureter organ culture.

# Chapter 2: Materials and Methods

## 2.1 General

All laboratory work was carried out at the Jack Birch Unit for Molecular Carcinogenesis, Department of Biology, University of York. Support and use of equipment was also provided by the Department of Environment, University of York. Human tissue biopsies were taken at multiple sites (see section 2.6.1).

## 2.2 Suppliers

Commercial manufacturers and suppliers of laboratory equipment and reagents are named in the text at first mention. A full list detailing names and addresses can be found in the Appendix.

## 2.3 Glassware and Plastic-ware

All glassware (including glass pipettes; Scientific Laboratory Supplies) and plastic-ware (including microfuge tubes; Sarstedt, and pipette tips; Starlab) were sterilised by autoclaving at 121ºC for 20 min followed by air drying in an oven at 60ºC. Glass pipettes were placed in a metal container (Jencons) for the sterilisation process. All sterile single-use plastic-ware were manufactured by Sterilin and provided by SLS, with the exception of serological pipettes which were supplied by Sarstedt.

## 2.4 Stock Solutions

Formulae for all stock solutions used can be found in the Appendices (section 9.1). All chemicals used were of either analytical reagent grade or tissue culture grade. All solutions were prepared using ultra-pure water ($H_2O$) from a Purelab Ultra Genetic ultra-violet water purification system (ELGA). Sterilisation of water and solutions was carried out by autoclaving at 121ºC for 20 min or use of a 0.2 µm nitrocellulose syringe filter (Millipore).

## 2.5 Handling and Use of Cadmium Chloride

Cadmium chloride is known to be a human carcinogen as recognised by the International Agency for Research on Cancer (IARC). It is toxic if inhaled or swallowed and an irritant to skin, as well as posing a significant threat to aqueous organisms. Prior to purchase a risk assessment was carried out by the Biology Department Safety Officer, and a Standard Operating Procedure was prepared (see Appendices; section 8.7) in order to minimise exposure and risk to the aquatic environment.

### 2.5.1 Storage and Handling

Stock powder of cadmium chloride ($CdCl_2$; Sigma) was kept in a tightly closed container containing silica gel beads as desiccant. The container was kept in a locked and labelled 'Dangerous Chemicals' cabinet. Once powder had been dissolved in water to produce a working stock solution, aliquots were kept in a clearly labelled box in a locked -20 °C freezer.

When handling $CdCl_2$ a lab safety coat and nitrile gloves were worn at all times. $CdCl_2$ was only used in externally-vented hoods with safety cabinet shields which provided adequate protection for the eyes and minimised risk of inhalation.

### 2.5.2 Making up Stock Solutions

All weighing of powder stock was carried out in an externally vented fume hood (model number E32841; Fumetec Ltd). A tray containing damp blue roll was used to catch any spillage and strength of air flow was tested on a non-toxic substance to ensure powder was not blown into the air. A disposable spatula was used to place an undefined amount of $CdCl_2$ powder into a pre-weighed bijou tube (Greiner Bio-one) which was then sealed. The bijou was then placed in an Explorer® Pro (Ohaus) enclosed digital scale. $H_2O$ was added to make up a working stock solution, which was then passed through an Acrodisc 0.02 µM syringe filter (VWR) and stored appropriately.

### 2.5.3 Disposal

Any equipment that came into contact with $CdCl_2$ was placed in a small autoclave bag, which contained enough blue roll to capture any excess liquid. Bags were then sealed and placed into double-bagged clinical waste bags for disposal by incineration.

Liquid waste (including aspirated tissue culture medium) was stored in a clearly-labelled waste bottle containing 10 % (w/v) Virkon™. The bottle was kept in a locked 'Dangerous Chemicals' cabinet when not in use. When 90 % full, bottles were further labelled with the required paperwork and taken to Biology Stores for disposal by incineration. $CdCl_2$ was not allowed to enter the water system at any point.

### 2.5.4 Use of other Carcinogenic Metalloids

The work also involved the use of the carcinogenic metalloids arsenite and nickel chloride. For health and safety measures these substances were handled in the same manner as $CdCl_2$.

## 2.6 Tissue Specimens

### 2.6.1 Source of Human Tissue Specimens

*2.6.2.1 'Normal' Human Urothelial Tissue*

Surgical specimens of human urothelium were collected with NHS Research and Ethics Committee (REC) approval and informed consent as required. Samples of ureter and renal pelvis were obtained from patients undergoing urological surgery with no known history of urothelial malignancy from St. James's University Hospital, Leeds and Pinderfields Hospital, Wakefield (REC references 99/095, 02/208, respectively).

All samples were anonymous and provided with basic details of the surgical procedure, patient age, gender and urological diagnosis (if appropriate). Upon arrival, normal human urothelial specimens were allocated an arbitrary Y-number for laboratory records (all Y-numbers used during this work are detailed in Table 14). Surgical samples were collected aseptically in sterile Transport Medium (see Appendices) in a 30 mL Universal container. Samples were stored at 4 ºC until use (generally <5 days). For each sample obtained, a small representative sample was taken for routine histology using Haematoxylin and Eosin (H&E; see section 2.8.3) staining to confirm a normal urothelium, with absence of metaplasia, dysplasia or neoplasia.

## 2.7 Cell and Organ Culture

### 2.7.1 Cell and Organ Culture Equipment

All procedures for cell and organ culture were carried out under strict aseptic conditions using class II laminar air flow safety hoods with HEPA filters (Medical Air Technology). A vacuum pump connected to a Buchner flask was used for aspiration of waste medium and subsequently decontaminated in 10 % (w/v) Virkon™ solution. Hood surfaces were wiped before, during and after use with 70 % (v/v) EtOH.

All cell cultures were maintained in HERAcell™ 240 incubators (Thermo Scientific) at 37 ºC in a humidified atmosphere, with 5 % or 10 % $CO_2$ in the air depending on medium used. All organ cultures were maintained in a Forma Steri-cult $CO_2$ humidified incubator with HEPA filter (Thermo Scientific) at 37ºC in 10% $CO_2$ in air. In accordance with the Human Tissue Act (HTA) license the incubator was only used for the growth of human tissue and was kept locked at all times.

Cell cultures were observed and phase-contrast images captured using an EVOS® XL Core cell imaging system (Life Technologies). All images were captured using x10 objective. Centrifugation of cells was carried out using a Sigma 2-4 centrifuge (Philip

Harris). All centrifugation steps were performed at 250 g for 4 min unless otherwise stated.

Cell enumeration was performed using a Neubauer haemocytometer (VWR). Once cells were suspended in medium, 2 x 10 µL cell suspension were placed under each side of the coverslip. Cell counts were performed for the four individual 1 mm squares, from both sides of the haemocytometer. Counts were then averaged to give a mean cell count and multiplied by $10^4$ to obtain mean cell number per mL. Cell suspension was then diluted accordingly to give the desired cell seeding density.

### 2.7.2 Cell and Organ Culture Media

NHU cells were maintained in low-calcium [0.09 mM] Keratinocyte Serum-Free Media (KSFM; Gibco). Prior to use, KSFM was 'completed' (known as KSFMc) by the addition of bovine pituitary extract (BPE; 50 µg/ml; Gibco) and recombinant epidermal growth factor (rEGF; 5 ng/ml; Gibco) as recommended by the manufacturer. Cholera toxin (30 ng/ml) was also added in order to augment plating efficiency and suppress the growth of fibroblasts (Southgate et al., 1994).

Bladder cancer cell lines (EJ, RT112 and RT4; ATCC) and organ cultures were maintained in Dulbecco's Modified Eagle Medium (DMEM; Gibco) and Roswell Park Memoriam Institute 1640 medium (RPMI; Gibco) in a 1:1 ratio. The DMEM:RPMI medium was further supplemented with 5% (v/v) fetal bovine serum (FBS; Seralabs) and 1% (v/v) L-Glutamine (Sigma) was added before use due to its lability. Bladder cancer cell lines were also tested for *Mycoplasma spp.* infection (see section 2.7.7) and genotyped to ensure authenticity of the cell line.

Depending on cell type, cultures were incubated at different $CO_2$ concentrations in order to maintain optimum medium pH levels. Established bladder cancer cell lines were maintained in 10% $CO_2$ in air, whereas normal human urothelial (NHU) cells were maintained in 5 % $CO_2$.

### 2.7.3 Isolation of NHU Cells

Isolation and culturing of NHU cells was performed as previously described (Southgate et al., 1994).

Surgical samples of normal urothelium were placed in Petri-dishes containing Transport medium and aseptically dissected in order to remove excess tissue. Following this, samples were sectioned into approximately 1 $cm^2$ pieces and placed into a Universal tube containing Stripper medium (see Appendix). Samples in the Stripper medium were incubated at either 37 ºC for 4 h or at 4 ºC overnight in order to promote urothelial

separation from the underlying stroma. The tissue was then transferred into a Petri-dish and the urothelial sheet was physically separated using a pair of sterile forceps. Sheets were centrifuged for collection and then further disaggregated by re-suspension in 2 ml (400 U) collagenase type IV (see Appendix) at 37 ºC for 20 min, which disaggregates cells with minimum damage and primes them for primary culture. After another centrifugation step the cell pellet was re-suspended in KSFMc and seeded into Cell+™ tissue culture flasks (Sarstedt) at a minimum seeding density of 4 x $10^4$ cells/$cm^2$. This was the minimum seeding density used for all primary NHU cell culture experiments. KSFMc was removed and replenished twice a week in order to maintain primary cultures.

**2.7.4 Subculture of NHU Cells**

Once in culture, NHU cells adopt a non-differentiated proliferative phenotype and propagate as a monolayer (Southgate et al., 1994). Upon reaching approximately 95 % confluence, cultures were passaged in order to maintain proliferation and prevent contact-inhibited growth. All cultures were used for experiments between passage 2 and 6 to reduce any extraneous effects of long-term culture, which can induce culture senescence. When routinely passaged, cells were generally split in a 1:3 ratio. However, for experiments involving cadmium exposure cells were seeded at a density of 6 x $10^4$ cells/$cm^2$, the minimum density required for 'normal' proliferation (see Figure 21).

For routine passage, the culture medium was aspirated and replaced with 0.1 % (w/v) ethylenediaminetetra-acetic acid (EDTA) in phosphate-buffered saline (PBS; see Appendix). Cultures were then incubated at 37 ºC for approximately 5 min, until the cells began to 'round up' and dissociate from each other. EDTA was aspirated and depending on culture-ware size 0.5-1 mL Trypsin-Versene® (TV; see Appendix) was added, before incubation at 37 ºC for a further 1-2 min. At this point gentle tapping of the flask facilitated the detachment of cells, and trypsin activity was quickly inhibited by the addition of KSFMc containing 1.5 mg/mL of soybean trypsin inhibitor (TI; see Appendix). This TI step was omitted for cultures whose medium already contained serum, such as established cell lines (section 2.7.5). Cells were centrifuged at 250 g for 4 min to form a pellet, which was then flicked and re-suspended in KSFMc at the required seeding density before deposition onto either Cell+™ tissue culture flasks, Primaria™ 6-well plates (SLS) or ThinCert™ membranes (Greiner) as appropriate for the subsequent experiment. After subculture cells were left for 24 h to reattach and stabilise before any experimentation was started.

### 2.7.5 Subculture of Urothelial Cancer Cell Lines

Established bladder cancer cell lines were passaged using the same method as described above (2.7.4), with the omission of the TI step. Cells were seeded onto Cell+™ tissue culture flasks at different ratios depending on the cell line and sub-cultured when confluent (see Table 4).

***Table 4: Summary of the urothelial cancer cell lines used for this thesis.*** *The name of each urothelial cancer cell line is provided, as well as tissue of origin, grade of cancer and subculture ratio.*

| Cell Line | Tissue of Origin | Cancer Grade | Subculture Ratio |
|---|---|---|---|
| **EJ** | Human bladder carcinoma | 3 | 1:80 |
| **RT112** | Human bladder carcinoma | 2 | 1:40 |
| **RT4** | Human bladder papilloma | 1 | 1:10 |

### 2.7.6 Cryopreservation of NHU Cells

Cells were harvested from tissue culture flasks as described in section 2.7.4. However once cells were pelleted, instead of re-suspension in KSFMc they were re-suspended in Freezing mix at approximately 1 x $10^6$ cells/mL. Freezing mix consisted of the appropriate culture medium, 10 % (v/v) FBS and 10 % (v/v) dimethylsulphoxide (DMSO), and 1 mL of mix was used for each 25 $cm^2$ area of cells harvested. 1 mL cell suspension was transferred into a pre-labelled 2 mL cryovial (Starstedt), and the cryovial was placed into an isopropanol freezing bath (Nalgene) at -80 ºC overnight. This was to allow the cells' temperature to be gradually reduced to -80 ºC at a steady rate of -1 ºC per min. The following morning the vial was then transferred to a liquid nitrogen dewar for long-term storage.

For recovery of cells, vials were immediately placed into a 37 ºC water bath for rapid thawing. The Freezing mix was then aspirated and added to 9 mL pre-warmed KSFMc in a 30 mL Universal tube. Cells were then pelleted at 250 g for 4 min, re-suspended in 10 mL KSFMc and seeded onto a 75 $cm^2$ Cell+™ tissue culture flask for further culturing.

### 2.7.7 Cell Culture Screening for *Mycoplasma spp.* Infection

All cell cultures (NHU and cell line) were routinely checked for bacterial infection by *Mycoplasma spp.* using the DNA intercalating dye bisbenzimide (Hoescht 33258; Molecular Probes). Cell suspensions were seeded onto a Teflon™-coated 12-well multi-test slide (Hendley-Essex) at a volume of 50 µL per well and a density of approximately 5 x $10^4$ cells/mL. Cells were allowed to attach by incubating at 37 ºC for 3 h. At this point the slides were flooded with 5 mL appropriate medium (enough to cover the slide) and returned to the incubator overnight. The following morning medium was aspirated and the cells washed twice with PBS, before fixation for 30 secs by immersion in a 1:1 ratio of methanol and acetone (Fisher Scientific). Slides were then allowed to air-dry. Following this the cells were stained by Hoescht 33258 (1 µg/mL in PBS) by washing the slides and incubating on a Primix 7 orbital shaker (Jencons PLS) at ambient temperature for 5 min (slides were covered in foil during this incubation to exclude light). Cells were rinsed in $H_2O$ to remove Hoescht 33258 and mounted with antifade (see Appendices) before being left to dry. Cells were then viewed using an Olympus BX60 microscope (Olympus) using epifluorescent illumination to look for extra-nuclear DNA staining. Absence of ectopic staining indicated a negative result for infection.

### 2.7.8 Induction of NHU Cell Differentiation

Stimulation of NHU cells to terminally differentiate was performed using a previously developed method (Cross et al., 2005). Proliferating NHU cells were grown until approximately 95 % confluent, when KSFMc medium was aspirated and replaced with KSFMc supplemented with 5 % (v/v) adult bovine serum (ABS; Seralab). Cells were cultured for a further 5 days, passaged and seeded at 5 x $10^5$ cells/mL onto 12-well ThinCert™ (Greiner Bio-One) membranes with a 0.4 µm pore size. Cultures were maintained with 500 µL medium in the apical chamber and 2 mL in the basal chamber. 24 h after seeding, the exogenous calcium concentration was increased to 2 mM (near physiological) and cells cultured for a further 7-9 days, with medium changes every 2-3 days. This differentiation protocol is summarised in Figure 6.

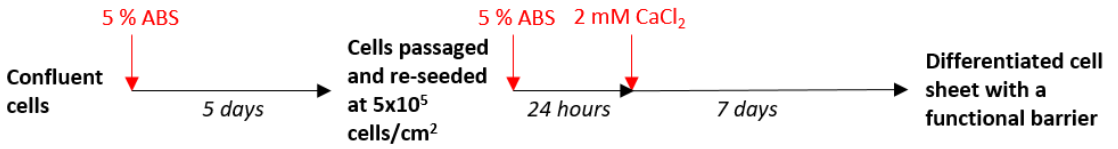


***Figure 6: Diagram demonstrating the biomimetic approach for differentiation of NHU cells.*** *Confluent NHU cells were cultured for 5 days in KSFMc + 5 % adult bovine serum (ABS). Cells were then passaged and seeded at a density of 5 x $10^5$ cells/$cm^2$ and further cultured in the presence of 5 % ABS for 24 hours. At this point the exogenous calcium concentration was increased to [2 mM] and cells cultured for a further 7 days, forming cell sheets. Differentiation was confirmed by the formation of a functional barrier which could generate transepithelial electrical resistance (see section 2.7.9 below).*

### 2.7.9 Transepithelial Resistance Readings

For measurement of transepithelial resistance (TER), which is indicative of barrier formation associated with urothelial differentiation, an EVOM™ epithelial voltohmmeter (World Precision Instruments) was used on cells previously seeded onto 12-well ThinCert™ membranes. Prior to use the electrode was placed in a Universal tube containing 10 mL activated Cidex Plus (see Appendix; World Precision Instruments) for 15min to allow sterilisation. The electrode was then washed once with appropriate culture medium (KSFMc supplemented with 5 % ABS and 2 mM $CaCl_2$) and placed into another Universal tube containing fresh medium in order to calibrate. To perform the TER reading, the electrode was slowly lowered into the well until the longer probe made contact with the bottom of the basal chamber, meaning the shorter probe stopped just above the membrane. The electrode was then held in place until a settled reading was obtained on the Voltohmeter. For each well 3 separate readings were taken and averaged in order to give the most accurate reading in kΩ/$cm^2$. A function barrier was considered to be a TER reading >0.5 kΩ/$cm^2$. When finished, the electrode was washed in sterile $H_2O$ and allowed to air-dry on blue roll.

### 2.7.10 AlamarBlue® Growth Assay

AlamarBlue® (Serotec) is an indicator dye used to infer cell viability, based on the assumption that metabolic activity proportionately reflects cell number. It relies on the oxidative reduction of the compound resazurin (the active ingredient of AlamarBlue®) by cells to the flurorescent molecule rezorufin. Viable cells constantly facilitate this conversion and therefore the amount of fluorescence can be used to quantitate change in cell biomass. Proliferating NHU cells were seeded at the required experimental density

onto a Primaria™ 96-well plate at a volume of 200 µL/well. For each experiment 6 technical repeats were included. The outside wells of the plate were filled with sterile water in order to prevent cultures from drying out. Once seeded, cells were left to adhere for 24 h before the addition of any treatments (day 0). On the day of treatment, medium change was performed and treatments added; no further medium change was conducted during the experiment. Absorbance readings were taken on days 1, 3, 5 and 7. On the day of each reading medium was removed from the cells and replaced by 200 µL AlamarBlue® diluted 1:10 with corresponding culture medium. Cells were left for 4 h to incubate with the solution. The 96-well plate was then transferred to a Multiskan Ascent 96/384 Plate Reader (Thermo Scientific) and the optical density of each well (NHU cells and no cell controls) measured at test (570 nm) and reference (630 nm) wavelengths. Absorbance was directly proportional to mitochondrial activity within cells, and was therefore taken to be directly proportional to cell number. Percentage reduction in AlamarBlue® was calculated using the following equation:

$$\left(\frac{(34798 \times NHU\ Cells570) - (80586 \times NHU\ Cells630)}{(155677 \times No\ Cells630) - (5494 \times No\ Cells570)}\right) \times 100$$

### 2.7.11 Organ Culture Sample Preparation

All preparation took place under aseptic conditions. Ureteric samples were removed from a universal container and placed into a Transport medium-containing Petri-dish using sterile forceps. Surgical scissors were used to strip excess fat from the sample so that only the ureter remained. Scissors were the n used to cut along one side of the sample, revealing the urothelium. Ureter pieces were dissected into approximately 1 $cm^2$ sections and kept in the Petri-dish in Transport medium until transfer to organ culture.

### 2.7.12 Organ Culture Constructs

Ureter pieces were placed urothelial side-up on cell culture inserts with 3 µM pore size (BD Falcon™) in a 6-well plate (Corning® Costar®). Samples were maintained in appropriate organ culture medium (described in 2.7.2) at a liquid:liquid interface, with 2 mL medium in the basal chamber and a small amount of medium just covering the surface of the urothelium in the insert (approximately 4-5 drops from a Pasteur pipette). Medium was changed every 2-3 days to remove waste and provide nutrients. For exposure, cadmium was added to both chambers to maintain the concentration, as there was no

urothelial barrier present to prevent diffusion of solutes through the membrane. A diagram summarising the organ culture method can be found in Figure 7.

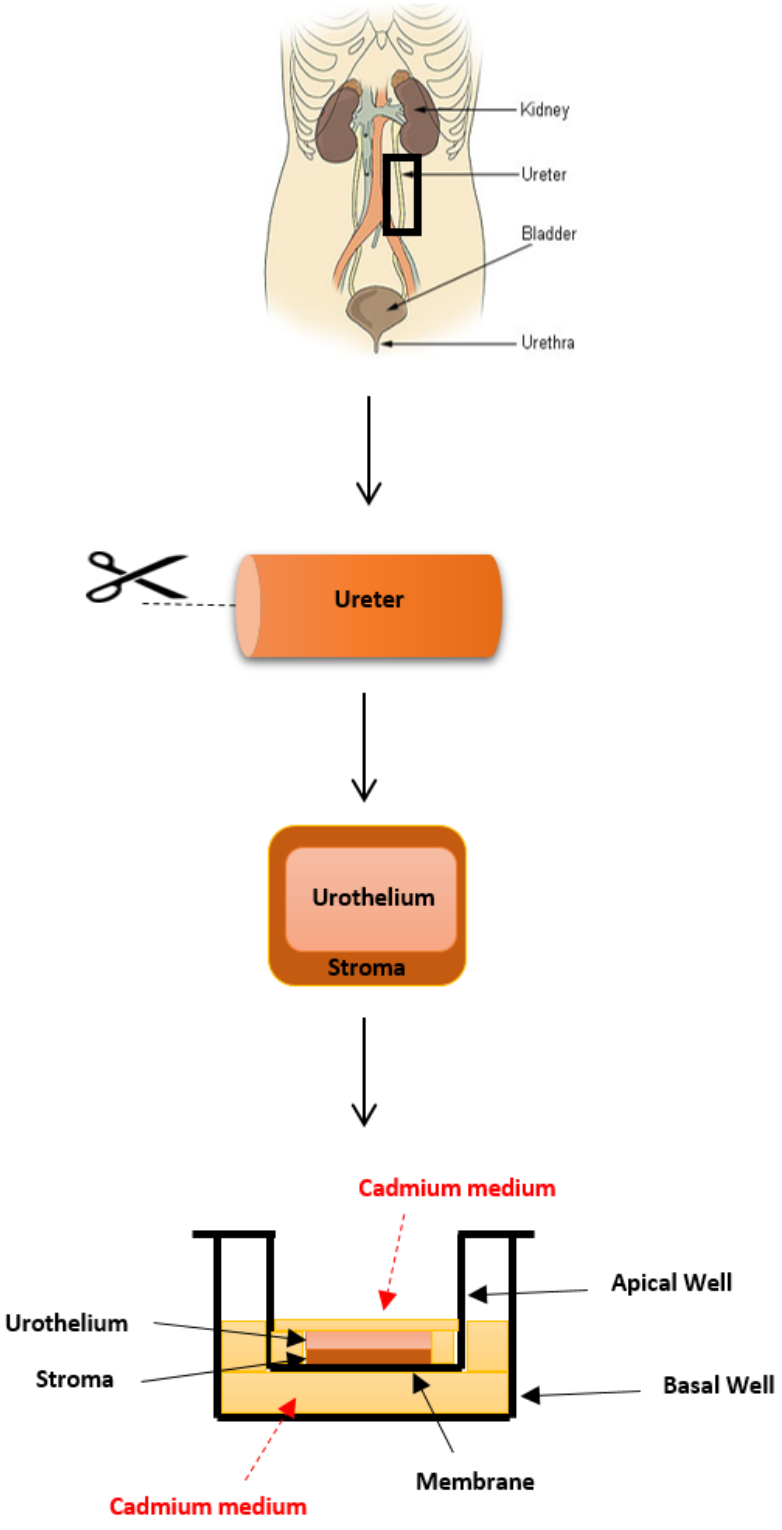


***Figure 7: Diagram summarising the method for cadmium-exposed ureter organ culture.*** *A small piece of healthy human ureter was cut open and laid flat to reveal the urothelium, which lies on top of stromal tissue. The ureter was placed urothelium-side up on a 3 µm pore-size membrane and cultured within a well. Both the apical and basal chambers were filled with medium supplemented with cadmium, with the apical medium just covering the surface of the*

*urothelium in order to maintain a liquid:liquid interface. For control conditions the same method applied but the medium did not contain cadmium.*

## 2.8 Histology

### 2.8.1 Embedding of Cultured NHU Cell Sheets

Differentiated NHU cell sheets that had been cultured on ThinCert™ membranes in wells were harvested intact for histological analysis. Medium was aspirated from cultures and the sheets were washed with pre-warmed (37 ºC) Dulbecco's phosphate-buffered saline (D-PBS) solution (Gibco). D-PBS was aspirated and 2 % (w/v) Dispase II (Sigma D-4693) added, as this is gentler than trypsin for cell disaggregation. 500 µL dispase was placed in the apical chamber and 2 mL in the basal chamber, and cultures were left to incubate at 37ºC for 30-45 min under frequent observation. When sheets began to lift the membrane was immediately placed in a Petri-dish containing pre-warmed D-PBS. A Pasteur pipette was then used in order to 'float' the cell sheet off the membrane and into a 'Cell Safe' histology cassette (CellPath) in the appropriate orientation. Cassettes were labelled, submerged in 10 % (v/v) formalin in PBS (see Appendix) for fixation and left for 24 h. After this time point cassettes were transferred into 70 % EtOH and stored until further processing.

To finish the embedding process, cassettes were transferred to fresh 70 % EtOH for 5 min. They were then submerged in absolute EtOH for 3x5 min, isopropanol for 2x5 min and finally in xylene for 4x5 min. Cassettes were then transferred to molten paraffin wax at 60ºC (Fisher Scientific) for 4 separate incubations of 15 min. Cell sheets were removed from cassettes using forceps and placed into a metal mould. Sheets were then orientated correctly, the mould filled with wax, and the blocks placed to set on a cold table (RA Lamb).

For sectioning, pre-cooled wax blocks were cut into 5 µm thick sections using a Leica RM2135 microtome (Leica Microsystems) and placed into a 37 ºC water bath. Sections were collected on electrostatically charged Superfrost Plus™ microscope slides (BDH), allowed to air-dry and then baked for 1 h on a hot plate (RA Lamb) before further processing.

### 2.8.2 Embedding of Tissue Samples

Tissue specimens were placed into 10 % (v/v) formalin in PBS for at least 24 h depending upon the size of the sample. Samples were then transferred to 70 % EtOH (v/v) until further processing.

Tissue samples were placed into a labelled 'Cell Safe' histology cassette and submerged in fresh 70 % (v/v) EtOH for 10 min. The cassettes were then submerged in absolute EtOH for 3x10 min washes on an orbital shaker. Following this, cassettes were submerged in isopropanol (Fisher Scientific) for 2x10 min washes, and further in xylene (Fisher Scientific) for 4x10 min washes; all of which took place inside an externally vented fume food. Samples were then placed sequentially in molten paraffin wax and embedded as described in section 2.8.1.

### 2.8.3 Haematoxylin and Eosin (H&E) Staining

H&E staining was used for histological analysis of embedded samples. Sections were de-waxed in xylene (Fisher Scientific) using 4 sequential submersions of 10 mins, 10 min, 1 min and 1 min duration. Sections were then re-hydrated in 3 sequential 1 min submersions in absolute EtOH, followed by a 1 min submersion in 70 % (v/v) EtOH and washing for 1 min in tap water. For staining, sections were then sequentially submerged in haematoxylin (see Appendix) for 2 min, running tap water for 1 min, Scott's tap water (see Appendix) for 1 min, running tap water for 1 minute, 1 % (w/v) Eosin (RA Lamb) for 30 secs and finally a 1 min wash in running tap water to remove any residual stain. Slides were de-hydrated by sequential submersions in 70% (v/v) EtOH (1 min), absolute EtOH (3x1 min) and xylene (2x1 min). Sections were then mounted using DPX fluid (CellPath) and sealed under cover slips (SLS).

### 2.8.4 Immunolabelling

To analyse protein expression in embedded tissue, immunohistochemical methods were used. Either an indirect streptavidin/biotin 'ABC' immunoperoxidase method or an amplified horseradish-peroxidase (HRP) polymer staining kit was used (see sections 2.8.7 and section 2.8.8 respectively) as appropriate for the protein of interest.

Details of antibodies used for immunolabelling are given in Table 12. Antibodies were kept at 4 °C, -20 ºC or -80 ºC according to suppliers' guidelines, with working stock solutions being kept at 4 ºC for up to 6 months. Working stocks were made up in either Tris-buffered saline pH 7.6 (TBS; see Appendix) or Tris-buffered saline supplemented with 0.1 % (v/v) Tween 20 (SLS) pH 7.6 (TBS-T; see Appendix) as appropriate for the immunolabelling method. Optimal antibody concentrations for each antibody were titrated using known negative and positive control tissues (Figure 8; see Table 13 for concentrations).

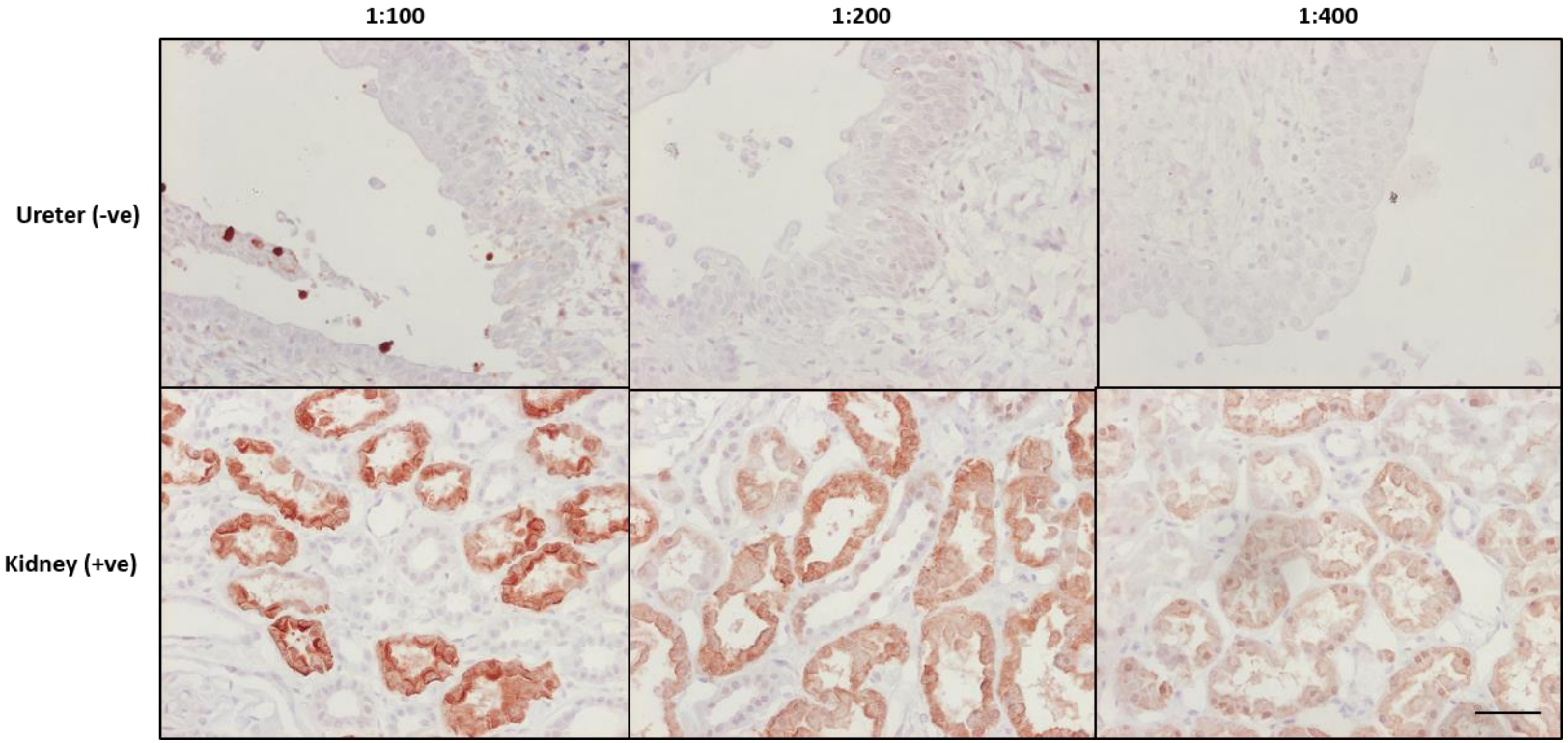


***Figure 8: Immunohistochemical labelling of ureter and kidney demonstrating MT-1/2 protein expression.*** *For all antibodies used a range of dilutions were tested in order to determine the optimal working concentration. In this example, the E9 primary antibody was tested at 1:100, 1:200 and 1:400 dilutions on tissues with negative (ureter) and positive (kidney) target protein expression. 1:400 was selected as the optimum dilution. Scale bar: 25 µm.*

For all IHC experiments conducted, a number of experimental controls were included (Figure 9). A secondary antibody-only control was used on the sample in order to detect any non-specific background labelling. An antibody known to work on the sample was included as a positive method control. Lastly, a sample of tissue known to express the target protein was used to ensure the proficiency of the test antibody.

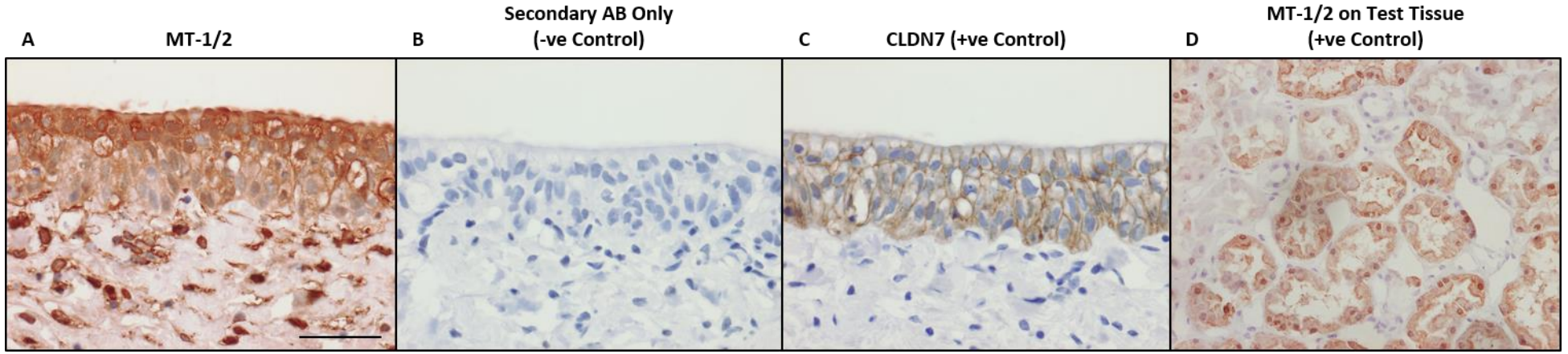


***Figure 9: Immunohistochemical labelling of ureter (Y1770) cultured in 10 µM $CdCl_2$ for 7 days.*** *For each IHC experiment a number of controls were included to ensure robustness of the primary result. (A) The primary antibody was used on the sample tissue. (B) A secondary antibody-only negative control was used to check for any non-specific background labelling, and (C) an antibody specific to a protein known to exist within the sample was used as a positive control to show that the method had worked. (D) Lastly, a sample known to express the target protein was included as an internal positive control in order to demonstrate the proficiency of the primary antibody. In this case, the control sample used was kidney tissue. Scale bar: 25 µm.*

### 2.8.5 Preparation of Sections and Endogenous Peroxidase Blocking

Samples were de-waxed and re-hydrated prior to immunolabelling as described in section 2.8.3. If samples contained vasculature and/or red blood cells endogenous peroxidase activity was blocked using 3 % (v/v) hydrogen peroxide (Fisher Scientific) for 10 min, followed by rinsing in running tap water for 10 min.

### 2.8.6 Antigen Retrieval

Antigenic sites can become masked during the tissue fixation process and can therefore be unable to bind antibodies (Arnold et al., 1996). To unmask antigens, thereby restoring antigen reactivity, a number of antigen retrieval methods were used:

a) Heat-induced epitope retrieval (HIER) in appropriate buffer. Samples were placed in a 900 W microwave at full power for 13 min (to boil for 10 min) in either 10 mM citric acid buffer pH 6 (see Appendix) or 1 mM EDTA pH 8 (see Appendices), using a Pyrex™ dish covered with perforated Clingfilm™. Dishes were then immediately placed on ice to accelerate the cooling down process.
b) Enzymatic digestion (trypsinisation). 0.1 g trypsin from porcine pancreas (Sigma) was added to 0.1 % (w/v) pre-warmed calcium chloride pH 7.8 (see Appendix) to make a 0.1 % (w/v) trypsin solution. Slides were incubated in this solution at 37 ºC for 10 min using a water bath.
c) HIER combined with enzymatic digestion. Slides were incubated in the 0.1 % (w/v) trypsin solution in calcium chloride pH 7.8 at 37 ºC for 1 min before microwaving in citric acid buffer as described in a).

After antigen retrieval, slides were rinsed in running tap water for 1 min. They were then placed in Shandon™ Sequenza™ cover-plates (Thermo Scientific) submersed in either TBS or TBST-T as appropriate for the immunolabelling method.

### 2.8.7 Immunolabelling using Streptavidin/Biotin 'ABC' Method

Endogenous avidin-binding sites were blocked using an avidin/biotin blocking kit (Vector). 100 µL avidin was added to each coverplate and incubated at ambient temperature for 10 min. Avidin was then removed by 2 washes with TBS and biotin applied to the slides. Slides were incubated at ambient temperature for 10 min, followed by 2 TBS washes. To minimise non-specific antibody binding, 100 µL 10% (v/v) serum (Dako) was incubated on the slides for 5 min. The serum used was dependent on the host of the secondary antibody; rabbit serum was used for rabbit secondary antibodies, and goat serum used for goat secondary antibodies. After blocking, 100 µL primary antibody was added at a pre-determined optimal dilution in TBS and slides were incubated at 4ºC

for 16 h. Negative control samples had an irrelevant antibody or did not have any primary antibody applied.

After incubation, unbound primary antibody was removed by 3 washes with TBS. 100 µL biotinylated secondary antibody (Dako) at a pre-determined dilution in TBS was incubated on the slides for 30 min at ambient temperature Unbound secondary antibody was removed by 2 TBS washes. A streptavidin-biotin-horseradish peroxidase (Strep-HRP/ABC) complex (Vectastain Elite ABC Kit; Vector) was prepared according to the manufacturer's instructions and 100 µL added to the slides for incubation at ambient temperature for 30 min. Slides were then washed twice with TBS and once with $H_2O$. To visualise the antibody-bound complex a diaminobenzidine (DAB) substrate reaction was used. Sigma Fast™ DAB tablets were added to 5 mL $H_2O$ following the manufacturer's instructions and the freshly-made solution added to the slides at a volume of 200 µL per slide. DAB solution was incubated on the slides for 12 min before removal with 2 $H_2O$ washes. Slides were counterstained in Haematoxylin for 5 secs, washed in tap water for at least 1 min and dehydrated/mounted as described in section 2.8.3.

### 2.8.8 Immunoballeing using Polymer-Based Horseradish-Peroxidase (HRP) Amplification Method

This method was used in order to improve the sensitivity of antibody labelling detection. The kit used was an Impress™ Excel staining kit (Vector) which is based on an enzymatic, non-biotin amplification system. The kit comes with ready-to-use affinity-purified and cross-adsorbed reagents including an amplifier antibody and polymer reagent.

After placing slides in cover-plates submersed in TBS-T, 100 µL 2.5 % (v/v) normal horse serum was applied to block any non-specific background labelling. Serum was incubated at ambient temperature on the slides for 20 min. 100 µL primary antibody diluted in TBS-T was applied and incubated at 4 ºC for 16 h. Unbound antibody was removed by 3 washes with TBS-T and 100 µL secondary amplifier antibody incubated on the slides for 30 min at ambient temperature. Secondary amplifier was either directed against mouse or rabbit depending on the primary antibody used. Unbound amplifier antibody was removed by 2 TBS-T washes and 100 µL Impress™ Excell anti-IgG reagent incubated on the slides for 30 min at ambient temperature. Slides were washed twice with TBS-T and once with $H_2O$ before the addition of the ImmPACT™ DAB EqV reagent, which was used to visualise the bound antibody via the same reaction described above (section 2.8.7). DAB reagent was incubated for 5 min at ambient temperature and then

the slides were immediately washed once with $H_2O$ before being transferred to a metal rack and further rinsed in tap water. Slides were then counter-stained and mounted as described previously (section 2.8.3).

## 2.9 Microscopy

An Olympus BX60 microscope was used to view slides under bright-field illumination, using x20, x40 and x60 oil immersion objectives. Images were captured using an Olympus DP50 digital camera and Image-Pro Plus™ software version 4.5.1.29 (Media Cybernetics).

## 2.10 Gene Expression Analysis

All RNA work was carried out in a designated area of the lab, separate from polymerase chain reaction (PCR) work. The work area was cleaned by regular wiping with 70 % (v/v) EtOH, as well as RNase*Zap*® wipes (Fisher Scientific) which were used to remove any RNase enzymes on the bench, pipettes and tip boxes. Fresh gloves were worn and regularly changed and cleaned with the wipes throughout the protocols, as a measure to maintain sample RNA integrity and minimise the risk of RNase and/or genomic DNA contamination. Single use DNase and RNase-free 1.5 mL microfuge tubes (Ambion) and filter pipette tips (Starlab, Starstedt) were used to minimise contamination. All water used for gene expression analysis had been treated with 0.1 % (v/v) diethylpyrocarbonate (DEPC) to inactivate RNase enzymes, and then autoclaved.

### 2.10.1 RNA Extraction

All RNA extractions were carried out using Trizol™ reagent (Invitrogen) based on the single-step method of RNA extraction by acid guanidinium thiocyanate-phenol-chloroform (Chomczynski and Sacchi, 1987). Medium was aspirated from cell cultures and 1 mL Trizol™ reagent added. Cultures were incubated at ambient temperature for 5 min on an orbital shaker. Cells were then scrape-harvested (cell scrapers; Starstedt) into 1.5 ml microfuge tubes, labelled and stored at -80 ºC until further processing.

Samples were thawed on ice and then left at ambient temperature for 5 min to permit complete dissociation of nucleoprotein complexes. 200 µL chloroform (Fisher Scientific) was added to each tube, each of which were vortexed for 15 seconds and then left to incubate at ambient temperature for 2 min. Tubes were then placed in a Hettich Mikro 200R refrigerating benchtop centrifuge (Hettich) and centrifuged at 12000 g for 15 min at 4 ºC. Following centrifugation, the RNA-containing aqueous supernatant was collected into fresh 1.5 ml microfuge tubes. 0.5 mL isopropanol (Fisher Scientific) was added to each tube, mixed by multiple inversions, and incubated at ambient temperature for 10

min. Tubes were then centrifuged at 12000 g for 20 min at 4 ºC. Following this, the supernatant was quickly removed by blotting onto blue roll. Two cycles of washing were carried out by adding 1 mL 75 % (v/v) EtOH, vortexing, centrifuging at 4 ºC for 5 min at 7500 g and removing the supernatant by blotting. The resulting RNA pellets were left to air-dry for approximately 15 min, re-suspended in 30 mL DEPC-treated water and then transferred to a 0.5 mL microfuge tube.

To remove any DNase contamination all samples were treated with a DNA-free™ kit (Ambion) following the manufacturer's recommendations. DNase 1 buffer was added at a dilution of 1:10 to each tube, along with 1 µL of the enzyme rDNase 1, and incubated at 37 ºC for 30 min. DNase inactivation reagent was thawed, re-suspended by vortexing and added to tubes at a dilution of 1:10. The tubes were incubated at ambient temperature for 2 min, and vortexed every 30 seconds. Following this tubes were centrifuged at 10000 g for 1 min 30 seconds at ambient temperature and the supernatant collected into a fresh 0.5 mL microfuge tube. RNaseOUT™ (Invitrogen) was added at a concentration of 40 U/30 µL and samples stored at -80 ºC.

**2.10.2 cDNA Synthesis**

Prior to cDNA synthesis, RNA concentration and quality was measured using a NanoDrop® ND-1000 spectrophotometer (Fisher Scientific). cDNA first strand synthesis was performed using the Superscript™ II first strand synthesis system (Invitrogen) following manufacturers' protocol. 1 µg RNA was added to two separate microfuge tubes for each sample; 1 tube for reverse transcriptase positive (RT +ve) and 1 tube for reverse transcriptase (RT -ve) reactions. 50 ng/µL random hexamers was added to each tube and incubated at 65 ºC for 10 min to anneal primers. Tubes were then cooled at 4ºC for 1 min and the contents collected by brief centrifugation. A master mix was prepared on ice so that each sample received 4 µL 5x First strand buffer, 2 µL 0.1 M DTT and 1 µL dNTPs (10 mM). Samples were then incubated at 25 ºC for 2 min. 1 µL (50 U) of the Superscript II reverse transcriptase enzyme was mixed into each RT+ tube but omitted from the RT- tubes. All samples were then incubated at 25 ºC for 10 min, 42ºC for 50 min, and finally 70 ºC for 15 min to inactivate the enzyme. cDNA was stored at -20 ºC in the short-term and transferred to -80 ºC for long-term storage. Prior to use, RT +ve and RT -ve samples were assessed for transcript expression of the housekeeping gene GAPDH. This was to confirm equal quantities of cDNA in the samples, and to ensure the absence of DNA contamination (see Figure 10).

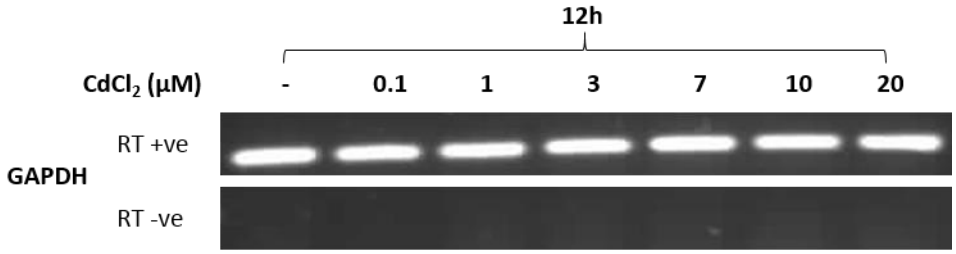


***Figure 10: RT-PCR demonstrating the reverse transcriptase-negative and reverse transcriptase positive-controls used for every RT-PCR experiment.*** *For every sample, two reactions were set up; one containing reverse transcriptase (RT +ve), one without (RT -ve). Once cDNA was synthesised, all samples were checked for the housekeeping gene GAPDH transcript expression in order to ensure equal cDNA/loading quantities (RT+ve) and to confirm the absence of genomic contamination (RT-ve).*

### 2.10.3 Primer Design

For each gene, all transcript information was downloaded from the EMBL™ genome browser (http://www.ensembl.org/index.html). Primers were designed to detect all splice variants of a gene and were checked for specificity using the NCBI Primer-BLAST tool (http://www.ncbi.nlm.nih.gov/tools/primer-blast/). All primers were produced by Eurofins, reconstituted to 100 mM concentration in DEPC-treated water and stored at -20 ºC.

All primers were optimised for use prior to performing reverse-transcriptase polymerase chain reaction (RT-PCR). Optimisation involved a series of gradient PCR reactions at increasing annealing temperatures, using genomic DNA as a positive control (Promega). The optimal annealing temperature was selected as the temperature that gave the brightest singular band at the correct product size (Figure 11; see Table 11 for primer information).

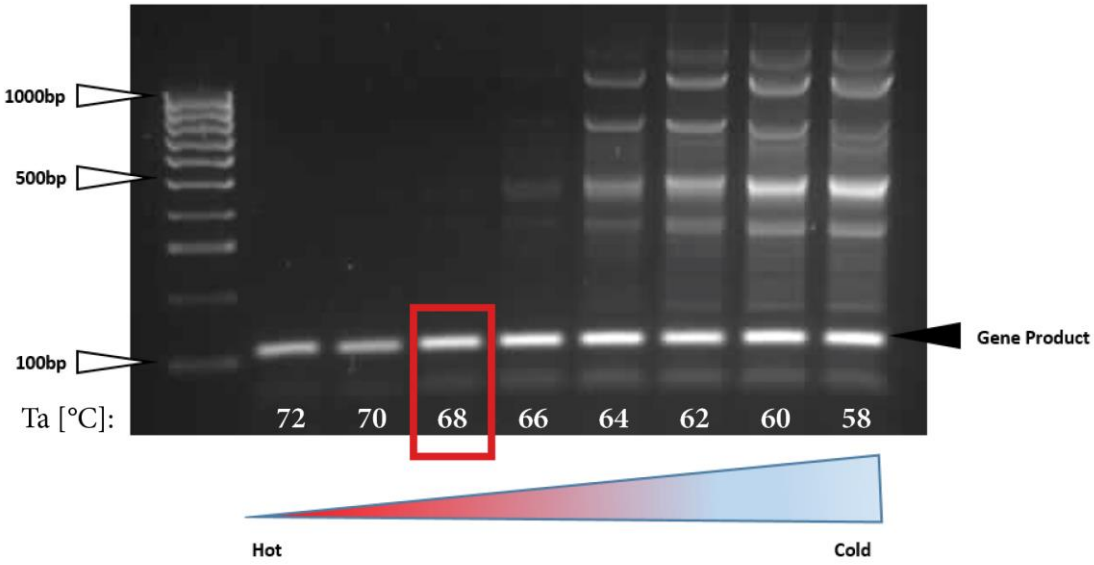


***Figure 11: Gradient RT-PCR was conducted to determine optimal primer annealing temperature.*** *Each primer set was tested by performing RT-PCR over a range of temperatures using gDNA. The temperature demonstrating the brightest product band of the correct size with the least non-specific binding was deemed optimal and used in subsequent RT-PCRs. The above example of gradient PCR was performed using primers for MTF-1 transcript, which had a product size of 108 base pairs. The optimal primer annealing temperature (Ta) was selected as 68 °C (demonstrated by the red rectangle).*

### 2.10.4 RT-PCR

All PCR reactions were carried out in a T100 thermal cycler (Bio-Rad). For each target gene a master mix was made up so that each 20 µL sample reaction received 8.5 µL DEPC-treated water, 4 µL GoTaq buffer (Promega), 0.4 µL dNTPs (10mM; Invitrogen), 2 µL $MgCl_2$ (25mM; Promega), 2 µL forward primer, 2 µL reverse primer and 0.1 µL GoTaq polymerase (Promega). 1 µg/µL cDNA was added for each sample bringing the total volume up to 20 µL for each reaction. Genomic DNA was used as a positive control and a no-template negative DEPC-treated water ($dH_2O$) control was also included (see Figure 12).

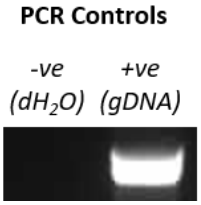


***Figure 12: RT-PCR showing experimental controls included for every reaction.*** *Negative controls ($dH_2O$) were used to check for contamination, whereas positive controls (gDNA) were used to determine whether the reaction had been successful.*

cDNA was initially denatured for 2 min at 95 ºC in the first cycle, changing to denaturation at 95 ºC for 30 seconds in subsequent cycles. After denaturation primers were annealed at a pre-determined optimum temperature for 30 seconds, followed by extension of template at 72 ºC for the required amount of time based on overall product size (30 seconds per 500 base pairs). A final cycle extension phase at 72 ºC for 5 min completed the reaction before cooling to 4 ºC. For each reaction 25 PCR cycles were performed.

**2.10.5 Gel Electrophoresis**

PCR products were visualised using gel electrophoresis and ultra-violet illumination. 2% flatbed gels were made using electrophoresis-grade agarose (Invitrogen) which was added to 1x Tris borate EDTA (TBE; see Appendix). The mixture was heated in a microwave for up to 3 min until the agarose had completely dissolved. The liquid was allowed to cool to approximately 60 ºC before the addition of SYBR® Safe DNA gel stain (Invitrogen) at a dilution of 1:10000. The molten gel was poured into a plastic gel case and allowed to set before being placed into an electrophoresis tank containing 1x TBE buffer.

18 µL from each PCR reaction was added to each well in order to ensure equal loading, and the gel run at 100 V until clear resolution of the DNA marker was achieved (approximately 1 h 30 min). The DNA marker used to track progress of the PCR products was HyperLadder™ 100bp (Bioline). Product bands were visualised using a Gene Genius Gel Imaging System (Syngene) and images captured using Genesnap software (Syngene).

## 2.11 Western Blotting

### 2.11.1 Harvesting of Whole Cell Lysates

Whole cell lysates were harvested from Cell+™ tissue culture flasks, Primaria™ 6-well plates or ThinCert™ membranes. The same protocol was used for all tissue culture-ware, however the amount of lysis buffer varied to account for overall cell number.

Medium was aspirated from cultures and cells washed twice with pre-chilled PBS. 2x sodium dodecyl sulphate (SDS; see Appendix) lysis buffer was 'completed' shortly before use by the addition of 13 mM DTT and 1:100 dilution Protease Inhibitor Cocktail (catalogue #P8340; Sigma Aldrich). 75 µL, 50 µL and 30 µL lysis buffer was added to T75 Cell+™ tissue culture flasks, T25 Cell+™ tissue culture flasks/Primaria™ 6-well plates and ThinCert™ membranes respectively. A cell scraper was used to scrape-harvest cells and lysates were transferred to pre-chilled 1.5 mL microfuge tubes. Lysates were sonicated on ice for 2x 10 sec bursts with a 10 sec rest in between. A Sonifier® (Branson) was used, set to 25 W and 40 % amplitude. Lysates were then left to rest on ice for 30 min, before centrifugation at 18000g for 30 min at 4 ºC. Supernatant was collected and placed in pre-chilled 0.5 mL microfuge tubes, and stored at -20 ºC.

### 2.11.2 Protein Determination of Lysates

A Coomassie protein assay reagent kit (Pierce) was used in order to determine the protein concentration of sample lysates. A 7-point protein standard was added in 10 µL duplicates to the wells of a 96-well plate (SLS) covering a range from 0-1 mg/mL, by dilution of bovine serum albumin (BSA) in $H_2O$. Lysate samples were diluted 1:12.5 in $H_2O$ and also added in 10 µL duplicates to the plate. 200 µL Coomassie reagent (pre-warmed to ambient temperature) was added to each of the wells and absorbance read at test (570 nm) and reference (630 nm) wavelengths using a MRX II 96-well plate spectrophotomer (Dynex). A standard curve was produced using the Revelation™ software (Dynex) and the average absorbance of each duplicate sample was used to estimate protein concentration, correcting for the dilution factor.

### 2.11.3 Sodium Dodecyl Sulphate-Polyacrylamide Gel Electrophoresis (SDS-PAGE)

20 µg protein samples (diluted with $H_2O$) were mixed with 10x NuPage™ reducing agent (Invitrogen) and 4x NuPage™ lithium dodecyl sulphate (LDS; Invitrogen) to a final reagent concentration of 1x. Samples were then heated for 10 min at 70 ºC and briefly centrifuged to collect contents.

Pre-cast 10- or 15-well 4-12 % Bis-Tris NuPage™ polyacrylamide gels (Invitrogen) were used for separation of proteins. Gels were placed in an XCell SureLock™

(Invitrogen) tank, with both outer and inner tank chambers filled with appropriate 1x running buffer depending on target protein size. 3-(N-morpholino) propanesulfonic acid (MOPS) buffer was used for separation of larger proteins, and its structural analogue 2-(N-morphilino) ethanesulfonic acid (MES) was used for smaller proteins (<10 kDa; buffers purchased ready-made from Life Technologies). 5 µL All-Blue Protein Precision Plus™ ladder (Bio-Rad) was loaded in the first well as a protein size reference (Figure 13), and samples were loaded in the rest of the wells. Empty wells were loaded with the same amount of LDS as used for samples in order to ensure equal running. 200 µL NuPage™ antioxidant (Invitrogen) was added to the inner tank chamber to maintain the reduced proteins, and electrophoresis was performed at 200 V until the blue dye-front reached the foot of the gel (approximately 1 h).

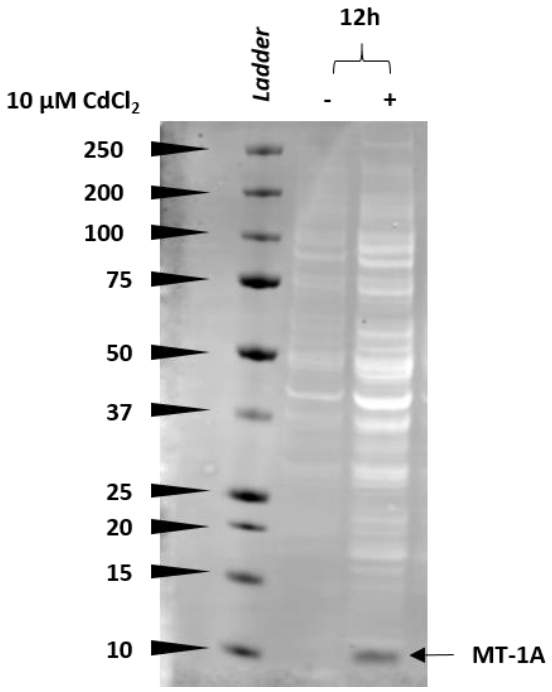


***Figure 13: Western blot showing MT-1A protein expression in proliferating NHU cells (Y1270) exposed to 10 µM $CdCl_2$ for 12 hours.*** *For each Western blot performed a molecular weight ladder was included to determine whether the detected protein was at the same weight as the target protein's estimated weight. Molecular weights are in kilodaltons (kDa). In this example, the predicted weight of MT-1A is ~6 kDa, and a protein band was detected at the correct estimated molecular weight.*

### 2.11.4 Electrophoretic Protein Transfer

Proteins were transferred from gels onto polyvinylfluoride (PVDF) membranes (Millipore) using the XCell II™ Blot Module (Invitrogen) following the manufacturer's recommendations.

PVDF membrane was cut to an appropriate size and activated by dipping in methanol (Fisher Scientific) before washing in $H_2O$. Prior to assembly E-PAGE™ blotting pads (Life Sciences), Whatman™ filter paper (cut to size) and PVDF membrane (cut to size) were all equilibrated in transfer buffer (see Appendix) for approximately 30 min. A gel membrane sandwich was then created in the order (from bottom to top); 2x blotting pads, filter paper, gel, PVDF membrane, filter paper, 3x blotting pads. The sandwich was placed in the blotting module and the inner chamber filled with transfer buffer, whereas the outside chamber was filled with tap water as a temperature buffer. The module was placed in an ice box and proteins were electrotransferred at 30 V for 3 h.

To confirm successful transfer, the retrieved membrane was stained with 5 mg/mL Ponceau red in 1% (v/v) glacial acetic acid in $H_2O$ for a few seconds before washing in $H_2O$ until resolution of protein bands.

### 2.11.5 Antibody Labelling

Before probing with antibodies, membranes were incubated for 1 h at ambient temperature on a shaker with 10 mL TBS (see Appendix) and Odyssey blocking buffer (LI-COR®) in a 1:1 ratio. This is an optimised buffer for the LI-COR® system which reduces background fluorescence. After blocking, membranes were incubated with 5-8 mL primary antibody at a pre-determined optimal dilution (Figure 14; see Table 12 for antibody concentrations) in a 1:1 mix of blocking buffer and TBS supplemented with 0.1 % (w/v) Tween 20 (TBST; see Appendix) for 1 h at ambient temperature or 16 h at 4ºC on an orbital shaker.

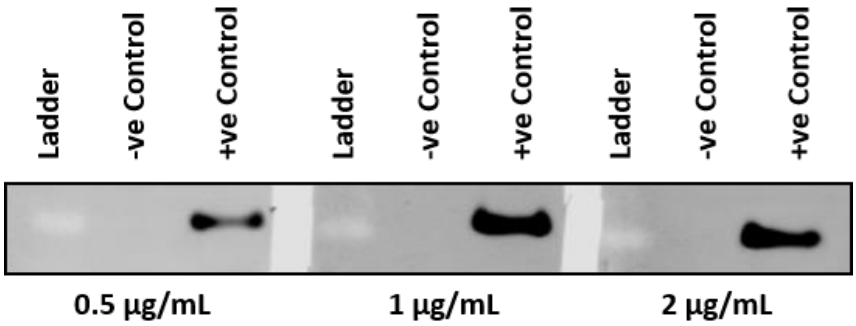


***Figure 14: Western blot demonstrating MT-1A protein expression in proliferating NHU cells (Y1531) exposed to 10 µM $CdCl_2$ for 72h.*** *For each antibody used for western blotting, a series of dilutions were tested on positive and negative controls in order to determine the optimal concentration. In this example, the negative samples were NHU cells grown in normal conditions, whereas the positive samples were NHU cells exposed to $CdCl_2$. The MT-1A antibody was tested at 3 different concentrations; 0.5 µg/mL, 1 µg/mL and 2 µg/mL. 1 µg/mL was selected as the best working concentration.*

To remove unbound primary antibody membranes were washed 4x5 min in TBST on an orbital shaker. Secondary antibody was diluted 1:10000 in 1:1 blocking buffer and TBST and incubated with the membrane in the dark for 1 h at ambient temperature on a shaker. Either an Alexa Fluor® 680-conjugated anti-mouse secondary antibody (Invitrogen) or an IRDye 800-conjugated anti-rabbit secondary antibody (Tebu-Bio) was used depending on the primary host species. To remove unbound secondary antibody, membranes were washed 4x5 min in blocking buffer/TBST solution on a shaker. Finally, membranes were rinsed once with TBS to remove residual TBST and stored in TBS at 4 ºC.

### 2.11.6 Membrane Imaging and Analysis

Western blot membranes were scanned using an Odyssey® Sa Infrared Imaging System (LI-COR®), with laser excitation and emission wavelengths as appropriate for the fluorophores used. Images were captured and analysed using Odyssey® Image Studio™ software v5.0 (LI-COR®). A positive control where the target protein was known to be expressed was included for every western blot performed, in order to ensure successful completion of the protocol (see Figure 15).

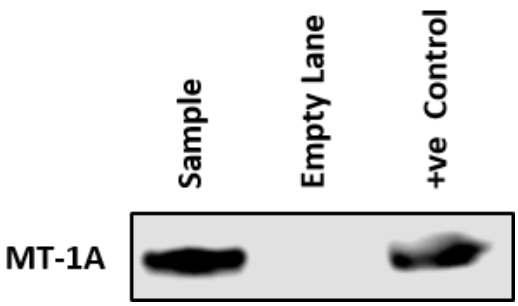


***Figure 15: Western blot showing MT-1A protein expression in proliferating NHU cells (Y1426) exposed to 10 µM $CdCl_2$ for 72h.*** *For all western blots conducted a positive (+ve) control was included, which was a sample known to have high expression of the target protein. In this case, the sample was from a different cell line chronically exposed to $CdCl_2$ which had previously demonstrated high MT-1A protein expression.*

Rectangular bands were auto-drawn by the software around the correct-sized protein bands for each lane. An additional, same-sized rectangle was placed randomly on the membrane where no bands were present and defined as the background. This allowed the relative intensities of each band to be measured. Densitometry was performed by measuring band intensity for β-actin as a loading control on the same membrane (see Figure 16), and normalising protein loading in each lane to obtain accurate protein quantification.

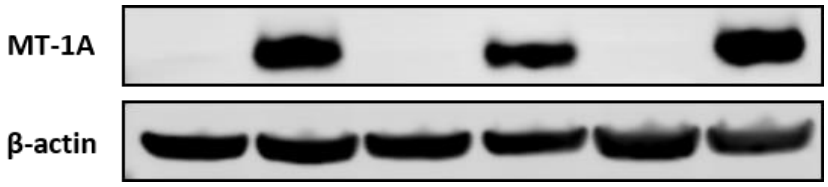


***Figure 16: Western blot demonstrating use of the housekeeper β-actin protein expression as a loading control.*** *Equal β-actin bands indicate accurate and equal protein sample loading into the gel. β-actin protein expression was included in every western blot performed.*

### 2.11.7 Stripping of Membranes for Re-use

Membranes occasionally needed to be stripped before they could be probed with another antibody (e.g. if proteins of interest were of a similar molecular weight). Membranes were stripped by incubation with antibody stripping solution (Western Blot Recycling Kit; Source Bioscience Autogen) diluted 1:10 with $H_2O$, for 30 min at ambient temperature on a shaker. Membranes were washed once with TBS and then re-scanned to ensure

stripping had been successful. Membranes were then re-blocked and re-probed as described in section 2.11.5.

## 2.12 Direct Intracellular Metal Quantification

Intracellular metal quantification was carried out using acid-digested biological samples and the spectroscopic technique inductively coupled plasma-optical emission spectroscopy (ICP-OES). This involves plasma excitation of samples, and the resulting emission of light wavelengths can be used to determine what trace metals are present in the sample and their concentration.

### 2.12.1 Digestion of Samples

NHU cells were seeded onto Primaria™ 6-well plates and stimulated to differentiate for 7 days using serum and calcium (as described in section 2.7.8). Once differentiation was confirmed by the formation of a functional barrier, cultures were treated with 10 µM $CdCl_2$ for a further 7 days. At this point medium was aspirated and cells washed 3 times with PBS to remove any non-cellular metal. Concentrated nitric acid (Sigma) was sub-boiled to 60 ºC using a water bath and 500 µL added to each well. Cells were incubated in acid at ambient temperature for 90 min to allow complete digestion of organic material. 400 µL of the digested cell solution was taken from each well and 2 wells for each condition (control and $CdCl_2$ exposure) were pooled together, resulting in a total of 800 µL acid per sample. This was diluted to 16 mL with $H_2O$ to form 5 % (v/v) nitric acid in water and stored in Corning® 50 mL centrifuge tubes at 4 ºC until analysis. All work involving nitric acid was performed in a fume hood and safety glasses were worn at all times.

### 2.12.2 Inductively-Coupled Plasma – Optical Emission Spectroscopy (ICP-OES)

A range of $CdCl_2$ standards was made up prior to running samples on the ICP-OES machine (iCAP 7000 Plus Series; Thermo Scientific). Standards consisted of $CdCl_2$ concentrations from 0 – 1 mG/L made up in $H_2O$ with 5 % (v/v) nitric acid, and were stored in Corning® 50 mL centrifuge tubes (required volumetric container for machine sampling). These standards and certified reference material were used in order to calibrate the machine. Accurate calibration was confirmed by a linear relationship between standard (predicted) and actual measurements (Figure 17). After calibration, samples were run on the machine and cadmium concentration of the digested cell solution calculated (taking into account the initial sample dilution). 2 technical repeats were included for each sample to ensure machine accuracy.

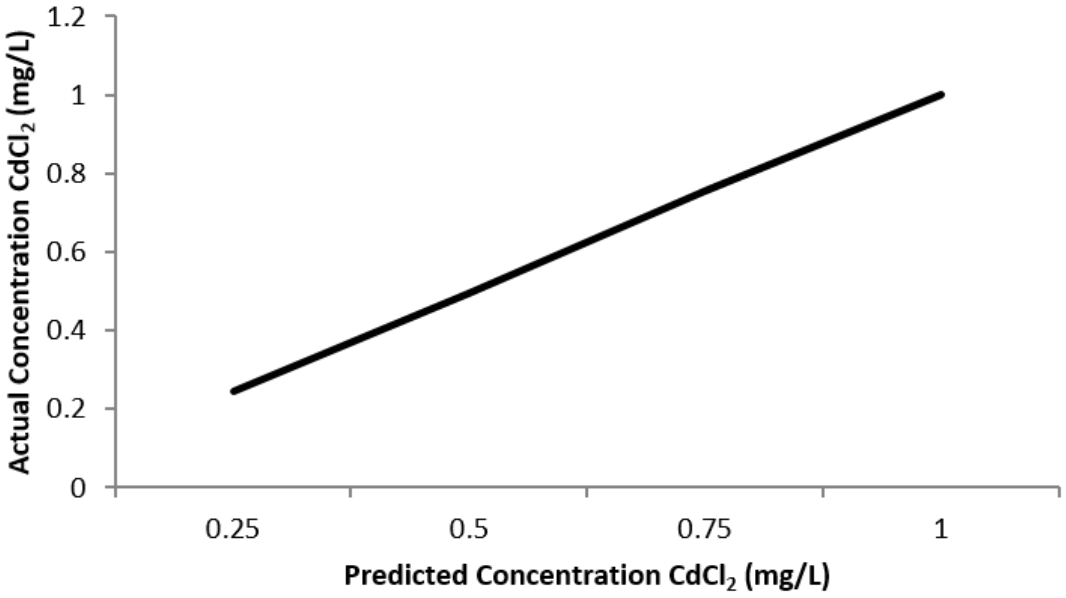


***Figure 17: Graph demonstrating the linearity of the range of standards used to calibrate the ICP-OES equipment.*** *When carrying out the ICP-OES procedure a known range of concentrations are input in order to calibrate the machine. The relationship between the standard (predicted) and actual concentrations should be linear in order to ensure the accuracy of readings, as demonstrated above.*

Once the acid-digested samples were entered into the ICP-OES machine they were combined with argon within a nebuliser, resulting in aeration of the sample. The sample was then passed to a spray chamber where a plasma torch excited the atoms and ions, producing specific wavelengths of light which were recorded by a receiver. This information was then used to determine which elements were present within the sample, and in what concentrations. Acid-washed equipment and wash buffers were utilised in order to avoid contamination. A summary of the ICP-OES workflow is provided in Figure 18.

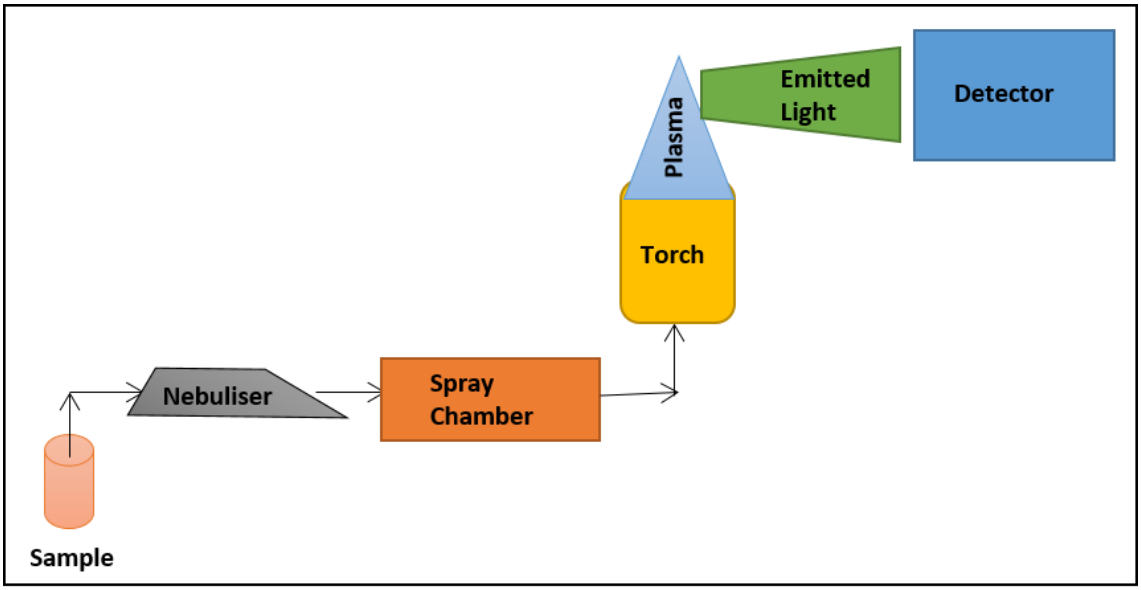


***Figure 18: Schematic diagram summarising the process of Inductively Coupled Plasma-Optical Emission Spectroscopy (ICP-OES).*** *Biological samples entered the machine and were combined with argon within the nebuliser, resulting in aeration of the sample. The sample then travelled through the spray chamber and encountered a plasma torch, whose function was to excite the atoms and ions of the sample. This resulted in wavelengths of light being emitted which were received and recorded by the detector. The specific wavelengths of light were used to determine precisely which elements were present in the sample and their resultant quantities.*

# Chapter 3: Characterisation of Control and Cadmium-Induced Metallothionein Isoform Expression in Normal Human Urothelium

## 3.1 Chapter Aims

The aim of this chapter was to characterise MT isoform expression in NHU cells under basal and cadmium-exposed culture conditions. Additionally, the use of novel MT isoform-specific antibodies was performed in order to discriminate between isoform expression at the protein level.

### 3.1.1 Objectives

1. Determine a human-relevant, non-cytotoxic cadmium concentration suitable for NHU cell culture.
2. Assess baseline MT isoform transcript expression in a variety of human urothelial cell culture models, including proliferating NHU cells, differentiated NHU cells and urothelial cancer cell lines.
3. Identify which, if any, MT isoform transcripts are induced in proliferating NHU cells exposed to cadmium and characterise this induction in relation to exposure time and cadmium concentration.
4. Determine whether MT protein is induced in proliferating NHU cells exposed to cadmium using novel isoform-specific antibodies, and characterise expression of the same using immunohistochemistry to determine protein localisation and expression patterns.

### 3.1.2 Experimental Approach

1. Growth assays were performed using proliferating NHU cells either cultured under control conditions or exposed to a range of cadmium concentrations, so that toxicant cytotoxicity could be assessed. The range of $CdCl_2$ concentrations selected was based on previous experiments in our laboratory, relevance to human exposure, and cell culture concentrations previously used in the literature (Chu et al., 1999; Takiguchi et al., 2003; Sens et al., 2004; Aimola et al., 2012; Fabbri et al., 2012; Mehus et al., 2014; Zhou et al., 2012). An intermediate cadmium concentration of 10 µM (Luevano and Damodaran, 2014) was selected for further experiments, as this concentration had previously been suggested to most closely reflect *in vivo* human exposure (Aimola et

al., 2012) and had also been shown malignantly cellular transform the human prostate epithelial cell line RWPE-1 (Achanzar et al., 2001). Further growth assays were then performed using this specific concentration, with the aim of establishing whether altering NHU cell seeding density could facilitate comparable cell growth in control and cadmium-exposed cells.

2. Before investigating MT isoform transcript induction by cadmium exposure it was important to determine baseline expression of their expression, as the literature had reported tissue-specific expression patterns (section 1.5.5.2; Jahroudi et al., 1990; Conway et al., 2010; Capdevila et al., 2012). Firstly, Next Generation Sequencing (NGS) data previously produced in the laboratory was mined for MT isoform expression using HT-seq gene analysis (Anders et al., 2015). NGS data was available for passage (P) 0 NHU cells (i.e. freshly isolated NHU cells that had not yet been passaged *in vitro*), proliferating (PRO) and differentiated (DIF) NHU cells. MT isoform transcript expression was normalised using housekeeping gene GAPDH transcription. Next, MT isoform transcript expression was assessed in proliferating and differentiated NHU cells grown *in vitro*, as well as three different urothelial cancer cell lines, using RT-PCR. Proliferating NHU cells and urothelial cancer cell lines were passaged prior to the experiment in order to maintain proliferation and then left to settle for 24 hours, before RNA was extracted at 12, 24 and 48 hour time-points. Separate cultures of proliferating NHU cells were stimulated to differentiate using a biomimetic method (see section 2.7.8) prior to the experiment, and differentiation was confirmed by expression of the differentiation-associated marker ZO-1 (see section 8.7.1). Once differentiated, NHU cells were maintained in culture and RNA extracted at the same time-points as used for proliferating NHU cells and urothelial cancer cell lines. Extracted RNA was used to assess MT isoforms transcript expression via RT-PCR.
3. Proliferating NHU cells were exposed to 10 µM $CdCl_2$ and RNA extracted at multiple time points. RT-PCR was used to determine MT isoform transcript expression, allowing identification of highly induced isoforms for more detailed investigation in further experiments. To characterise the relationship between exposure and transcript induction proliferating NHU cells were then exposed to a range of cadmium concentrations over a variety of exposure times, and RT-PCR used to determine transcript expression.

4. Proliferating NHU cells were exposed to 10 µM $CdCl_2$ for 72 hours, a time period previously shown as sufficient for MT protein translation (Wei et al., 2008; Urani et al., 2010; Mehus et al., 2014) and then underwent either protein extraction for subsequent western blotting or fixation for immunohistochemical analysis. Specific antibodies for two of the isoforms whose transcripts were highly induced by cadmium were obtained, titrated and then used to quantify and localise MT isoform protein induction in response to cadmium exposure.

## 3.2 Results

### 3.2.1 Identification of a Relevant Cadmium Concentration Suitable for *In Vitro* NHU Cell Culture

Proliferating NHU cells were exposed to a range of cadmium chloride concentrations ($CdCl_2$; 0.1 µM – 20 µM) and a growth curve generated over 7 days, using the AlamarBlue® cell biomass assay. For initial growth assays, the standard laboratory protocol for NHU cells was used, which indicates an NHU cell seeding density of $2 \times 10^4$ cells/$cm^2$. At this seeding density it was observed that exposure to $CdCl_2$ concentrations above 3 µM was cytotoxic to proliferating NHU cells, and that even 0.1 µM $CdCl_2$ was able to inhibit growth (Figure 19; n=1). As 0.1 µM $CdCl_2$ is a very low concentration, it was decided that the initial cell seeding density would be increased in order to assess whether this could improve NHU cell tolerance to cadmium exposure.

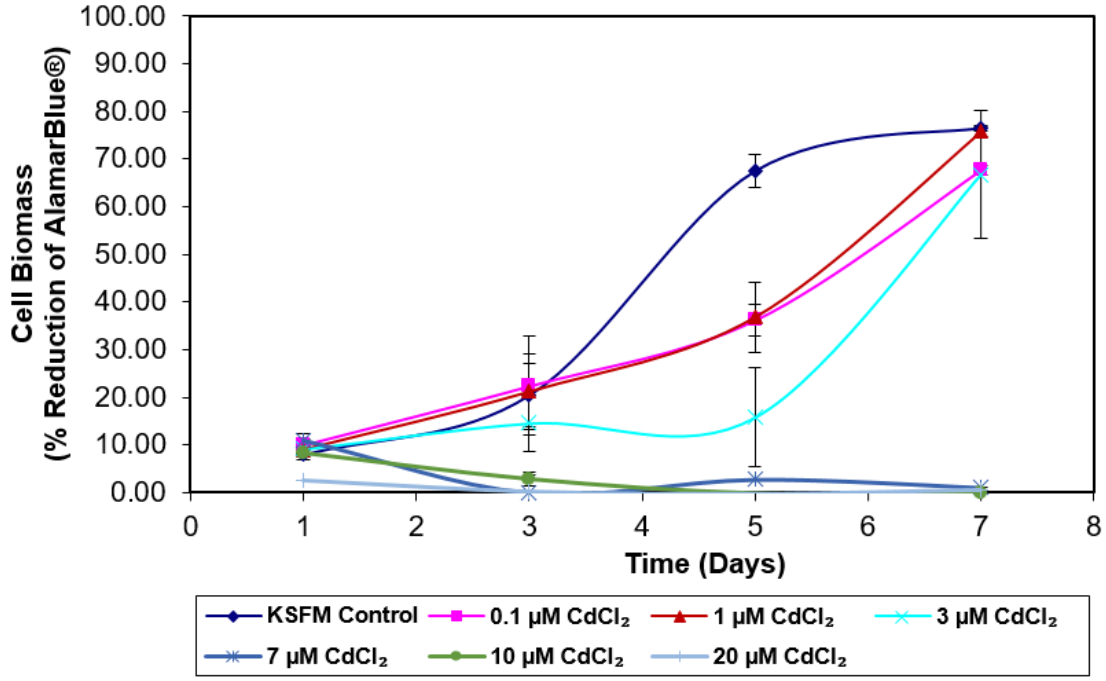


***Figure 19: AlamarBlue® assay demonstrating growth of NHU cells seeded at 2 x $10^4$ cells/$cm^2$ and exposed to cadmium.*** *Proliferating NHU cells (n=1; Y1470) were seeded and exposed to 0.1, 1, 3, 7, 10 or 20 µM $CdCl_2$ from day 0 for up to 7 days. Data points represent mean percentage reduction in AlamarBlue® ±S.D. (n=3; technical repeats).*

At a seeding density of 4 x $10^4$ cells/$cm^2$ growth assays indicated that the highest concentration of 20 µM $CdCl_2$ remained cytotoxic to the NHU cells, but that exposure to concentrations up to 3 µM $CdCl_2$ did not appear to affect NHU cell proliferation (Figure 20; n=1). However, treatment with 7 and 10 µM $CdCl_2$ were observed to inhibit population growth, and exposure to 10 µM $CdCl_2$ exerted a cytostatic effect. It was therefore decided to determine whether a further increase in cell seeding density could increase NHU cell tolerance to this concentration.

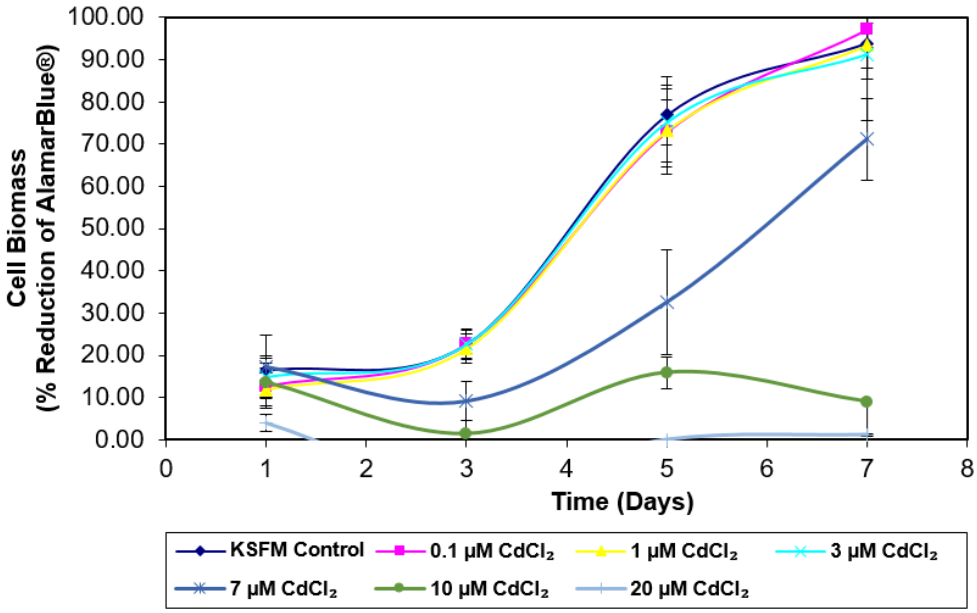


***Figure 20: AlamarBlue® assay demonstrating growth of NHU cells seeded at 4 x $10^4$ cells/$cm^2$ and exposed to cadmium.*** *Proliferating NHU cells (n=1; Y1497) were seeded and exposed to 0.1, 1, 3, 7, 10 or 20 µM $CdCl_2$ from day 0 for up to 7 days. Data points represent mean percentage reduction in AlamarBlue® ±S.D. (n=3; technical repeats).*

Final growth assays were performed using a cell seeding density of 6 x $10^4$ cells/$cm^2$. At this density, exposure to 20 µM $CdCl_2$ remained cytotoxic to proliferating NHU cells (Figure 21A). However, exposure to 10 µM $CdCl_2$ and lower no longer effected cell growth. Additionally, the growth curves indicated that NHU cells continued to proliferate throughout the experimental period, suggesting that confluency (and subsequent cell-cell contact inhibition) was not reached. To confirm these initial results the assays were repeated using NHU cells from a different patient donor and the data combined (Figure 21B; n=2). This growth curve revealed a possible lag phase in NHU cell cultures exposed to cadmium between days 1 – 3; however, by day 5 the cells had recovered and demonstrated similar growth to control cells for the rest of the experiment. These results suggested that the human-relevant concentration 10 µM $CdCl_2$ did not inhibit NHU cell growth when cells were seeded at a minimum density of 6 x $10^4$ cells/$cm^2$.

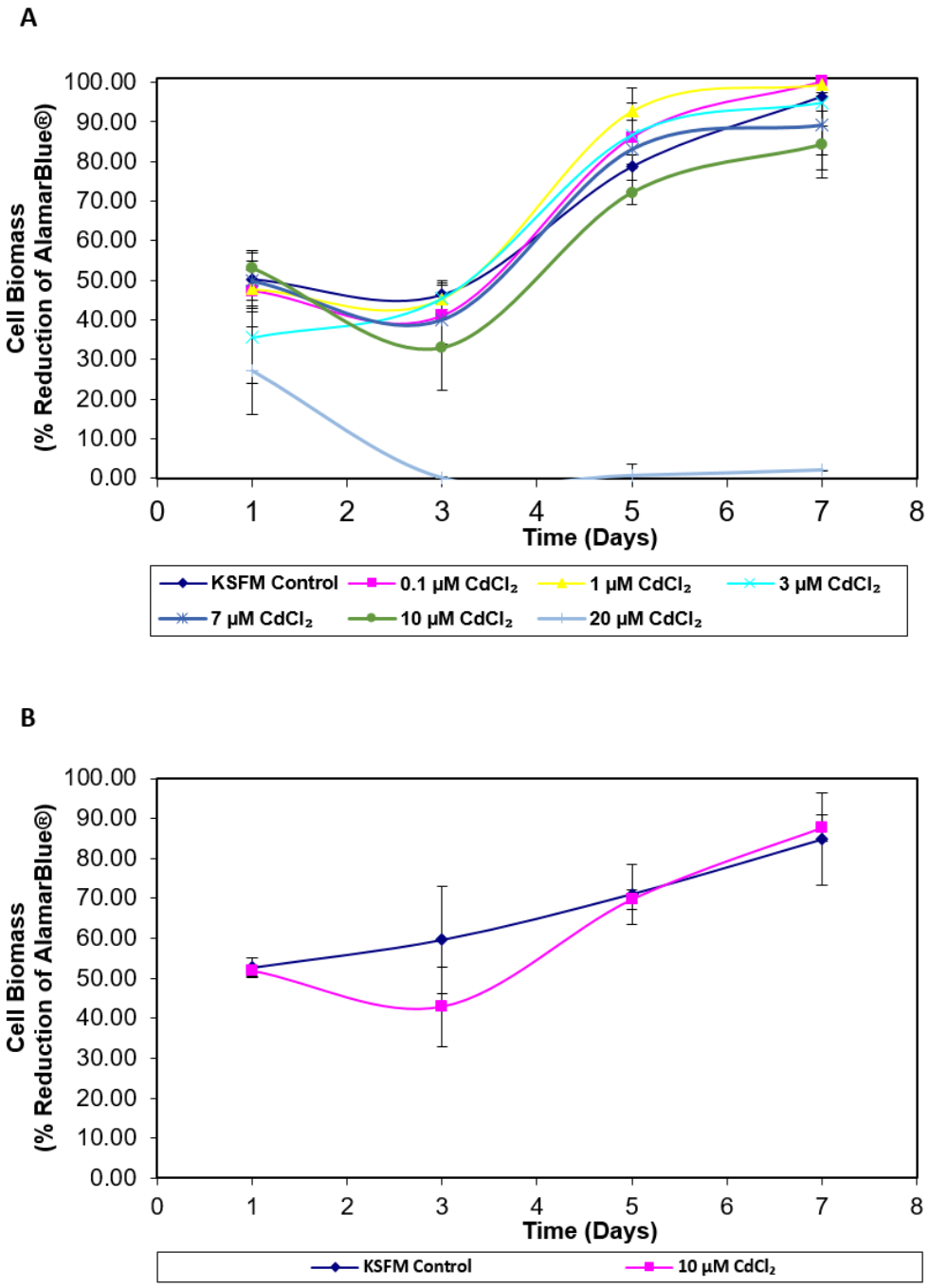


***Figure 21: AlamarBlue® assays demonstrating growth of NHU cell cultures seeded at 6 x $10^4$ cells/$cm^2$ and exposed to cadmium.*** *(A) NHU cells (n=1; Y1497) were seeded and exposed to 0.1, 1, 3, 7, 10 or 20 µM $CdCl_2$ for 7 days. Data points represent mean percentage reduction in AlamarBlue® ±S.D. (n=3; technical repeats). (B) NHU cells (n=2; Y1497, Y1470) were seeded at a density of 6 x $10^4$ cells/$cm^2$ and exposed to 10 µM $CdCl_2$ for 7 days. Data points represent mean percentage reduction in AlamarBlue® ±S.D. from the two biological repeats. The mean of each biological repeat was calculated from three technical repeats (n=3; technical repeats).*

Phase contrast images were captured of proliferating NHU cell cultures exposed to cadmium in order to observe any morphological changes. The resultant images (Figure 22A) revealed the formation of extended processes between the NHU cells at 24 and 48 hours exposure, along with less defined cell borders compared to control cells (magnified in Figure 22B). These morphological alterations could be observed in NHU cell cultures from three independent donors exposed to 10 µM cadmium (n=3), and were also observed to present frequently in subsequent experiments.

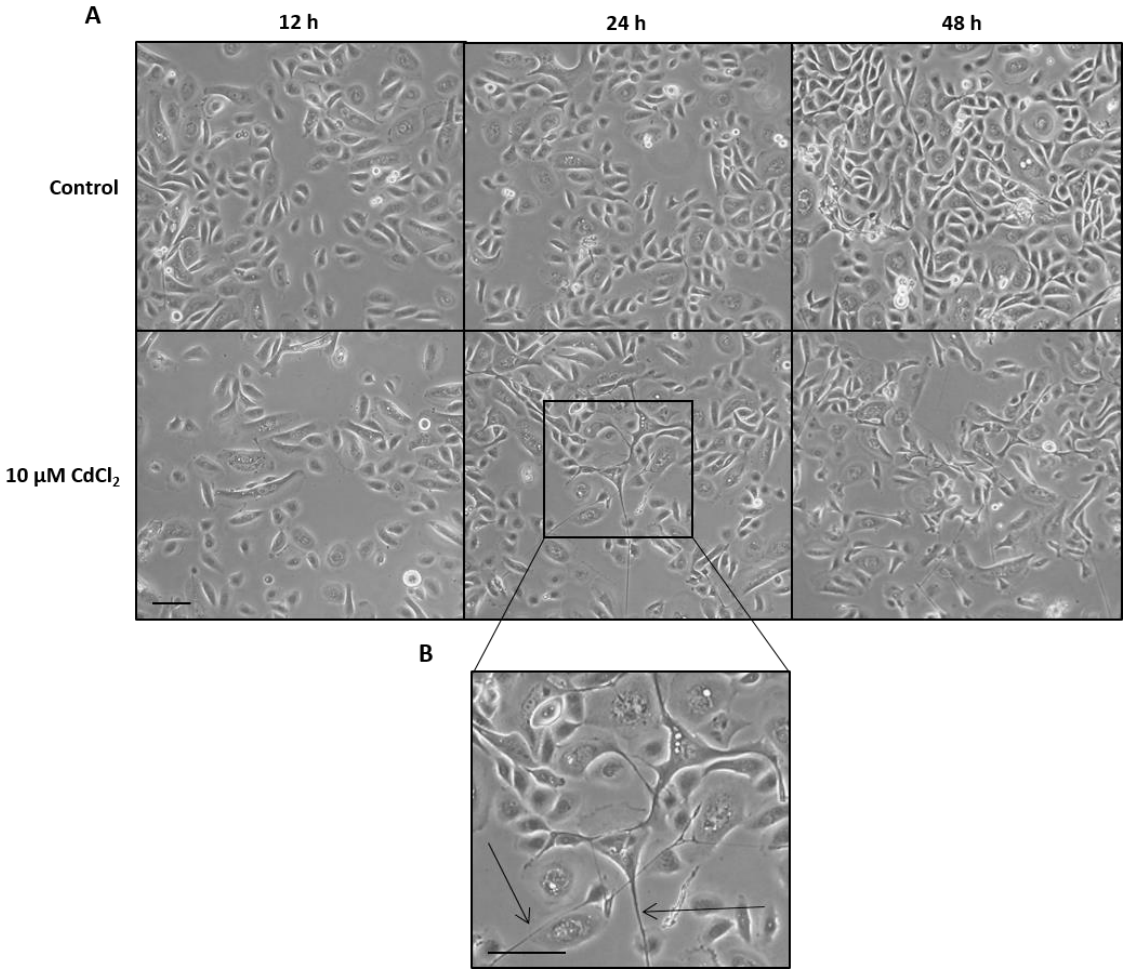


***Figure 22: Representative phase contrast images of proliferating NHU cells cultured in cadmium for 48 hours.*** *Three independent NHU cell lines (n=3; Y1089, Y1270, Y1426) were seeded at a density of 6 x $10^4$ cells/$cm^2$ and exposed to 10 µM $CdCl_2$ for up to 48 hours. (A) Phase contrast images were captured at various time-points of control and cadmium-exposed cell cultures. (B) Magnified image of proliferating NHU cells exposed to 10 µM $CdCl_2$ for 24 hours. Arrows indicate extended processes between cells. Scale bars = 50 µm. Representative NHU cell line was Y1089 (results from other cell lines are included in the Appendices).*

### 3.2.2 Baseline MT Transcript Expression in Normal Human Urothelium

NGS data analysis revealed that the most highly expressed isoforms in P0, PRO and DIF NHU cells were MT-2A, and MT-1X (Figure 23). In general, MT isoform expression was observed higher in PRO NHU cells than P0 or DIF. The majority of MT-1 isoforms were expressed at such low levels that expression was neglibible and may have been below the limit of detection., particularly the MT-1A, MT-1H and MT-1M isoforms. MT-3 was also expressed at neglible levels, and MT-4 transcription was absent.

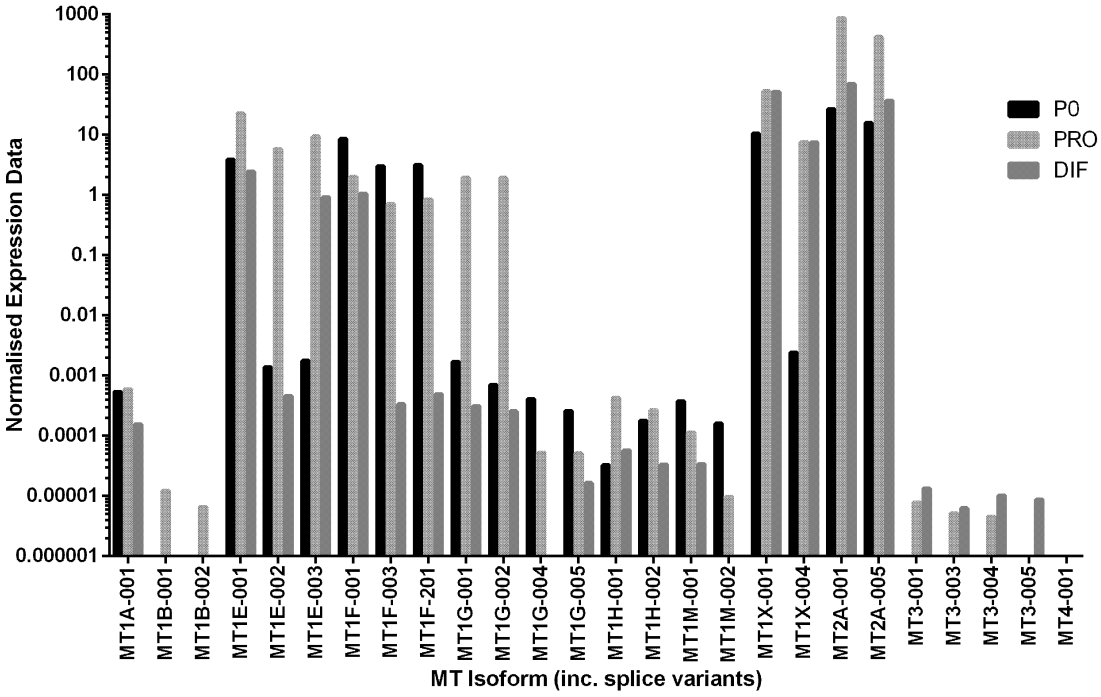


***Figure 23: Next Generation Sequencing (NGS) data analysis of MT isoform transcription in NHU cells.*** *NGS data was previously collected from passage (P) 0 NHU cells (i.e. freshly isolated NHU cells that had not yet been passaged in vitro), proliferating (PRO) and differentiated (DIF) NHU cells. Data was mined using HT-seq gene analysis (Anders et al., 2015) and MT isoform transcription determined. All isoform splice variant transciption is shown individually. Transcript expression was normalised to housekeeping gene GAPDH transcription.*

The baseline expression of MT isoform transcripts was next established in both proliferating (n=1) and differentiated (n=1) NHU cells using RT-PCR (Figure 23). MT-2A isoform transcript was constitutively highly expressed in both proliferating and differentiated NHU cells. However, many MT isoform transcripts were not expressed under control conditions in either NHU cell culture. This included a number of isoforms belonging to the MT-1 subfamily, such as MT-1B, MT-1G, MT-1H and MT-1M. The

MT-3 and MT-4 isoform transcripts were also absent in all NHU cell cultures. Other isoforms such as MT-1A demonstrated variable expression, appearing to alter with both differentiation state and time-point. Further, a number of isoforms showed increased transcript expression upon NHU cell differentiation, such as the MT-1E, MT-1F and MT-1X isoforms.

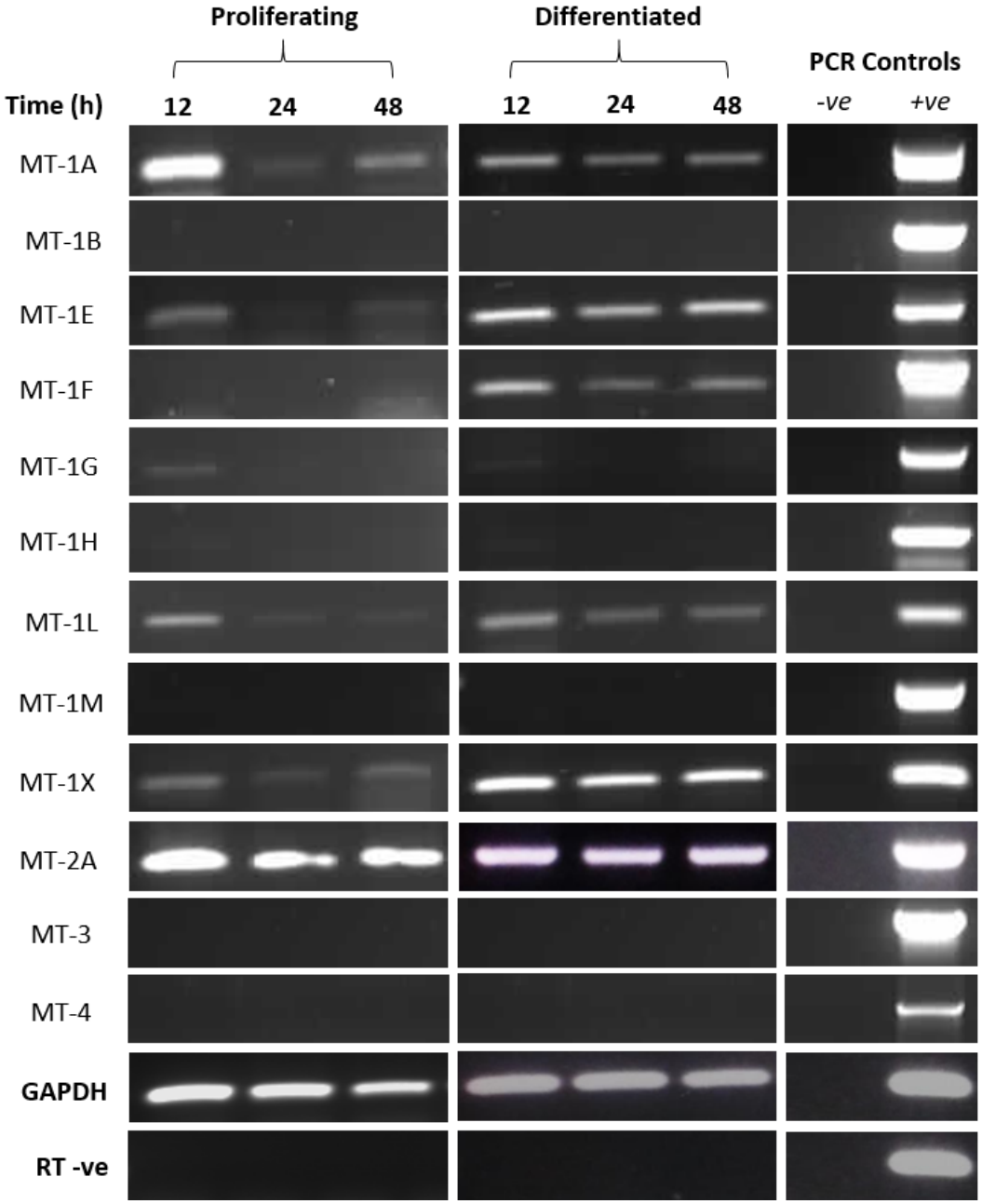


***Figure 24: RT-PCR showing baseline MT isoform transcript expression in proliferating and differentiated NHU cells.*** *Proliferating (n=1; Y1270) and differentiated (n=1; Y1456) NHU cell cultures were maintained under standard culture conditions for up to 48 hours and RNA extracted. Differentiated NHU cells were induced to differentiate prior to the start of the experiment using the biomimetic protocol (see section 2.7.8) and differentiation was confirmed*

*by the presence of a functional barrier (see Figure 31). PCR controls included genomic DNA as a positive control and $dH_2O$ as a negative control. GAPDH transcript expression was used as a loading control, and RT-ve samples confirmed the absence of genomic contamination.*

### *3.2.2.1 MT Transcript Expression in Urothelial Cancer Cell Lines*

MT isoform transcript expression was assessed in a number of urothelial cancer cell lines to determine how expression might change with malignancy (and/or the immortalisation process). Proliferating NHU cells were cultured in parallel with the EJ, RT112 and RT4 urothelial cancer cell lines, and RNA extracted at 24 hours. As MT-4 transcript expression has only been reported in squamous tissue (section 1.5.2), and under basline conditions NHU cells did not express MT-4 transcript (Figure 24), this isoform's expression was not assessed. Although NHU cells did not demonstrate MT-3 transcript expression it was decided to keep this isoform in the MT gene panel, as previous literature had suggested it is expressed in malignant urothelial cells (see section 1.5.6.3).

Consistent with the findings in NHU cells, under control conditions the urothelial cancer cell lines were negative for the majority of MT isoform transcript expression (Figure 25; n=1). The RT-4 cell line in particular expressed no MT gene isoforms, apart from low expression of the MT-2A transcript. Interestingly, the MT isoforms with increased and/or constitutive transcript expression in proliferating and differentiated NHU cells (such as MT-1X and MT-2A) showed decreased expression in the malignant cell lines, especially in RT112 and RT4 cells. Lastly, MT-3 and MT-4 transcripts were found to be absent in all 3 urothelial cancer cell lines.

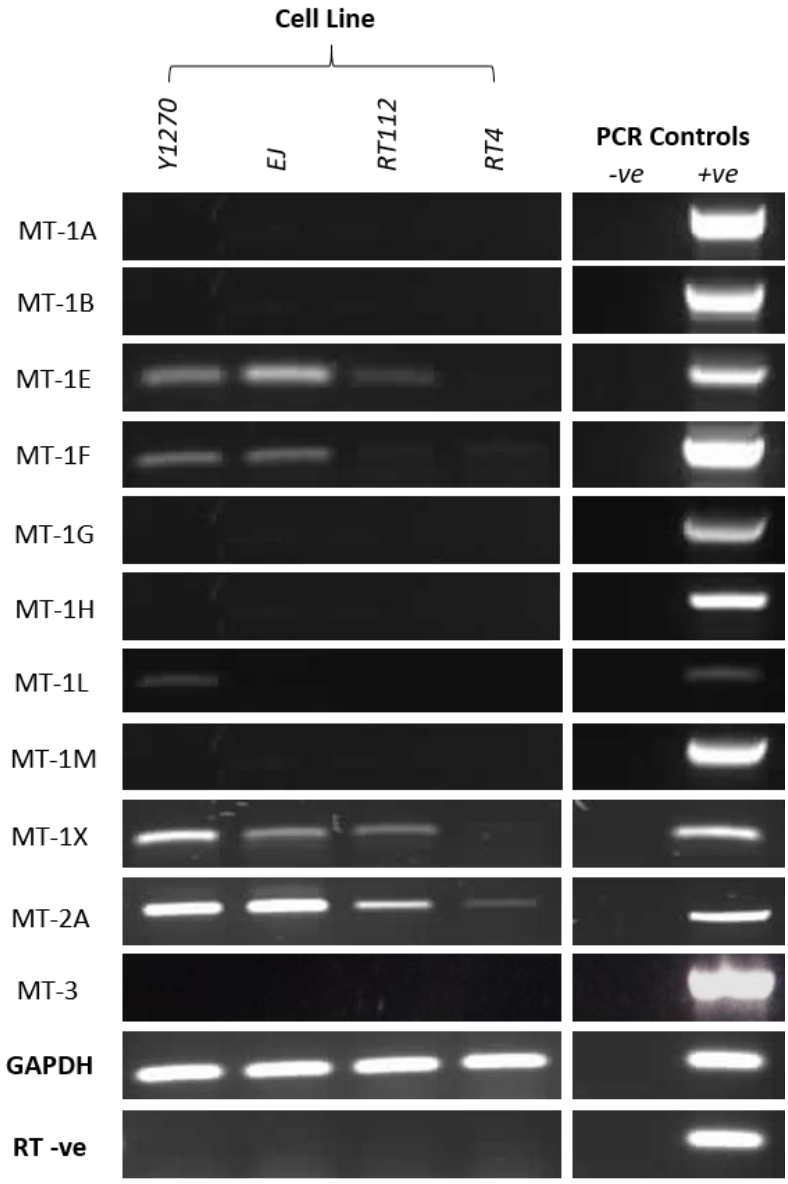


***Figure 25: RT-PCR showing basal MT isoform transcript expression in NHU cells and three urothelial cancer cell lines.*** *Proliferating NHU cells (n=1; Y1270) and 3 urothelial cancer cell lines (EJ, RT112, RT4; n=1; technical repeat) were cultured under standard growth conditions for 24 hours. RNA was then extracted and MT isoform transcript expression assessed. PCR controls included genomic DNA as a positive control and $dH_2O$ as a negative control. GAPDH transcript expression was used as a loading control, and RT-ve samples confirmed the absence of genomic contamination.*

### 3.2.3 Characterisation of MT Isoform Expression in NHU Cells Exposed to Cadmium

RT-PCR results revealed induction of all but one of the MT-1 subfamily isoforms in proliferating NHU cells exposed to cadmium, particularly at the 12-hour time-point

(Figure 26; n=3). The only isoform unaffected by exposure was MT-1L. MT-1 isoform transcript induction was lost over time, as transcript expression of 5 isoforms returned to baseline expression after 48 hours continuous cadmium exposure. The isoform transcripts most prominently induced were MT-1A, MT-1G, MT-1H and MT-1M. MT-1X transcript was also highly induced in exposed cells, as there no obvious transcript expression in control cells; contradictory to results from other NHU cell lines where this isoform has been found to be highly expressed in control conditions (Figures 24, 74 and 75). By contrast, transcription of the other MT subfamilies did not appear to change with cadmium exposure. MT-2A transcript remained highly expressed under all conditions, and neither MT-3 or MT-4 transcripts were expressed.

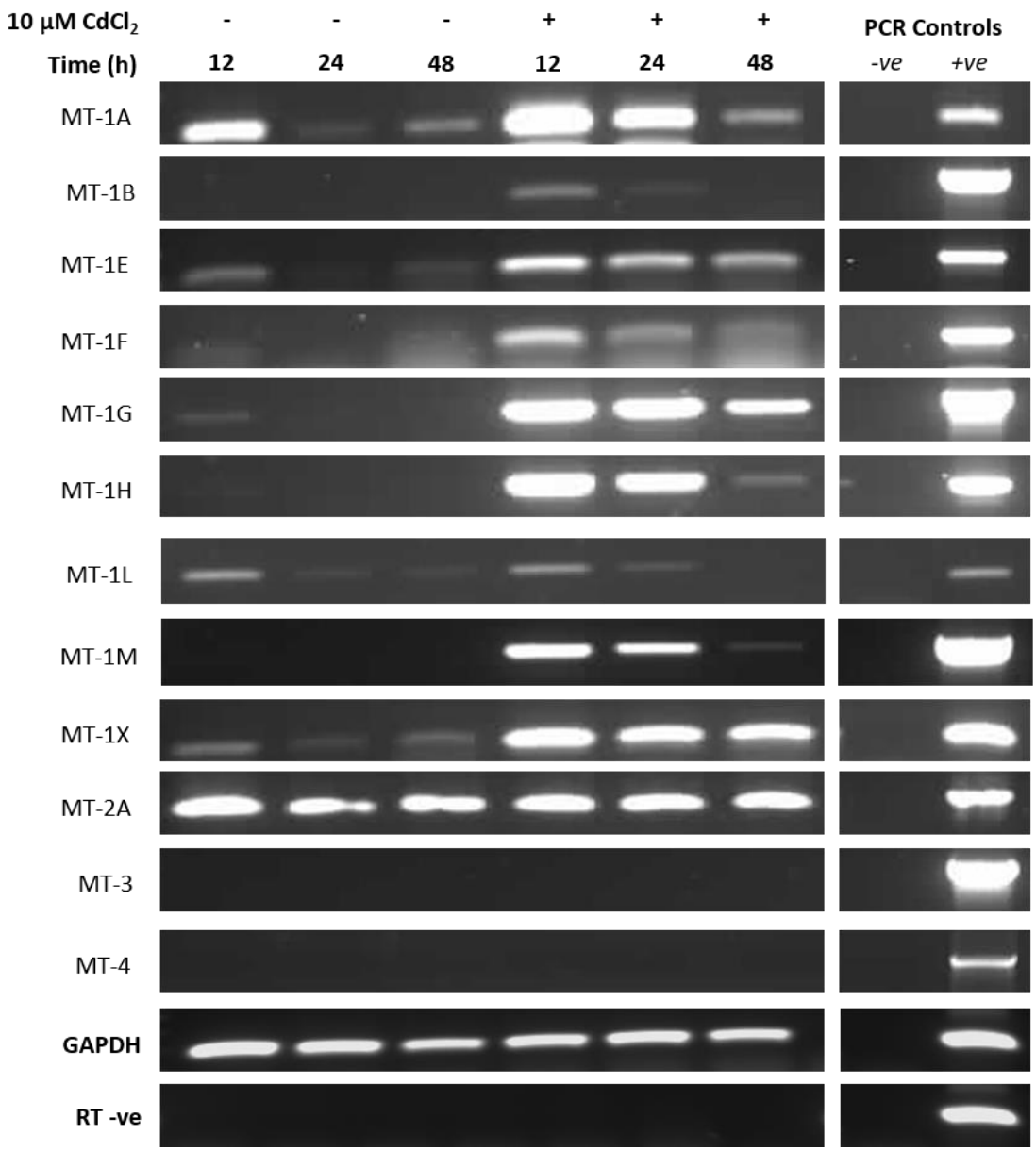


***Figure 26: Representative RT-PCR showing MT isoform transcript expression in proliferating NHU cells exposed to cadmium.*** *Proliferating NHU cells (n=3; Y1270, Y1344, Y1426) were exposed to 10 µM $CdCl_2$ for up to 48 hours, RNA extracted and MT isoform transcript expression assessed. PCR controls included genomic DNA as a positive control and $dH_2O$ as a negative control. GAPDH transcript expression was used as a loading control, and RT-ve samples confirmed the absence of genomic contamination. Representative cell line was Y1270 (results from other cell lines are included in the Appendices).*

The dose-response relationship between cadmium exposure and MT isoform induction was then investigated. Proliferating NHU cells were exposed to the same range of concentrations as used in the growth assays (0.1 µM – 20 µM $CdCl_2$; section 3.2.1) for 12 hours and transcript expression assessed using RT-PCR. The results showed that MT-

2A transcript expression remained constitutively expressed in all conditions and that MT-3/MT-4 demonstrated no transcription (Figure 27), as observed in previous results. However, the MT-1 subfamily showed a striking dose-response induction of transcript, as isoform induction occurred in cells exposed to concentrations as low as 1 µM $CdCl_2$ (n=1). Once again the most prominently induced isoforms were MT-1A, MT-1G, MT-1H and MT-1M. By contrast, MT-1B transcript was only minimally induced, and required exposure to at least 7 µM $CdCl_2$ for expression to occur. Interestingly, in this cell line (Y1426) MT-1E and MT-1X transcripts were highly expressed in proliferating NHU cells under both normal and exposed conditions, which was also sporadically observed in NHU cell lines from other donors (see section 3.2.2).

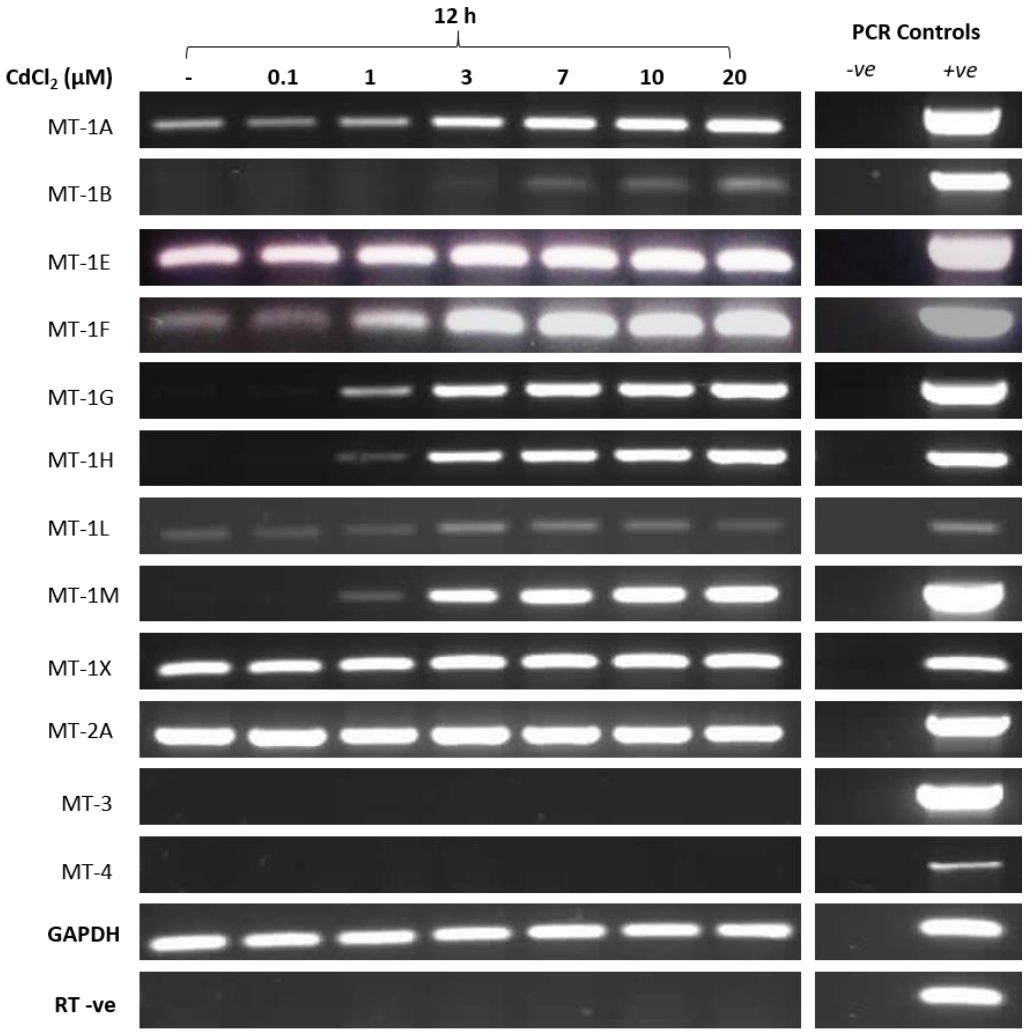


***Figure 27: RT-PCR showing the dose-response of MT isoform transcript induction in proliferating NHU cells exposed to cadmium.*** *Proliferating NHU cells (n=1; Y1426) were exposed to 0.1, 1, 3, 7, 10 or 20 µM $CdCl_2$ for 12 hours, RNA extracted and MT isoform transcript expression assessed. PCR controls included genomic DNA as a positive control and $dH_2O$ as a negative control. GAPDH transcript expression was used as a loading control, and RT-ve samples confirmed the absence of genomic contamination.*

To further characterise the relationship between urothelial MT isoform induction and cadmium exposure, the timing of transcript induction was investigated. As the MT-1A, MT-1G, MT-1H and MT-1M isoforms had been observed to be consistently highly induced in response to cadmium exposure, it was decided to focus on these targets for subsequent experiments. Proliferating NHU cultures were exposed to 10 µM $CdCl_2$ for up to 12 hours and RNA extracted at 1, 3, 6 and 12-hour time-points. RT-PCR once again

confirmed the prominent transcript induction of these isoforms in response to cadmium exposure (Figure 28). However, the results also showed that the isoforms differed in respect to their timing and extent of induction (n=1). MT-1G and MT-1M isoform transcript expression was induced as early as 1 hour into exposure, whereas MT-1A and MT-1H transcripts were not induced until 3 hours exposure. MT-1H transcript induction was decreased compared to the other isoforms, even after 12 hours exposure. MT-1A transcript expression was constitutively present at low levels in control cells, suggesting cadmium may not be the only inducer of this isoform. However, upon cadmium exposure MT-1A transcript expression increased strikingly, indicating that the metal is at least a highly potent inducer of this isoform.

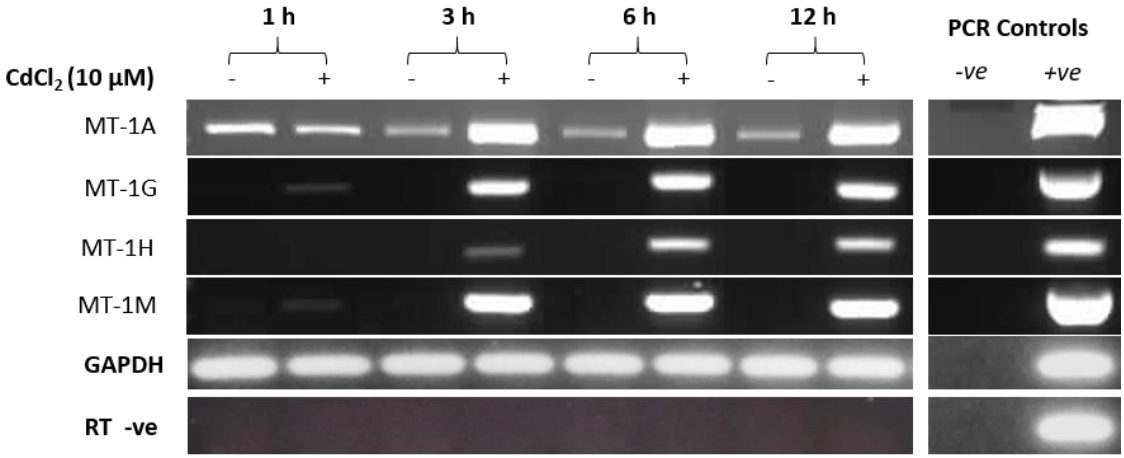


***Figure 28: RT-PCR showing the time-response of MT isoform transcript induction in proliferating NHU cells exposed to cadmium.*** *Proliferating NHU cells (n=1; Y1594) were continuously exposed to 10 µM $CdCl_2$ and analysed at 1, 3, 6 and 12-hour time-points, RNA extracted and MT isoform transcript expression assessed. PCR controls included genomic DNA as a positive control and $dH_2O$ as a negative control. GAPDH transcript expression was used as a loading control, and RT-ve samples confirmed the absence of genomic contamination.*

### 3.2.4 Detection of Cadmium-Induced MT Isoform Protein Expression using Novel MT Isoform-Specific Antibodies

It was next important to determine whether the prominent MT-1 isoform transcript inductions observed in cadmium-exposed NHU cells were translated to protein expression. However, as discussed earlier (section 1.5.5.4) the most specific MT antibody commercially available can only detect the MT-1/2 subfamily as a whole, and is therefore

also unable to discriminate between the the MT-1 isoforms. Determining individual isoform protein expression has therefore been problematic and previously only been attempted using mass-spectrometry in the literature (section 1.5.6.1). For this thesis, commercially untested isoform-specific antibodies were obtained, validated and optimised for use in a number of protocols (see Figures 8, 9, 14 and 15). The antibodies obtained were specific for the MT-1A and MT-1M isoforms, both of which had demonstrated high transcript induction in response to cadmium exposure.

Initial experiments were performed to determine whether MT-1A and MT-1M isoform protein induction could be detected using western blotting. Proliferating NHU cells were exposed to 10 µM $CdCl_2$ for 72 hours, protein lysates extracted and western blotting performed using the newly optimised MT-1A and MT-1M antibodies. The results showed no expression of either MT-1A or MT-1M protein in NHU cells under control conditions (Figure 29), despite low MT-1A transcript expression having been observed in control cells. However, cadmium exposure caused a striking induction of both MT-1A (Figure 29A) and MT-1M (Figure 29B) protein expression, which was observed in all three independent NHU cell lines tested (n=3).

To confirm these results, and to attempt localisation of MT isoform protein expression, immunohistochemistry was also performed. Proliferating NHU cells exposed to 10 µM $CdCl_2$ for 72 hours were centrifuged to form cell pellets, which were then fixed and probed for MT-1A/MT-1M protein expression. Control cell pellets did not express either MT-1A and MT-1M protein, whereas cadmium-exposed cell pellets revealed strong immunolabelling for both protein isoforms (Figure 30; n=1). Interestingly, the isoforms showed differential protein localisation. MT-1A protein expression was observed to occur in both the cytoplasm and nucleus, forming punctate protein deposits (as indicated by the arrows). However, MT-1M protein was observed confined to the cytoplasm and did not form such distinguishable deposits, as localisation was observed to be more diffuse.

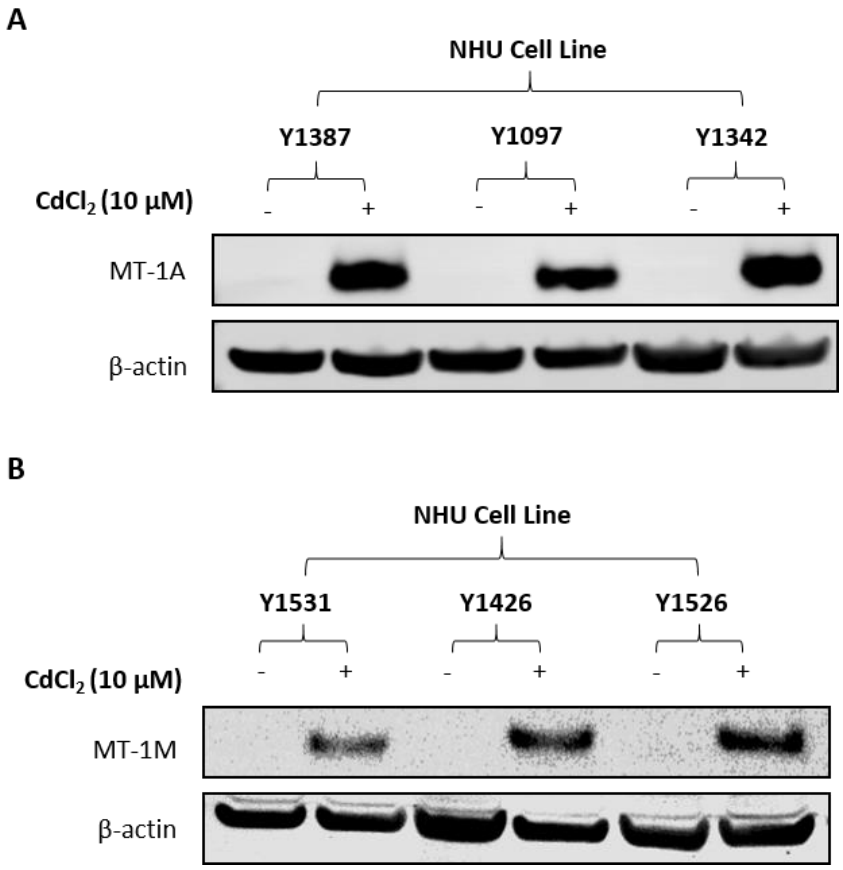


***Figure 29: Western blot showing MT-1A and MT-1M protein expression in proliferating NHU cells exposed to cadmium.*** *Proliferating NHU cells (n=3; Y1387, Y1097, Y1342 for MT-1A and Y1531, Y1426, Y1526 for MT-1M) were exposed to 10 µM $CdCl_2$ for 72 hours, protein lysates extracted and western blotting performed. Protein expression of (A) MT-1A and (B) MT-1M was then determined using novel, isoform-specific antibodies. β-actin protein expression was used as a loading control.*

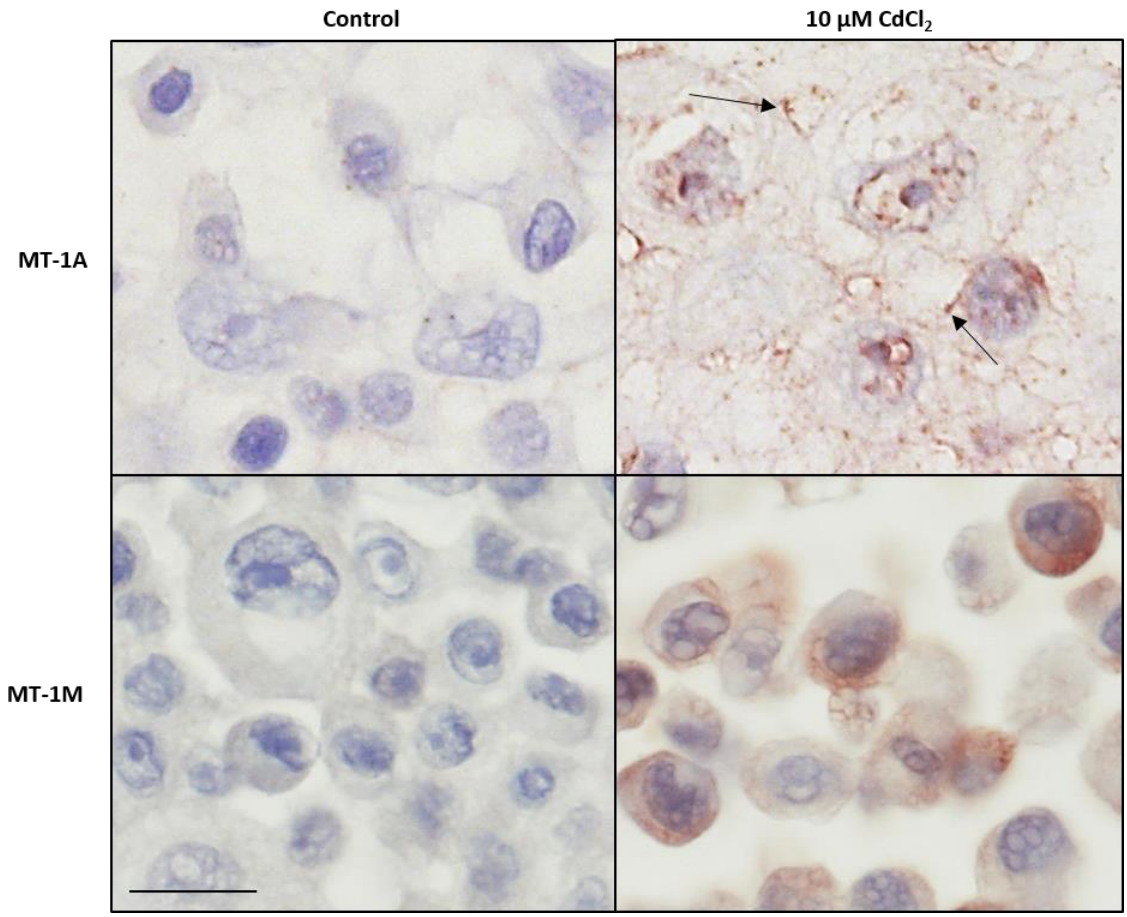


***Figure 30: Immunohistochemical labelling of MT-1A and MT-1M protein expression in proliferating NHU cells.*** *Proliferating NHU cells (n=1; Y1497) were exposed to 10 µM $CdCl_2$ for 72 hours and centrifuged to form cell pellets. Pellets were then fixed and immunolabelled for MT-1A or MT-1M protein using novel isoform-specific antibodies. Arrows indicate punctate MT-1A protein deposits visible within the cells. Scale bar = 25 µm.*

## 3.3 Summary of Key Findings

- 10 µM $CdCl_2$, a concentration suggested to closely reflect human *in vivo* exposure, did not inhibit NHU cell proliferation at a minimum cell seeding density of 6 x $10^4$ cells/$cm^2$.
- Most MT-1 isoforms showed no or minimal transcript expression in NHU cells under baseline conditions, although MT-1A gene transcription was sporadically observed and MT-1X transcript constitutively expressed. MT-2A isoform transcript was also ubiqitously present. No expression of MT-3 isoform transcript was observed in either cadmium-exposed NHU cells or urothelial cancer cell lines.
- NHU cell exposure to cadmium caused transcript induction of the majority of MT-1 isoforms, with preferential induction of the MT-1A, MT-1G, MT-1H and MT-1M isoforms, which were the selected as target isoforms for study in subsequent experiments.
- MT isoforms showed differential transcript induction depending on cadmium concentration and length of exposure.
- MT-1A and MT-1M proteins were induced in proliferating NHU cells exposed to cadmium and demonstrated differential localisation and presentation. MT-1A protein formed punctate deposits throughout the cell, whereas MT-1M protein was observed as diffuse in the cytoplasm.

## 3.4 Discussion

### 3.4.1 Development of Cell Culture Conditions for NHU Cell Cadmium Exposure

When determining a human-relevant, non-cytotoxic concentration of cadmium for NHU cell exposure, it was observed that use of the standard cell seeding density for the proliferation assay resulted in cytotoxicity at the selected intermediate concentration 10 µM $CdCl_2$. It was therefore decided to determine whether an increased cell seeding density could increase NHU cell tolerance to this concentration. However, the density had to be remain low enough to still permit NHU cell proliferation for the duration of the experiment (i.e. without confluence being reached). Further experiments were successful in determining a minimum cell seeding density that permitted cellular proliferation throughout the experiment, yet eliminated cadmium-induced cellular cytotoxicity, resulting in proliferation of exposed NHU cells that did not significantly alter compared to proliferation by control cells.

### 3.4.2 Cadmium-Induced NHU Cell Morphological Changes

The development of extended processes between NHU cells exposed to cadmium (Figure 22) has also been observed in other cadmium-exposed epithelial cell lines. One such study found that the rat liver cell line TLR1215 adopted a more fibroblastic morphology upon chronic cadmium exposure, a change which is often associated with the malignant transformation (Takiguchi et al., 2003). A similar morphological alteration has also been found in the human urothelial cancer cell line T24 upon exposure to cigarette smoke extract (Sun et al., 2017); a substance which is known to contain cadmium (section 1.2.4.1). In this case the cells underwent a significant morphological change from a cobblestone-like to a spindle-like mesenchymal form, accompanied by increased expression of mesenchymal markers and decreased expression of epithelial markers.

Other carcinogenic heavy metals such as arsenic have also been shown to induce epithelial-to-mesenchymal transition (EMT); however, in this study the immortalised human lung peripheral epithelial cell line HPL-1D was used, not a urothelial one (Person et al., 2015). Of note, the authors also observed a significant increase in MT-1A and MT-2A transcript expression in these cells, concluding that the results supported an association between MT expression and the development of a malignant cell phenotype. Based on these results, it is tempting to speculate that the formation of extended processes in NHU cells exposed to cadmium may be an early indicator of EMT. Further studies

exposing NHU cells to cadmium for a prolonged time period would be required, combining morphological alterations with changes in gene expression (for example of epithelial and mesenchymal markers) in order to confirm whether cells may be undergoing EMT.

### 3.4.3 MT Isoform Expression in NHU Cells

RT-PCR assessment of MT isoform transcript expression in proliferating and differentiated NHU cells under control conditions revealed that the majority of MT-1 isoforms were not expressed in baseline conditions, supported by the NGS data. However, these isoforms could be induced by cadmium exposure, consistent with literature suggesting that MT-1 is the inducible MT subfamily (Miles et al., 2000; Thirumoorthy et al., 2007; Capdevila et al., 2012). In proliferating NHU cells it was observed that both MT-1E and MT-1X transcription was variable, demonstrating constitutively high baseline expression in some NHU cells derived from certain donors, but having minimal or no expression in cells from others. NGS data partially supported these findings, demonstrating high MT-1E and MT-1X transcription in proliferating NHU cells. Variable expression could be linked to the high amounts of polymorphism observed in the MT-1 subfamily (Sigel et al., 2009; Capdevila et al., 2012) which can affect isoform expression and function (Yang et al., 2008; Raudenska et al., 2013; Starska et al., 2014). RT-PCR showed that MT-2A transcript was constitutively highly expressed in both proliferating and differentiated NHU cells from all donors, which was also found in the NGS data, consistent with literature which suggests that this is the most widely expressed MT isoform (section 1.5.2).

NHU cells derived from one patient donor demonstrated minimal transcript expression of the MT-1X isoform in control conditions, but a prominent upregulation of transcript expression was observed upon cadmium exposure. Results in NHU cells from other donors (see Appendices section 8.6.2) showed that MT-1X transcript expression was constitutively high in control conditions and remained unaffected by cadmium exposure. These contradictory results raise two questions; firstly, why does MT-1X baseline transcript expression vary between individuals? As suggested above, differential baseline transcription could be due to polymorphisms (e.g. single nucleotide polymorphisms), which could be further investigated using direct DNA sequencing. The second question is whether MT-1X transcript expression was still increased in individuals demonstrating high baseline transcription, but the increase was unobservable using RT-PCR due to PCR

band saturation. To answer this question quantitative PCR methods would need to be used to compare MT-1X transcript expression in cadmium-exposed NHU cells derived from different donors demonstrating either high or no MT-1X transcript expression under baseline conditions. The results would determine whether NHU cell lines demonstrating low baseline MT-1X transcript expression show a unique increased expression of MT-1X in response to cadmium exposure.

As mentioned in the introduction (section 1.5.6.2) MT-3 transcript and protein expression has previously been reported in urothelial cancer specimens, and no obseravle expression in normal urothelial samples (Sens et al., 2000; Zhou et al., 2006b). Absent MT-3 expression in healthy urothelial controls is supported by the results from this thesis, as neither proliferating nor differentiated NHU cells demonstrated MT-3 transcription. However in contradiction to previous findings, which suggested MT-3 as a potential biomarker of urothelial cancer (Sens et al., 2000), this thesis additionally found no detectable MT-3 transcript expression in any of the urothelial cancer cell lines analysed. This included the high-grade urothelial cancer cell line EJ, despite the study by Sens et al. having reported particularly elevated MT-3 expression in high-grade urothelial cancer. Moreover, in this thesis MT-3 transcript expression was also absent in proliferating NHU cells exposed to cadmium, despite a previous study having reported induction of MT-3 in the urothelial cell line UROtsa after malignant transformation by chronic cadmium exposure (Zhou et al., 2006b).

Lack of MT-3 transcript expression in all human urothelial cells assessed in this thesis is supported by the widely held view that MT-3 expression is confined to neural tissue (Palmiter et al., 1992). It is therefore unclear why the studies by Sens et al. (2000) and Zhou et al. (2006b) observed positive MT-3 expression in urothelial cancer specimens. One possible explanation for the MT-3 transcript expression observed in urothelial cancer samples is that the transcript may have originated from other, non-urothelial cells. In order to perform RT-PCR the authors cut thick sections from paraffin-embedded tissue specimens, but did not attempt to isolate the urothelium, and thus the samples analysed most likely contained a mixture of cell types (e.g. stromal, lymphocyte). However, this does not explain why the authors were able to observe MT-3 protein expression in the urothelium of urothelial cancer specimens. A second possibility is that the antibody used was not specific for MT-3 protein expression. Clearly, further investigation is needed to establish whether MT-3 expression is truly associated with the presence of urothelial cancer.

Lastly, commercially untested antibodies were able to successfully discriminate between cadmium-induced MT-1A and MT-1M protein expression (section 3.2.4). This was the first time that differentiation between MT-1 isoforms had been performed at the protein level using non-spectroscopic methods, and that localisation of the individual MT-1 isoforms had been attempted. Differential localisation and protein expression characteristics of the isoforms was observed in cadmium-exposed NHU cells (Figure 30), not only suggesting that the antibodies could discriminate between the isoforms, but inferring that the different isoforms may possess distinct functions.

# Chapter 4: Cadmium Exposure and the Urothelial Barrier

## 4.1 Chapter Aims

The aim of this chapter was to determine whether cadmium could cross a functional, tight urothelial barrier, either by direct access or by compromising barrier function and thereby indirectly accessing the underlying urothelial cells.

### 4.1.1 Objectives

1. Determine whether exposure of differentiated NHU cells to a human-relevant concentration of cadmium alters barrier function over time.
2. Assess whether cadmium exposure can cause MT transcript and protein induction in differentiated NHU cells despite the presence of a tight urothelial barrier.
3. Directly quantify cadmium in exposed differentiated NHU cell sheets despite the presence of a tight urothelial barrier.

### 4.1.2 Experimental Design

1. To achieve the overall aim of determining whether cadmium could penetrate an intact tight urothelial barrier, it was first important to assess whether cadmium exposure compromised urothelial barrier function. To investigate this, proliferating NHU cell cultures were stimulated to differentiate using a biomimetic method (described in section 2.7.8). Differentiation was confirmed by expression of differentiation associated markers and/or the development of a functional barrier (determined using TER readings; section 2.7.9). Once differentiated, the cultures were exposed apically to 10 µM $CdCl_2$ (Figure 31) in order to reflect *in vivo* exposure, where the apical surface of the urothelium would be exposed to cadmium in the urine. Differentiated NHU cells were exposed to cadmium for up to 72 hours and TER measured in triplicate at various time-points to monitor barrier function.

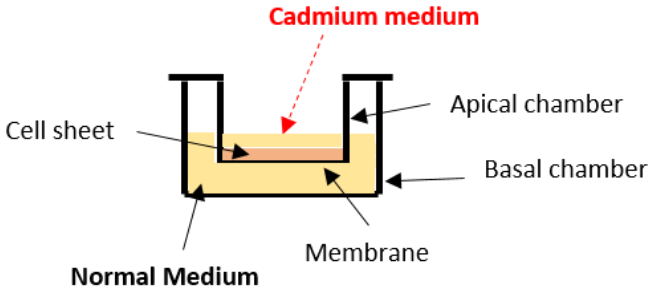


***Figure 31: Diagram illustrating the set-up of a ThinCert™ membrane for culturing differentiated NHU cell sheets in the presence of cadmium.*** *NHU cells were seeded onto the membrane and stimulated to differentiate (as described in section 2.7.8). For cadmium exposure, all medium was first aspirated from the wells. Normal medium was then placed in the basal well, and medium containing 10 µM $CdCl_2$ was placed in the apical chamber in order to mimic in vivo exposure.*

2. The next step was to indirectly assess whether cadmium could penetrate the urothelial barrier. Based on the finding from Chapter 3 that MT-1 isoform transcript/protein induction appears a robust biomarker of cadmium exposure in NHU cells, differentiated NHU cell sheets demonstrating a tight urothelial barrier were exposed to 10 µM $CdCl_2$ for up to 72 hours and MT isoform transcript and protein expression determined. TER was monitored throughout the experiment to ensure the continuous presence of a functional urothelial barrier. At the end of the experiment RNA and protein lysates were extracted for RT-PCR and western blotting respectively. Additionally, differentiated cell sheets were fixed and used for immunohistochemical labelling of MT protein.
3. To further investigate and quantify any potential cadmium penetration through the urothelial barrier, inductively coupled plasma-optical emission spectroscopy (ICP-OES) was performed to directly measure cadmium concentration in the underlying urothelial cells. Differentiated NHU cell sheets were taken from the above experiment, as they had maintained a tight urothelial barrier but still shown induction of the MT-1 isoforms post cadmium-exposure, suggesting cadmium may have penetrated the urothelium. The NHU cell sheets were washed, acid-digested and prepared for use in the ICP-OES machine (see section 2.12). Two separate NHU cell cultures from the same cell line were used for each condition (control and cadmium-

exposed) to provide duplicate technical repeats. Cadmium concentration in digested cell solutions was then calculated, along with concentration per $mm^2$ cell sheet.

## 4.2 Results

### 4.2.1 Effect of Cadmium Exposure on Urothelial Barrier Function

The results indicated that both control and cadmium-exposed differentiated NHU cells maintained a tight urothelial barrier throughout the experiment (Figure 32A). Moreover, TER readings remained similar between control and cadmium-exposed NHU cell cultures. In order to validate these findings, the experiment was repeated in NHU cells from 3 individual donors and the results combined. The data revealed that after 72 hours cadmium exposure differentiated NHU cells still retained a tight urothelial barrier with a TER reading >3 $k\Omega.cm^2$ (Figure 32B). This reading was not significantly different to control cells ($p>0.05$), suggesting that cadmium exposure did not alter urothelial barrier function (n=3 biological repeats, in experimental triplicates).

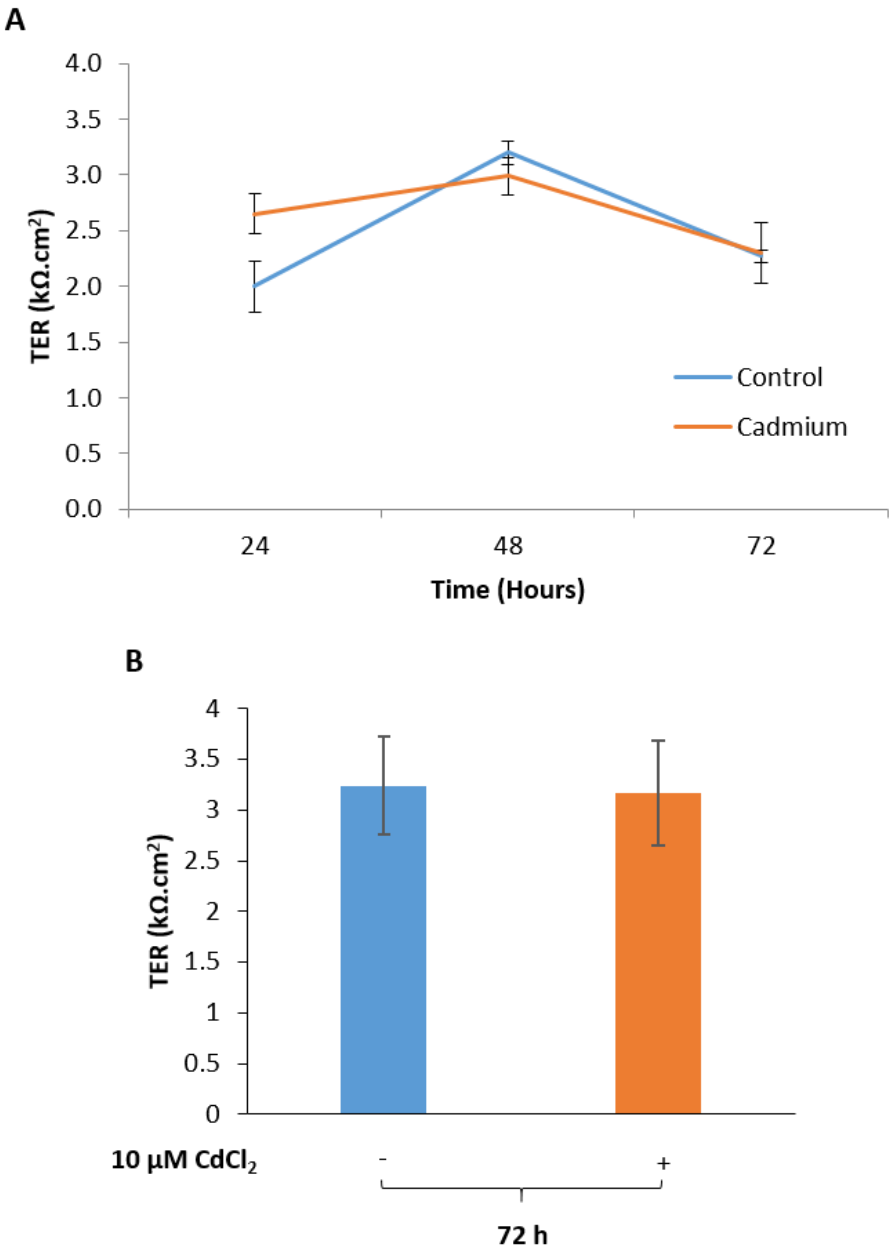


***Figure 32: Transepithelial electrical resistance (TER) readings from differentiated NHU cell sheets exposed to cadmium.*** *(A) Representative graph of differentiated NHU cells (n=1; Y1493) that were apically exposed to 10 µM $CdCl_2$ for 24, 48 and 72 hours showing TER readings over time. Each data point represents mean electrical resistance from 3 technical replicates (kΩ.cm$^2$) ±S.D. (B) NHU cells from 3 independent donors (n=3; Y1493, Y1531, Y1456) were differentiated and exposed to 10 µM $CdCl_2$ for 72 hours to determine whether exposure affected barrier function. Mean TER readings for each donor were calculated from 3 technical replicates. Each column represents the overall mean electrical resistance calculated from triplicate readings in 3 independent donors (kΩ.cm$^2$) ±S.D.*

### 4.2.2 MT Isoform Transcript and Protein Expression in Differentiated NHU Cells Exposed to Cadmium

RT-PCR was performed for all MT-1 and MT-2 transcripts to examine possible induction of isoforms. KRT13 transcript expression was used as a marker of transitional differentiation (see Appendices section 8.4.1) and the presence of a functional barrier was also confirmed (see Figure 32B). Qualitatively, the results showed a strong induction of the majority of the MT-1 subfamily, although MT-1B and MT-1L demonstrated minimal induction (Figure 33; n=3). In support of previous findings (see section 3.2.3), the MT-1A, MT-1G, MT-1H and MT-1M transcripts were the most highly induced. The data also indicated constitutively high expression of MT-1X and MT-2A transcripts, which had been previously observed (section 3.2.2). Despite its constitutive expression, MT-1X transcript also increased in expression with cadmium exposure.

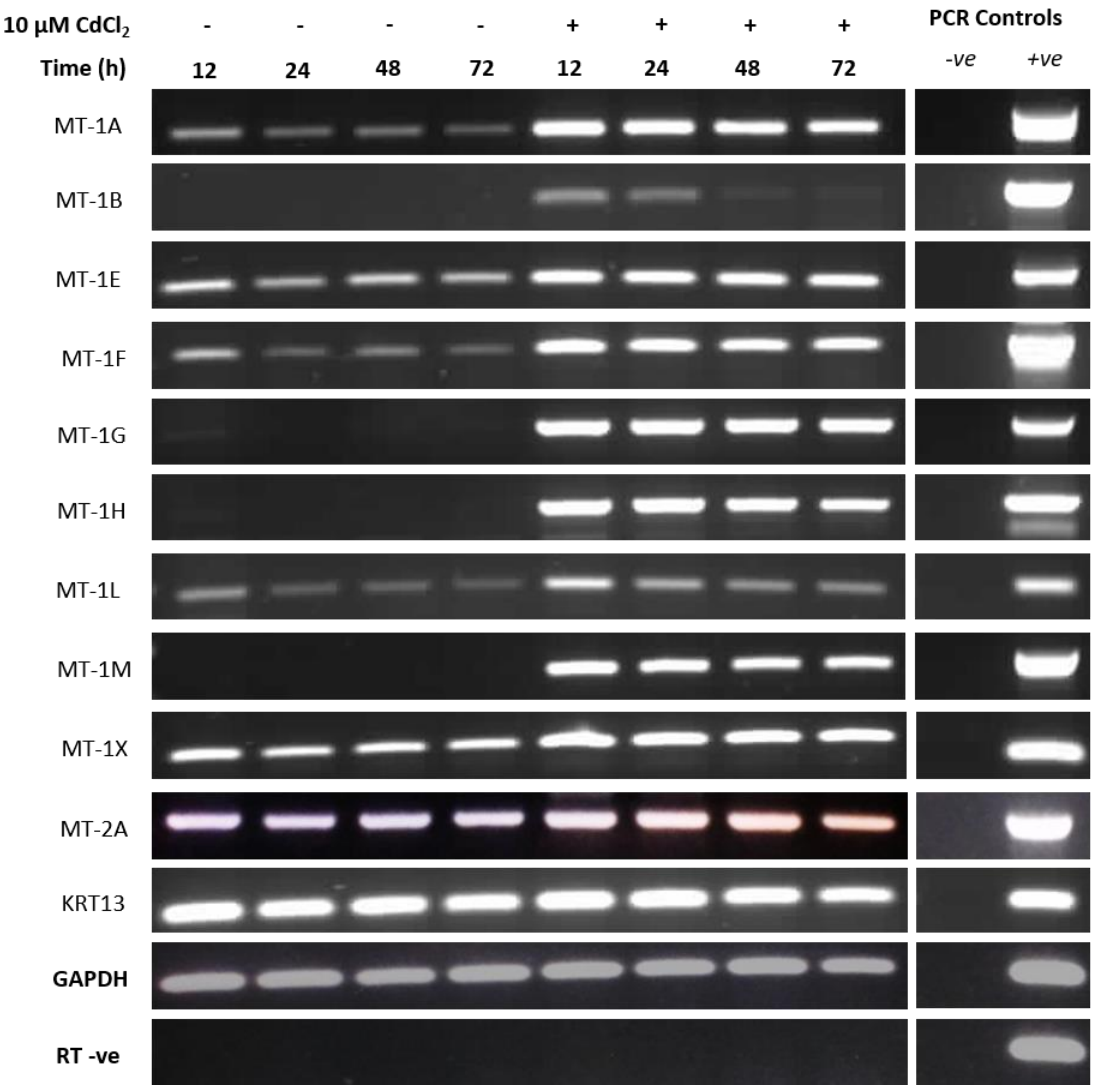


***Figure 33: Representative RT-PCR showing MT isoform transcript expression in differentiated NHU cells with functional barriers that were exposed to cadmium.*** *NHU cells (n=3; Y1456, Y1493, Y1531) were differentiated and exposed to 10 µM $CdCl_2$ for up to 72 hours. Differentiation was inferred by expression of the transitional epithelial marker KRT13 and confirmed using TER readings (see Figure 32B). PCR controls included genomic DNA as a positive control and $dH_2O$ as a negative control. GAPDH transcript expression was used as a loading control, and RT-ve samples confirmed the absence of genomic contamination. Representative cell line was Y1456 (results from other cell lines are included in the Appendices).*

Protein expression of the MT-1A and MT-1M isoforms was next determined. Western blotting revealed a prominent induction of MT-1A protein in differentiated NHU cells exposed to cadmium (Figures 34A and 34C; n=3). No MT-1A protein was expressed in control cells, despite the presence of low levels of transcript expression observed in control NHU cells previously (section 3.2.2). MT-1M protein induction could also be

detected in cadmium-exposed cells (Figure 34B; n=1), however not to the same extent as MT-1A protein. To confirm these findings, and attempt to localise the proteins within the differentiated cell sheets, immunohistochemistry was performed. The results showed immunolabelling for both MT-1A and MT-1M proteins in the exposed cell sheets (Figure 35; n=1). In support of previous findings in proliferating NHU cells (section 3.2.4) MT-1A protein was observed as punctate protein deposits, whereas MT-1M protein presented as diffuse immunolabelling. MT-1A protein expression also appeared

much stronger than MT-1M, supporting the western blot results.

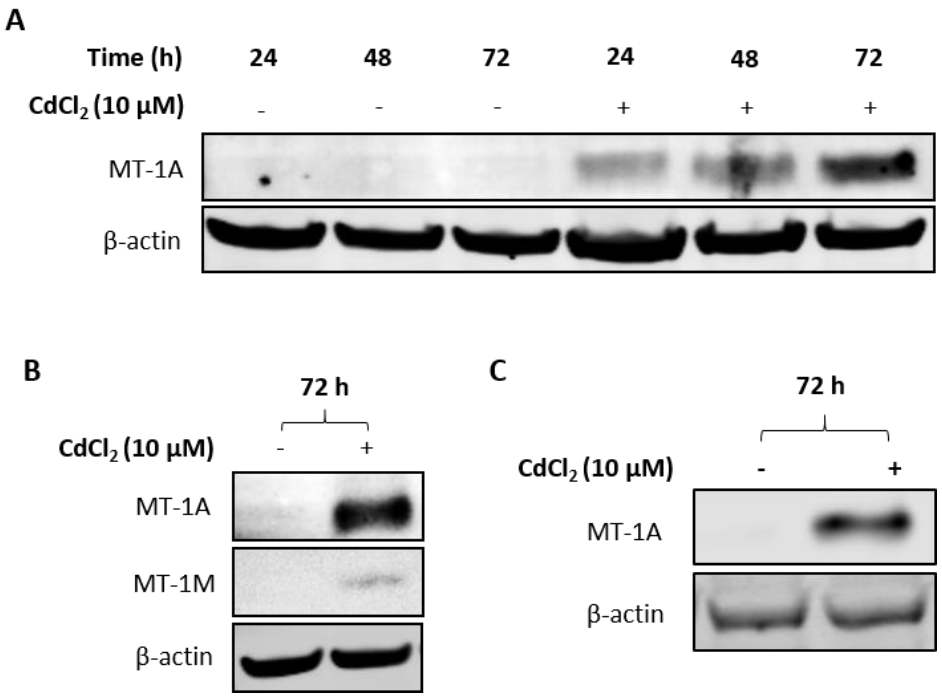


***Figure 34: Western blots demonstrating MT-1A and 1M protein expression in differentiated NHU cells with functional barriers that were exposed to cadmium.*** *NHU cells were stimulated to differentiate and form a functional barrier, before exposure to 10 µM $CdCl_2$ for up to 72 hours. Protein lysates were then extracted and MT protein expression determined. (A) MT-1A protein expression was assessed at multiple time-points to ensure exposure time was adequate for protein translation in differentiated NHU cells (n=1; Y1493). (B) Western blots showing MT-1A and MT-1M protein expression (n=1; Y1531) and (C) MT-1A protein expression (n=1; Y1426) in differentiated NHU cells exposed to cadmium for 72 hours.*

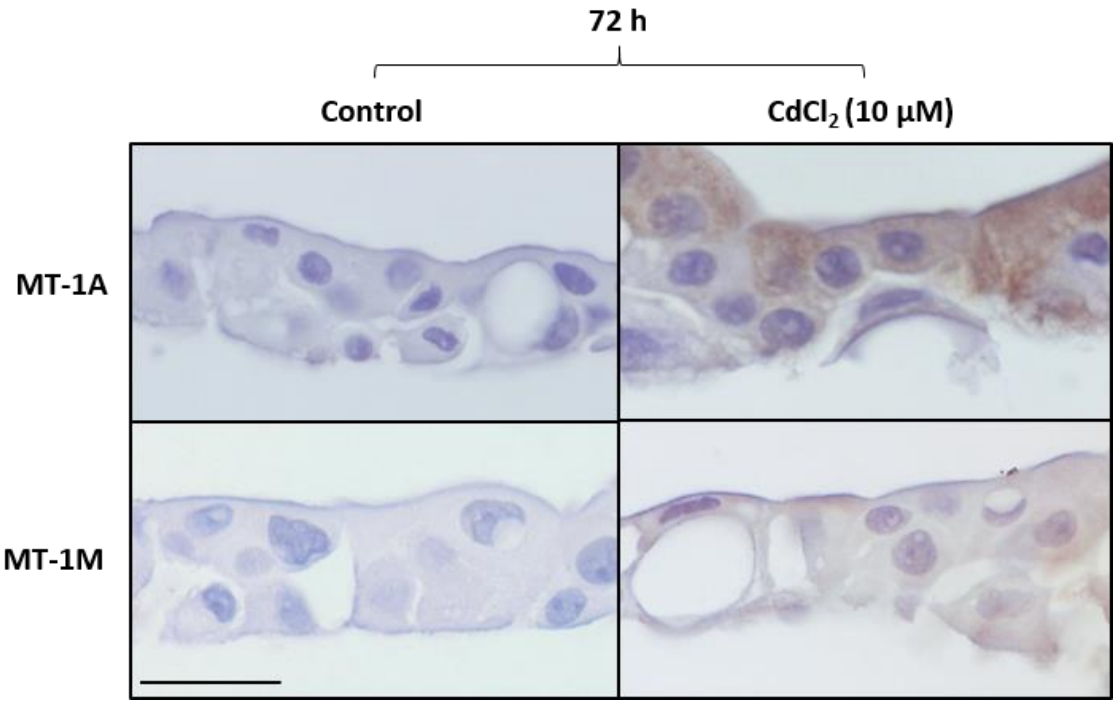


***Figure 35: Immunohistochemical labelling of MT-1A and MT-1M protein expression in differentiated NHU cell sheets with functional barriers that were exposed to cadmium.*** *NHU cells (n=1; Y1531) were differentiated forming cell sheets with a functional barrier. Cells were then apically exposed to 10 µM $CdCl_2$ for 72 hours, and TER readings monitored throughout in order to ensure the continuous presence of a tight barrier (TER readings can be seen in Figure 32B). NHU cell sheets were then fixed and immunolabelled for MT-1A and 1M protein expression. Control images were differentiated NHU cell sheets which had not undergone cadmium exposure. Scale bar = 25 µm.*

These results demonstrated that cadmium could cause MT transcript and protein induction in differentiated NHU cell sheets despite the presence of a 'tight' urothelial barrier. This therefore suggested that cadmium was able to penetrate an intact urothelial barrier and enter urothelial cells, causing MT induction. However, this could only be inferred from the data indirectly, and thus a direct method of determining the presence of cadmium in differentiated urothelial cell sheets was additionally performed.

### 4.2.3 Direct Quantification of Cadmium in Exposed Differentiated NHU Cell Sheets using Spectroscopic Methods

Cadmium concentration readings of all solutions tested are shown in Figure 36A, which revealed that the cadmium concentration of the digested control cell solution was comparable to wash buffer concentrations; i.e. negligible. However, the digested cell

solution from cadmium-exposed NHU cells demonstrated a much higher cadmium concentration (n=1). When data from two technical repeats was combined and the means compared, it was found that the digested cadmium-exposed cell solution had an approximately 10 times higher mean cadmium concentration than the digested cell solution from control cells (0.08 µM and 0.94 µM, respectively; Figure 36A). Conversion of the data to cadmium concentration per $mm^2$ NHU cell sheet supported these findings, with cadmium-exposed cells containing 0.008 µM/$mm^2$ and control cells containing 0.0007 µM/$mm^2$ (Figure 36B).

**A**

| $CdCl_2$ Concentration (µM) | Wash Buffer | Control Cells | $CdCl_2$-Exposed Cells |
|---|---|---|---|
| Repeat 1 | 0.08 | 0.08 | 0.95 |
| Repeat 2 | 0 | 0.08 | 0.93 |
| **MEAN:** | **0.04** | **0.08** | **0.94** |

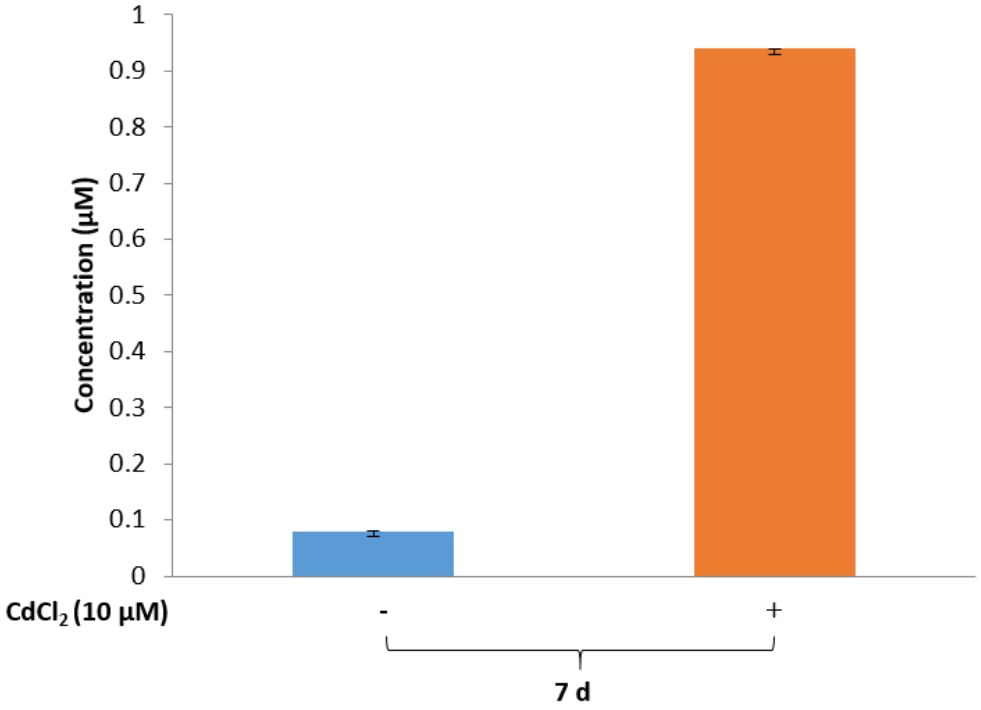

| $CdCl_2$ (µM/mm² cell sheet) | Control Cells | $CdCl_2$ Cells |
|---|---|---|
| Sample 1 | 0.00071 | 0.0084 |
| Sample 2 | 0.00071 | 0.00822 |
| **MEAN:** | 0.00071 | 0.00831 |

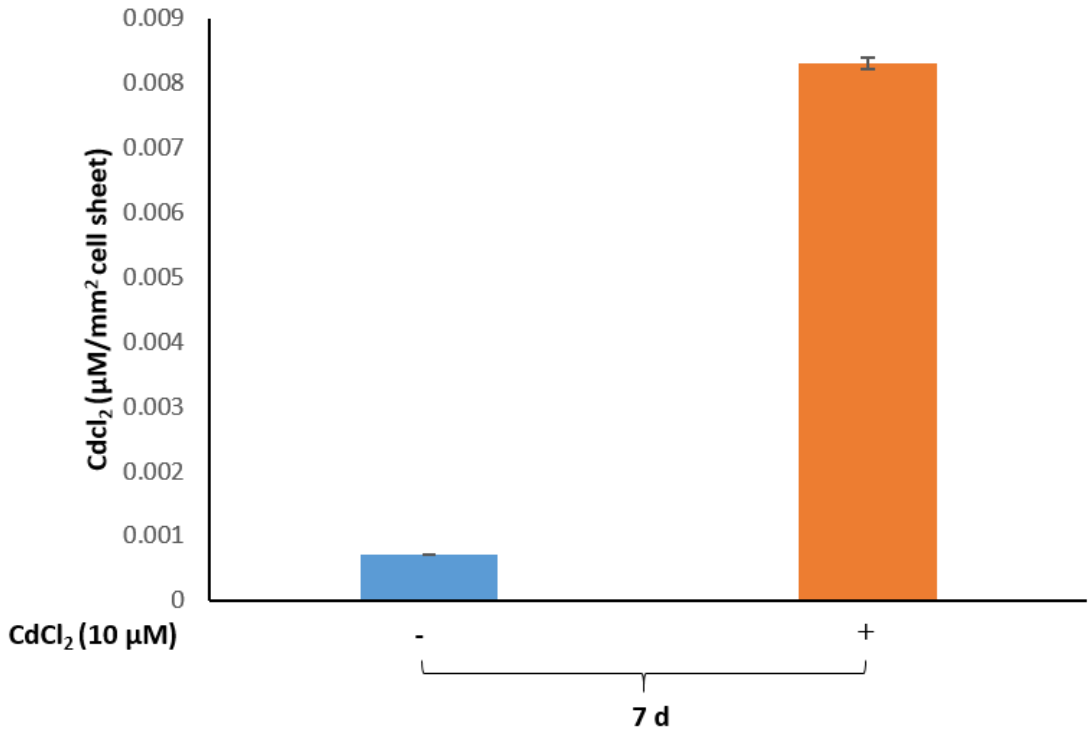


***Figure 36: ICP-OES was used to detect and quantify cadmium in differentiated NHU cells with a functional barrier that were exposed to cadmium.*** *NHU cells (n=1; Y1531) were differentiated forming cell sheets with a functional barrier (see Figure 32B) and apically exposed to 10 µM $CdCl_2$ for 7 days. Samples were then washed 3 times with PBS to remove extracellular metal, acid-digested and diluted for use in the ICP-OES machine. Dilutions were taken into account when calculating final measurements. (A) Cadmium concentrations in wash buffer solution, digested control and digested cadmium-exposed NHU cell solutions are shown. Each column represents mean cadmium concentration ±S.D. (n=2; technical repeats). (B) Cadmium concentration per $mm^2$ cell sheet in control and cadmium-exposed differentiated NHU cells. Each column represents mean cadmium concentration ±S.D. (n=2; technical repeats).*

## 4.3 Summary of Key Findings

- Cadmium exposure did not compromise the urothelial cell barrier, yet it could still cause MT-1 subfamily transcript and protein induction in differentiated NHU cells; suggesting that cadmium could potentially penetrate the protective epithelial barrier.
- Direct quantification of cadmium in the digested cell solution from exposed NHU cell sheets revealed an ~10-fold higher cadmium concentration compared to controls, despite the presence of a ‘tight’ urothelial barrier, further suggesting that cadmium could penetrate the protective urothelial barrier.

## 4.4 Discussion

### 4.4.1 The Ability of Cadmium to Penetrate an Intact Urothelial Barrier

The results from this chapter suggest that cadmium is able to penetrate an intact urothelial barrier. This contradicts previous studies which have investigated the effect of cadmium exposure on barrier function of other epithelial cells. One publication observed that different cadmium concentrations had opposing effects on the TER of Sertoli cells, as intermediate to high concentrations caused a decrease in TER and low concentrations resulted in an increased TER reading (Janecki et al., 1992). Another study found that exposure of renal epithelial cells to cadmium decreased TER, especially when cadmium was applied to the apical surface (Faurskov and Bjerregaard, 1997). A limitation of these studies is that the cells used were not human, but instead originated from rats and toads respectively, questioning the applicability of the findings to *in vivo* human exposure. However, these findings are also supported by a recent study which used primary normal human bronchial epithelial cells (Cao et al., 2015). These cells were used to develop in an *in vitro* air-liquid-interface airway tissue model, which was exposed to non-cytotoxic concentrations of cadmium. The authors found that exposure caused a collapse of barrier function, as monitored by TER, as well as decreased expression of tight junction markers such as ZO-1 (see section 3.1.2).

There is the possibility that the discrepancy in these findings may be due to the difference in the type of epithelium being tested. Urothelial cells are known to form one of the tightest epithelial barriers in the human body so that they may protect the underlying tissue from harmful constituents of the urine (see Introduction section 1.1.3), and thus maintenance of this barrier is essential. While other epithelium could be susceptible to cadmium-induced damage, the urothelium may be unique in its resistance. However, it should be noted that ICP-OES analysis was only conducted on an NHU cell culture from one individual donor; cultures from at least another two independent donors should therefore be analysed to verify this finding. Further, although cadmium was only applied apically to differentiated NHU cells after the development of a tight urothelial barrier (section 4.1.2), it is still possible that some cadmium may have entered the bottom chamber via the cell sheet edges and penetrated the cell sheets basally. This would have circumnavigated the need to cross the urothelial barrier, and thus future experiments should aim to remove the possibility of basal urothelial penetration by cadmium as an extraneous variable.

# Chapter 5: Specificity and Longevity of MT-1 Isoform Induction in Cadmium-Exposed NHU Cells.

## 5.1 Chapter Aims

The aims of this chapter were to investigate the specificity of MT-1 isoform induction in cadmium-exposed NHU cells, and to investigate how long this isoform induction persisted at both the transcript and protein level.

### 5.1.1 Objectives

1. Determine whether a variety of potential inducers can stimulate MT-1 isoform transcript and protein expression in NHU cells.
2. Compare MT-1 isoform transcript and protein induction caused by extraneous factors from Objective 1 to induction caused by cadmium, focusing on isoform specificity and extent of induction.
3. Analyse the arrangement of MTF-1 binding sites in MT-1 isoform genes as a potential mechanism of induction specificity.
4. Determine how long MT-1 isoform transcript and protein induction persists in NHU cells post-exposure to cadmium.

### 5.1.2 Experimental Approach

1. As reviewed in section 1.5.5.3, it has been suggested that the MT isoforms show differential induction depending on the causative agent. In order to determine the cadmium-specificity of the MT-1 target isoform induction identified in Chapters 4 and 5, it was important to establish whether other extraneous factors could also regulate MT-1 isoform expression. This was especially important for the MT-1A isoform, which had already demonstrated varied expression in control cells, suggesting factors other than cadmium exposure were able to regulate its transcript expression. Positive control genes were used to ensure NHU cell exposure to effective treatment concentrations where necessary (see Appendices section 8.4.1). A number of potential inducers identified from the literature (see section 1.5.5.3) were tested to determine their ability to induce MT-1 isoform transcript expression. If transcript expression was observed to be altered, protein expression was also investigated. All results from candidate inducers are summarised in section 5.2.2, Table 7. The ‘inducers’ tested and the experimental approach taken are summarised below:

a. **Cell Culture Conditions** – MT-1A transcript expression had varied under control conditions in previous experiments (see sections 3.2.2 and 3.2.3), and thus it was important to determine whether standard cell culture procedures such as medium change and passage may be able to influence MT-1 isoform expression. Proliferating NHU cells were cultured under standard conditions and underwent either a medium change or passage every 24 hours for 3 days. After the last passage, cells were left for 12 hours in order to allow them to adhere, meaning the total experimental time was 84 hours. A separate culture of NHU cells was exposed to 10 µM $CdCl_2$ throughout this time period without undergoing any cell culture procedures, so that MT-1 isoform induction could be compared between cadmium exposure and the cell culture procedures. At the end of the experiment RNA and protein were extracted for analysis using RT-PCR and western blotting. A flow chart summarising the experimental plan is shown below in Figure 37.

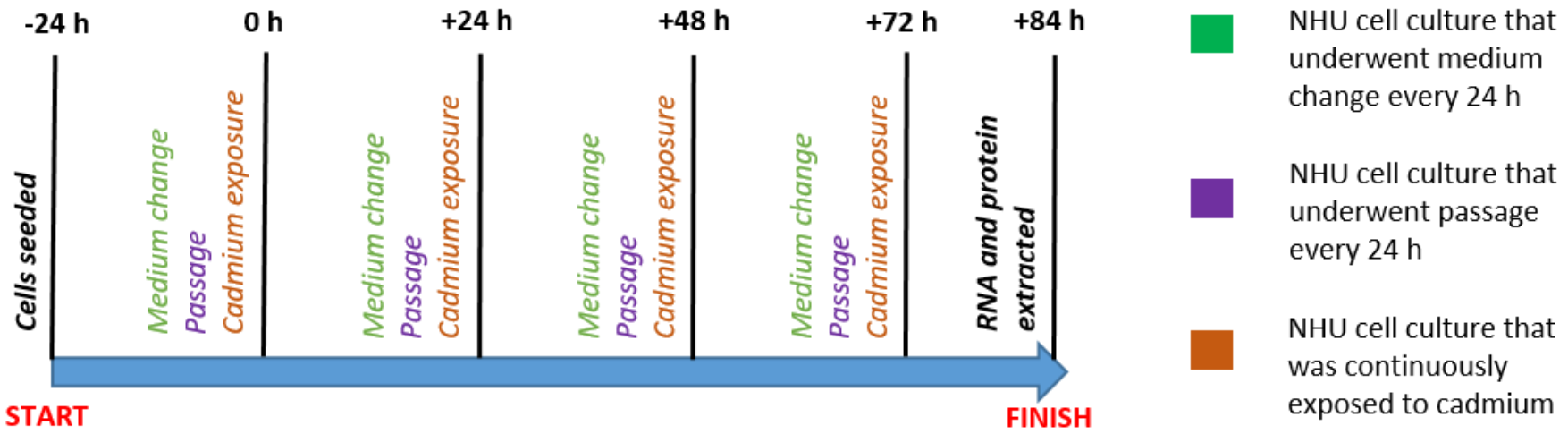


***Figure 37: Flow diagram summarising the experimental plan for assessing the ability of standard cell culture procedures to influence MT-1 isoform transcript induction.*** *Three proliferating NHU cell cultures were seeded and left to adhere for 24 h. One cell culture underwent medium change every 24 h and one cell culture underwent passage every 24 h. This was performed for 72 h, and cells were then left for 12 h post final medium change/passage so that passaged cells could adhere before lysis. This resulted in a total experimental timeline of 84 h. A third cell culture was exposed to 10 µM $CdCl_2$ continuously throughout the experiment. At 84 h all cell cultures were lysed and RNA and protein extracted.*

b. **Reactive Oxygen Species** - The ability of reactive oxygen species (ROS) to induce MT isoform expression was determined. This was particularly important to establish, as cadmium exposure is reported to indirectly induce ROS via inhibition of the mitochondrial electron transfer chain (Wang et al., 2004; Heyno et al., 2008). Therefore, it was essential to determine whether MT isoform induction in cadmium-exposed NHU cells was due to increased cellular ROS, or due to cadmium itself. To investigate this, the ROS-inducing chemical sulforaphane was titrated using NHU cell cultures in order to identify a concentration that induced similar levels of ROS to cadmium exposure (5 µM; see Appendices section 8.6.2). ROS induction was inferred using transcript expression of the ROS-sensitive heme oxygenase-1 (HMOX1) gene (Ryter and Choi, 2005; Sarma et al., 2011). Proliferating NHU cells were then exposed to either 10 µM $CdCl_2$ or 5 µM sulforaphane for 12 hours, and RNA extracted for RT-PCR analysis. To further determine whether ROS could cause MT-1 subfamily induction, a second experimental approach was taken. This involved exposure to cadmium in the presence of the ROS-scavenger ascorbic acid. The ascorbic acid concentration was based on preliminary titration work that identified a concentration that could inhibit cadmium-induced ROS (25 µg/mL; see Appendices section 8.7.2), as inferred by HMOX1 transcript expression. Proliferating NHU cells were then exposed to 10 µM $CdCl_2$ either alone or in combination with 25 µg/mL ascorbic acid for 12 hours and RNA extracted.

c. **Hypoxia** - Another factor that has been proposed to induce MT expression is hypoxia (see section 1.5.5.3). To investigate whether hypoxic conditions could induce MT-1 subfamily expression, proliferating NHU cells were cultured in a hypoxic incubator where atmospheric oxygen ($O_2$) was maintained at 2 %. A separate NHU cell culture was exposed to 10 µM $CdCl_2$ under normal cell culture conditions, and after 12 hours RNA was extracted from both cultures for analysis. HIF-1α gene transcript expression was used as a positive control for hypoxia (see Appendices section 8.4.1).

d. **Steroids and Hormones** - The literature has also suggested that both glucocorticoids and cytokines may be able to induce MT expression (see section 1.5.5.3). To assess whether these factors could cause MT-1 subfamily expression, proliferating NHU cells were exposed to two reported inducers;

either the glucocorticoid dexamethasone (Dex) or the cytokine interleukin-1β (IL-1β). Both these substances were titrated prior to use (see Appendices section 8.4.2) in order to determine functional concentrations capable of altering target gene expression (Figure 43A). Cells were either exposed to one of these agents or 10 µM $CdCl_2$ for 12 hours and RNA extracted for RT-PCR analysis.

e. **Essential Metals** – Previous studies had reported that some essential metals such as zinc were able to induce MT-1 isoform expression. The next step was therefore to determine whether the addition of essential metals at the same exogenous concentration as cadmium (10 µM) could induce MT-1 isoform expression, and if so, whether to the same extent. Proliferating NHU cells were exposed to either 10 µM cadmium ($CdCl_2$), copper ($CuSO_4$), iron ($FeSO_4$) or zinc ($ZnCl_2$) for 12 hours and RNA extracted.

f. **Other Heavy Metals** - As it is well documented that heavy metals can cause induction of MT (section 1.5), it was decided to investigate whether exposure to other occupationally-related carcinogenic heavy metals could also induce transcript expression of the MT-1 target isoforms, and whether induction was comparable to that caused by cadmium exposure. Proliferating NHU cells were exposed to a range of non-cytotoxic concentrations of either sodium arsenite ($NaAsO_2$; 0.25 – 2 µM) or nickel ($NiCl_2$; 25 – 200 µM; Dally and Hartwig, 1997; Gadhia et al., 2012; Severson et al., 2012; Treas et al., 2012; also determined by previous experiments in the laboratory) for 12 hours and RNA extracted.

2. To confirm the specificity of MT-1 isoform transcript induction, and to determine whether these changes were translated to protein expression, all factors that were capable of inducing MT-1 isoform transcript expression were compared in the same experiment. Proliferating NHU cells were exposed to either 10 µM $CdCl_2$, 10 µM $CuSO_4$, 10 µM $FeSO_4$, 10 µM $ZnCl_2$, 2 µM $NaAsO_2$, 200 µM $NiCl_2$ or 5 µM sulforaphane for 72 hours. RNA and protein were then extracted for analysis.
3. To further investigate the initial findings of differential MT-1 isoform induction, and potentially identify a regulatory mechanism, bioinformatics was used to determine the presence and spatial arrangement of MTF-1 binding sites in the non-coding DNA region upstream of MT-1 isoform genes (see section 1.5.3). The rVISTA (v. 2.0) computer web tool was used for this approach

(http://genome.lbl.gov/vista/index.shtml). The tool works by identifying all transcription factor binding sites (TFBSs) in target genes using positional weight matrices from the TRANSFAC® database (Figure 38). TFBSs are then selected based on criteria such as local alignment and high DNA conservation, and the tool produces a list of transcription factors (TFs) that have binding sites within the target genes. The user then selects which TF(s) they are interested in, and the programme produces a graphical display of the TFBSs for this selected TF(s) within the target genes. These displays can then be used to compare target genes and identify shared and unique TFBSs for the specific TF(s) in question. For this thesis, MTF-1 binding sites were compared between the MT-1 target isoforms (MT-1A, MT-1G, MT-1H, MT-1M), focusing specifically on the MT-1A and MT-1M isoforms. MT-1A and MT-1M were each compared to the other MT-1 isoforms individually as 'cases', with the aim of identifying any unique MTF-1 binding sites in the gene promoters. Unique MTF-1 binding sites were identified in each case by comparing the location of all MTF-1 binding sites (denoted by MTF1_all) to the location of shared binding sites (denoted by MTF1_aligned and MTF1_conserved). Any unique binding sites observed in the individual cases were then compared to MTF-1 binding sites from all cases, to confirm if they were truly unique and not present in any of the other isoforms.

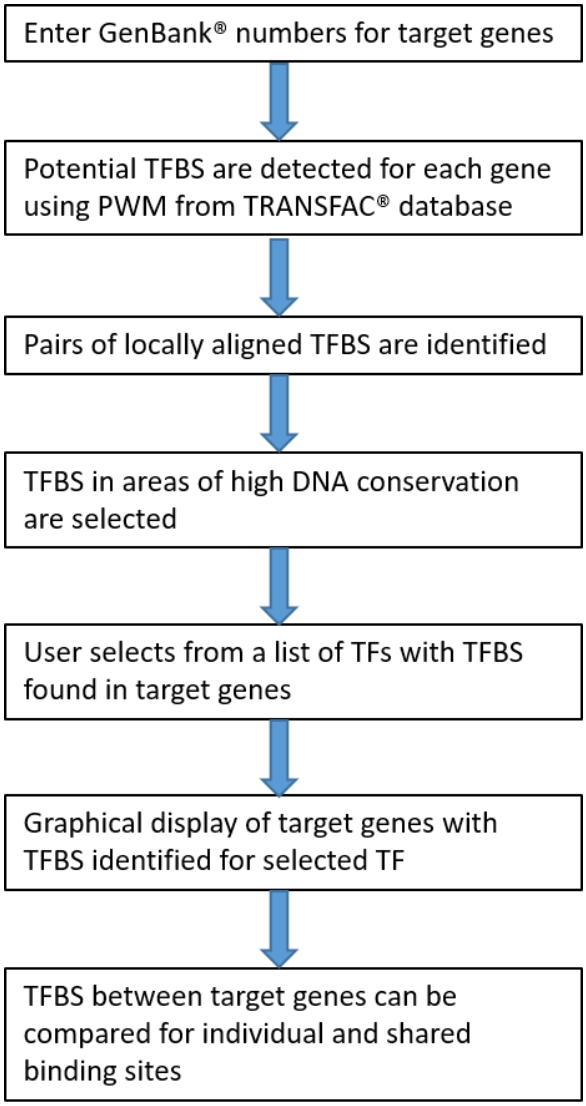


***Figure 38: Diagram showing the workflow for using the rVISTA (v. 2.0) web tool.*** *The purpose of the web tool is to identify transcription factor (TF) binding sites (TFBSs) in target genes, allowing gene comparisons and unique binding sites to be found. The tool firstly identifies all TFBSs in the target genes using positional weight matrices (PWM) obtained from the TRANSFAC® database. TFBSs are then filtered using local alignment and DNA conservation. The programme then provides the user with a list of TFs that have binding sites within the target genes, and the user can select which TF(s) they wish to analyse. Graphical displays are produced which show all TFBSs for the TF(s) in question within the non-coding DNA of target genes, allowing comparisons of TFBSs to be made. Website: http://genome.lbl.gov/vista/index.shtml.*

4. The longevity of MT-1 target isoform induction was investigated in order to determine whether expression persisted post-cadmium exposure. This was important to investigate in order to assess their potential use as biomarkers of cadmium exposure, as not all occupational heavy metal exposure is current. Longevity of MT-

1 isoform expression was determined in both proliferating and differentiated NHU cells as both cell phenotypes are found *in vivo* in human urothelium (see Introduction; section 1.1.2), and additionally that any dilutive effects caused by cell division could be observed and eliminated as an extraneous effect.

a. **Transcript Expression** - MT-1 isoform transcript longevity was first assessed. Proliferating NHU cells were pre-exposed to 10 µM $CdCl_2$ for 24 hours before removal of cadmium (time-point 0 h). Cells were then further cultured for 48 hours, and RNA extracted at various time-points. MT-1 isoform transcript expression post-cadmium exposure was also assessed in differentiated NHU cells. To achieve this, differentiated NHU cell cultures were apically exposed to 10 µM $CdCl_2$ for 3 days (0 d), before removal of exposure and continued culturing for up to 11 days. A description of the method used for NHU cell differentiation and apical cadmium exposure can be found in Chapter 5 (section 5.1.2). RNA was extracted at various time-points for RT-PCR analysis.

b. **Protein Expression** - The next step was to determine the longevity of MT-1A and MT-1M protein induction post-exposure to cadmium. This was firstly investigated in undifferentiated NHU cells; proliferating NHU cells that had been allowed to reach confluence prior to exposure. The purpose of allowing confluence to be reached was to prevent protein dilution due to cell proliferation post-exposure, as protein dilution could be falsely interpreted as a decrease in protein expression. Once NHU cells had reached confluence they were exposed to 10 µM $CdCl_2$ for 72 hours, before removal of exposure and continued culturing for a further 5 days. Protein was then extracted and western blotting performed. The longevity of MT protein expression was also investigated in differentiated NHU cell cultures. Upon differentiation (confirmed by TER measurements), NHU cell cultures were apically exposed to 10 µM $CdCl_2$ for 3 days (0 d time-point). Cadmium was then removed from the medium and the differentiated cell sheets cultured for another 4 days. Protein lysates were extracted both before and after removal of exposure and MT-1A and MT-1M protein expression determined. Immunohistochemistry was also performed to assess MT-1A and MT-1M protein longevity. Differentiated NHU cells were apically exposed to 10 µM $CdCl_2$ for 3 days before removal of exposure and continued culturing for 4 days. NHU cell

sheets were then fixed and immunolabelled for MT-1A and MT-1M protein expression.

## 5.2 Results

### 5.2.1 Effect of Candidate Inducers on MT-1 Isoform Expression to Investigate Isoform Specificity

#### *5.2.1.1 Cell Culture Conditions*

NHU cell culture medium change caused induction of all MT-1 transcripts, although induction of the MT-1H and MT-1M transcripts was minimal (Figure 39A; n=1). However, induction of all isoforms was not as prominent as when NHU cells were exposed to cadmium. The results also indicated that passage resulted in downregulation of MT-1A transcript expression. Despite these changes in MT-1A transcript expression, MT-1H and MT-1M isoforms were unaffected by cell culture procedures, and transcript induction only induced by cadmium exposure.

As MT-1A transcript expression was altered by both medium change and passage, it was important to determine whether these changes were translated to MT-1A protein expression. Western blotting indicated low relative levels of MT-1A protein in both control and medium change cell cultures, and a slight upregulation of protein expression in the passaged cell culture (Figure 39B; n=1). However, quantification of protein expression using densitometry revealed that both medium change and passage were unable to increase MT-1A protein expression (Figure 39C; n=1). By contrast, western blotting clearly demonstrated a high induction of MT-1A protein expression in cells exposed to cadmium, which was supported by densitometry analysis.

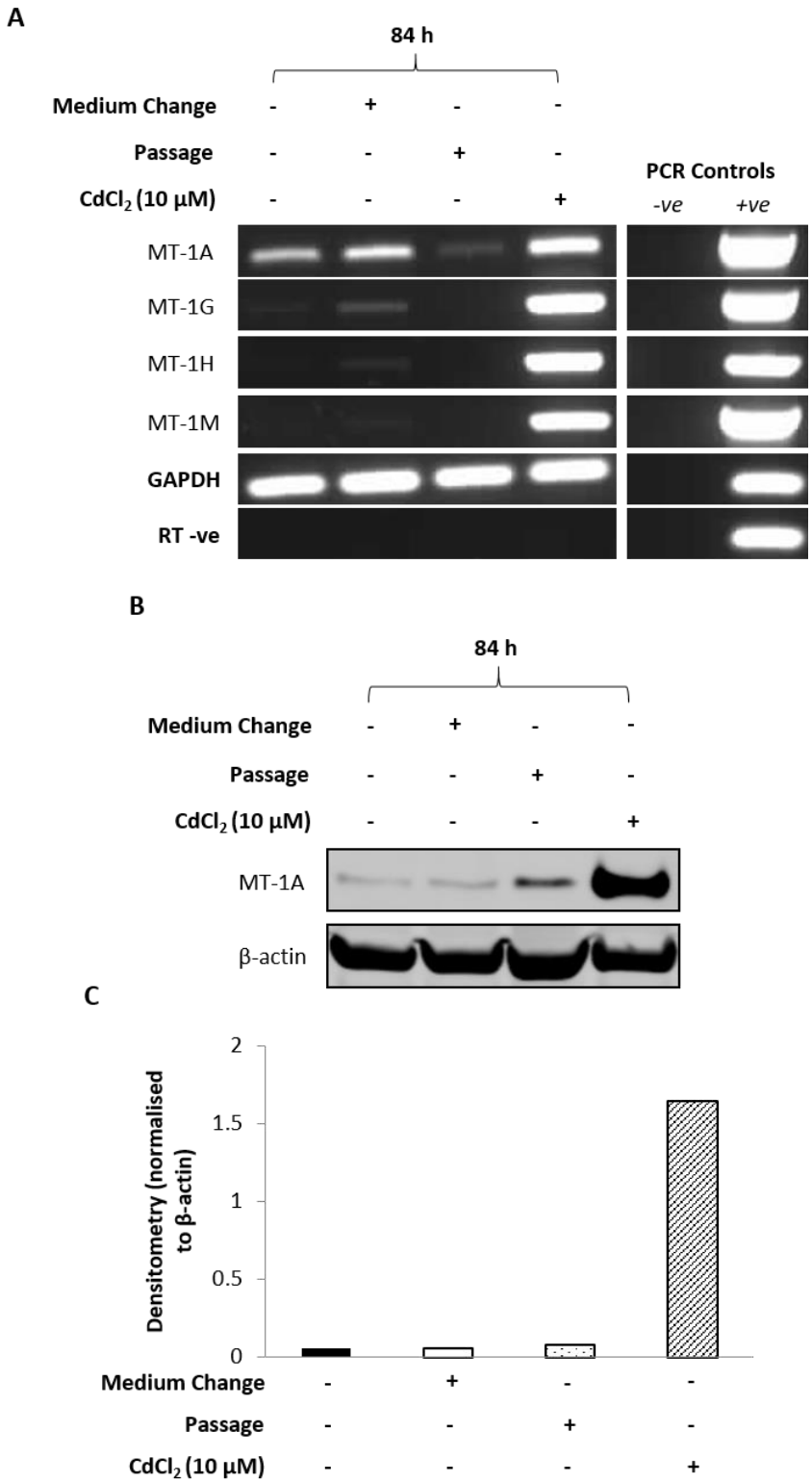


***Figure 39: The effects of cell culture conditions on MT isoform transcript and protein expression in NHU cells.*** *Proliferating NHU cells (n=1; Y1483) were cultured in vitro, and were either medium changed or passaged every 24 hours for a total of 3 days. After the final subculture, cells were allowed to settle and adhere for 12 hours before RNA and protein extraction, meaning the total experimental period was 84 hours. A parallel NHU cell culture was continuously exposed to 10 µM $CdCl_2$ in order to compare MT-1 isoform transcript and protein expression.*

*(A) Transcript expression was assessed by RT-PCR for MT-1 target isoforms. PCR controls included genomic DNA as a positive control and $dH_2O$ as a negative control. GAPDH transcript expression was used as a loading control, and RT-ve samples confirmed the absence of genomic contamination. (B) MT-1A transcript changes were investigated at the protein level by western blotting, and (C) densitometry was performed to quantify MT-1A protein expression.*

#### *5.2.1.2 Reactive Oxygen Species*

HMOX1 gene transcription was induced by both cadmium and Sulforaphane, suggesting that ROS was induced by both treatments (Figure 40A; n=3). Sulforaphane-induced ROS caused induction of both MT-1A and MT-1G transcription . However, this induction was decreased in comparison to cadmium-induced transcription. MT-1H and MT-1M transcription also showed some transcript induction in response to ROS exposure, however this was only minimal, and once again cadmium demonstrated a more striking induction of transcription.

It was important to determine whether the induction of MT-1A transcript expression by ROS was translated to MT-1A protein expression. To achieve this, proliferating NHU cells were exposed to 5 µM Sulforaphane for 72 hours (allowing sufficient time for protein translation) and protein extracted for analysis. Western blotting of protein lysates showed that ROS exposure did not cause induction of MT-1A protein expression (Figure 40B; n=2). This observation was further supported when the immunoblot was analysed by densitometry and corrected for loading, as MT-1A protein expression was observed to slightly decrease in ROS-exposed cells (Figure 40C). However, in cadmium-exposed NHU cells there was a high induction of MT-1A protein expression, as observed in previous results (sections 3.2.4 and 4.2.2). This suggested that although ROS was capable of inducing MT-1A transcript expression, these changes were not translated to protein expression (n=2).

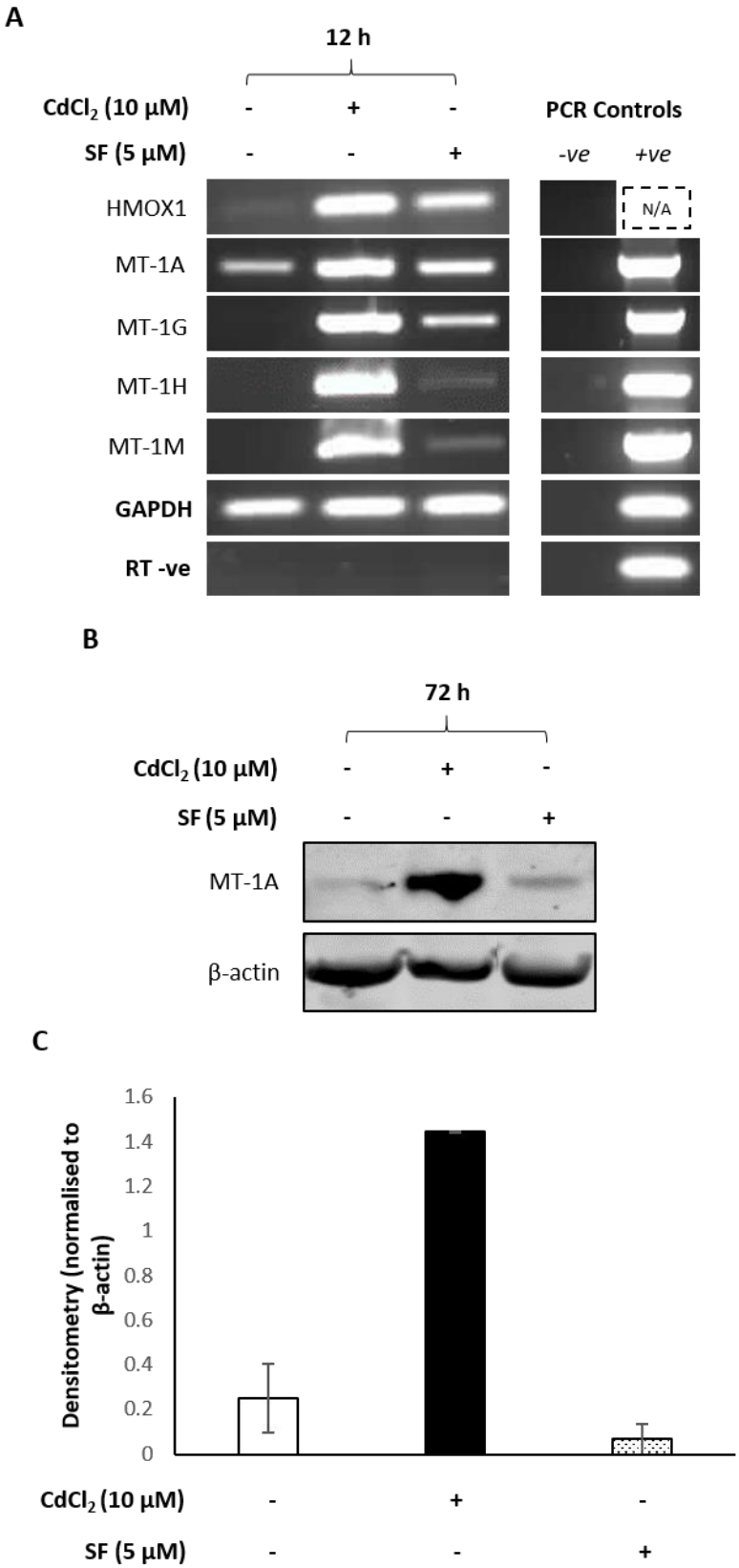


***Figure 40: The effect of reactive oxygen species (ROS) on MT-1 isoform transcript and protein expression in NHU cells.*** *(A) Representative RT-PCR showing the effects of ROS on MT isoform transcript expression. The chemical sulforaphane (SF) was used to induce ROS, having been titrated to a concentration that mimicked the amount of cadmium-induced ROS (determined by*

*transcript expression of the target gene HMOX1; section 8.4.1). Proliferating NHU cells (n=3; Y1426, Y1344, Y1526) were treated with either 10 µM $CdCl_2$ or 5 µM Sulforaphane for 12 hours and RNA extracted for analysis. The production of ROS was confirmed using HMOX1 gene transcript expression. PCR controls included genomic DNA as a positive control and $dH_2O$ as a negative control. GAPDH transcript expression was used as a loading control, and RT-ve samples confirmed the absence of genomic contamination. A positive genomic DNA control for HMOX1 expression was not possible due to intron-spanning primers (N/A; not applicable). Representative NHU cell line was Y1426 (results from other cell lines are included in the Appendices). (B) Representative western blot showing the effects of ROS on MT-1A protein expression. Proliferating NHU cells (n=2; Y1426, Y1526) were treated with 5 µM Sulforaphane or 10 µM $CdCl_2$ for up to 72 hours and western blotting performed. Representative NHU cell line was Y1426 (results from other cell lines are included in the Appendices). (C) Densitometry was performed in order to quantify and compare MT-1A protein expression induced by ROS and cadmium (n=2; Y1426, Y1526).*

To further determine whether ROS could cause MT-1 subfamily induction, the ROS-scavenger ascorbic acid was used to inhibit cadmium-induced ROS, and MT-1 isoform induction assessed. RT-PCR confirmed successful inhibition of cadmium-induced ROS, as indicated by the reduction in HMOX1 transcript expression (Figure 41). The results also suggested that a reduction in cadmium-induced ROS did not inhibit induction of MT-1 isoform transcript expression (n=1). All isoforms showed high transcript induction in both conditions, and this expression did not change with ROS inhibition.

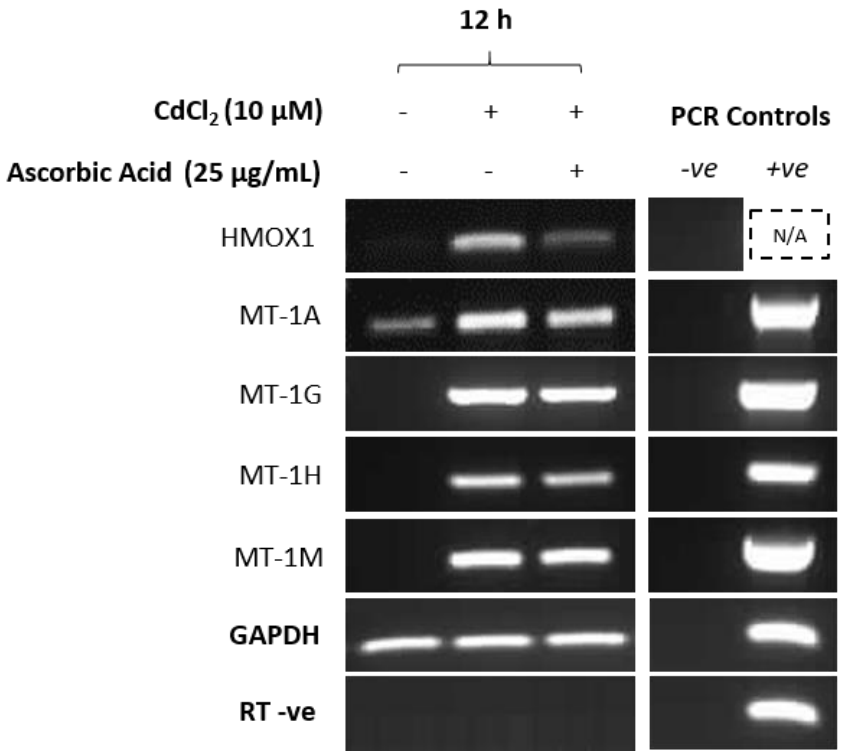


***Figure 41: RT-PCR showing the effects of inhibition of cadmium-induced reactive oxygen species (ROS) on MT-1 isoform transcript expression.*** *Proliferating NHU cells (n=1; Y1526) were exposed to 10 µM $CdCl_2$ for 12 hours either alone or in combination with 25 µg/mL ascorbic acid. Ascorbic acid is a ROS scavenger and was previously titrated to a concentration that inhibited ROS induction by cadmium exposure (see Appendices, section 8.4.2). Transcript expression of the ROS-sensitive gene HMOX1 was used to infer ROS production. PCR controls included genomic DNA as a positive control and $dH_2O$ as a negative control. GAPDH transcript expression was used as a loading control, and RT-ve samples confirmed the absence of genomic contamination.*

### *5.2.1.3 Hypoxia*

RT-PCR showed that whereas cadmium could cause a prominent induction of all MT-1 isoform target genes, hypoxia was unable to induce expression of any of these genes (Figure 42; n=1). Hypoxia was confirmed by induction of the hypoxia-sensitive HIF-1α gene.

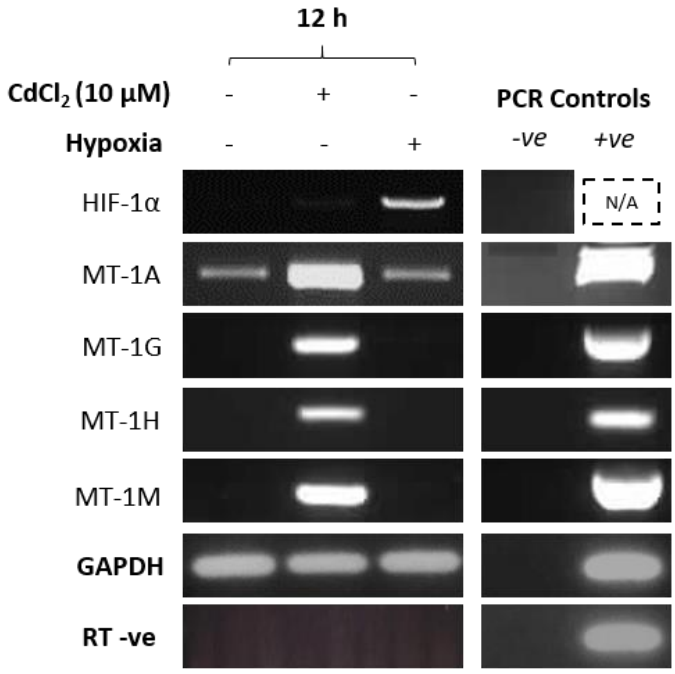


***Figure 42: RT-PCR showing the effects of hypoxia on MT-1 isoform transcript expression in NHU cells.*** *Proliferating NHU cells (n=1; Y1594) were exposed to either hypoxia (2 % $O_2$) or 10 µM $CdCl_2$ for 12 hours, and MT-1 isoform transcript expression assessed. HIF-1α gene expression was used to confirm hypoxic conditions (see Appendices, section 8.4.1). PCR controls included genomic DNA as a positive control and $dH_2O$ as a negative control. GAPDH transcript expression was used as a loading control, and RT-ve samples confirmed the absence of genomic contamination. A positive genomic DNA control for HIF-1α expression was not possible due to intron-spanning primers (N/A; not applicable).*

### *5.2.1.4 Dexamethasone (Glucocorticoid) and Cytokine IL-1β (Hormone)*

Successful treatment of NHU cells with functional concentrations of both Dexamethasone and IL-1β was confirmed using target gene transcript expression (Figure 42A). The usual induction of MT-1 isoform transcript expression by cadmium exposure was observed, however treatment with Dexamethasone or IL-1β demonstrated no induction of the isoforms (Figure 43B; n=1). The results therefore suggested that this specific glucocorticoid and cytokine were unable to induce MT-1 isoform target gene expression.

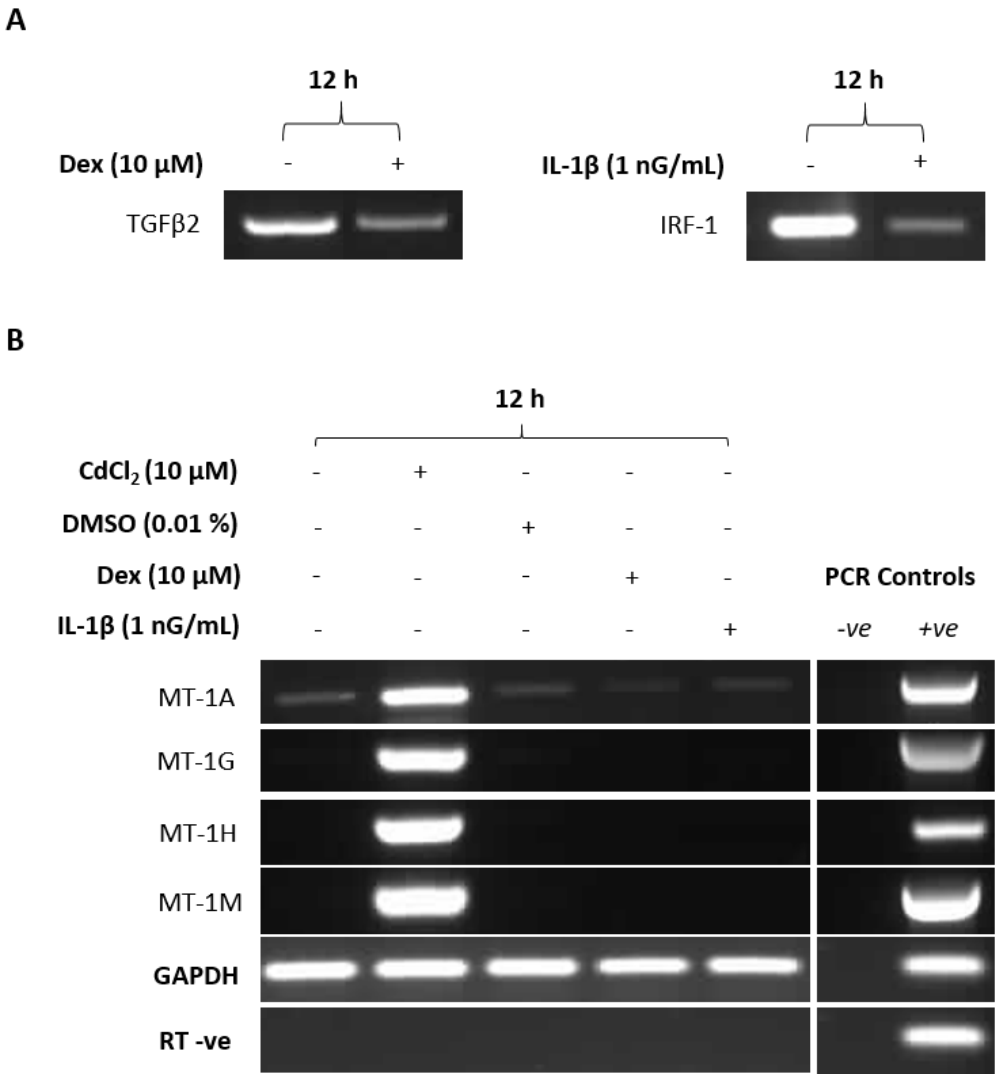


***Figure 43: RT-PCR showing the effects of glucocorticoid and cytokine treatment on MT-1 isoform transcript expression in NHU cells.*** *Proliferating NHU cells (n=1; Y1426) were cultured with either 10 µM $CdCl_2$, 10 µM Dexamethasone (Dex; glucocorticoid) or 1 nG/mL IL-1β (cytokine) for 12 hours. As the vehicle for dexamethasone, dimethyl sulphoxide (DMSO) treatment was included as a control. (A) Dexamethasone and IL-1β were titrated prior to use (see Appendices, section 8.4.2) in order to determine functional concentrations that were capable of altering target gene transcript expression. (B) MT-1 isoform transcript expression was assessed to determine whether either Dexamethasone or IL-1β could cause induction comparable to cadmium exposure. PCR controls included genomic DNA as a positive control and $dH_2O$ as a negative control. GAPDH transcript expression was used as a loading control, and RT-ve samples confirmed the absence of genomic contamination.*

### *5.2.1.5 Essential Metals*

RT-PCR analysis indicated that the MT-1 isoforms demonstrated differential induction depending upon the specific metal exposure (Figure 44; n=2). For example, MT-1G transcript expression was induced by both copper and zinc treatment, but not iron. Moreover, zinc was capable of inducing MT-1G transcript expression to a similar extent to cadmium exposure. Zinc was also the only essential metal able to induce either MT-1H or MT-1M transcript expression, but this induction was minimal compared to cadmium-induced expression. Lastly, all the essential metals tested were able to upregulate MT-1A transcript expression, although not to the same extent as cadmium exposure.

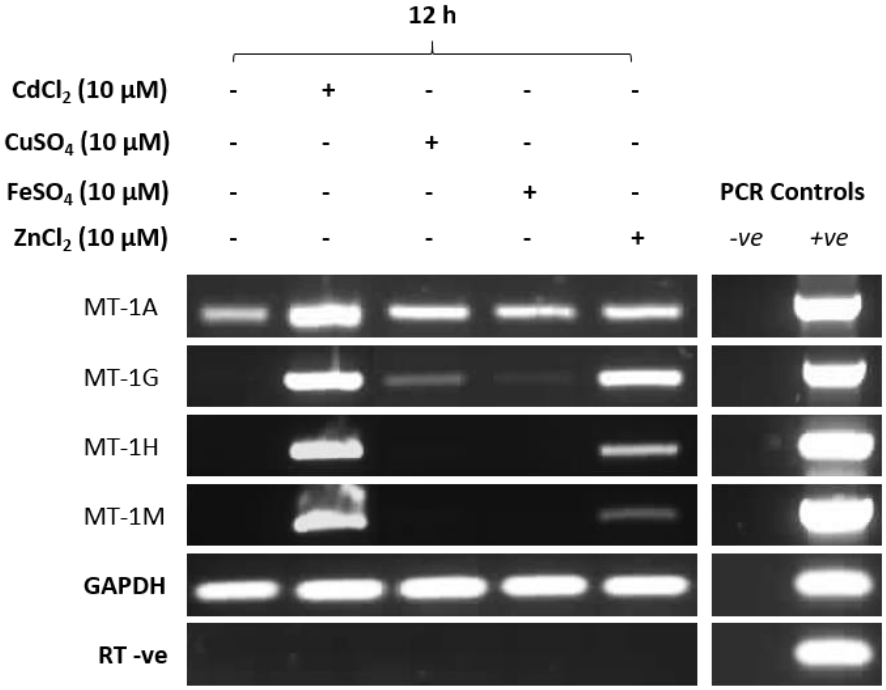


***Figure 44: RT-PCR showing the effects of essential metal exposure on MT-1 isoform transcript expression in NHU cells.*** *Essential metals copper, iron or zinc were added to NHU cell culture at the same exogenous concentration as cadmium, in order to determine whether they could also induce MT-1 isoform transcript expression. Proliferating NHU cells (n=2; Y1426, Y1526) were exposed to either 10 µM $CdCl_2$, 10 µM $CuSO_4$, 10 µM $FeSO_4$, or 10 µM $ZnCl_2$ for 12 hours and RNA extracted for RT-PCR. PCR controls included genomic DNA as a positive control and $dH_2O$ as a negative control. GAPDH transcript expression was used as a loading control, and RT-ve samples confirmed the absence of genomic contamination. Representative cell line was Y1426 (results from the other cell line are shown in Figure 46).*

### *5.2.1.6 Other Heavy Metals*

RT-PCR showed that the NHU cell line used in this experiment demonstrated constitutive expression of MT-1A transcript, which remained unaffected by exposure to either arsenite or nickel (Figure 45). However, MT-1G, MT-1H and MT-1M transcript expression demonstrated a dose-response relationship to both arsenite and nickel exposure (n=1). Preferential metal induction of MT-1 isoforms was again observed, as exposure to the highest non-cytotoxic concentration of nickel was capable of inducing MT-1H and MT-1M transcripts to a greater extent than the highest non-cytotoxic concentration of arsenite. Indeed, MT-1M transcript expression remained largely unaffected by arsenite exposure (n=2).

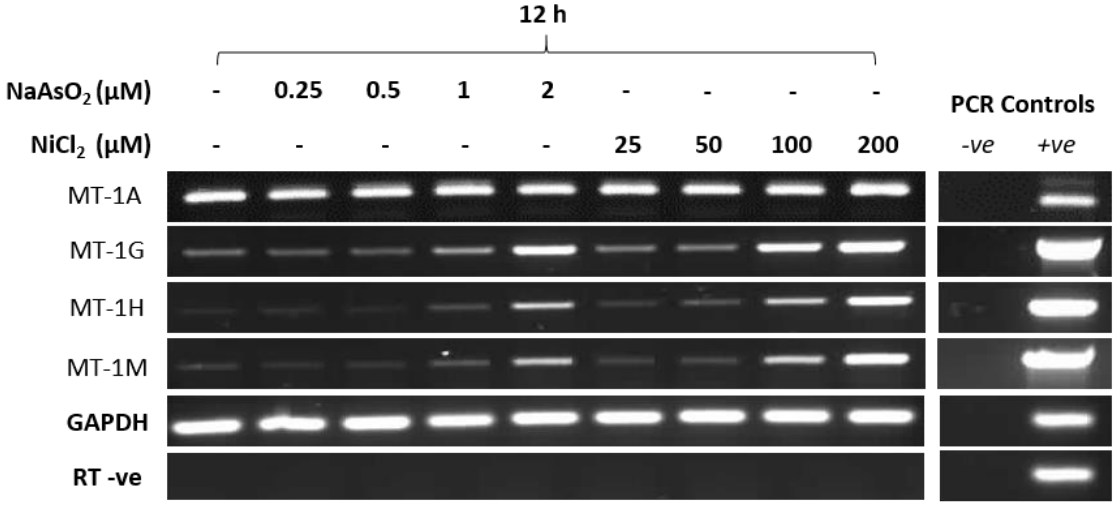


***Figure 45: Representative RT-PCR showing the effects of exposure to the carcinogenic metals arsenite and nickel on MT-1 isoform transcript expression in NHU cells.*** *Proliferating NHU cells (n=2; Y1344, Y1526) were exposed to a range of non-cytotoxic concentrations of arsenite (0.25 µM – 2 µM; $NaAsO_2$) and nickel (25 µM – 200 µM; $NiCl_2$) for 12 hours and MT-1 isoform transcript expression assessed. Non-cytotoxic concentrations were established using the literature (see section 5.1.2) and previous experiments in the laboratory. PCR controls included genomic DNA as a positive control and $dH_2O$ as a negative control. GAPDH transcript expression was used as a loading control, and RT-ve samples confirmed the absence of genomic contamination. Representative NHU cell line was Y1344 (results from the other cell line are shown in Figure 46).*

### 5.2.2 Comparison of MT-1 Isoform Induction by Cadmium and other Candidate Inducers

The RT-PCR results further supported differential induction of the MT-1 isoforms (Figure 46A; n=2). For example, MT-1G transcript was induced by cadmium, zinc, nickel and SF-induced ROS. By contrast, MT-1M transcript expression was only strongly induced by cadmium exposure, although there was minimal induction by zinc. MT-1A isoform transcription was constitutively minimal, but similar to MT-1M, could only be strongly upregulated by cadmium and zinc. MT-1H showed high induction by cadmium, but also some minimal induction by both zinc and SF-induced ROS. Neither of the heavy metals tested were observed able to induce transcript expression of MT-1A, MT-1H or MT-1M (n=1), which contradicts the previous findings (Figure 45). Overall the RT-PCR data further suggested that MT-1M transcript expression was highly specific to cadmium exposure, and though MT-1A transcript expression appeared less specific, it demonstrated preferential induction by cadmium.

Initial MT-1A protein expression results had suggested that the transcript expression changes caused by candidate inducers were not translated (Figures 39 and 40). It was important however to determine the specificity of both MT-1A and MT-1M protein expression as well as transcript. Western blotting showed that low amounts of MT-1A protein could be detected in control, zinc, arsenite and SF-induced ROS conditions; however, protein expression was also strikingly high in cadmium-exposed cells (Figure 46B; n=2). MT-1M protein exposure also showed prominent induction in NHU cells exposed to cadmium. However, in contrast to MT-1A protein, no expression of MT-1M protein was detected under other conditions. Densitometry was therefore only performed to quantify and compare MT-1A protein expression between the conditions (Figure 46C; n=2). Densitometry revealed that MT-1A protein was minimally expressed under baseline conditions, and that no treatments other than cadmium could increase its expression, which caused ~6 times higher MT-1A protein abundance.

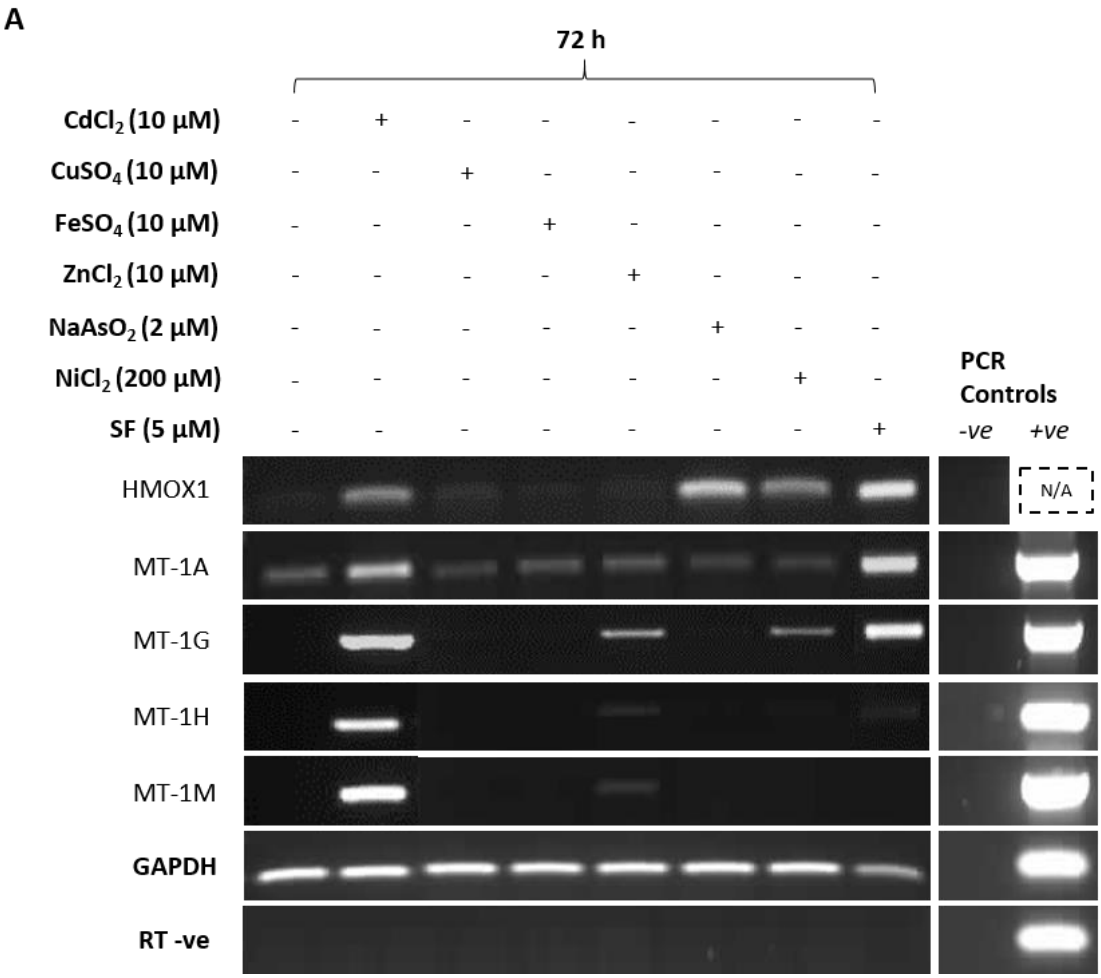
A
72 h
CdCl2 (10 µM)
CuSO4 (10 µM)
FeSO4 (10 µM)
ZnCl2 (10 µM)
NaAsO2 (2 µM)
NiCl2 (200 µM)
SF (5 µM)
PCR Controls
-ve
+ve
N/A
HMOX1
MT-1A
MT-1G
MT-1H
MT-1M
GAPDH
RT -ve

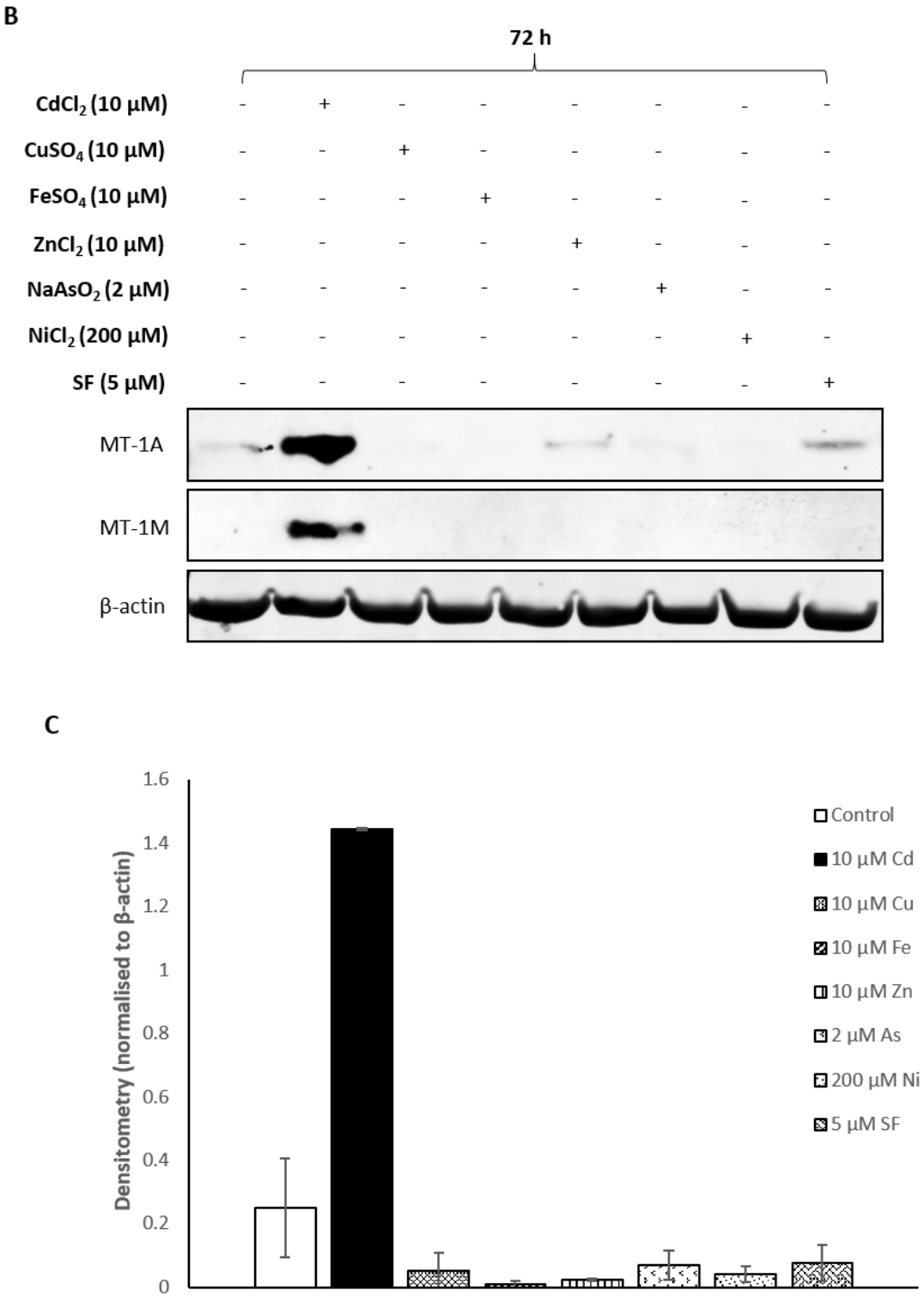


***Figure 46: A comparison of MT-1 isoform expression in NHU cells exposed to a variety of potential inducers.*** *Factors that had been found capable of inducing MT-1A or MT-1M isoform transcript expression in previous experiments were assessed in order to compare transcript induction and determine if changes were translated to protein expression. Proliferating NHU cells were exposed to either $CdCl_2$ (10 µM), $CuSO_4$ (10 µM), $FeSO_4$ (10 µM), $ZnCl_2$ (10 µM), $NaAsO_2$ (2 µM), $NiCl_2$ (200 µM), or SF (5 µM) for 72 hours, and RNA and protein extracted. (A)*

*Representative RT-PCR showing MT-1 target isoform transcript expression in NHU cells. PCR controls included genomic DNA as a positive control and $dH_2O$ as a negative control. GAPDH transcript expression was used as a loading control, and RT-ve samples confirmed the absence of genomic contamination. Representative NHU cell line was Y1526 (results from other cell lines can be seen earlier in the chapter in Figures 44 and 45). (B) Representative western blot showing MT-1A and MT-1M protein expression in NHU cells. Representative NHU cell line was Y1426. (C) Densitometry was performed in order to quantify and compare MT-1A protein expression between the different potential inducers (n=2; Y1426, Y1526).*

***Table 5: Summary of MT-1 isoform potential inducers.*** *Table showing the different factors tested for their ability to induce MT-1A, MT-1G, MT-1H and MT-1M isoform expression. The concentration of each factor is given (where appropriate), and whether it could influence MT-1 isoform expression at the transcript and/or protein level. For each result the 'n' number (biological repeats) is provided. Results which are starred (*) denote mixed findings.*

| **Potential Inducer** | **Concentration Used** | **Isoform(s) with Altered Transcript Expression** | **Isoform(s) with Altered Protein Expression** |
|---|---|---|---|
| **Medium Change** | N/A; 4x | MT-1A, MT-1G (n=1) | None (n=1) |
| **Passage** | N/A; 4x | None (n=1) | None (n=1) |
| **ROS**<br>**1. Induction (sulforaphane)**<br>**2. Inhibition (ascorbic acid)** | 1. 5 µM<br>2. 25 µg/mL | 1. MT-1A, MT-1G (n=3)<br>2. None (n=1) | 1. None (n=2)<br>2. Not tested |
| **Hypoxia** | N/A; 2 % $O_2$ | None (n=1) | Not tested |
| **Dexamethasone (Glucocorticoid)** | 10 µM | None (n=1) | Not tested |
| **IL-1β (Cytokine)** | 1 ng/mL | None (n=1) | Not tested |
| **Copper ($CuSO_4$)** | 10 µM | MT-1A, MT-1G (n=2) | None (n=2) |
| **Iron ($FeSO_4$)** | 10 µM | MT-1A (n=2) | None (n=2) |
| **Zinc ($ZnCl_2$)** | 10 µM | MT-1A, MT-1G, MT-1H, MT-1M (n=2) | None (n=2) |

| | | | |
|---|---|---|---|
| **Arsenite ($NaAsO_2$)** | 2 µM | *MT-1G, MT-1H, MT-1M (n=1)<br>None (n=1) | None (n=2) |
| **Nickel ($NiCl_2$)** | 200 µM | *MT-1G, MT-1H, MT-1M (n=1)<br>None (n=1) | None (n=2) |
| **Cadmium ($CdCl_2$)** | 10 µM | MT-1A, MT-1G, MT-1H, MT-1M (n= >3) | MT-1A, MT-1M (n= >3) |

### 5.2.3 Presence and Spatial Arrangement of MTF-1 Binding Sites in MT-1 Isoform Genes as a Potential Mechanism of Differential Induction

Analysis of MTF-1 binding sites in the X1000 bp upstream non-coding DNA of the MT-1A isoform gene showed that it contained 1 unique TFBS compared to MT-1G, no unique TFBSs compared to MT-1H, and 4 unique TFBSs compared to MT-1M (Figure 47A). However, upon comparison of TFBSs from all isoforms combined, it was found that no TFBSs were truly unique to MT-1A. MT-1M analysis revealed that its non-coding DNA contained 13 unique TFBSs compared to MT-1A, 10 unique TFBSs compared to MT-1G, and 9 unique TFBSs compared to MT-1H (Figure 47B). Upon comparison to the TFBSs from all isoforms, it was found that MT-1M contained 9 truly unique MTF-1 binding sites in its gene promoter. Moreover, MT-1M contained 29 MTF-1 binding sites overall, whereas MT-1A only contained 17.

A

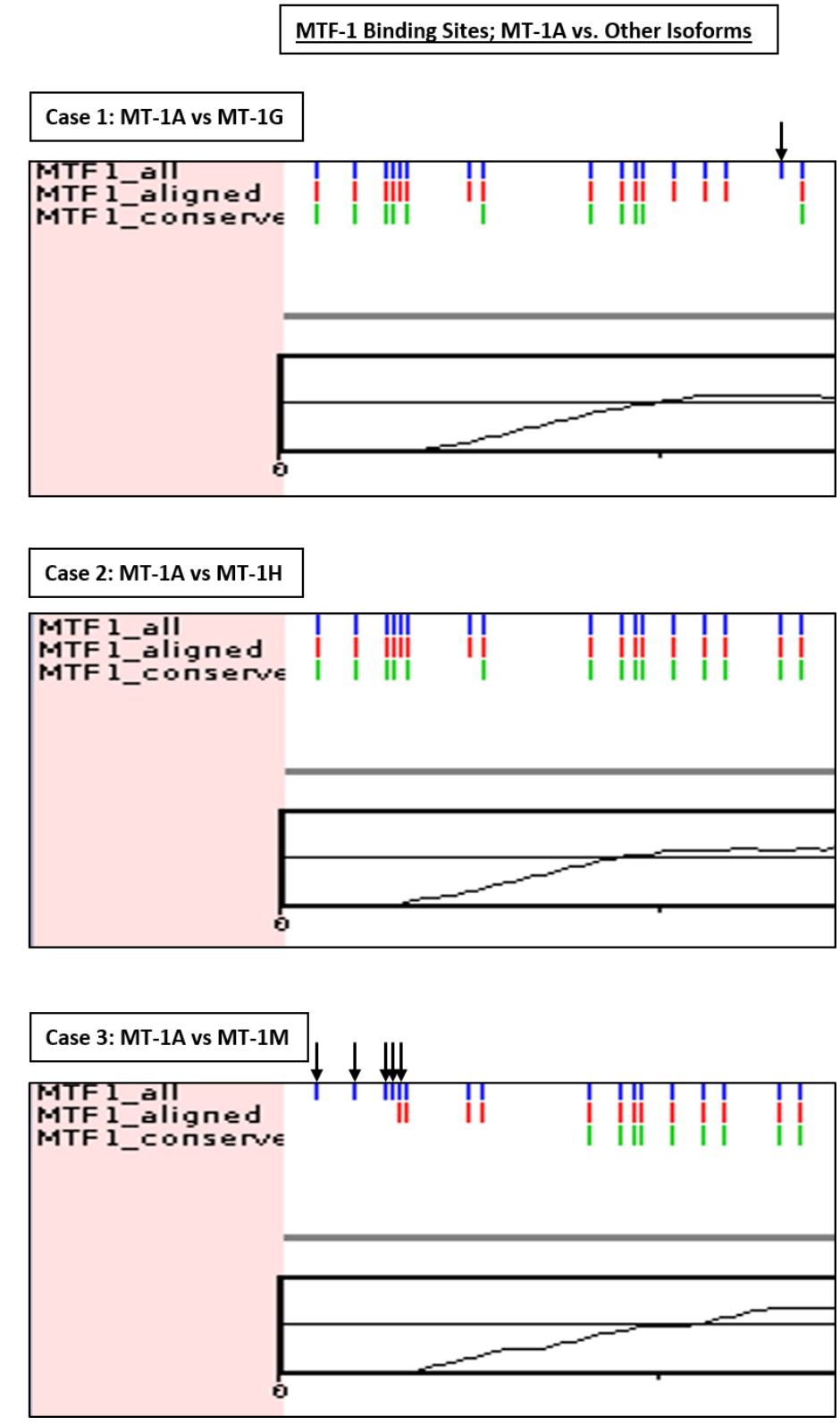
MTF-1 Binding Sites; MT-1A vs. Other Isoforms
Case 1: MT-1A vs MT-1G
MTF1_all
MTF1_aligned
MTF1_conserve
0
Case 2: MT-1A vs MT-1H
MTF1_all
MTF1_aligned
MTF1_conserve
0
Case 3: MT-1A vs MT-1M
MTF1_all
MTF1_aligned
MTF1_conserve
0

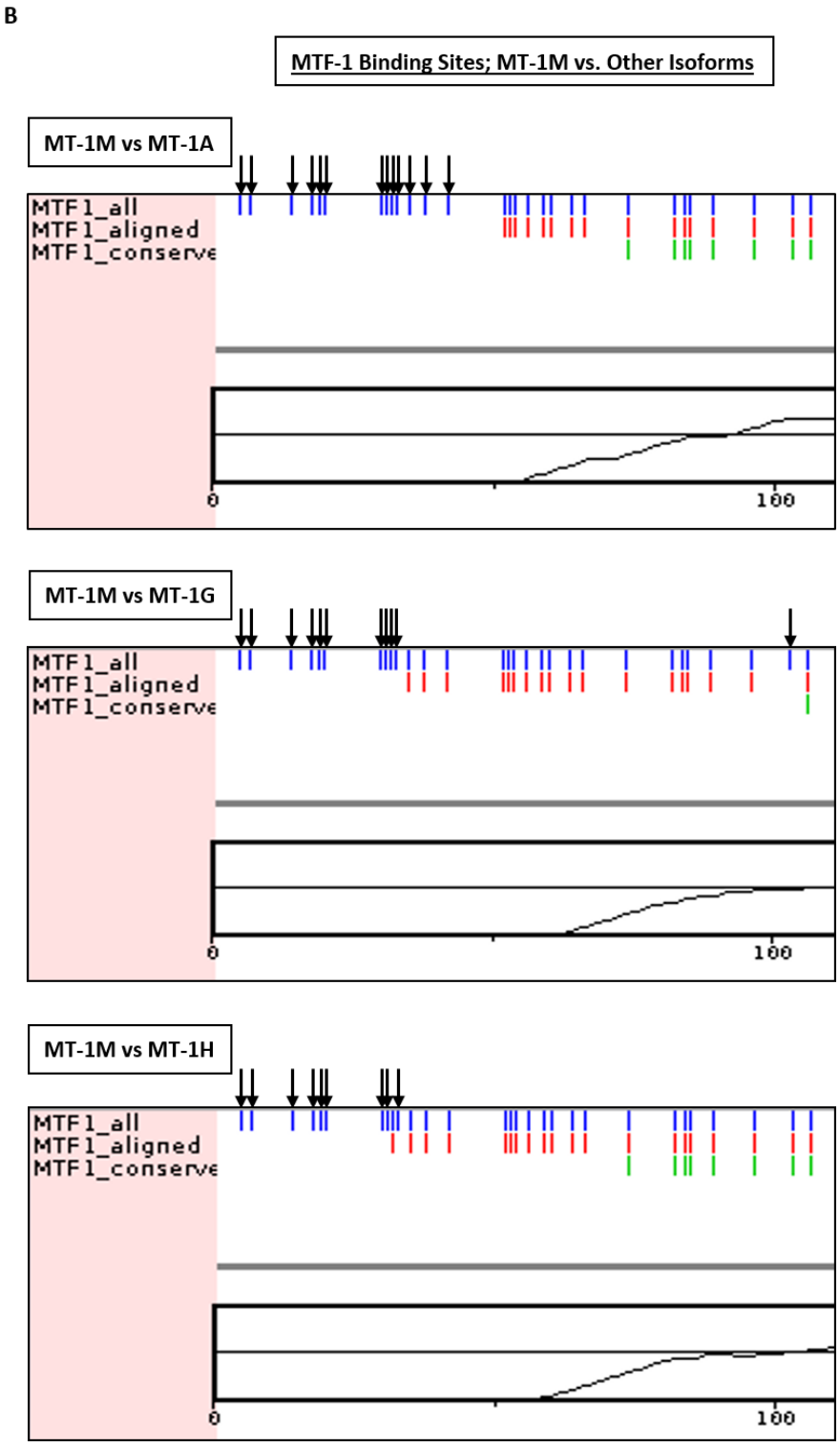


***Figure 47: rVISTA (v. 2.0) analyses showing shared and unique MTF-1 binding sites in MT-1 isoform non-coding DNA****. (A) MT-1A isoform was compared to MT-1G, 1H and 1M isoforms. (B) MT-1M isoform was compared to MT-1A, 1G and 1H isoforms. Unique MTF-1 binding sites were identified by comparing shared (MTF1_aligned; red, and MTF1_conserved; green) and all (MTF1_all; blue) TFBSs present in the target isoform. Any unique binding sites found between*

*two isoforms was then compared to all other isoforms in order to check if it was truly unique. Website: http://genome.lbl.gov/vista/index.shtml.*

Overall, the data obtained from performing these analyses indicated that the MT-1 isoforms have differential arrangement and total number of MTF-1 binding sites within their non-coding DNA, which could be seen from the graphical comparisons. Moreover, the data indicated that the MT-1M isoform contains up to 9 unique MTF-1 binding sites and possesses 12 additional sites compared to MT-1A.

### 5.2.4 Longevity of MT-1 Isoform Expression Post-Exposure to Cadmium

#### *5.2.4.1 Transcript Expression*

RT-PCR analysis showed that cadmium exposure caused transcript induction of all MT-1 isoforms, as previously observed (Figure 48). However, once cadmium exposure was removed and cells cultured under standard conditions, transcript induction began to recede over time (n=1). The rate of this reduction was observed to be dependent on the isoform. For example, MT-1A transcript expression returned to control levels by 24 hours post-exposure, whereas MT-1G and MT-1H transcript expressions remained elevated up to 48 hours post-exposure. By contrast, at 48 hours post-exposure MT-1M transcript induction had dissipated and expression was comparable to controls.

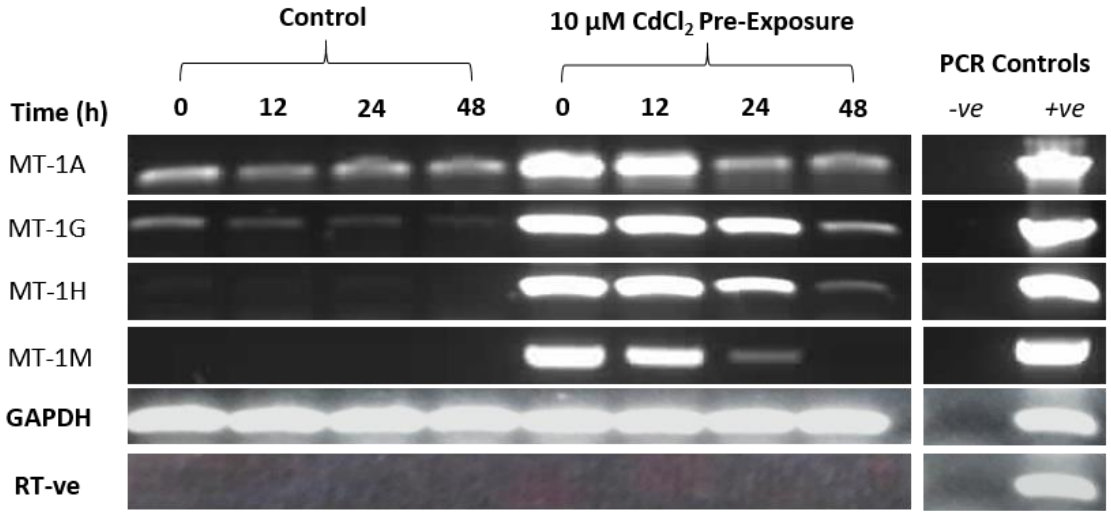


***Figure 48: RT-PCR showing MT-1 isoform transcript expression in NHU cells post exposure to cadmium.*** *Proliferating NHU cells (n=1; Y1270) were exposed to 10 µM $CdCl_2$ for 24 hours before removal of cadmium and further culturing for 48 hours. RNA was extracted at regular time points and MT isoform transcript expression assessed. PCR controls included genomic DNA as a positive control and $dH_2O$ as a negative control. GAPDH transcript expression was used as a loading control, and RT-ve samples confirmed the absence of genomic contamination.*

In differentiated NHU cells, high induction of all MT-1 isoform transcripts pre-exposed to cadmium was observed, as in previous experiments (Figure 49). However, transcript induction again receded once cadmium exposure was removed, albeit at a slower rate than proliferating NHU cells (n=1). For example, MT-1M transcript expression remained highly induced at 4 days post-exposure in differentiated cells, whereas in proliferating cells transcript expression returned to control levels after only 48 hours. The rate of transcript de-induction also differed between the isoforms, as observed in proliferating cells. MT-1A transcript induction was the most transient, showing loss of induction by 4 days post-exposure, whereas MT-1G transcript induction was still present up to 11 days post-exposure.

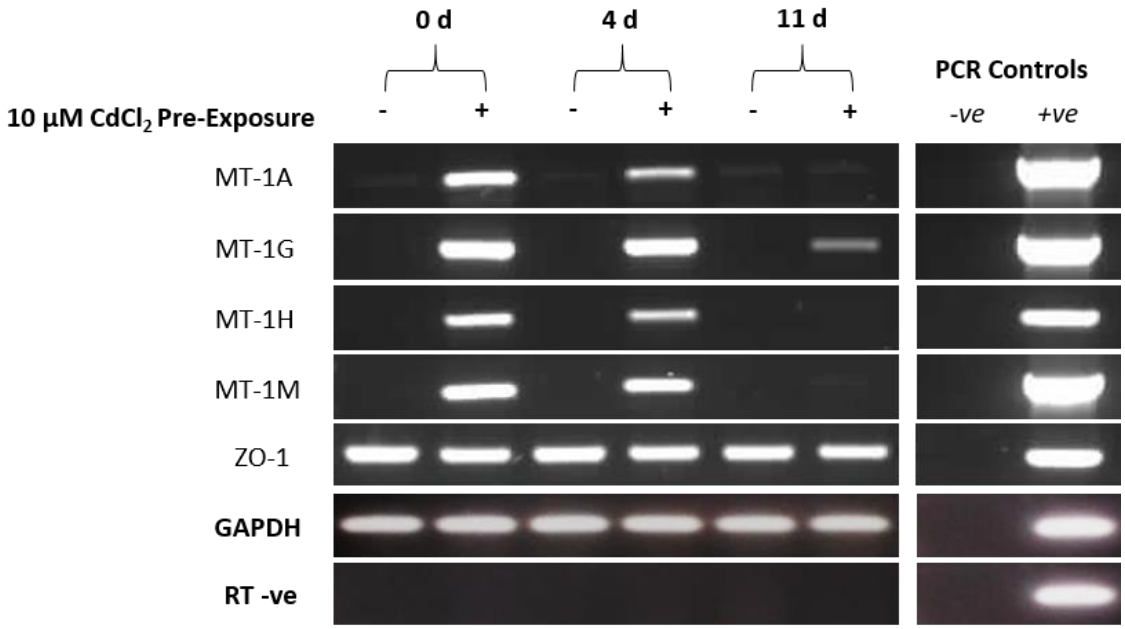


***Figure 49: RT-PCR showing MT-1 isoform transcript expression in differentiated NHU cells post exposure to cadmium.*** *NHU cells (n=1; Y1531) were differentiated and pre-exposed to 10 µM $CdCl_2$ for 3 days. Cadmium was then removed (0 d) and cells further cultured for 11 days. RNA was extracted at various time-points and MT-1 isoform transcript expression assessed. Differentiation of cells was confirmed by formation of a 'tight' urothelial barrier, and transcript expression of the differentiation marker ZO-1 (see Appendices, section 8.4.1). PCR controls included genomic DNA as a positive control and $dH_2O$ as a negative control. GAPDH transcript expression was used as a loading control, and RT-ve samples confirmed the absence of genomic contamination.*

### *5.2.4.2 Protein Expression*

The results from undifferentiated NHU cells revealed high protein expression of both MT-1A and MT-1M isoforms that could be detected up to 5 days post exposure to cadmium, and no protein expression detected in control cells (Figure 50; n=1). This suggested that MT-1 isoform protein expression was more stable than transcript expression in undifferentiated NHU cells, at least for the MT-1A and MT-1M isoforms.

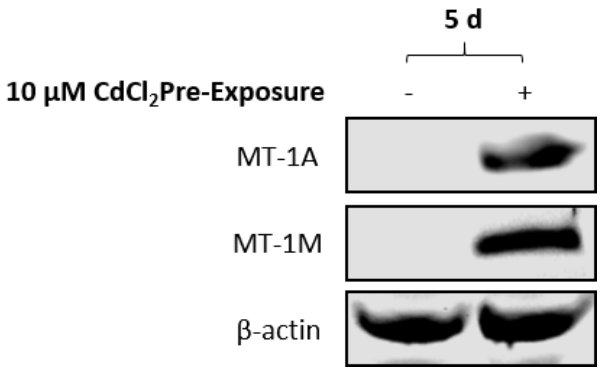


***Figure 50: Western blot showing MT-1A and MT-1M protein expression in confluent undifferentiated NHU cells post exposure to cadmium.*** *Proliferating NHU cells (n=1; Y1277) were cultured until confluence was reached, and then exposed to 10 µM $CdCl_2$ for 72 hours. Cadmium exposure was then removed and cells further cultured for another 5 days. Protein lysates were extracted and MT-1A and MT-1M protein expression determined.*

Western blotting from differentiated NHU cell cultures showed that both MT-1A and MT-1M proteins were induced after 72 h cadmium exposure (0 d), although MT-1M protein expression was not induced to the same extent as MT-1A (Figure 51). Both proteins could still be detected 4 d post-exposure, and expression did not significantly decrease during this time-period (n=1).

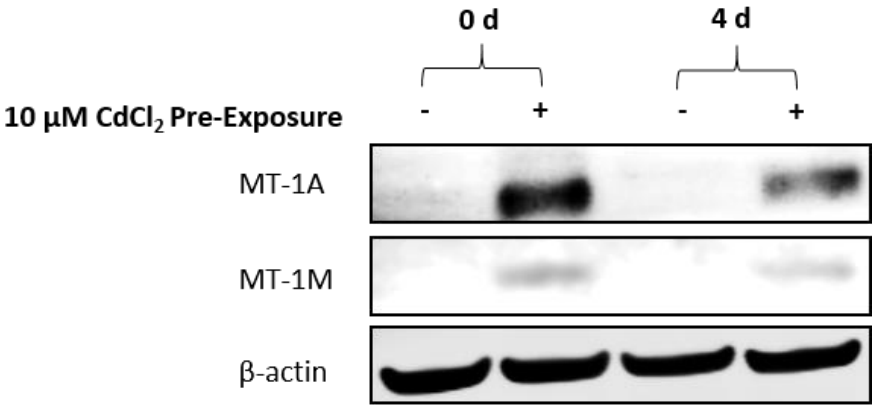


***Figure 51: Western blot showing MT-1A and MT-1M protein expression in differentiated NHU cells post exposure to cadmium.*** *NHU cells (n=1; Y1531) were differentiated and then apically exposed to 10 µM $CdCl_2$ for 3 days (0 d time-point). Cadmium was then removed and cells cultured for a further 4 days. Protein was extracted at 0 d and 4 d post exposure, and MT-1A and MT-1M protein expression assessed. Differentiation was confirmed by the presence of a 'tight' urothelial barrier and transcript expression of a differentiation-associated marker (see Appendices section 9.4.1).*

Both MT-1A and MT-1M protein expression was detectable in cell sheets at 4 d post cadmium exposure (Figure 52; n=1), supporting the western blot data. MT-1A protein formed punctate deposits, whereas MT-1M protein demonstrated a mainly diffuse expression pattern, both of which have been observed in previous results (sections 3.2.4 and 4.2.2). These results further suggest that MT-1 isoform protein expression was more stable than transcript expression, as protein induction persisted post cadmium exposure for a longer time period.

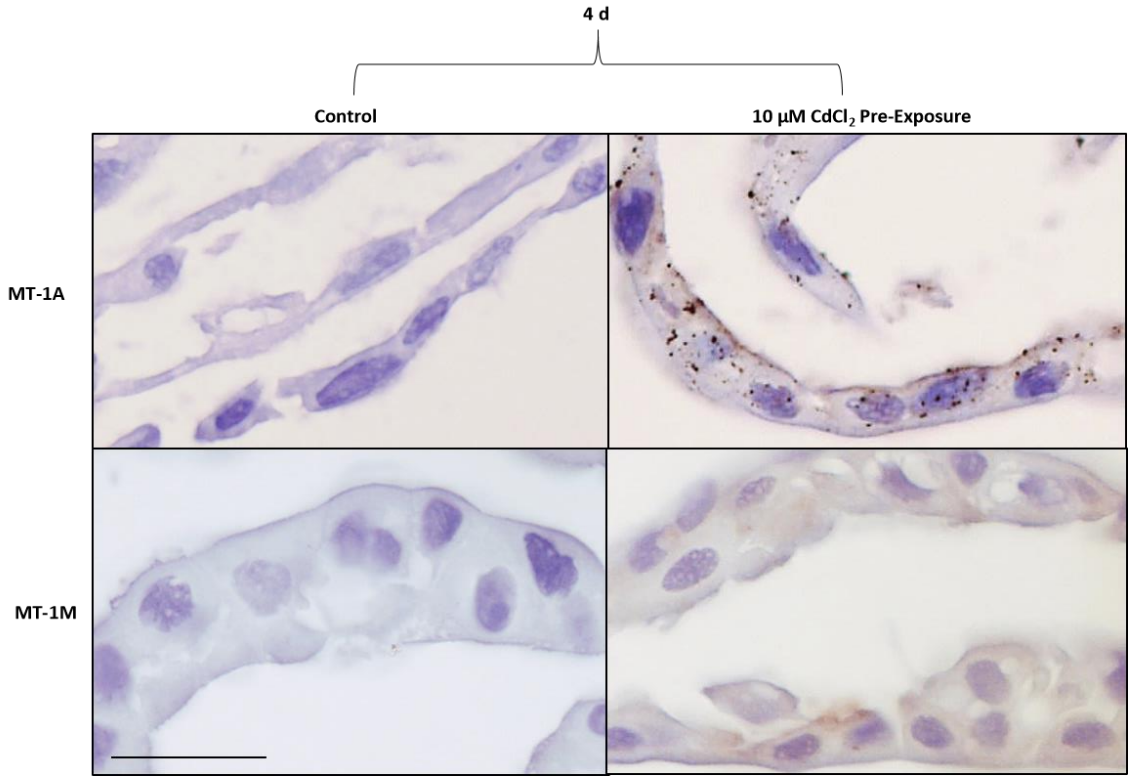


***Figure 52: Immunohistochemical labelling of MT-1A and MT-1M protein expression in differentiated NHU cell sheets post exposure to cadmium.*** *NHU cells (n=1; Y1426) were differentiated and then apically exposed to 10 µM $CdCl_2$ for 3 days, before removal of cadmium exposure and further culturing for 4 days. Cell sheets were harvested, fixed and prepared for immunohistochemical labelling to determine MT-1A and MT-1M protein expression. NHU cell differentiation was confirmed by the presence of a 'tight' urothelial barrier and transcript expression of a differentiation-associated marker (see Appendices section 8.4.1). Scale bar = 25 µm.*

## 5.3 Key Findings

- MT-1 target isoforms showed differential transcript induction.
- Comparison of MTF-1 binding sites in MT-1 isoforms revealed differences in the spatial arrangement and total number of MTF-1 binding sites. The MT-1M isoform was the only isoform to demonstrate uniquely located MTF-1 binding sites, and contained an additional 12 sites compared to MT-1A.
- MT-1A transcript expression could be induced by a number of factors; however, these changes were not usually translated to protein, and only cadmium exposure was able to cause high induction of MT-1A protein expression.
- MT-1M transcript and protein expression were highly specific to cadmium exposure.
- MT-1 isoform transcript induction was transient, and a loss of induction was observed after cessation of cadmium exposure; moreover, this reduction occurred at different rates depending on the gene isoform.
- MT-1A and MT-1M protein expression was observed to persist for prolonged time periods post-cadmium exposure, suggesting protein induction was more stable than transcript.

## 5.4 Discussion

### 5.4.1 Specificity of MT Isoform Induction

As explored in the Introduction (section 1.5.5.3), the MT isoforms are thought to show differential induction depending on the specific inducer present, and a range of potential factors have been suggested as capable of inducing MT-1 isoform expression. However, this was the first time that these potential inducers have been studied using a normal human urothelial cell model. The results revealed the extent to which urothelial MT isoforms can differ in their individual expression, as specific isoforms were induced by different factors and to differing extents (sections 5.2.1. and 5.2.2). These findings support the hypothesis of differential induction of MT isoforms, and demonstrate the importance of discriminating between individual isoforms.

Standard cell culture procedures such as passage and medium change were able to alter MT-1A transcript expression. Moreover, medium change was observed to cause a slight induction of all MT-1 isoforms (section 5.2.1.1). The reasons for this are currently unclear, and to the author's knowledge these results have not been reported before. However, there is the possibility that these changes in isoform transcription were due to altered levels of cellular stress caused by medium change (Garcia-Montero et al., 2001). They could also be linked to changes in cellular proliferation, which is known to be significantly reduced after passage and reseeding (known as the 'lag' phase; Freshney, 2016). Further work would be required to elucidate the mechanism(s) by which standard cell culture may be capable of inducing MT-1 isoform transcript induction, particularly MT-1A.

Several of the potential inducers tested were unable to induce any MT-1 isoform expression, an observation which was particularly evident with the non-metal factors tested (sections 5.2.1.3 and 5.2.1.4). Neither dexamethasone, hypoxia nor IL-1β were able to cause MT isoform transcript induction. A possible reason why these proposed inducers failed to induce MT-1 isoform expression is that no previous studies have specifically studied MT induction by these factors in normal human urothelium, and as explored in the Introduction (section 1.5.5.2), MT isoform expression and induction appears to be highly tissue-specific. Moreover, most previous studies using these potential inducers have not attempted to discriminate between the MT-1 isoforms, and thus it is unclear which isoform(s) may have been responsible for the reported increase in MT expression.

It was particularly important to determine whether the MT-1 isoform induction observed in response to cadmium exposure was due to cadmium itself, or the ROS produced as a by-product of exposure. The results from this thesis suggested that although SF-induced ROS was able to induce transcript expression of MT-1A and MT-1G, these changes were not translated to MT-1A protein expression (section 5.2.1.2). These findings contradict previous studies which have demonstrated increased MT transcript and/or protein expression in response to ROS (Futakawa et al., 2006; Mita et al., 2008; Cortese-Krott et al., 2009; Kadota et al., 2010). However, these studies did not discriminate between the isoforms of the MT-1 subfamily. Discrimination between the MT-1 and MT-2 subfamilies was performed at most, and even then was only completed at the transcript level; and additionally did not include all functional isoforms (Kadota et al., 2010). Moreover, when increased MT protein was detected, only total cellular MT protein was analysed (Futakawa et al., 2006); meaning any of the MT isoforms from any subfamily could have been responsible. The results from this thesis therefore may not be contradictory to previous studies, only more comprehensive due to discrimination between isoforms. This further demonstrates the importance of differentiating between the MT isoforms at both the transcript and protein level, so that individual specificities and expression of the isoforms may be determined.

The results obtained using inhibition of ROS (Figure 41) slightly contradict the original ROS-induction experiment (Figure 40). If SF-induced ROS was able to induce MT-1A/1G isoform expression, inhibition of ROS should have been able to inhibit their cadmium-induced expression, yet did not appear able to. However, it is possible that SF and cadmium may induce different types of ROS, which could cause differential induction of the MT-1 isoforms and account for the apparent discrepancy in results. Cadmium has been reported to induce both superoxide anion and hydrogen peroxide (Hassoun and Stohs, 1996 and Heyno et al., 2008 respectively), whereas the type of ROS induced by SF remains unclear. Further, it appears that cadmium and SF may induce ROS via different mechanisms; cadmium has been reported to generate ROS via the mitochondria (section 5.1.2), whereas SF been shown to deplete intracellular glutathione levels and thus is thought to induce ROS via a non-mitochondrial mechanism (Singh et al., 2005).

Exposure of proliferating NHU cells to both essential and heavy metals illustrated metal-specific induction of the MT-1 isoforms (sections 5.2.1.5 and 5.2.1.6). This metal specificity supports previous research conducted in other cell types which have also

demonstrated metal-dependent differential induction (section 1.5.5.3). Moreover, metal-specificity has been shown as tissue-specific; in a previous study using HeLa cells copper was unable to induce MT-1A transcript expression (Miura and Koizumi, 2007), whereas in this thesis copper was observed to induce MT-1A transcript expression in NHU cells. These results further demonstrate the need to study the metal specificity of MT isoform induction within the specific cell type being investigated, as results from a different tissue type cannot necessarily be applied to other tissues.

Comparison of MT-1 isoform transcript and protein expression in response to the potential inducers revealed that although MT-1A transcript expression could be induced by several factors, only cadmium could induce strong protein expression (section 5.2.2). Although low MT-1A protein expression could be detected under other conditions (such as zinc exposure), cadmium was by far the most potent inducer, suggesting preferential activation. MT-1M transcript induction was highly specific to cadmium, as the only other treatment able to cause induction was zinc, and induction was minimal (section 5.2.1.5). Low transcript induction was not translated to protein, and only cadmium exposure could cause MT-1M protein expression, suggesting that MT-1M protein induction is highly cadmium-specific.

The reasons for the poor translation of MT-1A transcript to protein under non-cadmium conditions are unknown. However, it is possible that MT-1A transcript generally has a poor translation efficiency (Tian et al., 2004; Vogel et al., 2010), and subsequently translation may require high amounts of transcript in order for protein expression to be detectable. As cadmium was a potent transcript inducer, this could explain why MT-1A protein expression was only detectable in cadmium-exposed NHU cells. Alternately, the translational efficiency of MT-1A transcript may be inducer-specific, with different inducers potentially utilising different post-transcriptional controls (reviewed by Day and Tuite, 1998).

A limitation of these MT isoform specificity results is that for factors which were not observed to alter MT-1 isoform transcript induction (such as hypoxia), NHU cells from only one donor were used. To truly demonstrate whether these factors are unable to induce MT-1 isoform expression, the experiments would need repeating in NHU cells derived from at least another two individual donors. A further limitation is that only qualitative methods were used to assess isoform transcript expression (RT-PCR). These methods were adequate for investigating initial isoform transcript induction as a series of

pilot experiments, but for in-depth comparison between inducing factors and assessment of individual isoform expression, a quantitative method such as real-time PCR should be used. With regards to cytokine treatment, it should also be noted that only IL-1β was tested, whereas IL-1α has specifically been suggested to induce MT isoform transcript expression (Kikuchi et al., 1993). However, studies have suggested that the IL-1 family as a whole can induce MT expression (Karin et al., 1985), and have also shown that IL-1α specifically requires the addition of zinc to be able to cause MT-1 isoform induction (Alvarez et al., 2012).

The unique number and spatial arrangement of MTF-1 binding sites found in the MT isoforms supports the hypothesis of differential induction (section 1.5.5.3). However, the exact mechanism(s) behind this is not clear. Previous studies have observed that MTF-1 can bind to different non-overlapping genomic regions depending on the specific type of metal treatment used in *D. melanogaster* (Sims et al., 2012). A similar mechanism was reported in a human hepatocarcinoma cell line, where MTF-1 was observed to bind to a different combination of MTF-1 binding sites depending on the type of metal exposure (Balesaria et al., 2010). Although MTF-1 binding sites are composed of MREs, other transcription factors are also able to bind to these sites (such as MREBP), and it has been suggested that cadmium induces MT expression via its own unique mechanism that is independent of MTF-1 yet still dependent on MREs (section 1.5.3). It is therefore possible that transcription factors other than MTF-1 may bind to the MREs, resulting in cadmium-specific induction. Further work analysing MREs should be conducted in order to determine what factors may bind to these sites under normal and cadmium-exposed conditions. To achieve this, one possible approach would be to perform a DNA pull-down assay based on the principles of reverse ChIP, where a DNA probe is used to isolate the DNA region of interest and mass-spectrometry performed to identify the proteins bound to it (Rusk, 2009). Reverse-ChIP would allow the identification of TFs bound to the MT-1 isoform MREs under cadmium-induced activation, determining whether MTF-1 is involved or whether other potentially novel TFs may also play a role.

### 5.4.2 MT Induction Longevity after the Cessation of Cadmium Exposure

The results from this thesis indicated that cadmium-induced MT-1 isoform transcript induction was transient, as removal of exposure caused a gradual return to control expression. These findings are consistent with results from previous research (Waalkes et al., 1984; Morris and Huang, 1987; Garrett et al., 2002); however, discrimination

between the MT isoforms was not performed in these studies. The experiments in this thesis differentiated between the MT-1 isoforms, which revealed that the rate of de-induction appeared to be isoform-specific. These MT isoform-specific differences in transcript longevity have not been reported before, presumably due to a lack of discrimination, further showing the need to determine individual isoform expression. The isoform-specific rates of transcript de-induction also lend support to the hypothesis that individual isoforms may have different roles within the cell.

To the author's knowledge, longevity of MT protein expression post-cadmium exposure has not been investigated in a human cell system before, although some exploratory studies have been conducted in rats (Liang et al., 2010; Madejczyk et al., 2015). The results from this thesis found that high MT-1A and MT-1M protein expression could still be detected in undifferentiated NHU cells up to 5 days post-cadmium exposure, despite de-induction of transcript generally occurring within 48 hours. This suggests that protein expression is longer-lived and may persist within the cell for a prolonged period post-cadmium exposure, warranting further investigation into the use of MT protein as a biomarker of cadmium exposure.

# Chapter 6: Translation of *In Vitro* Findings to *Ex Vivo* Organ Culture.

## 6.1 Chapter Aims

The main aim of this chapter was to determine whether the cadmium-induced MT-1 isoform protein expression previously observed in *in vitro* NHU cell cultures could also be observed in the urothelium of *ex vivo* ureter organ culture. The advantages of using this type of 3-dimensional model are explained in detail in section 1.1.5, but one of the primary reasons to use organ culture is that it is more reflective of *in vivo* conditions. Therefore, if the MT-1A and MT-1M proteins could be found induced in this model, it would suggest these proteins may also be found induced *in situ* in the urothelium of a cadmium-exposed human.

A further aim of this chapter was to determine whether cadmium exposure could affect the expression of various other proteins whose expression had previously been reported to be altered by exposure. These target proteins were as follows;

- **CK13** - protein expression of the differentiation-associated marker CK13 was determined in order to assess transitional differentiation of urothelium (Varley et al., 2004; Southgate et al., 2007). Although this protein has not been reported as directly altered by cadmium, a loss of tissue differentiation has been associated with exposure (Achanzar et al., 2001; Qu et al., 2012).
- **FOXA1** – a second marker of urothelial differentiation was also assessed in order to further investigate the potential effect of cadmium exposure on loss of tissue differentiation (Varley et al., 2009).
- **CK5** - CK5 protein expression was investigated as its expression has been reported as increased by cadmium-induced malignant cellular transformation (Benbrahim-Tallaa et al., 2009), and it is also a well-characterised marker of basal urothelial cells (Reis-Filho et al., 2003; Castillo-Martin et al., 2010). Thus, characterising its expression could help to determine the phenotype of urothelial cells in cadmium-exposed ureter organ culture.
- **Ki67** - protein expression of the cellular proliferation marker Ki67 (Gerdes et al., 1983) was assessed, as previous studies have reported increased cellular proliferation due to cadmium exposure (Takiguchi et al., 2003; Kundu et al., 2011; Lacorte et al., 2011).

- **H3K27me3 –** protein expression of the histone post-translational modification H3K27me3 was determined, having been previously reported as increased in cadmium-exposed UROtsa cells (Somji et al., 2011b). This epigenetic mark is strongly repressive, and as such is often found associated with genetic silencing (Filion et al., 2010; Kharchenko et al., 2011; Li, Huang, Bickel, & Brenner, 2014).

### 6.1.1 Objectives

1. Determine whether MT protein is induced in the urothelium from ureter organ cultures acutely and chronically exposed to cadmium.
2. Investigate whether MT protein expression persists in the urothelium of ureter organ cultures post-acute exposure to cadmium.
3. Assess whether cadmium exposure can alter the protein expression of several candidate targets identified from the literature.

### 6.1.2 Experimental Approach

#### *6.1.2.1 Use of the MT-1/2 (E9) Antibody*

In addition to the MT-1A and MT-1M antibodies, the commercially available E9 antibody was also used for these experiments. As explained earlier (section 1.5.5.4) this antibody detects all MT-1/2 proteins and does not discriminate between the isoforms. This antibody was therefore included to ensure that any changes in gross MT protein expression were not missed due to only focusing on MT-1A and MT-1M isoform protein expression. Results using all 3 antibodies to determine MT protein expression in cadmium-exposed ureter organ culture can be found summarised in section 6.2.2, Table 9.

#### *6.1.2.2 Ureter Organ Culture*

The detailed protocol used for ureter organ culture can be found in section 2.7.12. It is important to note that exposure of ureter to cadmium was both apical and basal, the reasons for which are explained in the Materials and Methods (also section 2.7.12).

1. In order to determine whether any changes in MT protein expression could be detected in the urothelium of ureter organ cultures acutely exposed to cadmium, ureter was continuously exposed to 10 µM $CdCl_2$ for 3, 7 or 14 days. The pieces of ureter were then fixed, sectioned and immunolabelled for MT-1/2, MT-1A and MT-1M protein expression.

2. The next experiment was designed to fulfil Objectives 2 and 3, and the second half of Objective 1. Ureter from one individual donor was exposed to 10 µM $CdCl_2$ for either 7 days (acute exposure) or 56 days (chronic exposure). A further culture was exposed for 14 days (found to be sufficient for MT protein induction; section 6.2.1) before removal of cadmium and continuous culturing for 42 days (post-exposure). Ureter sections were then used to achieve the Chapter's Objectives in the following ways;
    a. **Objective 1 (partial)** – the effect of chronic cadmium exposure on MT protein expression was assessed by immunolabelling ureter sections for MT-1A, MT-1M and MT-1/2 protein expression.
    b. **Objective 2** – post-exposure ureter sections were immunolabelled for MT-1A, MT-1M and MT-1/2 protein expression in order to determine whether expression could be detected post-cadmium exposure.
    c. **Objective 3** - acutely and chronically exposed ureter sections were immunolabelled to determine the protein expression of several other potential targets of cadmium. Post-exposure samples were included as they had the potential to support any changes found in chronically exposed urothelium, and could possibility indicate whether cadmium-induced alterations persisted even after cadmium exposure.

## 6.2 Results

### 6.2.1 MT Protein Expression in the Urothelium of Cadmium-Exposed Ureter Organ Culture

The urothelium from control cultures was largely negative for MT-1/2 protein expression, showing only faintly diffuse immunolabelling at the apical surface of superficial cells (Figure 53). By contrast, after 7 days continuous cadmium exposure there was a strong induction of MT-1/2 protein expression in the urothelium, which was both nuclear and cytoplasmic. Protein expression was observed in all 3 urothelial cell zones, although expression was strongest in the superficial urothelial cells. The stromal cells underlying the urothelium also showed an increase in MT-1/2 protein expression upon cadmium exposure, although this was confined to nuclear expression.

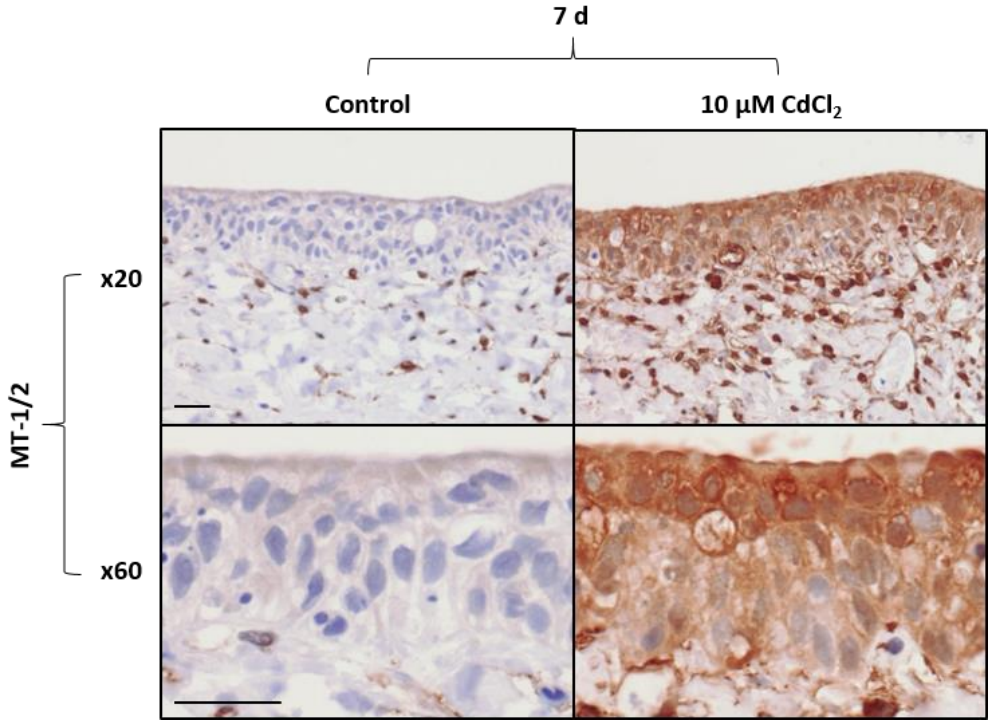


***Figure 53: Immunohistochemical labelling of MT-1/2 protein expression in ureter organ culture exposed to cadmium.*** *Ureter pieces (n=1; Y1770) were continuously exposed to 10 µM $CdCl_2$ for 7 days and MT-1/2 protein expression determined. Scale bar = 25 µm.*

The next step was to determine whether the MT-1A and/or MT-1M proteins were specifically induced. To achieve this, ureter sections were continuously exposed to 10 µM $CdCl_2$ for 3 or 7 days and immunolabelled for MT-1A and MT-1M protein expression. By day 3 there was strong immunolabelling for the MT-1A protein in exposed

urothelium, which could be seen in both the nucleus and cytoplasm in the majority of cells, and in all 3 urothelial cell zones (Figure 54). By contrast, MT-1M protein expression was barely detectable after 3 days exposure, and most cells were negative for expression. After 7 days exposure, MT-1A protein expression was still present, remaining expressed in both the nucleus and cytoplasm. MT-1M protein expression was also observed highly induced by this time-point, demonstrating a diffuse expression pattern. MT-1M protein expression was mainly confined to superficial urothelial cells, although sporadic intermediate cells also showed expression. Additionally, MT-1M protein induction only occurred in the cytoplasm, and no nuclear immunolabelling was observed.

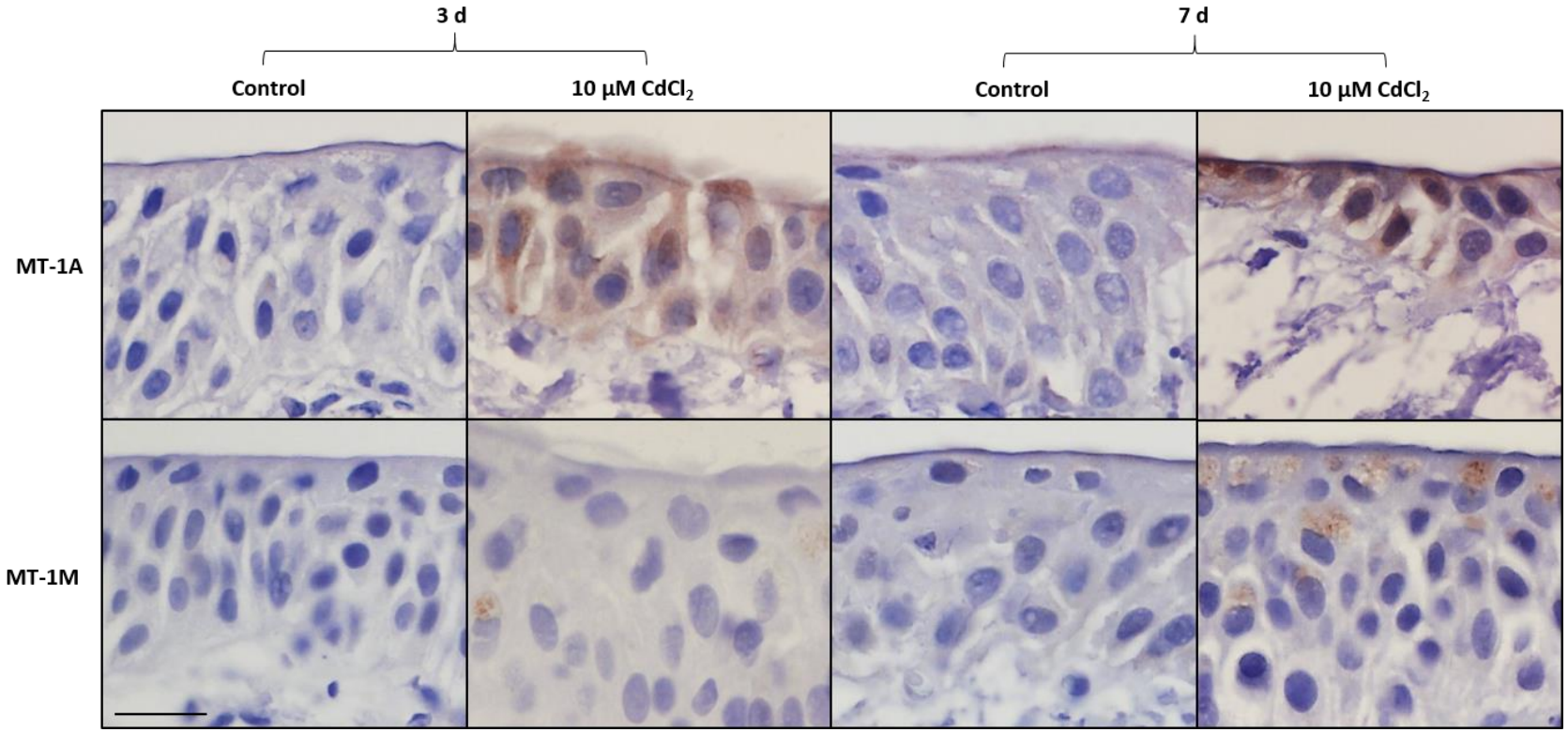


***Figure 54: Immunohistochemical labelling of MT-1A and 1M protein expression in ureter organ culture exposed to cadmium.*** *Ureter pieces (n=1; Y1566) were continuously exposed to 10 µM $CdCl_2$ for 3 or 7 days and immunolabelled for MT-1A and MT-1M protein expression. Scale bar = 25 µm.*

Ureter continuously exposed to 10 µM $CdCl_2$ for 14 days was also immunolabelled for MT-1A, MT-1M and MT-1/2 protein expression. After 14 days exposure a strong induction of MT-1/2 protein expression was observed, which occurred throughout the urothelium as well as the stroma, as observed previously (Figure 55; n=2). However, in this organ culture the difference in immunolabelling intensity between the individual urothelial cell zones was more prominent; MT-1/2 protein expression decreased with penetration through the cell zones, from superficial to basal cells. MT-1A protein expression was also induced after cadmium exposure in all cell zones, supporting the initial findings (n=2). However, in contrast to the previous experiment, MT-1A immunolabelling was confined to nuclei throughout the urothelium and also presented in stromal cells. Lastly, MT-1M protein expression was found sporadically induced in urothelial cells after exposure to cadmium (n=2). As observed previously, protein expression presented as diffuse in the cytoplasm, and was mainly confined to the superficial and intermediate cell zones.

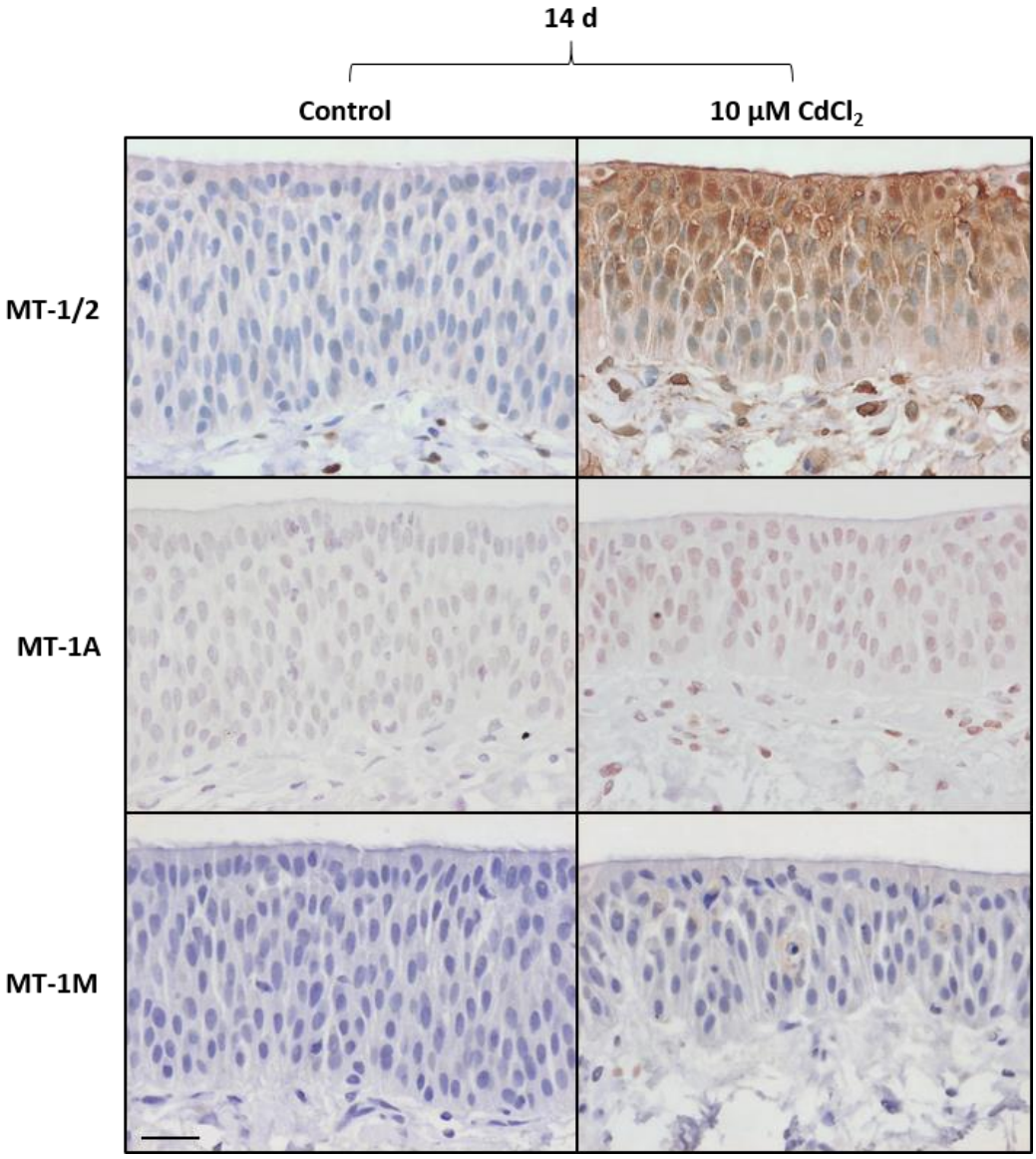


***Figure 55: Immunohistochemical labelling of MT-1/2, MT-1A and MT-1M protein expression in ureter organ culture exposed to cadmium.*** *Ureter pieces (n=1; Y1644) were continuously exposed to 10 µM $CdCl_2$ for 14 days and immunolabelled for MT-1A, MT-1M and MT-1/2 proteins. Scale bar = 25 µm.*

### 6.2.2 MT Protein Expression in Ureter Organ Cultures Chronically Exposed or Post-Acute Exposure to Cadmium

#### *6.2.2.1 Chronic Cadmium Exposure*

From this single specimen, all long-term organ cultures showed a high number of nuclear fragments in the urothelium which resembled apoptotic bodies (Figures 56 and 57). The reasons for this prominent urothelial cell death are unknown, but may be associated with the prolonged (56 day) organ culture. Additionally, the width of the urothelium varied

greatly between control and chronically exposed ureters, as the width of the latter appeared approximately 3-fold narrower than control.

After 56 days continuous cadmium exposure a strong induction of MT-1/2, MT-1A and MT-1M protein expression was observed in the urothelium (Figure 56; n=1). Immunolabelling of these proteins occurred in all three cell zones, in both the nucleus and cytoplasm. These results differed from previous experiments which suggested that MT-1A protein expression was nuclear and MT-1M protein expression confined to the cytoplasm. Additionally, MT-1/2 protein was equally expressed throughout all cell zones, whereas in acutely exposed ureter it was observed to be strongest in the superficial urothelial cells. In general, after 56 days' cadmium exposure immunolabelling of all 3 different MT proteins was quite similar. The most obvious difference was that a number of urothelial cells did not express MT-1M expression, whereas nearly all cells demonstrated immunolabelling for MT-1A and MT-1/2 protein expression.

#### *6.2.2.2 Post-Acute Cadmium Exposure*

42 days after removal of acute cadmium exposure, MT-1M protein expression could no longer be detected in the urothelium. However, MT-1A and MT-1/2 protein expression could both still be observed (n=1). MT-1A protein expression was confined to the nucleus post exposure, and could also be detected in the nuclei of stromal cells. This nuclear presentation of MT-1A protein was similar to results previously observed after acute (7 or 14 days) cadmium exposure (Figures 54 and 55). MT-1/2 protein expression was observed in both the nucleus and cytoplasm of urothelial cells post-cadmium exposure, and some immunolabelling in stromal cells was also visible (also observed previously; Figures 53 and 55). However, in contrast to ureter cultures that had undergone 56 days continuous exposure, MT-1/2 protein expression once again differed in strength between the cell zones. Immunolabelling was observed strongest in the superficial urothelial cells and some intermediate cell labelling was present, whereas the basal cell zone was negative for MT-1/2 protein expression.

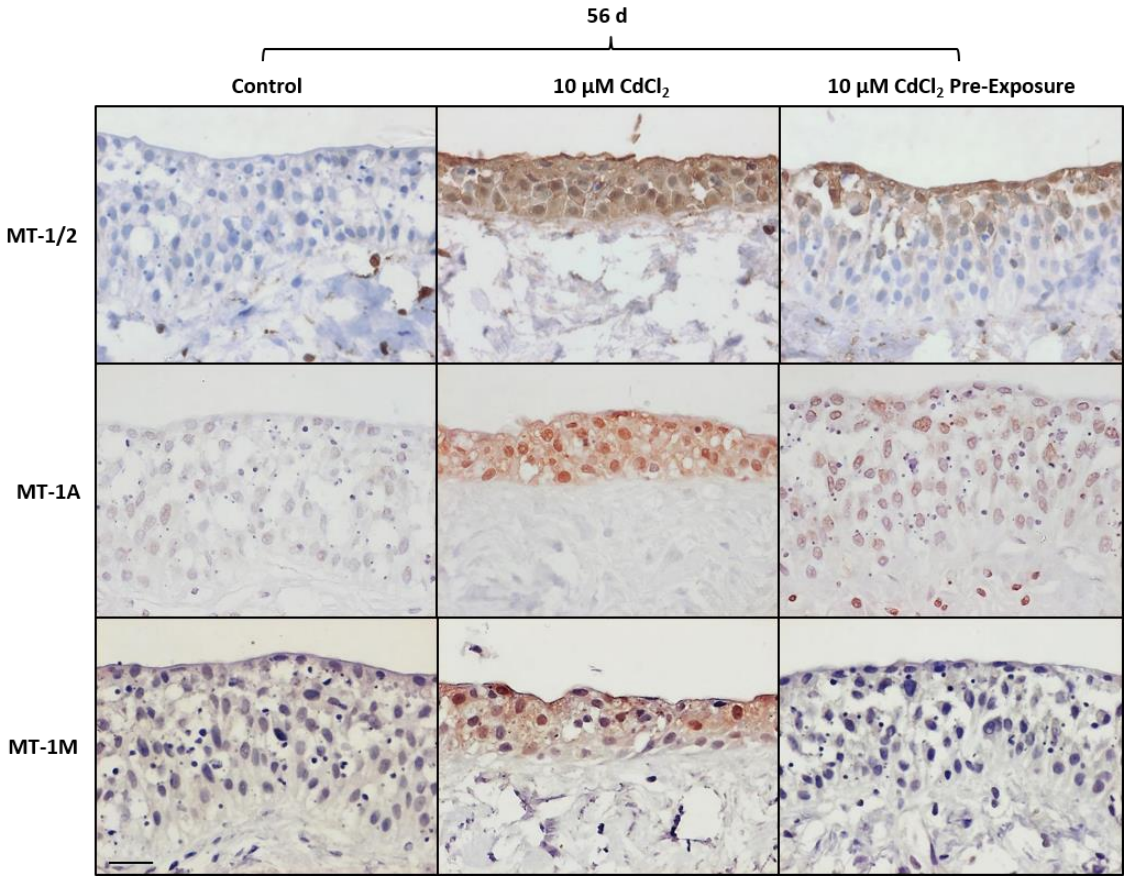


***Figure 56: Immunohistochemical labelling of MT-1/2, MT-1A and MT-1M protein expression in ureter organ culture during and after cadmium exposure.*** *Ureter pieces (Y1644) were exposed to 10 µM $CdCl_2$ for 56 days continuously, or exposed for 14 days before removal of cadmium and further culture for 42 days (pre-exposure). Scale bar = 25 µm.*

***Table 6: Summary of MT protein expression in urothelium from cadmium-exposed ureter organ culture.*** *Normal human ureter was exposed to 10 μM $CdCl_2$ for short (≤ 14 days; 'Acute') or prolonged (56 days; 'Chronic') time periods, or were acutely exposed (14 days) before removal of exposure and continued culturing (42 days; 'Post-'). Immunolabelling for MT-1/2, MT-1A and MT-1M proteins was performed on samples and the expression of each is summarised in the table below.*

| | **Cadmium Exposure** | | |
|---|---|---|---|
| ***Protein*** | Acute (≤14 d.) | Chronic (56 d.) | Post- (14 d. exposure; 42 d. post-exposure) |
| *MT-1/2* | Cytoplasmic and nuclear localisation. Immunolabelling intensity decreased with penetration through the cell zones. | Cytoplasmic and nuclear localisation. Equally intense immunolabelling in all cell zones. | Cytoplasmic and nuclear localisation. Immunolabelling intensity decreased with penetration through the cell zones. |
| *MT-1A* | Nuclear localisation with some cytoplasmic. Immunolabelling in all cell zones. | Cytoplasmic and nuclear localisation. Strong immunolabelling in all cell zones. | Nuclear localisation. Immunolabelling in all cell zones. |
| *MT-1M* | Cytoplasmic localisation. Sporadic immunolabelling in superficial and intermediate cell zones. | Cytoplasmic and nuclear localisation. Strong immunolabelling in all cell zones. | None. |

### 6.2.3 Protein Expression of other Candidate Targets of Cadmium in Exposued Ureter Organ Culture

*CK13*

After 7 days ureter organ culture, the urothelium in control samples showed strong immunolabelling for CK13 protein in the basal and intermediate cell zones, although protein expression was strongest in basal cells (Figure 57). Superficial urothelial cells were mostly negative for CK13 protein expression. These results were as expected for normal human urothelium, indicating the presence of a transitional differentiation morphology (Southgate et al., 2007). However, after 7 days continuous cadmium exposure, urothelial expression of CK13 protein expression was decreased (n=1). This was particularly evident in basal urothelial cells, several of which did not express CK13 protein, in direct contrast to control results. After 56 days in culture, CK13 protein expression was lost in both control and exposed samples, although very weak immunolabelling could be sporadically observed in areas of control urothelium.

*FOXA1*

At day 7 strong immunolabelling of FOXA1 was observed in the urothelium from control ureter (Figure 58). FOXA1 protein expression was confined to the nucleus and observed in the majority of urothelial cells from all cell zones. FOXA1 protein expression was also present in most urothelial cells from cadmium-exposed ureter; however, there was a distinct decrease in expression in ~50 % of cells. After 56 days in culture, strong FOXA1 immunolabelling was still visible in control urothelium, whereas chronically exposed urothelium again demonstrated reduced expression, although this was less obvious at this time-point. In support of this observation, a small reduction in FOXA1 protein expression also occurred in the urothelium of ureters post-acute exposure to cadmium.

*CK5*

Strong immunolabelling for CK5 protein expression was observed in both control and cadmium-exposed urothelium at day 7 (Figure 59). Expression was mostly confined to the basal cell zone, although immunolabelling also occurred in some intermediate urothelial cells. By day 56 the results showed that although CK5 protein expression was still detectable in control urothelium, it was greatly reduced, and only sporadic cells were immunolabelled. By contrast, in ureters post-acute cadmium exposure, CK5 protein expression presented more frequently. Moreover, there was strikingly higher CK5 protein

expression in the urothelium from chronically cadmium-exposed ureter cultures compared to both control and pre-exposed conditions (n=1). Not only was CK5 protein expression more intense, but it was also more frequently expressed in urothelial cells. Additionally, CK5 protein expression was no longer confined to only the basal and intermediate cell zones, as the majority of superficial urothelial cells were also positive for protein expression.

*Ki67*

After 7 days in culture, several superficial urothelial cells in both control and cadmium-exposed urothelium immunolabelled for Ki67 protein expression (Figure 60). At day 56 however, no urothelial cells were observed to express Ki67 protein in control samples. By contrast, a small number of urothelial cells demonstrated Ki67 protein expression in both the cadmium post-exposure and chronically exposed ureter organ cultures, indicating the presence of cells that were still actively proliferating (n=1).

*H3K27me3*

Strong H3K27me3 protein expression was observed in the nucleus of most urothelial cells from all cell zones in both control and cadmium-exposed ureters at day 7 (Figure 61). By day 56, H3K27me3 protein expression could only be detected in ~50 % urothelial cells from all ureters samples, suggesting expression was lost with time in culture. Despite this, it was observed that H3K27me3 protein expression was markedly stronger in chronically cadmium-exposed urothelium compared to control and post-exposure organ cultures (n=1). Urothelial cells from post-exposure ureter cultures also demonstrated stronger immunolabelling compared to controls, although this difference in protein expression was less prominent.

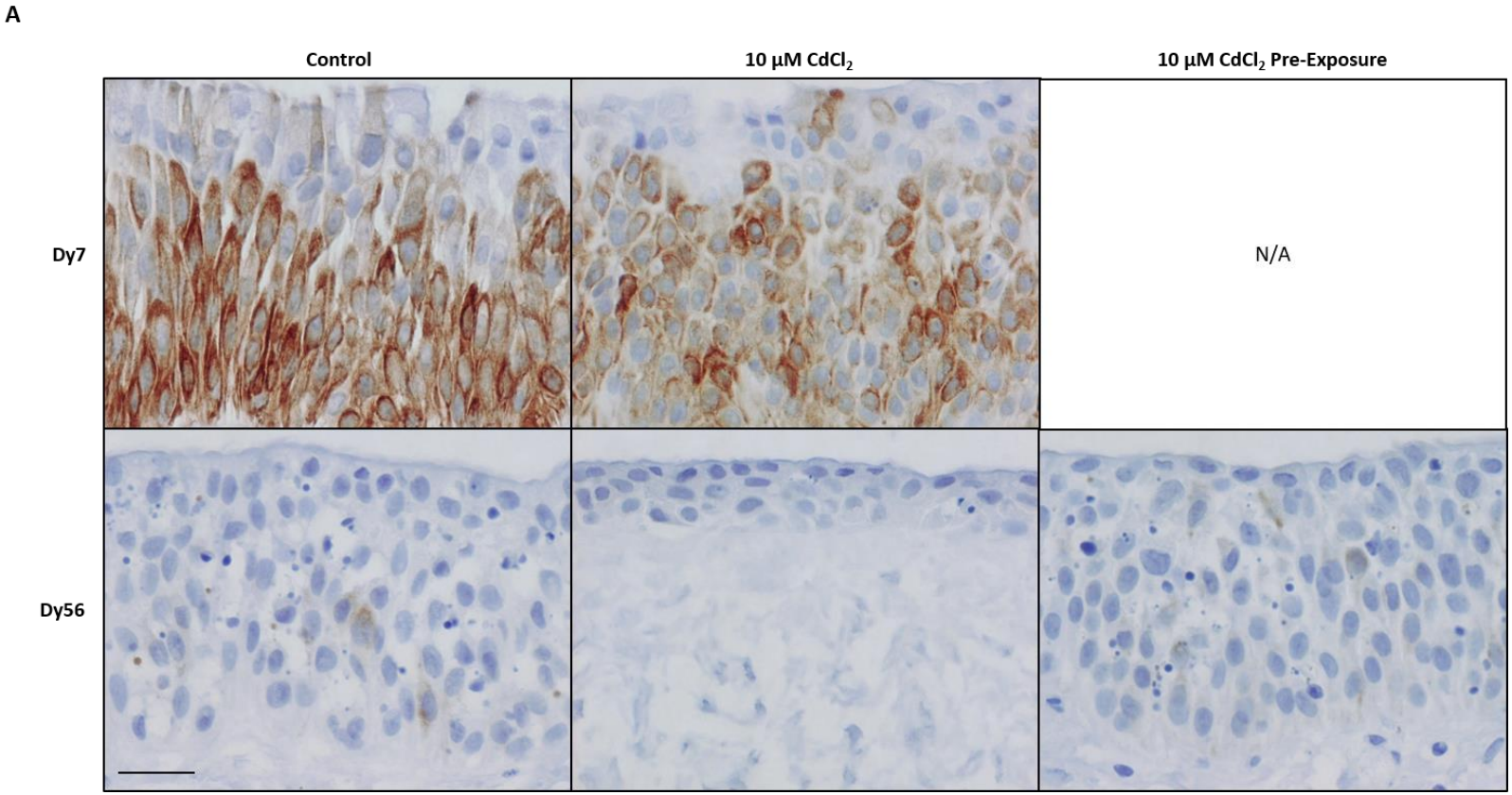


***Figure 57: Immunohistochemical labelling of other protein targets potentially affected by cadmium exposure (CK13).*** *Ureter pieces (Y1644) were exposed to 10 µM CdCl2 for 7 or 56 days continuously, or exposed for 14 days before removal of cadmium and further culture for 42 days (pre-exposure). Immunolabelling was performed to determine the protein expression of markers previously identified in the literature as being affected by cadmium exposure. IHC for candidate protein target CK13 is shown above. Scale bar = 25 µm.*

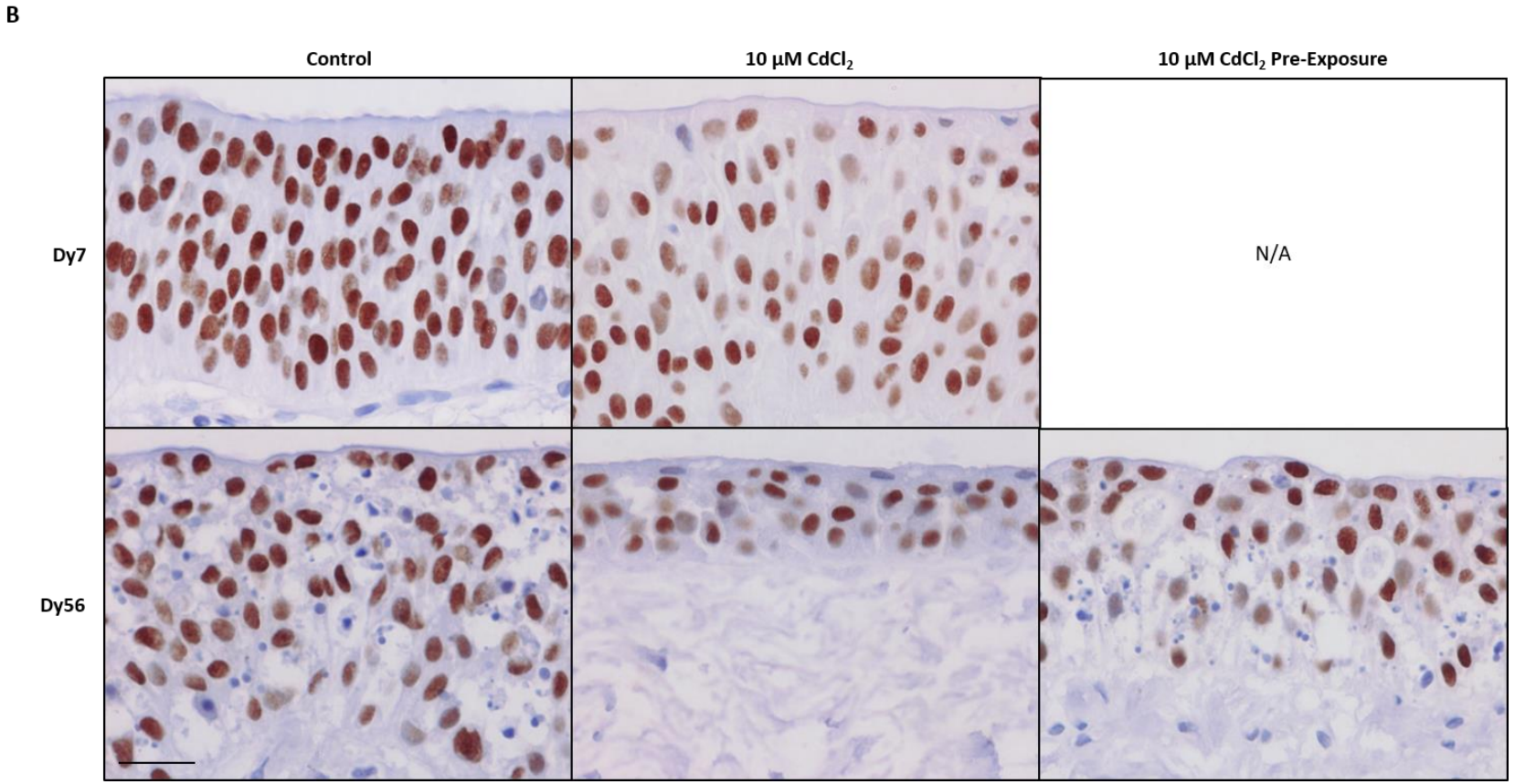


***Figure 58: Immunohistochemical labelling of other protein targets potentially affected by cadmium exposure (FOXA1). Ureter pieces (Y1644) were exposed to 10 µM CdCl2 for 7 or 56 days continuously, or exposed for 14 days before removal of cadmium and further culture for 42 days (pre-exposure). Immunolabelling was performed to determine the protein expression of markers previously identified in the literature as being affected by cadmium exposure.*** *IHC for candidate protein target FOXA1 is shown above.* ***Scale bar = 25 µm.***

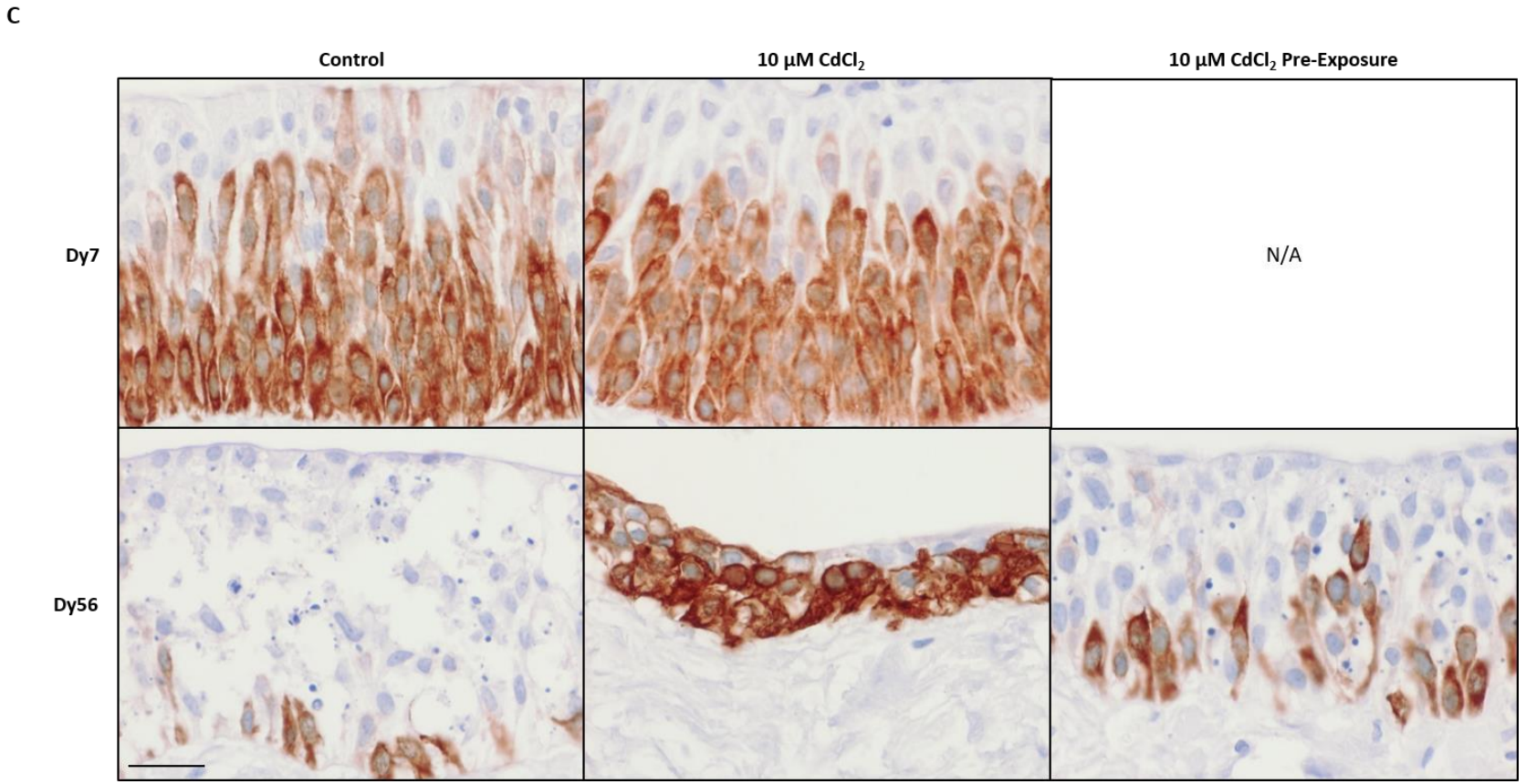


***Figure 59: Immunohistochemical labelling of other protein targets potentially affected by cadmium exposure (CK5).*** *Ureter pieces (Y1644) were exposed to 10 µM CdCl2 for 7 or 56 days continuously, or exposed for 14 days before removal of cadmium and further culture for 42 days (pre-exposure). Immunolabelling was performed to determine the protein expression of markers previously identified in the literature as being affected by cadmium exposure. IHC for candidate protein target CK5 is shown above. Scale bar = 25 µm.*

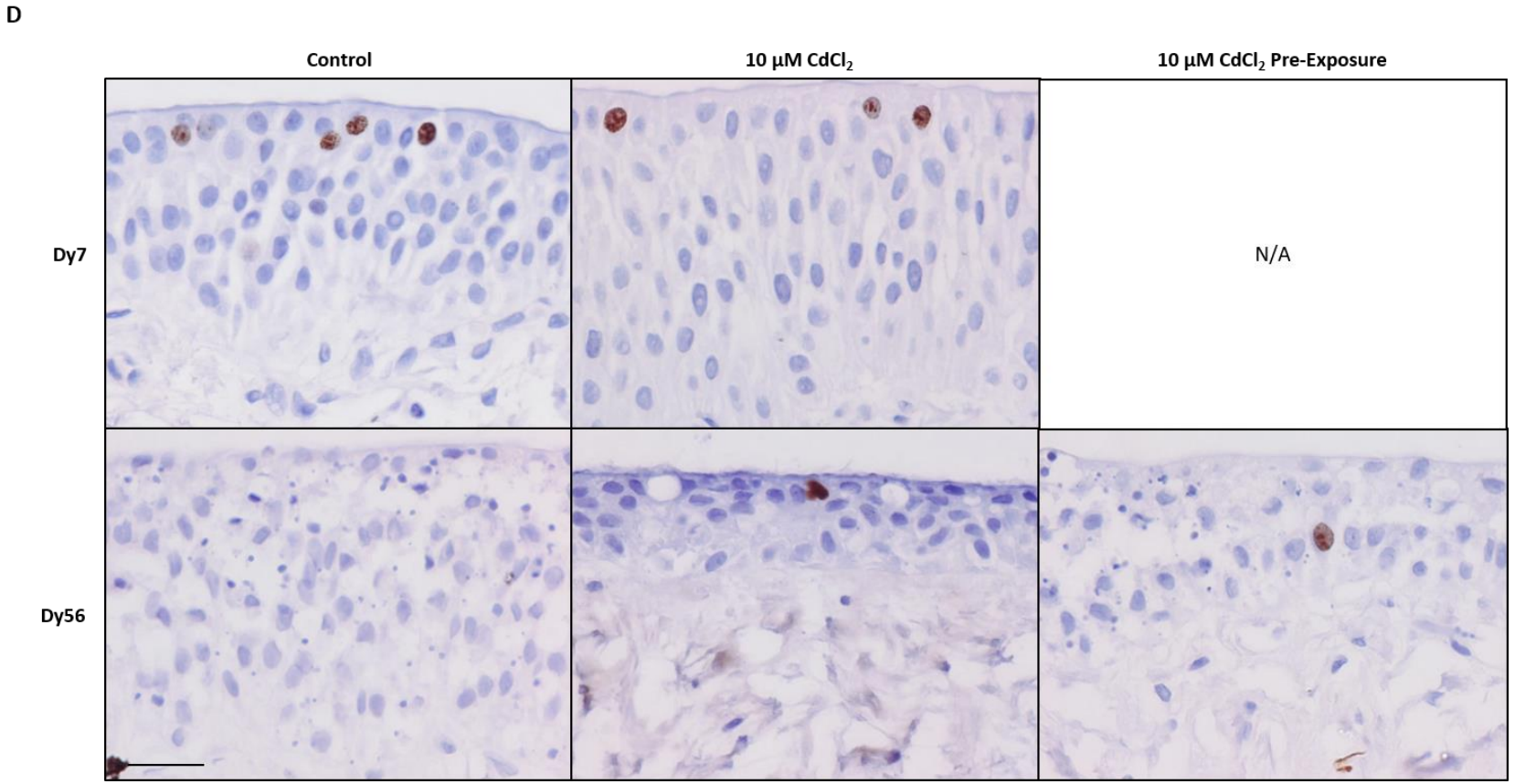


***Figure 60: Immunohistochemical labelling of other protein targets potentially affected by cadmium exposure (Ki67).*** *Ureter pieces (Y1644) were exposed to 10 µM CdCl2 for 7 or 56 days continuously, or exposed for 14 days before removal of cadmium and further culture for 42 days (pre-exposure). Immunolabelling was performed to determine the protein expression of markers previously identified in the literature as being affected by cadmium exposure. IHC for candidate protein target Ki67 is shown above. Scale bar = 25 µm.*

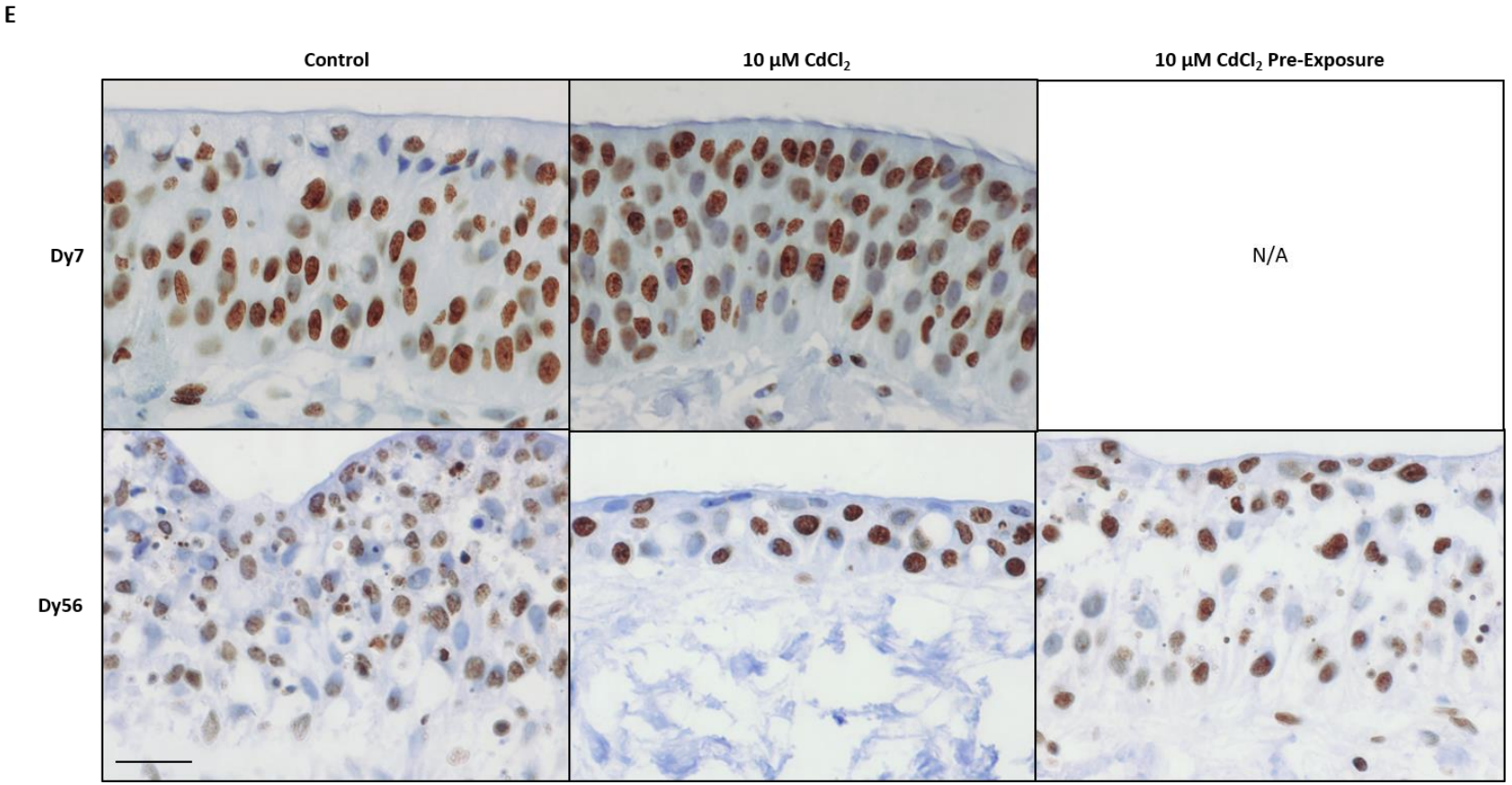


***Figure 61: Immunohistochemical labelling of other protein targets potentially affected by cadmium exposure (H3K27me3).*** *Ureter pieces (Y1644) were exposed to 10 µM $CdCl_2$ for 7 or 56 days continuously, or exposed for 14 days before removal of cadmium and further culture for 42 days (pre-exposure). Immunolabelling was performed to determine the protein expression of markers previously identified in the literature as being affected by cadmium exposure. IHC for candidate protein target H3K27me3 is shown above. Scale bar = 25 µm.*

## 6.3 Key Findings

- MT-1/2 protein expression was highly induced in the urothelium of ureter organ culture acutely and chronically exposed to cadmium. MT-1A and MT-1M protein isoforms were specifically found induced, and demonstrated differential expression patterns.
- Cadmium-induced MT-1/2 protein expression was observed to be strongest in superficial urothelial cells, and decreased with penetration through the cell zones.
- MT-1/2 and MT-1A protein expression could still be detected in the urothelium of ureter organ cultures up to 6 weeks post exposure to cadmium.
- Other protein markers also seemed to demonstrate altered expression due to cadmium exposure; including apparent increased CK5, Ki67 and H3K27me3 protein expression, and decreased CK13 and FOXA1 protein expression.

## 6.4 Discussion

### 6.4.1 MT Protein Expression in Cadmium-Exposed Ureter Organ Culture

Use of human ureter organ culture revealed that MT-1/2, MT-1A and MT-1M proteins were all induced in human urothelium acutely exposed to cadmium, supporting the *in vitro* results (Chapters 4, 5 and 6). The isoforms were also observed to exhibit differential timing of induction, as well as individual expression patterns, further suggesting individual differing roles (section 1.5.5.4). Chronic exposure of human ureter to cadmium also resulted in strong induction of all three MT proteins in the urothelium, although the isoforms no longer displayed their individual expression patterns (section 6.2.2.1). This may have been due to urothelial tissue saturation by cadmium after prolonged exposure (Urani et al., 2007), potentially causing an over-abundance of MT protein expression, and thereby masking normal individual isoform expression patterns.

The MT-1/2 and MT-1A proteins were found to remain expressed up to 6 weeks after the removal of cadmium exposure (Figure 56), also supporting the *in vitro* results (section 5.2.4.2). MT-1A protein expression relocalised from a nuclear localisation during acute cadmium exposure to a perinuclear localisation after cessation of exposure. This finding is supported by previous studies, which have demonstrated that MT-1 subfamily transcription occurs in the perinuclear cytoplasm, and that transcripts can be specifically found bound to cytoskeletal polysomes (Mahon et al., 1997). Moreover, it has been suggested that perinuclear localisation and association with the cytoskeleton has the physiological role of facilitating efficient shuttling of the MT-1 protein into the nucleus, which is its proposed site of function (Levadoux et al., 1999; Chabanon et al., 2004). A flaw in these studies however is that they did not discriminate between the MT-1 subfamily isoforms, and thus it is not clear from their results which isoform(s) may be associated with perinuclear localization, although the results in this thesis suggest that it may be MT-1A.

The strength of MT-1/2 immunolabelling was observed to increase throughout the cell zones in an apical direction, both in urothelium acutely exposed to cadmium and post-exposure, and superficial urothelial cells demonstrated the strongest MT-1/2 protein expression. Change in protein expression appeared to occur along a gradient, which has not been reported in humans before, and was observed in two ureters derived from independent donors. There is the possibility that this change in MT-1/2 protein expression may reflect the presence of a cadmium concentration gradient in the urothelium due to

exposure. A similar observation has been made in plant crops exposed to cadmium, where a declining cadmium concentration gradient was reported in the stem in the direction of the developing leafy tissues (Harris and Taylor, 2013). A study using shark testis also reported the presence of a cadmium concentration gradient along the developmental stages, which are topographically separated (Betka and Callard, 1999). Further, accumulation of cadmium along a gradient has been observed in the kidney of brown trout, where cadmium concentration was found to increase with progression from the posterior kidney tail to the kidney head (Woodling et al., 2001). It has additionally been suggested that in metal-exposed marine organisms the metals demonstrate an inward-directed tissue diffusion gradient, due to the metal ions binding to a variety of ligands within the tissue cells, which may also act to slow overall metal efflux from the organism (Mason et al., 1988; Neff, 2002).

These studies support the hypothesis that the change in MT-1/2 protein expression observed in cadmium-exposed urothelium may reflect a cadmium concentration gradient, which decreased with penetration into the urothelial tissue. The reasons behind a potential concentration gradient are not clear, but may be due to cadmium sequestration by MT as it passes through the cells, meaning less cadmium reaches the underlying cells. It may also be that transcellular movement becomes more difficult with penetration into the urothelium, thus reducing the depth reached by cadmium. Future studies could isolate the individual urothelial cell zones after cadmium exposure and determine whether different cadmium concentrations are present using ICP-OES. This approach could also be combined with western blotting of protein lysates from the individual urothelial cell zones in order to determine whether differential MT-1/2 protein expression correlated with cadmium concentration changes.

Strong immunolabelling of MT-1/2 protein was detected in the stromal cells of control ureters. Expression was predominantly nuclear, and occurred in approximately 50 % of the stromal cells. The E9 antibody can detect protein expression of any isoform from the MT-1 and MT-2 subfamilies, meaning that it is unclear which protein isoform(s) was highly expressed within the stromal cells. As explained previously, the MT-2A isoform is the most abundant isoform in the human body (section 1.5.2), and it is therefore possible that the E9 antibody detected high protein expression of this isoform. Moreover, the stromal MT-1/2 immunolabelling was nuclear, and MT-2A has been reported to regulate cell cycle progression and proliferation, requiring a nuclear localisation (Studer et al., 1997; Jin et al., 2002; Lim et al., 2009; Yap et al., 2009; Kim et al., 2011).

### 6.4.2 Protein Expression Changes in other Potential Targets of Cadmium Exposure

After long-term ureter organ culture, control urothelium was observed to contain a high number of apoptotic bodies (indicated by cell shrinkage and chromatin condensation; Elmore, 2007) . The cause of cell death was most likely due to prolonged *in vitro* culture, as organ cultures cannot survive indefinitely (Yadav and Tyagi, 2006). However, it has been shown that ureter organ culture can be maintained for up to 18 weeks (Scriven et al., 1997), and thus extraneous variables affecting cell viability (such as patient donor health and sample time in transport medium) cannot be excluded (Resau et al., 1991). Chronically cadmium-exposed ureter also contained several apoptotic bodies, although to a lesser extent, suggesting increased cellular survival compared to control. This observation was supported by Ki67 immunolabelling, which showed protein expression in several urothelial cells from chronically cadmium-exposed ureter, whereas no expression was detectable in control urothelium (Figure 60).

Increased CK5 and decreased CK13/FOXA1 protein expression was observed in urothelial cells from cadmium-exposed ureters, inferring a possible loss of differentiation. The process by which cadmium may be able to inhibit differentiation is unclear. However, it could be related to the reported ability of cadmium to replace zinc in transcription factors, altering their physiological function and potentially deregulating important cellular pathways such as differentiation (see section 1.4.4.2). A potential approach to investigate this hypothesis would be to measure intracellular zinc levels pre-, during and post-cadmium exposure, which could be achieved using the labile zinc-specific fluorescent probe Zinquin (Nasir et al., 1999). Such as approach has previously been performed in the hepatic HepG2 cell line, as the authors reported an approximately 93 % increase in free intracellular zinc due to cadmium exposure (Urani et al., 2015). This study supports the hypothesis that cadmium may be able to displace zinc from its proteome, binding to TFs and altering normal cellular processes.

The observed increase in immunolabelling of H3K27me3 protein in chronically cadmium-exposed urothelium revealed a potential mechanism of cadmium-induced urothelial carcinogenesis. Elevated H3K27me3 protein expression has previously been demonstrated in UROtsa cells malignantly transformed by cadmium exposure (Somji et al., 2011b). Moreover, increased abundance of the H3K27me3 mark has been specifically associated with regions of chromosomal silencing found in a subset of urothelial cancers, termed the Multiple Regions of Epigenetic Silencing (MRES) phenotype (Vallot et al.,

2011). This subset of tumours was observed associated with a CIS-specific gene signature, and displayed a more aggressive phenotype. A further study investigating H3K27me3 expression in urothelial cancer found upregulated H3K27me3 expression in the majority of urothelial cancers analysed (Liu et al., 2013). They also found that increased H3K27me3 expression was associated with multifocal tumours and lymph node metastases, and was an independent prognostic indicator of cancer-specific survival. A more recent study additionally found that elevated expression of H3K27me3 protein may predispose urothelial tissue to development of the urothelial cancer (Balsara and Li, 2017). Taken together, these studies suggest that increased H3K27me3 protein expression may be linked with the development of aggressive urothelial cancer, possibly as a result of cadmium exposure.

# Chapter 7: Discussion

## 7.1 Main Findings

The first thesis objective was to perform novel characterisation of MT isoform expression in normal human urothelium. To achieve this, baseline and cadmium-induced MT isoform transcript expression was investigated for the first time in NHU cells derived from patient donors. Novel discrimination between all functional MT isoforms was performed in order to conduct a comprehensive characterisation of expression, and it was observed that the MT-1 subfamily was highly inducible by cadmium, and that the urothelium possessed its own unique MT isoform expressional profile. Further, novel iscrimination between MT-1 isoforms at the protein level was completed utilising commercially untested antibodies, revealing differential protein expression that supported the hypothesis of divergent MT isoform function.

Robust induction of the MT-1 subfamily facilitated achievement of the second objective, which was to determine whether cadmium could penetrate an intact human urothelial barrier. Using induction of MT-1 isoforms as a marker of cadmium exposure, it was indicated that cadmium could cross the protective urothelial barrier of differentiated NHU cells in culture. This finding was further supported using spectroscopic methods, which revealed direct detection of cadmium in exposed differentiated NHU cell cultures, despite the continuous presence of a functional urothelial barrier.

The third objective was to investigate specificity and longevity of cadmium-induced MT isoform expression. Individual MT isoform expression was assessed in NHU cell cultures exposed to a broad range of potential inducers, which allowed the identification of two MT-1 isoforms (MT-1A and MT-1M) whose induction was highly specific to cadmium. Moreover, results demonstrated the importance of discriminating between the MT isoforms at both the transcript and protein level, as the isoforms were observed to differ in their baseline expression, preferential induction, translational efficiency, transcript/protein longevity and protein localization. Bioinformatic analysis revealed that differential expression may be regulated by the number and location of MTF-1 binding sites within MT genes. It was also observed that while MT isoform transcript induction was transient, protein induction was long-lived and persisted for prolonged periods post-cadmium exposure.

The final objective was to determine whether the *in vitro* findings of cadmium-induced MT-1A and MT-1M protein expression could be translated to *ex vivo* ureter organ culture. Ureter organ culture supported the *in vitro* results, revealing MT-1A, MT-1M and generic MT-1/2 protein induction in the urothelium of cadmium-exposed ureters. Protein induction was found to be particularly strong after chronic (≥ 8 weeks) cadmium exposure, and MT-1A and MT-1/2 protein expression was observed to persist in the urothelium up to six weeks post-exposure. Additional investigation of cadmium-exposed ureter resulted in the observation of several other molecular changes, potentially indicating a change to a predominantly basal urothelium with increased cellular survival.

### 7.1.1 Key Findings

- The majority of MT-1 isoform transcripts were not expressed in NHU cells under baseline conditions; however, they were highly inducible by cadmium exposure
- Novel discrimination between the MT-1A and MT-1M proteins could be performed in cadmium-exposed NHU cells using commercially untested antibodies
- Cadmium appeared able to penetrate an intact urothelial barrier and enter the underlying urothelial cells
- Differential induction of the MT-1 isoforms was observed (including metal-specific activation), and MT-1A and MT-1M isoform induction appeared highly cadmium-specific
- MT-1 gene isoforms appeared to demonstrate individual spatial arrangements and total number of MTF-1 binding sites (MREs)
- MT-1A, MT-1M and MT-1/2 protein expression was induced in the urothelium of human ureters exposed to cadmium, along with other potential molecular changes
- MT-1A and MT-1/2 protein expression was still detectable in human urothelium up to 6 weeks post-exposure to cadmium

## 7.2 Discussion Points

### 7.2.1 Differential MT Isoform Expression

MT isoform expression was investigated in normal human urothelium for the first time in this thesis, and it was found that urothelial tissue possessed its own unique expressional profile (section 3.2.2). This finding was consistent with previous literature, which has suggested that MT isoform expression is tissue-specific (section 1.5.5.2). Moreover, the MT isoforms showed tissue-specific induction; MT isoforms previously found to be induced in other cell types by a specific agent (e.g. dexamethasone) could not be induced in NHU cells (section 5.2.1). Even other urothelial cell lines (thereby derived from the same source tissue) showed differential MT isoform expression to NHU cells under baseline and cadmium-exposed conditions (section 3.2.2.1), suggesting that the processes of immortalisation and/or carcinogenesis can also cause differential expression of MT isoforms. This observation is supported by previous literature, which has demonstrated altered MT-2A expression as a result of immortalisation of human primary cells (Duncan and Reddel, 1999; An et al., 2003). Therefore not only must the cell/tissue type be taken into consideration when investigating MT isoform expression, but also whether the cell has undergone carcinogenesis and/or immortalisation.

Novel discrimination of all known MT isoforms was successfully achieved within the same cell type. Previously, studies generally assessed combined MT-1 and MT-2 subfamily expression, or only selected a few specific MT-1 isoforms to analyse (section 1.5.6.1). However, this approach means that the whole picture is never truly evaluated, and changes in individual isoform expression may be missed. The work performed here demonstrates the urgent need to assess the MT isoforms individually, as each isoform was observed to differ in tissue-specific expression, preferential activation, rate of induction/de-induction, and even protein localisation (sections 3.2.2, 5.2.1, 5.2.4 and 6.2.1 respectively). These findings of differential MT isoform expression are supported by the bioinformatic analysis performed for this thesis, which suggested that the MT-1 isoforms possess different numbers and spatial arrangements of MREs (section 5.2.3). This is the first time that isoform-specific MRE localisation has been reported in human MT genes, and as well as supporting the observation of differential MT isoform expression, also provides a possible mechanism of the same.

The finding that each MT isoform demonstrated unique expressional characteristics supports the hypothesis that individual isoforms may perform related yet distinct functions (section 1.5.5.4). As discussed in the Introduction (section 1.5.2.1), the MT family has recently undergone rapid gene duplication due to a change in selection pressure, resulting in several new MT genes having been selected for and maintained. It is possible that the shift in selection pressure was due to the increased use and emittance of heavy metals in anthropological activity, resulting in the observation that the natural bio-geochemical cycle of heavy metals in ecosystems has become overwhelmed (Nriagu, 1996). *De novo* MT isoforms may have evolved and adapted in response to historical increased exposure, acting to both sequester these toxic metals and regulate cellular mechanisms to promote survival in the face of exposure.

### 7.2.2 The Metallothioneins as Possible Biomarkers of Cadmium Exposure

As explored in the Introduction (section 1.5.7.2), the MTs have long been suggested as possible biomarkers of cadmium exposure. However, the specificity of MT induction remained unclear, which is an essential prerequisite for a biomarker (Mayeux, 2004; Humpel, 2011). Research investigating the longevity of MT expression post-exposure in humans had also not been published, and is another important biomarker aspect to establish as not all exposure is current. For MT expression to qualify as a candidate biomarker of cadmium exposure, it would not only need to be specific to cadmium, but would also need to persist post-exposure, so that both current and historical cadmium exposure could be detected.

This thesis employed the use of commercially untested antibodies in order to perform novel discrimination between two of the MT-1 isoforms at the protein level (MT-1A and MT-1M). Previously, discrimination between MT-1 isoforms had only been attempted using spectroscopic techniques (section 1.5.5.4), which can be costly. In this work, discrimination between the MT-1A and MT-1M proteins allowed the specificity of their induction to be investigated, and therefore the isoforms could be assessed for their potential as biomarkers of cadmium exposure. MT-1A protein expression was found to be more promiscuous, but clearly showed preferential induction by cadmium, whereas MT-1M protein expression was found to be highly specific to cadmium alone (section 5.2.2). Importantly, ROS did not cause strong induction of either protein, suggesting that cadmium itself caused MT protein induction and not ROS as a by-product of exposure (sections 5.2.1.2 and 5.2.2).

However, a limitation of the use of these antibodies is that their specificity to the different MT-1 isoforms was not tested. It is therefore possible that the antibodies may have detected more than one MT-1 protein isoform. In order to confirm their specificity, co-immunoprecipitation could be performed. This methodology would involve the use of the MT-1A antibody to extract 'MT-1A protein' from cadmium-exposed NHU cells. The resultant protein fraction would then be probed with the MT-1M antibody in order to determine whether MT-1M protein was also present. This process could then be repeated using the MT-1M antibody to extract protein, and subsequent probing with the MT-1A antibody. It should also be noted that although the extent of protein induction was observed to vary between MT-1A and MT-1M, there is the possibility that this was due to antibody efficiency. Therefore caution should be use when comparing MT-1A and MT-1M protein expression.

Investigation of the longevity of MT protein expression in ureter organ culture showed that cadmium-induced MT-1A and MT-1/2 protein expression persisted up to 6 weeks after cessation of exposure (section 6.2.2.2). These findings of long-lived MT protein expression post-cadmium exposure were also supported by *in vitro* results (section 5.2.4.2). The initial results are promising, suggesting that MT protein expression may persist in the body for prolonged periods, and therefore could be utilised to detect both current and historical exposure. However, the experiment would need repeating in at least two other ureters from independent donors in order to make the results more robust. Future experiments would also need to extend the experimentation time, to determine whether MT protein expression can persist for longer than found in this thesis.

Results demonstrating long-lived protein expression of MT supports its putative role in metal sequestration, which has been suggested to occur via the formation of IBs (explained in the Introduction; section 1.5.4.2). Immunolabelling of MT-1A protein in NHU cells supported a sequestration hypothesis, as the protein was found to localise to both the cytoplasm and nucleus, which are the postulated sites of IB formation and migration respectively (Sigel et al., 2009). During cadmium exposure the protein presented as granular deposits, whereas post-exposure MT-1A protein presented as intranuclear circular structures, which suggests an association with the outer portion of an IB (section 6.2.2.2). Persistent MT protein expression may also have been caused by 'systemic cycling' of cadmium, which occurs when metal ions are re-released into the cell due to protein degradation of the MT-Cd complex (Bebianno and Langston, 1998; Sandbichler and Höckner, 2016). Release of free cadmium ions results in *de novo*

synthesis of MT protein and re-sequestration of the metal, meaning that cadmium is not only maintained in the cell for prolonged periods, but MT protein expression also persists long-term.

### 7.2.3 Possible Mechanisms of Cadmium-Induced Urothelial Carcinogenesis

Chronic cadmium exposure of normal human ureter revealed potential insights into the mechanisms by which cadmium can induce urothelial carcinogenesis. Long term ureter organ culture resulted in prominent urothelial cell death, the cause of which remains unclear, but it was observed that urothelial cells from chronically cadmium-exposed ureter demonstrated increased cellular survival. Exposed urothelium was additionally much narrower in width, demonstrating a less-differentiated, more basal phenotype and indicating a potential loss of the superficial cell zone (as indicated by Ki67, CK5, CK13 and FOXA1 protein expression; section 6.2.3).

Loss of the superficial urothelial cell zone has been reported previously in mouse bladders infected with UPEC, leaving the underlying intermediate urothelial cells exposed (Mysorekar et al., 2002; Colopy et al., 2014). These studies found that the loss of the superficial urothelial cell zone was followed by a rapid proliferation of CK5-posititive basal cells, supporting the observation of increased basal urothelial cell survival after chronic cadmium exposure in this thesis (section 6.4.2). Loss of the superficial urothelial cell zone could also explain the narrow urothelial width observed in exposed ureters and its apparent loss of differentiation, resulting in a predominantly basal phenotype. Loss of tissue differentiation is a characteristic property of malignant cells and closely coupled with abnormal proliferation, thereby providing a possible mechanism of cadmium-induced carcinogenesis (Cooper, 2000). Loss of the differentiation-associated marker FOXA1 expression (as observed in chronically cadmium-exposed urothelium; Figure 58) has specifically been linked to the development of undifferentiated cancers, and silencing of this gene has been demonstrated as sufficient to cause EMT in pancreatic ductal adenocarcinoma cell lines (Song et al., 2010). Moreover, loss of urothelial FOXA1 expression has specifically been reported to correlate with increased stage and histologic grade of urothelial cancers (DeGraff et al., 2012).

Although these initial results offer promising insight into cadmium-induced urothelial carcinogenesis, it should be noted that this was a preliminary study and only performed in ureter from one individual donor. Future experiments using ureters from two or more individual donors should therefore be performed in order to verify these observed protein

expression changes. To further determine whether chronic cadmium exposure can increase urothelial cell survival, experiments analysing expression of anti- and pro-apoptotic markers such as Bcl-2 and Bax (respectively) should be conducted (Adams and Cory, 1998; Pfister et al., 1999; Singh et al., 2009), perhaps in conjunction with the analysis of multiple markers of proliferation (Whitfield et al., 2006).

It is currently unclear whether the apparent increase in cellular survival could have been as a result of cadmium exposure, increased MT protein expression, or a combination of both. As explained in the Introduction, cadmium exposure has been demonstrated to induce malignant cellular transformation in a number of cell types (section 1.4.3). Transformation was characterised by reduced apoptosis and increased proliferation, which together may have contributed to the apparent increased cellular survival observed in this thesis (section 6.2.3). There is the additional possibility that elevated MT protein levels could have played a role, as MT protein expression has also been reported to directly increase cell survival by both promoting cell proliferation and inhibiting apoptosis (section 1.5.7.1). However, these results are so far only correlative. To determine whether MT protein does play a role increased cellular survival, functional analyses could be utilised. For example, if MT protein were to be knocked down in cadmium-exposed NHU cells and cellular survival remain unaffected, this would suggest that elevated MT protein expression does not play a role in cellular survival.

### 7.2.4 Thesis Implications

Comprehensive analysis of MT isoform expression revealed the extent to which the individual isoforms may differ in their expression, demonstrating the importance of discriminating not just between MT subfamilies, but also between all known MT subfamily isoforms. Important changes in individual isoform expression may otherwise be missed and/or masked by changes in other subfamily members. The results also show the need to establish MT isoform expression specifically in the target tissue being investigated, as normal human urothelium was observed to express its own unique MT isoform profile under both baseline and cadmium-induced conditions. This suggests that findings of altered MT expression from studies using other cell/tissue types are not cross-applicable, and individual investigation of target tissues must be performed. Moreover, this work also demonstrated the importance of using normal human primary cells, as both the processes of immortalisation and carcinogenesis may be able to alter MT isoform

expression. Isoform expression in cells that have undergone these processes may therefore not accurately reflect *in vivo* expression, reducing the validity of results.

The extent to which the MT isoforms differ in their expression is supportive of the theory that each individual may perform related but distinct roles in the cell (discussed in the Introduction; section 1.5.5.4). The results showed not only preferential induction of different isoforms by specific inducers, but also different rates of induction/de-induction, individual protein localisation, and isoform-specific number and spatial arrangement of MREs in the non-coding DNA; all of which are suggestive of divergent functions. Previous investigation of the MT-1G isoform supports such a hypothesis. This thesis and other studies have found strong preferential induction of MT-1G by zinc, potentially suggesting that the isoform's expression may be dependent upon intracellular zinc levels (Rahman and De Ley, 2001; Arriaga et al., 2014; section 5.2.1.5). Another study found that MT-1G transcript expression strongly correlated with cellular zinc levels in human Sertoli cells, leading the authors to propose that MT-1G has a predominant role in zinc homeostasis (Kheradmand et al., 2010). This was the first report of a MT isoform-specific function, and paves the way for future studies to elucidate such individual functions of the other isoforms. Functional analyses of the MT isoforms need to be performed, in order to observe the effects of under- and/or over-expression on the cell. Spectroscopic analysis could also be utilised, potentially combining the methods developed by Mehus et al. (2014) with those from Van Campenhout et al. (2004) and Wolf et al. (2009). Use of these methods would allow separation of the individual MT isoforms, and the identification of which specific metals they may be bound to, potentially providing novel insight into their individual functions within the cell.

A further implication of the research performed is that cadmium appears able to penetrate an intact urothelial barrier (Chapter 5). This is the first time that such a report has been made, as it was previously unclear whether cadmium may first damage the urothelium, thereby faciliating entry. The finding that cadmium appears able to cross one of the tightest epithelial barriers in the human body (section 1.1.3) and gain access to underlying tissue is of great public concern, and implies that the human body is not well-equipped to deal with this relatively recent health threat (section 1.4.1). The mechanisms that facilitate cadmium penetration of the urothelial barrier are unclear, but one possible explanation is that it can substitute for zinc in biological systems (see Introduction section 1.4.4.2). It is therefore possible that cadmium can utilise the same mechanisms as zinc to enter urothelial cells. This hypothesis is supported by several studies which have identified the

zinc importer protein (ZIP) 8 as a major facilitator of cadmium entrance into the cell, due to its high expression in cadmium-sensitive murine cells but minimal expression in cadmium-resistant cells (Fujishiro et al., 2009; He et al., 2009). ZIP8 expression has also been identified in normal human urothelium and in the UROtsa cell line (Ajjimaporn et al., 2012), further supporting the hypothesis that cadmium may enter urothelial cells by hijacking the use of zinc transporters.

Long term ureter organ culture revealed that chronic cadmium exposure may result in increased cellular survival, possibly via increased apoptotic-resistance induced by cadmium exposure and/or increased MT protein expression (section 6.4.2). This has implications not only for cadmium-induced carcinogenesis, but also for the development of chemotherapeutic resistance in cadmium-related malignancies. These cancers may be highly resistant to apoptosis and demonstrate increased proliferation (see Introduction; section 1.2.6.3), making them difficult to target using traditional apoptosis-inducing therapies, as well as potentially promoting the survival of highly aggressive malignant cells (Hart, 2000). Chemotherapeutic resistance in cadmium-related malignancies has already been observed, with Hatcher (1997) finding that cadmium exposure induced various forms of resistance in human lung carcinoma cell lines, including resistance against anti-neoplastic agents.

Whether increased treatment resistance was directly due to cadmium exposure, or increased MT expression as a result of exposure, is not yet clear. As explored in the Introduction, increased MT expression has also been postulated to cause increased cellular proliferation and resistance to apoptosis, and has also been linked to chemotherapeutic resistance (section 1.5.7.1). MT-induced resistance is potentially supported by the results in this thesis, which demonstrated high MT protein expression correlating with increased cellular survival (Chapter 7). Moreover, a previous study found that human ovarian cancer cells with acquired resistance to the anti-neoplastic cisplatin were also highly resistant to cadmium exposure, suggesting that another mechanism (such as MT expression) may be responsible for the acquired resistance (Lee et al., 1995). Further studies are needed to verify whether MT protein expression may directly influence chemotherapeutic resistance, as the proteins could potentially be targeted by future treatments with the aim of increasing tumour sensitivity to chemotherapy.

The work conducted here suggests that the MT isoforms MT-1A and MT-1M may potentially be utilised as specific biomarkers of cadmium exposure. Such markers would

be useful for monitoring both environmental and occupational exposure, with the aim of informing policy decisions and ultimately reducing human health risks. However, a non-invasive method of determining urothelial MT expression would be required, instead of basing analysis on invasive urothelial patient biopsies. An ideal patient sample source would be urine, which often contains sloughed off urothelial cells, and has already been used to determine MT protein concentration in exposed individuals (see Introduction; section 1.5.6.3). Protocols would need to be further developed in order to detect individual MT isoform expression for the test to be cadmium-specific, but this could potentially be achieved using a combination of the previously described spectroscopic methods (section 1.5.5.4).

Lastly, biomarkers of cadmium exposure would allow the stratification of urothelial cancers into a subgroup specifically linked to exposure, providing novel insights into cadmium-induced urothelial carcinogenesis. Gene expression profiles could be compared from non- and cadmium-induced urothelial samples, which may allow the identification of genes specifically altered in the exposed samples. This would not only elucidate the mechanisms by which cadmium may cause carcinogenesis, but also provide novel targets for treatment.

### 7.2.5 Future Work

A number of suggested experiments for future work have been suggested throughout the thesis, within discussion sections. However, there are a number of experiments which would be important next steps in order to verify and extend the current research. First and foremost, as explored in section 7.2.2, it would be essential to confirm the specificity of the MT-1A and MT-1M antibodies. This could be achieved not only via co-immunoprecipitation, but also by knocking out isoform gene expression in NHU cells and subsequent probing for protein expression. A knock-out NHU cell model could be further used for functional studies, aimed at determining whether the MT-1 isoforms may perform differential roles (section 7.2.3).

To further eludicate the mechanisms by which cadmium may enter and perturb NHU cellular function, future research should focus upon cellular zinc kinetics. Determination of zinc transporter presence and expression on NHU cells could reveal the mechanisms by which cadmium ions enter the cell, and possibly reflect alterations to intracellular zinc concentration (section 1.5.4.1). Experiments using the labile zinc-binding fluorescent probe Zinquin could additionally be utilised in order to directly

assess intracellular zinc levels during and after cadmium exposure (section 6.4.2), as increased labile zinc has been well-reported as a possible mechanism of cadmium-induced carcinogenesis (section 1.4.4.2)

The protein changes observed in ureter organ culture after chronic exposure to cadmium revealed insights into other potential mechanisms of cadmium-induced carcinogenesis, inferring increased cellular survival and loss of differentiation in exposed urothelium (sections 6.2.3 and 6.4.2). However, as this experiment was only performed in ureter from one donor, the experiment needs to be repeated using ureters from at least another two individual donors to verify the initial results. Experiments should not only aim to assess initial target protein expression, but include additional targets indicative of cellular apoptosis, such as Bcl-2 (section 7.2.3).

Lastly, as mentioned above (section 7.2.4), further work should aim to determine whether MT-1A and/or MT-1M could be used as biomarkers of cadmium exposure *in vivo*. This would allow the stratification of a subset of urothelial carcinoma specimens associated with cadmium exposure, facilitating identification of cadmium-specific gene signatures and potentially revealing mechanisms of cadmium-induced urothelial carcinogenesis. To determine whether such stratification may be possible, future experiments should aim to determine whether MT-1A/MT-1M protein expression can be detected in malignant urothelial samples obtained from patients who have been identified as being occupationally exposed to cadmium. Determination of exposure could be achieved using a questionnaire, aimed at determining current and historical occupations, as well as smoking habits (to control for extraneous variables). Immunolabelling of samples for MT-1A and MT-1M protein expression would then reveal whether a correlation could be found between cadmium exposure and MT protein expression, allowing the novel stratification of a subgroup of cadmium-related urothelial cancers.

Chapter 8: Appendices

## 8.1 NHU Cell Lines Used

All NHU cell lines used in experiments for this thesis are detailed in the table below.

***Table 7: Summary of NHU cell lines used in thesis. All NHU cell lines were obtained from independent donors.*** *Detailed in the table is their unique Y-number, their tissue of origin and the surgical procedure the patient underwent which allowed the tissue to be obtained.*

| Y Number | Tissue of Origin | Surgical Procedure |
|---|---|---|
| **1089** | Renal Pelvis | Pyeloplasty |
| **1097** | Ureter | Nephrectomy |
| **1234** | Renal Pelvis | Pyeloplasty |
| **1270** | Ureter | Nephrectomy |
| **1277** | Renal Pelvis | Pyeloplasty |
| **1342** | Ureter | Nephrectomy |
| **1344** | Ureter | Nephrectomy |
| **1387** | Ureter | Renal Transplant |
| **1426** | Ureter | Renal Transplant |
| **1456** | Ureter | Renal Transplant |
| **1470** | Ureter | Renal Transplant |
| **1483** | Ureter | Renal Transplant |
| **1493** | Ureter | Renal Transplant |
| **1497** | Ureter | Renal Transplant |
| **1526** | Ureter | Renal Transplant |

| | | |
|---|---|---|
| **1531** | Ureter | Renal Transplant |
| **1566** | Ureter | Nephrectomy |
| **1594** | Ureter | Renal Transplant |
| **1644** | Ureter | Renal Transplant |
| **1705** | Ureter | Renal Transplant |
| **1770** | Ureter | Renal Transplant |
| **1089** | Renal Pelvis | Pyeloplasty |

## 8.2 List of Suppliers

- Abnova - http://www.abnova.com/
- Bioline - http://www.bioline.com/
- Bio-Rad - http://www.bio-rad.com/
- CellPath - http://www.cellpath.co.uk/
- Dako - http://www.dako.com/
- Dynex Technologies - http://www.dynextechnologies.com/
- Elga - http://www.elgalabwater.com/en-gb/
- Eurofins - http://www.eurofins.co.uk/
- Fisher Scientific - https://www.fishersci.com/us/en/home.html
- Fumetec Limited - http://www.fumetec.co.uk/
- Greiner Bio-one - http://www.greinerbioone.com/en/start/
- Hendley-Essex - http://www.hendley-essex.com/
- Hettic - http://www.hettichlab.com/
- Jencos - https://uk.vwr.com/store/
- Leica Microsystems - http://www.leica-microsystems.com/home/
- Li-Cor- https://www.licor.com/
- Media Cybernetics - http://www.mediacy.com/
- Medical Air Technology - http://www.medicalairtechnology.com/
- Millipore - http://www.emdmillipore.com/
- Ohaus - http://europe.ohaus.com/europe/en/home.aspx
- Olympus - http://www.olympus.co.uk/
- Philip Harris - http://www.philipharris.co.uk/
- Promega - http://www.promega.co.uk/
- ProteinTech - http://www.ptglab.com/
- Sarsedt - https://www.sarstedt.com/en/home/
- Scientific Laboratory Supples - http://www.scientificlabs.co.uk/
- Seralab - http://www.seralab.co.uk/
- Serotec - https://www.abdserotec.com/
- Sigma-Aldrich - https://www.sigmaaldrich.com/
- Source Bioscience - http://www.sourcebioscience.com/
- Starlab - http://www.starlab.de/int/?l=3

- Syngene - http://www.syngene.com/
- Thermo Scientific - http://www.thermoscientific.com/en/home.html
- Vector Laboratories - http://vectorlabs.com/
- VWR - https://uk.vwr.com/store/
- World Precision Instruments - https://www.wpiinc.com/

## 8.3 Stock Solutions

### 8.3.1 General Lab Solutions

#### *8.3.1.2 Phosphate Buffered Saline (PBS)*

5 PBS tablets (Sigma) were dissolved in 1 L of $dH_2O$. The solution was then autoclaved at 121° for 20 minutes, and cooled to room temperature before use.

### 8.3.2 Cell Culture Solutions

#### *8.3.2.1 Transport Medium*

500 mL Hanks Balanced Salt Solution (HBSS; Gibco, Life Technologies) containing 140 mg/L $CaCl_2$, 100 mg/L $MgCl_2$, 10 mM hydroxyethyl-piperazineethanesulfonic acid (HEPES) buffer (Gibco, Life Technologies) and 500 000 kallikrein inactivating units (KIU) Trasylol (Nordic Pharma).

#### *8.3.2.3 Stripper Medium*

500 mL HBSS (-$Ca^{2+}$, -$Mg^{2+}$; Gibco, Life Technologies) containing 0.1 % (w/v) EDTA, 500 000 KIU Trasylol and 10 mM HEPES buffer (Gibco, Life Technologies).

#### *8.3.2.4 Cholera Toxin*

34.3 mL KSFM (keratinocyte serum-free medium; Gibco, Life Technologies) containing cholera toxin powder (Sigma Aldrich) was stored at 4°C until use. When diluted in 500 mL KSFM-complete (KSFM with supplements) for use the final cholera toxin concentration was 30 ng/mL.

#### *8.3.2.5 0.1 % EDTA Solution*

1 L dPBS containing 1 g EDTA (Fisher Scientific) was autoclaved at 120°C for a duration of 20 minutes. The solution was then cooled before use.

#### *8.3.2.6 Collagenase IV Solution*

10 000 units of Collagenase IV powder (Sigma Aldrich) was dissolved in 100 mL HBSS (+$Ca^{2+}$, +$Mg^{2+}$) containing 10 mM HEPES buffer (Gibco, Life Technologies). The solution was then filter-sterilised using a 0.2 µM low protein-binding filter syringe (Gelman, Sigma Aldrich) before storage at -20°C.

*8.3.2.7 Dispase II Solution*

dPBS was pre-warmed to 37°C before addition of dispase II powder to a final concentration of 0.5 % (w/v). The solution was then vortexed thoroughly, passed through Whatman 0 filter paper and filter sterilised using a 0.2 µM low protein-binding filter syringe (Gelman, Sigma Aldrich). The final solution was then aliquoted and stored at -20°C until use.

*8.3.2.8 Trypsin Versene*

4 mL 1 % EDTA was combined with 20 mL 10x Trypsin (Sigma Aldrich) and then made up to 200 mL with HBSS (-$Ca^{2+}$, -$Mg^{2+}$; Gibco, Life Technologies). The solution was aliquoted and then stored at -20°C until use.

*8.3.2.9 Trypsin Inhibitor*

100 mg Trypsin inhibitor (Sigma) was dissolved in 5 mL dPBS, filter sterilised using a 0.2 µM low protein-binding filter syringe (Gelman, Sigma Aldrich), aliquoted and stored at -20°C.

**8.3.3 Histology Solutions**

*8.3.3.1 Haemotoxylin*

850 mL $dH_2O$ containing 0.3 g sodium iodate, 1 g citric acid and 50 g aluminium potassium sulphate was combined with 20 mL 100 % ethanol containing 3 g haemotoxylin. Once thoroughly mixed 120 mL glycerol was added.

*8.3.3.2 Scott's Tap Water*

0.35 % (w/v) $NaHCO_3$ and 2 % (w/v) $MgSO_4$ in $dH_2O$.

*8.3.3.3 10% Formalin*

900 mL PBS containing 0.9 mM $CaCl_2$and 0.5 mM $MgCl_2$ was added to 100 mL 37 % (v/v) formaldehyde.

*8.3.3.4 Tris-Buffered Saline (TBS)*

1 L $dH_2O$ containing 0.5 M Tris-HCL (Sigma Aldrich) and 0.15 M NaCl (SLS), pH adjusted to 7.6.

*8.3.3.5 Tris-Buffered Saline plus Tween®20 (TBST)*

1 L $dH_2O$ containing 0.5 M Tris-HCL (Sigma Aldrich), 0.15 M NaCl (SLS) and 0.1 % Tween®20 (Sigma Aldrich), pH adjusted to 7.6.

### 8.3.4 PCR Electrophoresis

*8.3.4.1 10x Tris-Borate-EDTA (TBE) Buffer*

1 L $dH_2O$ containing 0.9 M Tris, 0.9 M Boric acid and 25 mM EDTA. The solution was diluted to 1x using $dH_2O$ prior to use.

### 8.3.5 Western Blotting

*8.3.5.1 2x Sodium Dodecyl Sulphate (SDS) Lysis Buffer*

20 % (v/v) glycerol, 2 % (w/v) sodium dodecyl sulphate (SDS), 18.4 mg sodium orthovanadate, 0.42 g sodium fluoride, 0.446 tetra-sodium pyrophosphate and 125 mM Tris-HCL (pH 6.8) made up to 50 mL with $dH_2O$. The solution was then stored at -20°C.

*8.3.5.2 Transfer Buffer*

1 L $dH_2O$ containing 12 mM Tris, 96 mM glycine and 20 % (v/v) methanol.

*8.3.5.3 Tris-Buffered Saline (TBS)*

1 L $dH_2O$ containing 10 mM Tris and 140 mM NaCl, pH adjusted to 7.4.

*8.3.5.4 Tris-Buffered Saline plus Tween®20 (TBST)*

1 L $dH_2O$ containing 10 mM Tris, 140 mM NaCl and 0.1 % Tween®20 (Sigma Aldrich), pH adjusted to 7.4.

## 8.4 Primer Table

***Table 8: Details of primers used for experiments.***

| Target Gene | Forward or Reverse | Sequence (5´-3´) | Product Size (bp) |
|---|---|---|---|
| **GAPDH** | Forward | CAAGGTCATCCATGACAACTTTG | 90 |
| **GAPDH** | Reverse | GGGCCATCCACAGTCTTCTG | 90 |
| **HIF-1α** | Forward | GCAGGGTCAGCACTACTTCG | 684 |
| **HIF-1α** | Reverse | TTTCCTCAGTCGACACAGCC | 684 |
| **IRF-1** | Forward | CCTGCAGCAGAGCCAACATG | 280 |
| **IRF-1** | Reverse | AGGGAGTTCATGGCACAGCG | 280 |
| **MT-1A** | Forward | CTCGAAATGGACCCCAACT | 219 |
| **MT-1A** | Reverse | ATATCTTCGAGCAGGGCTGTC | 219 |
| **MT-1B** | Forward | GGAACTCCAGGCTTGTCTTGG | 77 |

| | | | |
|---|---|---|---|
| **MT-1B** | Reverse | TTGCAGGAGGTACATTTG | 77 |
| **MT-1E** | Forward | TGCGCCGGCTCCTGCAAGTC | 118 |
| **MT-1E** | Reverse | ATGCCCCTTTGCAGACGCAGC | 118 |
| **MT-1F** | Forward | CCTGCACCTGCGCTGGTTCC | 110 |
| **MT-1F** | Reverse | ACAGCCCTGGGCACACTTGC | 110 |
| **MT-1G** | Forward | CTTCTCGCTTGGGAACTCTA | 309 |
| **MT-1G** | Reverse | AGGGGTCAAGATTGTAGCAAA | 309 |
| **MT-1H** | Forward | CCTCTTCTCTTCTCGCTTGG | 317 |
| **MT-1H** | Reverse | GCAAATGAGTCGGAGTTGTAG | 317 |
| **MT-1M** | Forward | CTAGCAGTCGCTCCATTTATCG | 180 |
| **MT-1M** | Reverse | CAGCTGCAGTTCTCCAACGT | 180 |
| **MT-1X** | Forward | GGACCCAACTGCTCCTGCTC | 151 |

| | | | |
|---|---|---|---|
| **MT-1X** | Reverse | TTTGCAGATGCAGCCCTGGGC | 151 |
| **MT-2A** | Forward | CCGACTCTAGCCGCCTCTT | 259 |
| **MT-2A** | Reverse | GTGGAAGTCGCGTTCTTTACA | 259 |
| **MT-3** | Forward | AGTGCGAGGGATGCAAATG | 98 |
| **MT-3** | Reverse | GCCTTTGCACACACAGTCCTT | 98 |
| **MT-4** | Forward | CATGGACCCCAGGGAATGTGT | 213 |
| **MT-4** | Reverse | GGGGTGGGCACGATGGA | 213 |
| **TGF-β2** | Forward | GCGCTACATCGACAGCAAAG | 381 |
| **TGF-β2** | Reverse | CAATAGGCCGCATCCAAAGC | 381 |
| **ZO-1** | Forward | GTGTCTTCCCGGAGATCCAA | 292 |
| **ZO-1** | Reverse | GCCAATACCAACAGTCCCGT | 292 |

## 8.5 Antibody Table

***Table 9: Primary antibodies used for research.*** **denotes antibodies that required use of the Impress IHC kit (see methods).*

| **Antigen** | **Clone** | **Host** | **Supplier** | **Dilution** | **Molecular Weight (kDa)** |
|---|---|---|---|---|---|
| **Beta-actin** | A5441 | Mouse | Sigma Aldrich | 1:10 000 (WB) | 42 |
| **Claudin 7** | 34-9100 | Rabbit | Zymed | 1:100 (IHC) | - |
| **Cytokeratin 5** | Ab53121 | Rabbit | Abcam | 1:200 (IHC) | |
| **Cytokeratin 7** | LP1K | Mouse | CRUK | 1:1000 (IHC) | - |
| **Cytokertain 13** | IHC: KS13.1 | IHC: Mouse | IHC: MP Biomedicals | IHC: 1:10 | - |
| ***FOXA1** | HF3α | Mouse | Santa Cruz | 1:250 | - |
| **H3K27me3** | C36B11 | Rabbit | Cell Signalling | 1:400 | - |
| **Ki67** | MM1 | Mouse | Leica | 1:200 | - |
| ***Metallothionein 1A** | B01P | Mouse | Abnova | 1:750 (WB) | 6 |

| | | | | | |
|---|---|---|---|---|---|
| | | | | 1:500 (IHC)* | |
| ***Metallothionein 1M** | 17281-AP | Rabbit | ProteinTech | 1 µg/mL (WB)<br>1:16 000 (IHC)* | 6 |
| **Metallothionein 1/2** | E9 | Mouse | Dako | 1:800 (IHC) | - |

***Table 10: Secondary antibodies used for research.***

| **Antigen** | **Conjugate** | **Host** | **Supplier** | **Application** |
|---|---|---|---|---|
| **Anti-mouse IgG** | Alexa 680 | Goat | Life Technologies | WB |
| **Anti-rabbit IgG** | Alexa 800 | Goat | Life Technologies | WB |
| **Anti-mouse IgG** | Biotin | Rabbit | Dako | IHC |
| **Anti-rabbit IgG** | Biotin | Goat | Dako | IHC |

## 8.6 Experimental Controls

### 8.6.1 Cell Culture

Induction of target gene expression was used as a positive control to ensure that treatment of cells with various compounds had been successful.

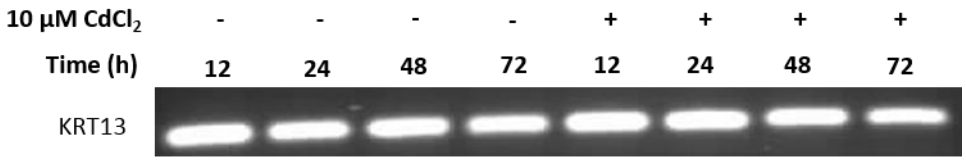


***Figure 622: Use of gene expression to ensure successful treatment of cells with a specific compound****. In this case, CK13 gene expression was used in order to confirm differentiation of NHU cells treated with ABS and calcium.*

### 8.6.2 Treatment Titrations

For treatments used in cell culture optimal doses were determined using concentration titrations and target gene expression changes.

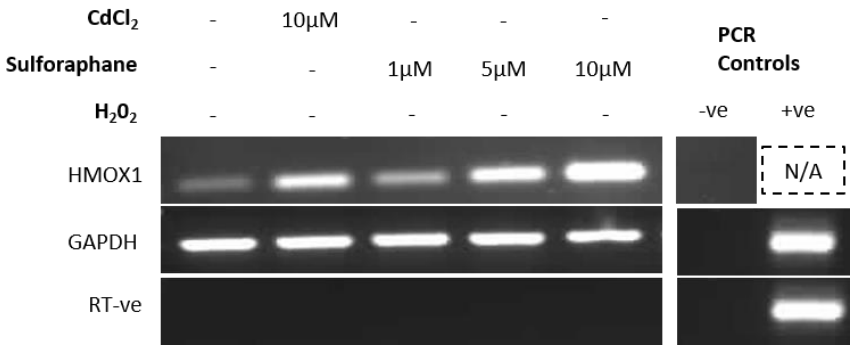


***Figure 633: RT-PCR showing Sulforaphane (SF) titration to determine an optimal dose for inducing reactive oxygen species (ROS).*** *Proliferating NHU cells (Y1344) were treated with a range of concentrations of the ROS-inducing agent SF for 12 hours, and the effect on the target gene HMOX1 transcript expression assessed in comparison to exposure to 10 µM $CdCl_2$. The concentration of SF that induced expression of HMOX1 to a comparable extent to cadmium was selected.*

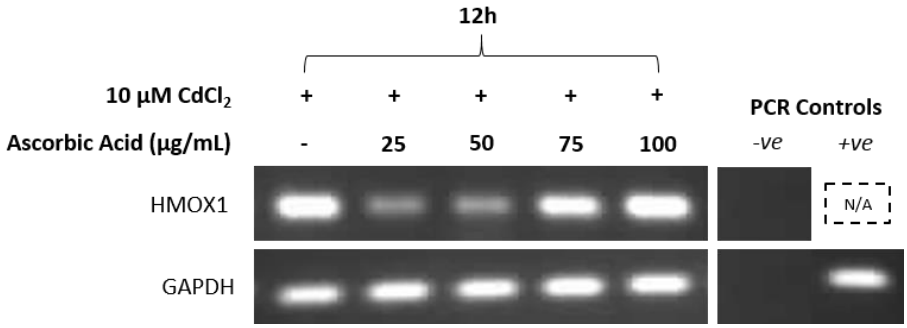


***Figure 64: RT-PCR showing ascorbic acid titration to determine an optimal dose for inhibiting production of reactive oxygen species (ROS).*** *Proliferating NHU cells (Y1594) were treated with 10 µM $CdCl_2$ in combination with a range of concentrations of the ROS inhibitor ascorbic acid for 12 hours. HMOX1 transcript expression was used to infer levels of ROS. A reduction in transcript expression was therefore indicative of inhibition of ROS production.*

## 8.7 Biological Experimental Replicates

Below are supplementary figures detailing results from biological replicates of experiments shown in the main results chapters. The representative figure number is given, followed by the supplementary images from biological replicates.

### 8.7.1 Biological Replicates from Representative Figure 22

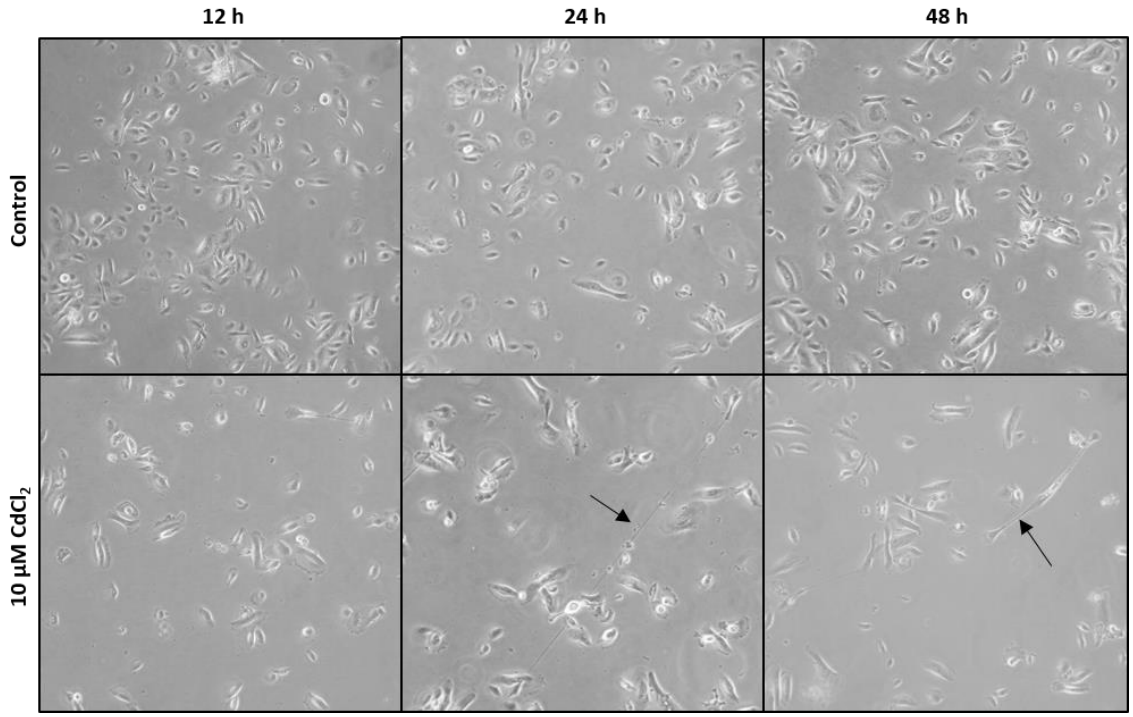


***Figure 65: Phase contrast images of NHU cells cultured in the presence of cadmium for 48 hours.*** *Proliferating NHU cells (n=1; Y1270) were seeded at a density of 6x10$^4$ cells/cm$^2$ and exposed to 10 µM $CdCl_2$ for up to 48 hours. Arrows indicate formation of extended processes between the cells. Scale bar = 50 µm.*

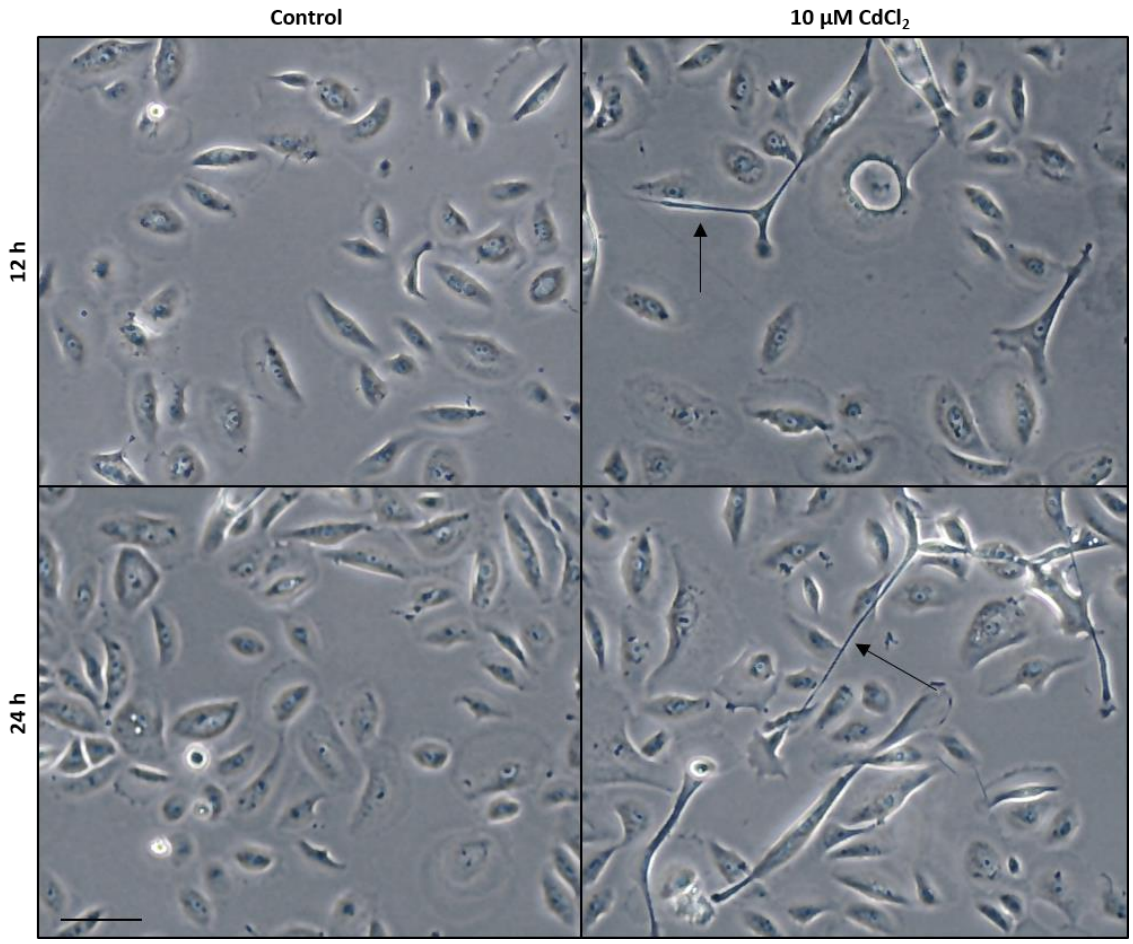


***Figure 66: Phase contrast images of NHU cells cultured in the presence of cadmium for up to 24 hours.*** *Proliferating NHU cells (n=1; Y1426) were seeded at a density of $6x10^4$ cells/$cm^2$ and exposed to 10 µM $CdCl_2$ for up to 48 hours. Arrows indicate formation of extended processes between the cells. Scale bar = 50 µm.*

### 8.7.2 Biological Replicates from Representative Figure 25

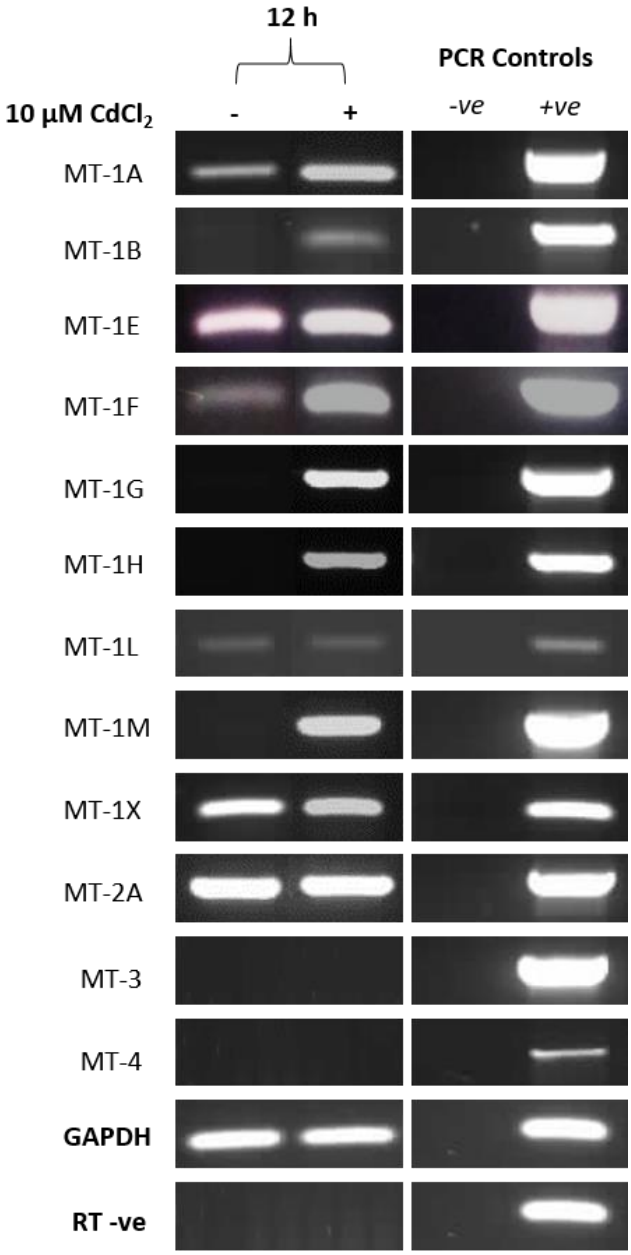


***Figure 67: RT-PCR showing MT isoform transcript expression in proliferating NHU cells exposed to cadmium.*** *Proliferating NHU cells (n=1; Y1426) were exposed to 10 µM $CdCl_2$ for up to 12 hours, RNA was then extracted and MT isoform transcript expression assessed. PCR controls included genomic DNA as a positive control and $dH_2O$ as a negative control. GAPDH transcript expression was used as a loading control, and RT-ve samples confirmed the absence of genomic contamination.*

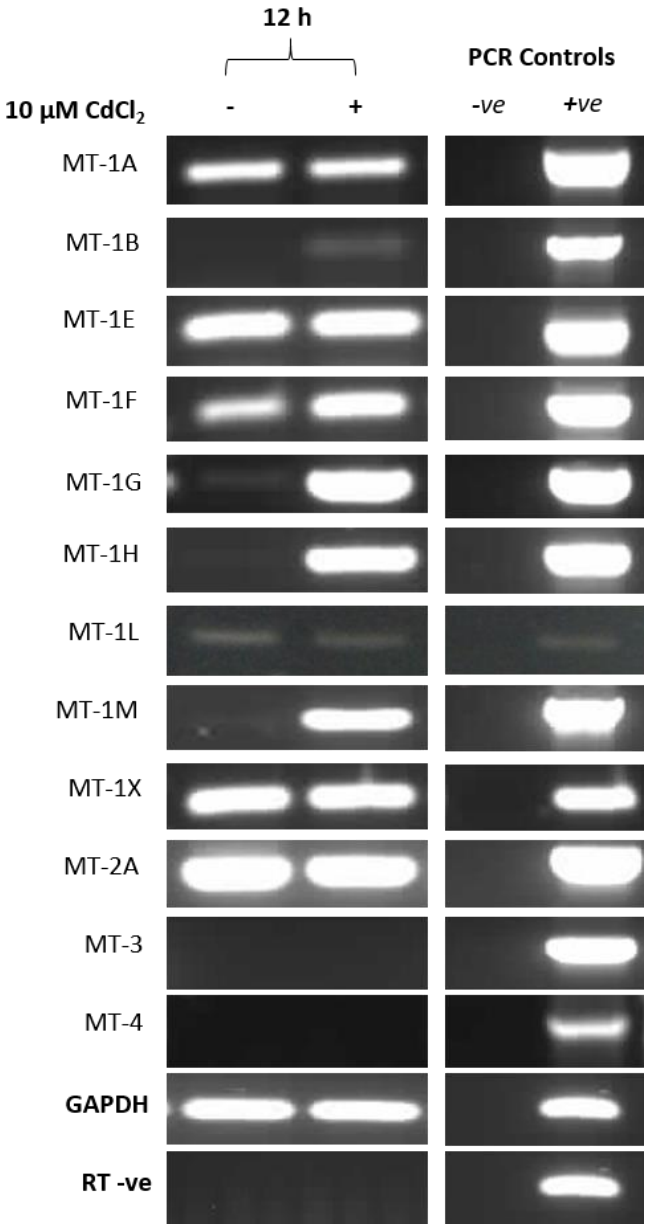


***Figure 68: RT-PCR showing MT isoform transcript expression in proliferating NHU cells exposed to cadmium.*** *Proliferating NHU cells (n=1; Y1344) were exposed to 10 µM $CdCl_2$ for up to 48 hours, RNA extracted and MT isoform transcript expression assessed. PCR controls included genomic DNA as a positive control and $dH_2O$ as a negative control. GAPDH transcript expression was used as a loading control, and RT-ve samples confirmed the absence of genomic contamination.*

### 8.7.3 Biological Replicates from Representative Figure 32

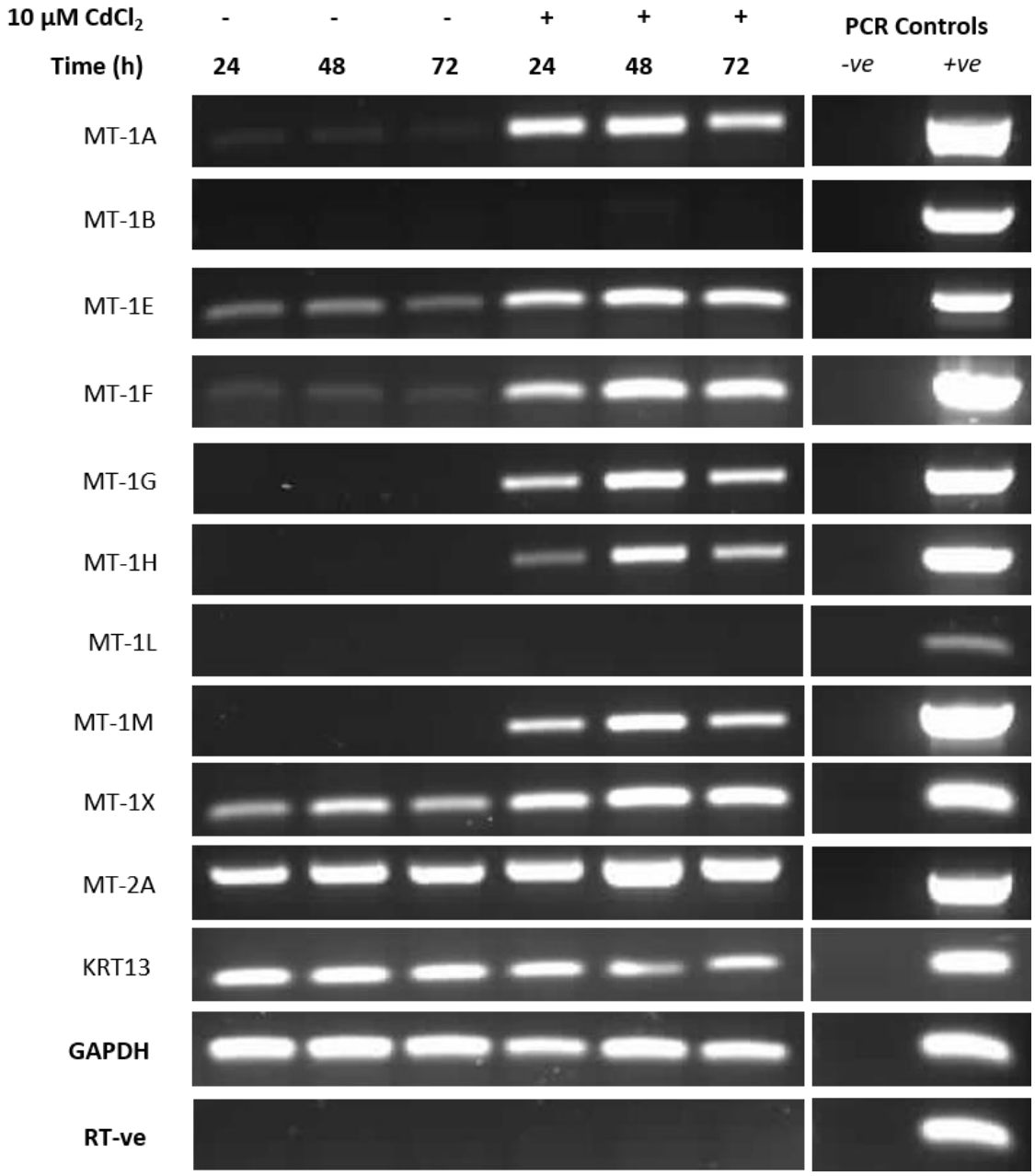


***Figure 69: RT-PCR showing MT isoform transcript expression in cadmium-exposed differentiated NHU cell sheets that demonstrated a functional barrier.*** *NHU cells (n=1; Y1493) were terminally differentiated and exposed to 10 µM $CdCl_2$ for up to 72 hours. Differentiation was confirmed using TER readings and expression of KRT13. PCR controls included genomic DNA as a positive control and $dH_2O$ as a negative control. GAPDH transcript expression was used as a loading control, and RT-ve samples confirmed the absence of genomic contamination.*

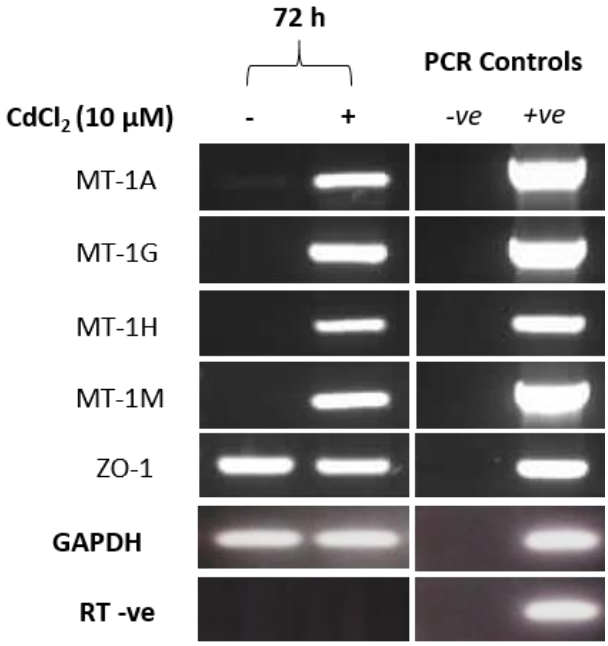


***Figure 70: RT-PCR showing MT isoform transcript expression in cadmium-exposed differentiated NHU cell sheets that demonstrated a functional barrier.*** *NHU cells (n=1; Y1531) were terminally differentiated and exposed to 10 µM CdCl2 for up to 72 hours. Differentiation was confirmed using TER readings and expression of ZO-1. PCR controls included genomic DNA as a positive control and $dH_2O$ as a negative control. GAPDH transcript expression was used as a loading control, and RT-ve samples confirmed the absence of genomic contamination.*

### 8.7.4 Biological Replicates from Representative Figure 39

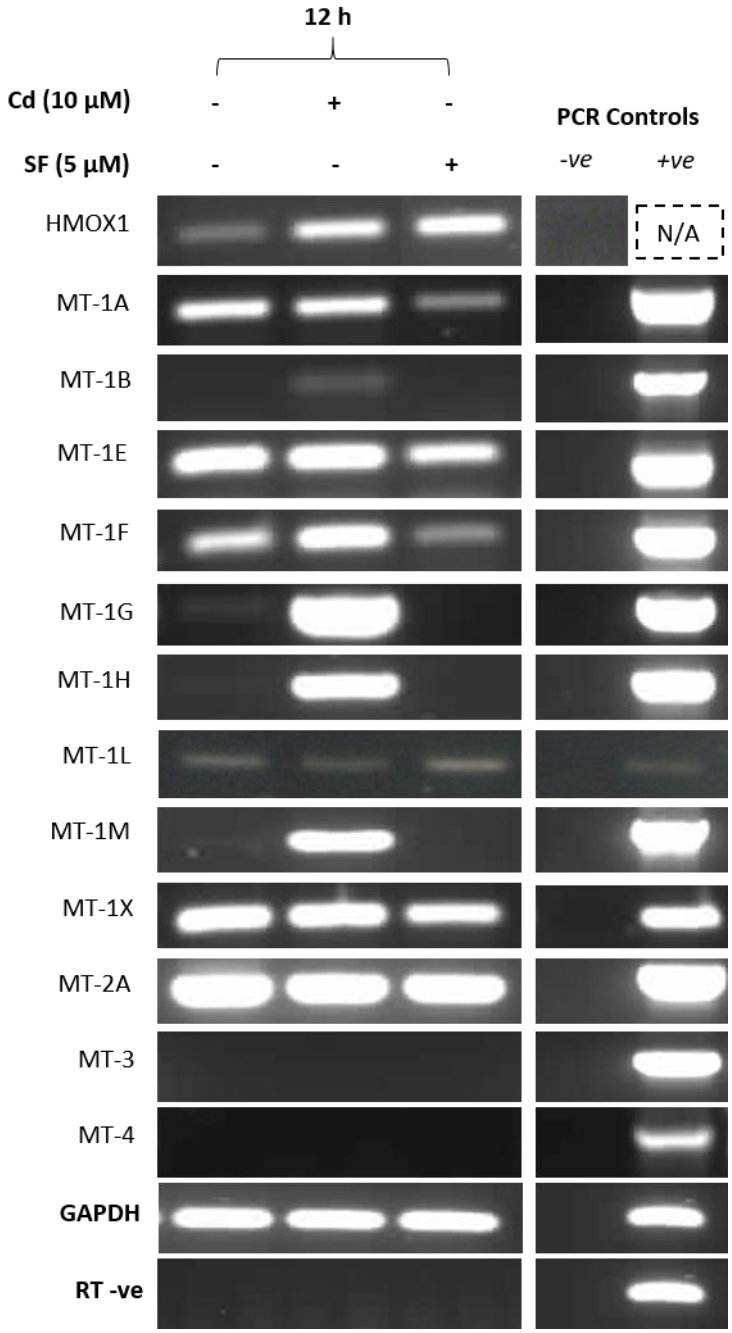


***Figure 71: RT-PCR showing the effects of ROS on MT isoform transcript expression in NHU cells.*** *The chemical Sulforaphane (SF) was used to induce ROS, having been titrated to a concentration that mimicked the levels of cadmium-induced ROS. Proliferating NHU cells (n=1; Y1344) were treated with either 10 µM $CdCl_2$ or 5 µM Sulforaphane for 12 hours and RNA extracted for analysis. The production of ROS was inferred using the ROS-sensitive HMOX1 gene transcript expression. PCR controls included genomic DNA as a positive control and $dH_2O$ as a negative control. GAPDH transcript expression was used as a loading control, and RT-ve*

*samples confirmed the absence of genomic contamination. A positive genomic DNA control for HMOX1 expression was not possible due to intron-spanning primers (N/A; not applicable).*

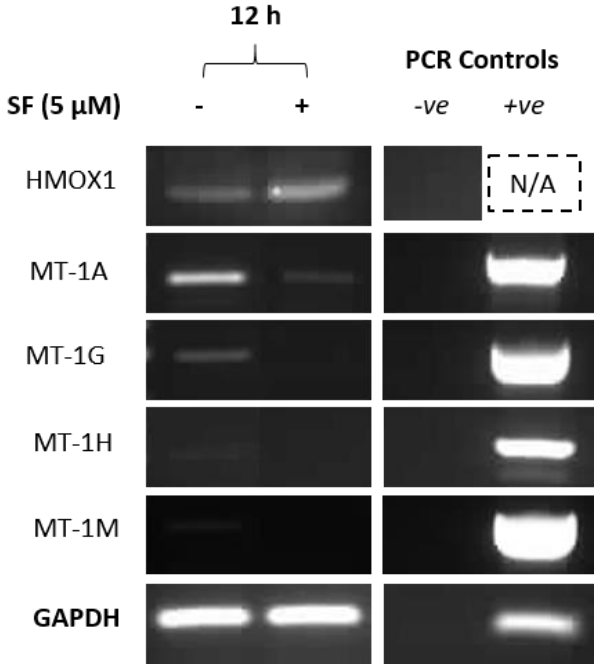


***Figure 72: RT-PCR showing the effects of ROS on MT isoform transcript expression in NHU cells.*** *The chemical Sulforaphane (SF) was used to induce ROS, having been titrated to a concentration that mimicked the levels of cadmium-induced ROS. Proliferating NHU cells (n=1; Y1526) were treated with 5 µM Sulforaphane for 12 hours and RNA extracted for analysis. The production of ROS was inferred using the ROS-sensitive HMOX1 gene transcript expression. PCR controls included genomic DNA as a positive control and $dH_2O$ as a negative control. GAPDH transcript expression was used as a loading control, and RT-ve samples confirmed the absence of genomic contamination. A positive genomic DNA control for HMOX1 expression was not possible due to intron-spanning primers (N/A; not applicable).*

### 8.7.5 Biological Replicates from Representative Figure 44

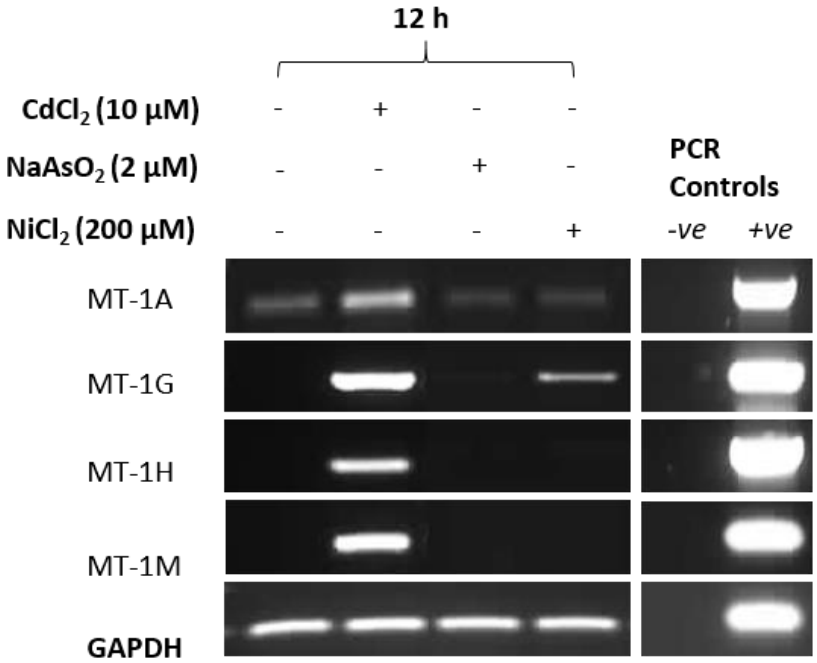


***Figure 73: RT-PCR showing the effects of exposure to the carcinogenic metals arsenite and nickel on MT-1 isoform transcript expression in NHU cells.*** *Proliferating NHU cells (n=1; Y1526) were exposed to 2 µM $NaAsO_2$ or 200 µM $NiCl_2$ for 12 hours and MT-1 isoform transcript expression assessed. PCR controls included genomic DNA as a positive control and $dH_2O$ as a negative control. GAPDH transcript expression was used as a loading control, and RT-ve samples confirmed the absence of genomic contamination.*

## 8.8 SOP for the Handling and Use of Cadmium Chloride

### 8.8.1 Safety Protocol for the handling and use of Cadmium Chloride (Hazard Level Code: 4)

*General*

Cadmium chloride is a known human non-genotoxic carcinogen that causes cancer following inhalation or ingestion, targeting the lung and prostate, with evidence to suggest that bladder and kidney cancers are linked to cadmium. It is toxic if inhaled or swallowed and is an irritant to skin. It can also cause sensitization by inhalation and skin contact. Cadmium chloride is also very toxic to aquatic organisms and may cause long term adverse effects in the aquatic environment. Inhalation of cadmium can be fatal.

Precautions for safe handling are to avoid inhalation and contact with skin, eyes and clothing. Hands should always be washed after working with cadmium chloride.

*8.9.1.1 Personal Protective Equipment*

Nitrile gloves and lab coat are essential. The safety cabinet shield on the fume hood and tissue culture hood will provide adequate protection for eyes and inhalation risk.

*8.9.1.2 Storage*

The cadmium chloride powder stock container should be tightly closed, contain silica gel beads for removal of air moisture, and be stored in the lockable dangerous chemicals cabinet. The contained should be labelled with researcher name and date of opening.

*8.9.1.3 Weighing*

The transfer of cadmium chloride powder from the original container to a bijou/universal tube should take place in the fume hood. Place a tray lined with damp blue roll into the fume hood to collect any powder spillages. Predetermine if the air flow in the hood is too strong by testing whether a non-harmful powder gets blown off a spatula. If this does occur turn off the fume hood while dispensing the cadmium chloride and then turn on again once the cadmium chloride has been put in bijou/universal tube.

Using a disposable spatula carefully dispense a small amount of cadmium chloride powder into a pre-weighed bijou/universal in the fume hood over the lined tray. Once the cadmium chloride is in the bijou, seal up the bijou/universal and cadmium chloride containers and replace the latter in the dangerous chemicals cabinet. Take the bijou/universal containing the cadmium chloride powder to the balance and weigh it.

Calculate the correct volume of purified $H_20$ needed for your stock solution based on the amount of cadmium chloride present in the bijou. Put any damp blue roll and disposable spatulas into a yellow clinical waste bag for incineration.

*8.9.1.4 Making up stock solution*

Where possible use the middle (externally vented) flow cabinet in the cell culture laboratory. Make up your stock solution in a tissue culture hood with the calculated amount of purified $H_20$ needed. Sterilize by passing through a 0.2 µm filter, aliquot into microfuge tubes, label clearly and store in the -20 ºC freezer until use.

*8.9.1.5 Treatment of Cells*

Thaw aliquot. In the tissue culture hood dilute the cadmium chloride solution in medium to the desired treatment concentration. Apply this medium to the cells, changing medium every 2-3 days. Aspiration of cadmium from cells should be performed using disposable serological pipettes taking care not to suck liquid into the filter of the pipette buoy. Liquid waste should then be dispensed into a bottle containing 10 % (w/v) Virkon™ (ensuring that this remains pink). Do not suck medium containing cadmium into the Virkon™ traps.

*8.9.1.6 Disposal*

Used filters, syringes, universal tubes, flasks, dishes, gloves, spatulas, blue roll etc. should be collected in small bags containing enough absorbent material to contain any leakage of excess liquids, sealed and then placed in a double-bagged clinical waste bag for disposal by incineration (take these bags to stores when half full). Pipette tips and serological pipettes shouldn't be placed in bags due to puncture risk; they should instead be placed in designated puncture-resistant 'cin' bins.

Stock powder should be either dissolved or mixed with a combustible solvent and put into Winchester bottles or retained in the original container and disposed of through the Biology Department internal chemical waste. Fill out an internal waste transfer note and take down to Biology Stores.

Liquid waste should be stored in a clearly labelled bottle, containing 10 % (w/v) Virkon™ if containing cell culture waste. This bottle should be stored in the lockable dangerous chemicals cupboard and taken to biology stores with the appropriate paperwork when 90 % full. Do not allow these bottles to sit long term in the dangerous chemicals cupboard. Take care to ensure that cadmium never enters the water system.

*8.9.1.7 Spillage*

Spillage <1 g of stock powder should be wiped up immediately with damp blue roll, put in a container and disposed of in yellow clinical waste bag. Spillage >1 g of stock powder in the open lab requires the lab members to be evacuated from the lab and cadmium to be contained and collected into a container for disposal whilst wearing a respiratory face mask (ie. a FFP2 type face mask which is available from Biology Stores). Spillage >1 g of stock powder in fume hood requires the shield of the hood to be closed down and the hood to be left running for a few minutes to allow removal of any air-borne material. Any spilled material should then be collected onto damp blue roll and placed into a container for disposal. Liquid spillages should be mopped up with blue roll, put in a container and disposed of in a yellow clinical waste bag.

# References

Achanzar, W.E., Diwan, B.A., Liu, J., Quader, S.T., Webber, M.M., Waalkes, M.P., 2001. Cadmium-induced Malignant Transformation of Human Prostate Epithelial Cells. Cancer Res. 61, 455–458.

Adams, J.M., Cory, S., 1998. The Bcl-2 Protein Family: Arbiters of Cell Survival. Science 281, 1322–1326.

Adams, S.V., Newcomb, P.A., Shafer, M.M., Atkinson, C., Bowles, E.J.A., Newton, K.M., Lampe, J.W., 2011. Sources of cadmium exposure among healthy premenopausal women. Sci. Total Environ. 409, 1632–1637.

Agency for Toxic Substances and Disease Registry, 2008. Cadmium Toxicity Clinical Assessment - Laboratory Tests [WWW Document]. ATSDR. URL https://www.atsdr.cdc.gov/csem/csem.asp?csem=6&po=15 (accessed 10.6.16).

Agency for Toxic Substances and Disease Registry, 1999. Toxicological profile for cadmium [WWW Document]. ATSDR. URL https://www.atsdr.cdc.gov/toxprofiles/tp.asp?id=48&tid=15 (accessed 9.14.16).

Agudo, A., Bonet, C., Travier, N., González, C.A., Vineis, P., Bueno-de-Mesquita, H.B., Trichopoulos, D., Boffetta, P., Clavel-Chapelon, F., Boutron-Ruault, M.-C., Kaaks, R., Lukanova, A., Schütze, M., Boeing, H., Tjonneland, A., Halkjaer, J., Overvad, K., Dahm, C.C., Quirós, J.R., Sánchez, M.-J., Larrañaga, N., Navarro, C., Ardanaz, E., Khaw, K.-T., Wareham, N.J., Key, T.J., Allen, N.E., Trichopoulou, A., Lagiou, P., Palli, D., Sieri, S., Tumino, R., Panico, S., Boshuizen, H., Büchner, F.L., Peeters, P.H.M., Borgquist, S., Almquist, M., Hallmans, G., Johansson, I., Gram, I.T., Lund, E., Weiderpass, E., Romieu, I., Riboli, E., 2012. Impact of cigarette smoking on cancer risk in the European prospective investigation into cancer and nutrition study. J. Clin. Oncol. Off. J. Am. Soc. Clin. Oncol. 30, 4550–4557.

Aimola, P., Carmignani, M., Volpe, A.R., Di Benedetto, A., Claudio, L., Waalkes, M.P., van Bokhoven, A., Tokar, E.J., Claudio, P.P., 2012. Cadmium Induces p53-Dependent Apoptosis in Human Prostate Epithelial Cells. PLoS ONE 7, e33647.

Ajjimaporn, A., Botsford, T., Garrett, S.H., Sens, M.A., Zhou, X.D., Dunlevy, J.R., Sens, D.A., Somji, S., 2012. ZIP8 expression in human proximal tubule cells, human urothelial cells transformed by Cd+2 and As+3 and in specimens of normal human urothelium and urothelial cancer. Cancer Cell Int. 12, 16.

Alvarez, L., Gonzalez-Iglesias, H., Garcia, M., Ghosh, S., Sanz-Medel, A., Coca-Prados, M., 2012. The stoichiometric transition from Zn6Cu1-metallothionein to Zn7-metallothionein underlies the up-regulation of metallothionein (MT) expression: quantitative analysis of MT-metal load in eye cells. J. Biol. Chem. 287, 28456–28469. doi:10.1074/jbc.M112.365015

Aminian, O., Saburi, A., Mohseni, H., Akbari, H., Chavoshi, F., Akbari, H., 2014. Occupational risk of bladder cancer among Iranian male workers. Urol. Ann. 6, 135–138.

An, Q., Pacyna-Gengelbach, M., Schlüns, K., Deutschmann, N., Guo, S., Gao, Y., Zhang, J., Cheng, S., Petersen, I., 2003. Identification of differentially expressed genes in immortalized human bronchial epithelial cell line as a model for in

vitro study of lung carcinogenesis. Int. J. Cancer 103, 194–204. doi:10.1002/ijc.10807

Anders, S., Pyl, P.T., Huber, W., 2015. HTSeq—a Python framework to work with high-throughput sequencing data. Bioinformatics 31, 166–169.

Antoni, S., Ferlay, J., Soerjomataram, I., Znaor, A., Jemal, A., Bray, F., 2016. Bladder Cancer Incidence and Mortality: A Global Overview and Recent Trends. Eur. Urol.

Arita, A., Chervona, Y., Costa, M., 2012a. Carcinogenic metals and the epigenome: understanding the effect of nickel, arsenic, and chromium. Met. Integr. Biometal Sci. 4, 619–627.

Arita, A., Shamy, M.Y., Clancy, H.A., Sun, H., Hall, M.N., Qu, Q., Gamble, M.V., Costa, M., 2012b. The effect of exposure to carcinogenic metals on histone tail modifications and gene expression in human subjects. J. Trace Elem. Med. Biol. Organ Soc. Miner. Trace Elem. 26, 174–178.

Arnold, M.M., Srivastava, S., Fredenburgh, J., Stockard, C.R., Myers, R.B., Grizzle, W.E., 1996. Effects of fixation and tissue processing on immunohistochemical demonstration of specific antigens. Biotech. Histochem. Off. Publ. Biol. Stain Comm. 71, 224–230.

Arriaga, J.M., Greco, A., Mordoh, J., Bianchini, M., 2014. Metallothionein 1G and Zinc Sensitize Human Colorectal Cancer Cells to Chemotherapy. Mol. Cancer Ther. 13, 1369–1381. doi:10.1158/1535-7163.MCT-13-0944

Babjuk, M., Burger, M., Zigeuner, R., Shariat, S.F., van Rhijn, B.W.G., Compérat, E., Sylvester, R.J., Kaasinen, E., Böhle, A., Palou Redorta, J., Rouprêt, M., European Association of Urology, 2013. EAU guidelines on non-muscle-invasive urothelial carcinoma of the bladder: update 2013. Eur. Urol. 64, 639–653.

Babula, P., Masarik, M., Adam, V., Eckschlager, T., Stiborova, M., Trnkova, L., Skutkova, H., Provaznik, I., Hubalek, J., Kizek, R., 2012. Mammalian metallothioneins: properties and functions. Met. Integr. Biometal Sci. 4, 739–750.

Balesaria, S., Ramesh, B., McArdle, H., Bayele, H.K., Srai, S.K.S., 2010. Divalent metal-dependent regulation of hepcidin expression by MTF-1. FEBS Lett. 584, 719–725. doi:10.1016/j.febslet.2009.12.023

Balsara, Z.R., Li, X., 2017. Sleeping Beauty: Awakening Urothelium from its Slumber. Am. J. Physiol. Renal Physiol. ajprenal.00337.2016.

Bassi, P., De Marco, V., De Lisa, A., Mancini, M., Pinto, F., Bertoloni, R., Longo, F., 2005. Non-invasive diagnostic tests for bladder cancer: a review of the literature. Urol. Int. 75, 193–200.

Basu, A., Mahata, J., Roy, A.K., Sarkar, J.N., Poddar, G., Nandy, A.K., Sarkar, P.K., Dutta, P.K., Banerjee, A., Das, M., Ray, K., Roychaudhury, S., Natarajan, A.T., Nilsson, R., Giri, A.K., 2002. Enhanced frequency of micronuclei in individuals exposed to arsenic through drinking water in West Bengal, India. Mutat. Res. 516, 29–40.

Bebianno, M.J., Langston, W.J., 1998. Cadmium and metallothionein turnover in different tissues of the gastropod Littorina littorea. Talanta 46, 301–313.

Benbrahim-Tallaa, L., Tokar, E.J., Diwan, B.A., Dill, A.L., Coppin, J.-F., Waalkes, M.P., 2009. Cadmium malignantly transforms normal human breast epithelial cells into a basal-like phenotype. Environ. Health Perspect. 117, 1847–1852.

Benbrahim-Tallaa, L., Waterland, R.A., Dill, A.L., Webber, M.M., Waalkes, M.P., 2007. Tumor Suppressor Gene Inactivation during Cadmium-Induced Malignant Transformation of Human Prostate Cells Correlates with Overexpression of de Novo DNA Methyltransferase. Environ. Health Perspect. 115, 1454–1459.

Betka, M., Callard, G.V., 1999. Stage-dependent accumulation of cadmium and induction of metallothionein-like binding activity in the testis of the Dogfish shark, Squalus acanthias. Biol. Reprod. 60, 14–22.

Billerey, C., Chopin, D., Aubriot-Lorton, M.-H., Ricol, D., Gil Diez de Medina, S., Van Rhijn, B., Bralet, M.-P., Lefrere-Belda, M.-A., Lahaye, J.-B., Abbou, C.C., Bonaventure, J., Zafrani, E.S., van der Kwast, T., Thiery, J.P., Radvanyi, F., 2001. Frequent FGFR3 Mutations in Papillary Non-Invasive Bladder (pTa) Tumors. Am. J. Pathol. 158, 1955–1959.

Binz, P.A., Kägi, J.H., 1997. Metallothionein: Molecular Evolution and Classification, in: Metallothionein IV. Berkhäuser, Basel, pp. 7–13.

Biton, A., Bernard-Pierrot, I., Lou, Y., Krucker, C., Chapeaublanc, E., Rubio-Pérez, C., López-Bigas, N., Kamoun, A., Neuzillet, Y., Gestraud, P., Grieco, L., Rebouissou, S., de Reyniès, A., Benhamou, S., Lebret, T., Southgate, J., Barillot, E., Allory, Y., Zinovyev, A., Radvanyi, F., 2014. Independent Component Analysis Uncovers the Landscape of the Bladder Tumor Transcriptome and Reveals Insights into Luminal and Basal Subtypes. Cell Rep. 9, 1235–1245.

Boonprasert, K., Ruengweerayut, R., Aunpad, R., Satarug, S., Na-Bangchang, K., 2012. Expression of metallothionein isoforms in peripheral blood leukocytes from Thai population residing in cadmium-contaminated areas. Environ. Toxicol. Pharmacol. 12, S1382-6689.

Botteman, M.F., Pashos, C.L., Redaelli, A., Laskin, B., Hauser, R., 2003. The health economics of bladder cancer: a comprehensive review of the published literature. PharmacoEconomics 21, 1315–1330.

Brazão-Silva, M.T., Rodriguez, M.F.S., Eisenberg, A.L.A., Dias, F.L., de Castro, L.M., Nunes, F.D., Faria, P.R., Cardoso, S.V., Loyola, A.M., de Sousa, S.C.O.M., 2015. Metallothionein gene expression is altered in oral cancer and may predict metastasis and patient outcomes. Histopathology 67, 358–367.

Bremner, I., 1987. Nutritional and physiological significance of metallothionein. Experientia. Suppl. 52, 81–107.

Brennan, P., Bogillot, O., Cordier, S., Greiser, E., Schill, W., Vineis, P., Lopez-Abente, G., Tzonou, A., Chang-Claude, J., Bolm-Audorff, U., Jöckel, K.H., Donato, F., Serra, C., Wahrendorf, J., Hours, M., T'Mannetje, A., Kogevinas, M., Boffetta, P., 2000. Cigarette smoking and bladder cancer in men: a pooled analysis of 11 case-control studies. Int. J. Cancer 86, 289–294.

Burger, M., Catto, J.W.F., Dalbagni, G., Grossman, H.B., Herr, H., Karakiewicz, P., Kassouf, W., Kiemeney, L.A., La Vecchia, C., Shariat, S., Lotan, Y., 2013. Epidemiology and risk factors of urothelial bladder cancer. Eur. Urol. 63, 234–241.

Burger, M., Stief, C.G., Zaak, D., Stenzl, A., Wieland, W.F., Jocham, D., Otto, W., Denzinger, S., 2009. Hexaminolevulinate is equal to 5-aminolevulinic acid concerning residual tumor and recurrence rate following photodynamic diagnostic assisted transurethral resection of bladder tumors. Urology 74, 1282–1286.

Cai, X., Wang, J., Huang, X., Fu, W., Xia, W., Zou, M., Wang, Y., Wang, J., Xu, D., 2014. Identification and Characterization of MT-1X as a Novel FHL3-Binding Partner. PLoS ONE 9, e93723.

Calabrese, E.J., Baldwin, L.A., 1992. Lead-induced cell proliferation and organ-specific tumorigenicity. Drug Metab. Rev. 24, 409–416.

Caldwell, J., Gardner, I., Swales, N., 1995. An Introduction to Drug Disposition: The Basic Principles of Absorption, Distribution, Metabolism, and Excretion. Toxicol. Pathol. 23, 102–114.

Calisi, A., Lionetto, M.G., De Lorenzis, E., Leomanni, A., Schettino, T., 2014. Metallothionein Induction in the Coelomic Fluid of the Earthworm Lumbricus terrestris following Heavy Metal Exposure: A Short Report. BioMed Res. Int. 2014, e109386.

Cancer Genome Atlas Research Network, 2014. Comprehensive molecular characterization of urothelial bladder carcinoma. Nature 507, 315–322.

Cao, X., Lin, H., Muskhelishvili, L., Latendresse, J., Richter, P., Heflich, R.H., 2015. Tight junction disruption by cadmium in an in vitro human airway tissue model. Respir. Res. 16, 30.

Capdevila, M., Bofill, R., Palacios, Ò., Atrian, S., 2012. State-of-the-art of metallothioneins at the beginning of the 21st century. Coord. Chem. Rev. 256, 46–62.

Carrel, A., 1937. THE CULTURE OF WHOLE ORGANS. J. Exp. Med. 65, 515–526.

Castillo-Martin, M., Domingo-Domenech, J., Karni-Schmidt, O., Matos, T., Cordon-Cardo, C., 2010. Molecular pathways of urothelial development and bladder tumorigenesis. Urol. Oncol. Semin. Orig. Investig. 28, 401–408.

Chabanon, H., Nury, D., Mickleburgh, I., Burtle, B., Hesketh, J., 2004. Characterization of the cis-acting element directing perinuclear localization of the metallothionein-1 mRNA. Biochem. Soc. Trans. 32, 702–704. doi:10.1042/BST0320702

Chaney, R.L., 2010. Cadmium and Zinc, in: Trace Elements in Soils. Wiley, New York, pp. 409–440.

Chang, C.-H., Liu, C.-S., Liu, H.-J., Huang, C.-P., Huang, C.-Y., Hsu, H.-T., Liou, S.-H., Chung, C.-J., 2016. Association between levels of urinary heavy metals and increased risk of urothelial carcinoma. Int. J. Urol. Off. J. Jpn. Urol. Assoc. 23, 233–239.

Chang, X., Jin, T., Chen, L., Nordberg, M., Lei, L., 2009. Metallothionein I Isoform mRNA Expression in Peripheral Lymphocytes as a Biomarker for Occupational Cadmium Exposure. Exp. Biol. Med. 234, 666–672.

Chapman, E.J., Hurst, C.D., Pitt, E., Chambers, P., Aveyard, J.S., Knowles, M.A., 2006. Expression of hTERT immortalises normal human urothelial cells without inactivation of the p16/Rb pathway. Oncogene 25, 5037–5045.

Chen, H., Giri, N.C., Zhang, R., Yamane, K., Zhang, Y., Maroney, M., Costa, M., 2010. Nickel ions inhibit histone demethylase JMJD1A and DNA repair enzyme ABH2 by replacing the ferrous iron in the catalytic centers. J. Biol. Chem. 285, 7374–7383.

Chen, L., Jin, T., Huang, B., Nordberg, G., Nordberg, M., 2006. Critical exposure level of cadmium for elevated urinary metallothionein-an occupational population study in China. Toxicol. Appl. Pharmacol. 215, 93–99.

Cheng, L., Cheville, J.C., Neumann, R.M., Leibovich, B.C., Egan, K.S., Spotts, B.E., Bostwick, D.G., 1999. Survival of patients with carcinoma in situ of the urinary bladder. Cancer 85, 2469–2474.

Cherian, M.G., Apostolova, M.D., 2000. Nuclear localization of metallothionein during cell proliferation and differentiation. Cell. Mol. Biol. 46, 347–356.

Cherian, M.G., Goyer, R.A., 1978. Methallothioneins and their role in the metabolism and toxicity of metals. Life Sci. 23, 1–9.

Cheung, G., Sahai, A., Billia, M., Dasgupta, P., Khan, M.S., 2013. Recent advances in the diagnosis and treatment of bladder cancer. BMC Med. 11, 13.

Chiba, M., Masironi, R., 1992. Toxic and trace elements in tobacco and tobacco smoke. Bull. World Health Organ. 70, 269–275.

Choi, A.O., Brown, S.E., Szyf, M., Maysinger, D., 2008. Quantum dot-induced epigenetic and genotoxic changes in human breast cancer cells. J. Mol. Med. 86, 291–302.

Choi, W., Porten, S., Kim, S., Willis, D., Plimack, E.R., Hoffman-Censits, J., Roth, B., Cheng, T., Tran, M., Lee, I.-L., Melquist, J., Bondaruk, J., Majewski, T., Zhang, S., Pretzsch, S., Baggerly, K., Siefker-Radtke, A., Czerniak, B., Dinney, C.P.N., McConkey, D.J., 2014. Identification of distinct basal and luminal subtypes of muscle-invasive bladder cancer with different sensitivities to frontline chemotherapy. Cancer Cell 25, 152–165.

Choie, D.D., Richter, G.W., 1972. Lead poisoning: rapid formation of intranuclear inclusions. Science 177, 1194–1195.

Chomczynski, P., Sacchi, N., 1987. Single-step method of RNA isolation by acid guanidinium thiocyanate-phenol-chloroform extraction. Anal. Biochem. 162, 156–159.

Chu, W.A., Moehlenkamp, J.D., Bittel, D., Andrews, G.K., Johnson, J.A., 1999. Cadmium-mediated Activation of the Metal Response Element in Human Neuroblastoma Cells Lacking Functional Metal Response Element-binding Transcription Factor-1. J. Biol. Chem. 274, 5279–5284.

Cohen, S.M., Greenfield, R.E., Ellwein, L.B., 1983. Multistage carcinogenesis in the urinary bladder. Environ. Health Perspect. 49, 209–215.

Colopy, S.A., Bjorling, D.E., Mulligan, W.A., Bushman, W., 2014. A Population of Progenitor Cells in the Basal and Intermediate Layers of the Murine Bladder Urothelium Contributes to Urothelial Development and Regeneration. Dev. Dyn. Off. Publ. Am. Assoc. Anat. 243, 988–998. doi:10.1002/dvdy.24143

Colt, J.S., Friesen, M.C., Stewart, P.A., Donguk, P., Johnson, A., Schwenn, M., Karagas, M.R., Armenti, K., Waddell, R., Verrill, C., Ward, M.H., Beane Freeman, L.E., Moore, L.E., Koutros, S., Baris, D., Silverman, D.T., 2014. A

case-control study of occupational exposure to metalworking fluids and bladder cancer risk among men. Occup. Environ. Med. 71, 667–674.

Colvin, R.A., Holmes, W.R., Fontaine, C.P., Maret, W., 2010. Cytosolic zinc buffering and muffling: their role in intracellular zinc homeostasis. Met. Integr. Biometal Sci. 2, 306–317.

Conway, D.E., Lee, S., Eskin, S.G., Shah, A.K., Jo, H., McIntire, L.V., 2010. Endothelial metallothionein expression and intracellular free zinc levels are regulated by shear stress. Am. J. Physiol. - Cell Physiol. 299, C1461–C1467.

Cookson, M.S., Herr, H.W., Zhang, Z.F., Soloway, S., Sogani, P.C., Fair, W.R., 1997. The treated natural history of high risk superficial bladder cancer: 15-year outcome. J. Urol. 158, 62–67.

Cooper, G.M., 2000. The Development and Causes of Cancer, in: The Cell; A Molecular Approach. Sinauer Associates, Sunderland (MA).

Cordon-Cardo, C., 2008. Molecular alterations associated with bladder cancer initiation and progression. Scand. J. Urol. Nephrol. Suppl. 218, 154–165.

Cordon-Cardo, C., Wartinger, D., Petrylak, D., Dalbagni, G., Fair, W.R., Fuks, Z., Reuter, V.E., 1992. Altered Expression of the Retinoblastoma Gene Product: Prognostic Indicator in Bladder Cancer. J. Natl. Cancer Inst. 84, 1251–1256.

Cordon-Cardo, C., Zhang, Z.F., Dalbagni, G., Drobnjak, M., Charytonowicz, E., Hu, S.X., Xu, H.J., Reuter, V.E., Benedict, W.F., 1997. Cooperative effects of p53 and pRB alterations in primary superficial bladder tumors. Cancer Res. 57, 1217–1221.

Cortese-Krott, M.M., Münchow, M., Pirev, E., Heβner, F., Bozkurt, A., Uciechowski, P., Pallua, N., Kröncke, K.-D., Suschek, C.V., 2009. Silver ions induce oxidative stress and intracellular zinc release in human skin fibroblasts. Free Radic. Biol. Med. 47, 1570–1577. doi:10.1016/j.freeradbiomed.2009.08.023

Costello, L.C., Fenselau, C.C., Franklin, R.B., 2011. Evidence for operation of the direct zinc ligand exchange mechanism for trafficking, transport, and reactivity of zinc in mammalian cells. J. Inorg. Biochem. 105, 589–599.

Coyle, P., Philcox, J.C., Carey, L.C., Rofe, A.M., 2002. Metallothionein: the multipurpose protein. Cell. Mol. Life Sci. 59, 627–647.

Crallan, R.A., Georgopoulos, N.T., Southgate, J., 2006. Experimental models of human bladder carcinogenesis. Carcinogenesis 27, 374–381.

Cross, W.R., Eardley, I., Leese, H.J., Southgate, J., 2005. A biomimetic tissue from cultured normal human urothelial cells: analysis of physiological function. Am. J. Physiol. Renal Physiol. 289, F459-468.

Cully, M., You, H., Levine, A.J., Mak, T.W., 2006. Beyond PTEN mutations: the PI3K pathway as an integrator of multiple inputs during tumorigenesis. Nat. Rev. Cancer 6, 184–192.

Cumberbatch, M.G., Rota, M., Catto, J.W.F., La Vecchia, C., 2016. The Role of Tobacco Smoke in Bladder and Kidney Carcinogenesis: A Comparison of Exposures and Meta-analysis of Incidence and Mortality Risks. Eur. Urol. 70, 458–466.

Dadhania, V., Zhang, M., Zhang, L., Bondaruk, J., Majewski, T., Siefker-Radtke, A., Guo, C.C., Dinney, C., Cogdell, D.E., Zhang, S., Lee, S., Lee, J.G., Weinstein,

J.N., Baggerly, K., McConkey, D., Czerniak, B., 2016. Meta-Analysis of the Luminal and Basal Subtypes of Bladder Cancer and the Identification of Signature Immunohistochemical Markers for Clinical Use. EBioMedicine 12, 105–117.

Dally, H., Hartwig, A., 1997. Induction and repair inhibition of oxidative DNA damage by nickel(II) and cadmium(II) in mammalian cells. Carcinogenesis 18, 1021–1026.

Dalton, T., Fu, K., Palmiter, R.D., Andrews, G.K., 1996. Transgenic mice that overexpress metallothionein-I resist dietary zinc deficiency. J. Nutr. 126, 825–833.

Damrauer, J.S., Hoadley, K.A., Chism, D.D., Fan, C., Tiganelli, C.J., Wobker, S.E., Yeh, J.J., Milowsky, M.I., Iyer, G., Parker, J.S., Kim, W.Y., 2014. Intrinsic subtypes of high-grade bladder cancer reflect the hallmarks of breast cancer biology. Proc. Natl. Acad. Sci. U. S. A. 111, 3110–3115.

Day, D.A., Tuite, M.F., 1998. Post-transcriptional gene regulatory mechanisms in eukaryotes: an overview. J. Endocrinol. 157, 361–371.

DeGraff, D.J., Clark, P.E., Cates, J.M., Yamashita, H., Robinson, V.L., Yu, X., Smolkin, M.E., Chang, S.S., Cookson, M.S., Herrick, M.K., Shariat, S.F., Steinberg, G.D., Frierson, H.F., Wu, X.-R., Theodorescu, D., Matusik, R.J., 2012. Loss of the urothelial differentiation marker FOXA1 is associated with high grade, late stage bladder cancer and increased tumor proliferation. PloS One 7, e36669. doi:10.1371/journal.pone.0036669

Dodmane, P.R., Arnold, L.L., Muirhead, D.E., Suzuki, S., Yokohira, M., Pennington, K.L., Dave, B.J., Lu, X., Le, X.C., Cohen, S.M., 2014. Characterization of intracellular inclusions in the urothelium of mice exposed to inorganic arsenic. Toxicol. Sci. Off. J. Soc. Toxicol. 137, 36–46.

Dozmorov, M.G., Kyker, K.D., Saban, R., Shankar, N., Baghdayan, A.S., Centola, M.B., Hurst, R.E., 2007. Systems biology approach for mapping the response of human urothelial cells to infection by Enterococcus faecalis. BMC Bioinformatics 8, S2.

Drayton, R.M., Catto, J.W., 2012. Molecular mechanisms of cisplatin resistance in bladder cancer. Expert Rev. Anticancer Ther. 12, 271–281.

Duncan, E.L., Reddel, R.R., 1999. Downregulation of metallothionein-IIA expression occurs at immortalization. Oncogene 18, 897–903.

Durnam, D.M., Palmiter, R.D., 1984. Induction of metallothionein-I mRNA in cultured cells by heavy metals and iodoacetate: evidence for gratuitous inducers. Mol. Cell. Biol. 4, 484–491.

Eble, J. N., Sauter, G., Epstein, J., Sesterhenn, I.A., 2004. Pathology and Genetics of Tumours of the Urinary System and Male Genital Organs, World Health Organisation Classification of Tumours. IARC Press, Lyon.

Elmore, S., 2007. Apoptosis: A Review of Programmed Cell Death. Toxicol. Pathol. 35, 495–516.

Eneman, J.D., Potts, R.J., Osier, M., Shukla, G.S., Lee, C.H., Chiu, J.-F., Hart, B.A., 2000. Suppressed oxidant-induced apoptosis in cadmium adapted alveolar epithelial cells and its potential involvement in cadmium carcinogenesis. Toxicology 147, 215–228.

European Commission Council, 1998. Directive 98/83/EC of 3 November 1998: on the quality of water intended for human consumption (Legislative). European Commission.

Fabbri, M., Urani, C., Sacco, M.G., Procaccianti, C., Gribaldo, L., 2012. Whole genome analysis and microRNAs regulation in HepG2 cells exposed to cadmium. ALTEX 29, 173–182.

Farquhar, M.G., Palade, G.E., 1963. Junctional complexes in various epithelia. J. Cell Biol. 17, 375–412.

Faurskov, B., Bjerregaard, H.F., 1997. Effect of cadmium on active ion transport and cytotoxicity in cultured renal epithelial cells (A6). Toxicol. Vitro Int. J. Publ. Assoc. BIBRA 11, 717–722.

Fearon, E.R., Vogelstein, B., 1990. A genetic model for colorectal tumorigenesis. Cell 61, 759–767.

Feki-Tounsi, M., Hamza-Chaffai, A., 2014. Cadmium as a possible cause of bladder cancer: a review of accumulated evidence. Environ. Sci. Pollut. Res. 21, 10561–10573. doi:10.1007/s11356-014-2970-0

Feki-Tounsi, M., Olmedo, P., Gil, F., Khlifi, R., Mhiri, M.-N., Rebai, A., Hamza-Chaffai, A., 2013. Cadmium in blood of Tunisian men and risk of bladder cancer: interactions with arsenic exposure and smoking. Environ. Sci. Pollut. Res. Int. 20, 7204–7213.

Feki-Tounsi, M., Olmedo, P., Gil, F., Mhiri, M.-N., Rebai, A., Hamza-Chaffai, A., 2014. Trace metal quantification in bladder biopsies from tumoral lesions of Tunisian cancer and controls subjects. Environ. Sci. Pollut. Res. Int. 21, 11433–11438.

Fergusson, J.E., 1990. The Heavy Elements: Chemistry, Environmental Impact and Health Effects, Civilization of the American Indian. Pergamon Press, Oxford.

Ferlay, J., Shin, H.-R., Bray, F., Forman, D., Mathers, C., Parkin, D.M., 2010. Estimates of worldwide burden of cancer in 2008: GLOBOCAN 2008. Int. J. Cancer 127, 2893–2917.

Filion, G.J., van Bemmel, J.G., Braunschweig, U., Talhout, W., Kind, J., Ward, L.D., Brugman, W., de Castro Genebra de Jesus, I., Kerkhoven, R.M., Bussemaker, H.J., van Steensel, B., 2010. Systematic protein location mapping reveals five principal chromatin types in Drosophila cells. Cell 143, 212–224.

Forti, E., Bulgheroni, A., Cetin, Y., Hartung, T., Jennings, P., Pfaller, W., Prieto, P., 2010. Characterisation of cadmium chloride induced molecular and functional alterations in airway epithelial cells. Cell. Physiol. Biochem. Int. J. Exp. Cell. Physiol. Biochem. Pharmacol. 25, 159–168.

Freedman, N.D., Silverman, D.T., Hollenbeck, A.R., Schatzkin, A., Abnet, C.C., 2011. Association between smoking and risk of bladder cancer among men and women. J. Am. Med. Assoc. 306, 737–745. doi:10.1001/jama.2011.1142

Freshney, R.I., 2016. Phases of the Growth Cycle, in: Culture of Animal Cells: A Manual of Basic Technique and Specialized Applications. Wiley, New Jersey, p. 502.

Frömter, E., Diamond, J., 1972. Route of passive ion permeation in epithelia. Nature. New Biol. 235, 9–13.

Fujishiro, H., Okugaki, S., Kubota, K., Fujiyama, T., Miyataka, H., Himeno, S., 2009. The role of ZIP8 down-regulation in cadmium-resistant metallothionein-null cells. J. Appl. Toxicol. 29, 367–373. doi:10.1002/jat.1419

Futakawa, N., Kondoh, M., Ueda, S., Higashimoto, M., Takiguchi, M., Suzuki, S., Sato, M., 2006. Involvement of oxidative stress in the synthesis of metallothionein induced by mitochondrial inhibitors. Biol. Pharm. Bull. 29, 2016–2020.

Gadhia, S.R., Calabro, A.R., Barile, F.A., 2012. Trace metals alter DNA repair and histone modification pathways concurrently in mouse embryonic stem cells. Toxicol. Lett. 212, 169–179.

Gaisa, N.T., Graham, T.A., McDonald, S.A.C., Cañadillas-Lopez, S., Poulsom, R., Heidenreich, A., Jakse, G., Tadrous, P.J., Knuechel, R., Wright, N.A., 2011. The human urothelium consists of multiple clonal units, each maintained by a stem cell. J. Pathol. 225, 163–171.

Ganguly, S., Taioli, E., Baranski, B., Cohen, B., Toniolo, P., Garte, S.J., 1996. Human metallothionein gene expression determined by quantitative reverse transcription-polymerase chain reaction as a biomarker of cadmium exposure. Cancer Epidemiol. Biomarkers Prev. 5, 297–301.

Garcia-Montero, A., Vasseur, S., Mallo, G.V., Soubeyran, P., Dagorn, J.C., Iovanna, J.L., 2001. Expression of the stress-induced p8 mRNA is transiently activated after culture medium change. Eur. J. Cell Biol. 80, 720–725. doi:10.1078/0171-9335-00209

García-Pérez, J., López-Abente, G., Castelló, A., González-Sánchez, M., Fernández-Navarro, P., 2015. Cancer mortality in towns in the vicinity of installations for the production of cement, lime, plaster, and magnesium oxide. Chemosphere 128C, 103–110.

García-Pérez, J., Pollán, M., Boldo, E., Pérez-Gómez, B., Aragonés, N., Lope, V., Ramis, R., Vidal, E., López-Abente, G., 2009. Mortality due to lung, laryngeal and bladder cancer in towns lying in the vicinity of combustion installations. Sci. Total Environ. 407, 2593–2602.

Garrett, S.H., Phillips, V., Somji, S., Sens, M.A., Dutta, R., Park, S., Kim, D., Sens, D.A., 2002. Transient induction of metallothionein isoform 3 (MT-3), c-fos, c-jun and c-myc in human proximal tubule cells exposed to cadmium. Toxicol. Lett. 126, 69–80.

Georgopoulos, N.T., Kirkwood, L.A., Varley, C.L., MacLaine, N.J., Aziz, N., Southgate, J., 2011. Immortalisation of normal human urothelial cells compromises differentiation capacity. Eur. Urol. 60, 141–149.

Gerdes, J., Schwab, U., Lemke, H., Stein, H., 1983. Production of a mouse monoclonal antibody reactive with a human nuclear antigen associated with cell proliferation. Int. J. Cancer 31, 13–20.

Gibas, Z., Prout, G.R., Connolly, J.G., Pontes, J.E., Sandberg, A.A., 1984. Nonrandom chromosomal changes in transitional cell carcinoma of the bladder. Cancer Res. 44, 1257–1264.

Goering, P., Waalkes, M., Klaassen, C., 1994. Toxicology of Cadmium, in: Handbook of Experimental Pharmacology: Toxicology of Metals, Biochemical Effects. Springer, New York, pp. 189–214.

Goering, P.L., Klaassen, C.D., 1984. Tolerance to cadmium-induced hepatotoxicity following cadmium pretreatment. Toxicol. Appl. Pharmacol. 74, 308–313.

Goyer, R.A., May, P., Cates, M.M., Krigman, M.R., 1970. Lead and protein content of isolated intranuclear inclusion bodies from kidneys of lead-poisoned rats. Lab. Investig. J. Tech. Methods Pathol. 22, 245–251.

Gunawardana, C.G., Martinez, R.E., Xiao, W., Templeton, D.M., 2006. Cadmium inhibits both intrinsic and extrinsic apoptotic pathways in renal mesangial cells. Am. J. Physiol. Renal Physiol. 290, F1074-1082.

Günther, V., Lindert, U., Schaffner, W., 2012. The taste of heavy metals: Gene regulation by MTF-1. Biochim. Biophys. Acta BBA - Mol. Cell Res. 1823, 1416–1425.

Guo, L., Lichten, L.A., Ryu, M.-S., Liuzzi, J.P., Wang, F., Cousins, R.J., 2010. STAT5-glucocorticoid receptor interaction and MTF-1 regulate the expression of ZnT2 (Slc30a2) in pancreatic acinar cells. Proc. Natl. Acad. Sci. U. S. A. 107, 2818–2823.

Hagrman, D., Goodisman, J., Dabrowiak, J.C., Souid, A.-K., 2003. Kinetic study on the reaction of cisplatin with metallothionein. Drug Metab. Dispos. Biol. Fate Chem. 31, 916–923.

Hamelink, J.L., Landrum, P.F., Bergman, H.L., Benson, W.H., 1994. Interactions of Organic Chemicals with Particulate and Dissolved Organic Matter in the Aquatic Environment, in: Bioavailability: Physical, Chemical, and Biological Interactions, SETAC Special Publications. Lewis, pp. 83–100.

Harney, J., Murphy, D.M., Jones, M., Mothersill, C., 1995. Expression of p53 in urothelial cell cultures from tumour-bearing and tumour-free patients. Br. J. Cancer 71, 25–29.

Harris, N.S., Taylor, G.J., 2013. Cadmium uptake and partitioning in durum wheat during grain filling. BMC Plant Biol. 13, 103. doi:10.1186/1471-2229-13-103

Hart, B.A., 2000. Cadmium-Induced Resistance and Suppression of Apoptosis, in: Molecular Biology and Toxicology of Metals. Taylor and Francis, London, p. 225.

Hart, B.A., Potts, R.J., Watkin, R.D., 2001. Cadmium adaptation in the lung - a double-edged sword? Toxicology 160, 65–70.

Hartung, T., Daston, G., 2009. Are In Vitro Tests Suitable for Regulatory Use? Toxicol. Sci. 111, 233–237.

Hassoun, E.A., Stohs, S.J., 1996. Cadmium-induced production of superoxide anion and nitric oxide, DNA single strand breaks and lactate dehydrogenase leakage in J774A.1 cell cultures. Toxicology 112, 219–226.

Hatcher, E.L., 1997. Decreased Sensitivity to Adriamycin in Cadmium-Resistant Human Lung Carcinoma A549 Cells. Biochem. Pharmacol. 53, 747–754.

Hayashi, Y., 1992. Overview of genotoxic carcinogens and non-genotoxic carcinogens. Exp. Toxicol. Pathol. 44, 465–471.

He, L., Wang, B., Hay, E.B., Nebert, D.W., 2009. Discovery of ZIP transporters that participate in cadmium damage to testis and kidney. Toxicol. Appl. Pharmacol. 238, 250–257. doi:10.1016/j.taap.2009.02.017

Hein, D.W., Doll, M.A., Fretland, A.J., Leff, M.A., Webb, S.J., Xiao, G.H., Devanaboyina, U.S., Nangju, N.A., Feng, Y., 2000. Molecular genetics and epidemiology of the NAT1 and NAT2 acetylation polymorphisms. Cancer Epidemiol. Biomark. Prev. Publ. Am. Assoc. Cancer Res. Cosponsored Am. Soc. Prev. Oncol. 9, 29–42.

Heuchel, R., Radtke, F., Georgiev, O., Stark, G., Aguet, M., Schaffner, W., 1994. The transcription factor MTF-1 is essential for basal and heavy metal-induced metallothionein gene expression. EMBO J. 13, 2870–2875.

Heyno, E., Klose, C., Krieger-Liszkay, A., 2008. Origin of cadmium-induced reactive oxygen species production: mitochondrial electron transfer versus plasma membrane NADPH oxidase. New Phytol. 179, 687–699.

Hicks, R.M., 1975. The mammalian urinary bladder: an accommodating organ. Biol. Rev. Camb. Philos. Soc. 50, 215–246.

Hinkel, A., Schmidtchen, S., Palisaar, R.-J., Noldus, J., Pannek, J., 2008. Identification of Bladder Cancer Patients at Risk for Recurrence or Progression: An Immunohistochemical Study Based on the Expression of Metallothionein. J. Toxicol. Environ. Health A 71, 954–959.

Hohlbrugger, G., 1996. Leaky urothelium and/or vesical ischemia enable urinary potassium to cause idiopathic urgency/frequency syndrome and urge incontinence. Int. Urogynecol. J. Pelvic Floor Dysfunct. 7, 242–255.

Hornigold, N., Devlin, J., Davies, A.M., Aveyard, J.S., Habuchi, T., Knowles, M.A., 1999. Mutation of the 9q34 gene TSC1 in sporadic bladder cancer. Oncogene 18, 2657–2661.

Howlett, A.R., Hodges, G.M., Rowlatt, C., 1986. Epithelial-stromal interactions in the adult bladder: urothelial growth, differentiation, and maturation on culture facsimiles of bladder stroma. Dev. Biol. 118, 403–415.

Humpel, C., 2011. Identifying and validating biomarkers for Alzheimer's disease. Trends Biotechnol. 29, 26–32.

International Agency for Research on Cancer, 1994. Shistosomes, liver flukes and Helicobacter pylori. IARC Monogr. Eval. Carcinog. Risks Hum. 61.

International Agency for Research on Cancer, 1993. Beryllium, cadmium, mercury, and exposures in the glass manufacturing industry. IARC Monogr. Eval. Carcinog. Risks Hum. 58.

Ioachim, E.E., Charchanti, A.V., Stavropoulos, N.E., Athanassiou, E.D., Michael, M.C., Agnantis, N.J., 2001. Localization of metallothionein in urothelial carcinoma of the human urinary bladder: an immunohistochemical study including correlation with HLA-DR antigen, p53, and proliferation indices. Anticancer Res. 21, 1757–1761.

Irvine, G.W., Pinter, T.B.J., Stillman, M.J., 2016. Defining the metal binding pathways of human metallothionein 1a: balancing zinc availability and cadmium seclusion. Metallomics 8, 71–81.

Jahroudi, N., Foster, R., Price-Haughey, J., Beitel, G., Gedamu, L., 1990. Cell-type specific and differential regulation of the human metallothionein genes. Correlation with DNA methylation and chromatin structure. J. Biol. Chem. 265, 6506–6511.

Janecki, A., Jakubowiak, A., Steinberger, A., 1992. Effect of cadmium chloride on transepithelial electrical resistance of Sertoli cell monolayers in two-compartment cultures--a new model for toxicological investigations of the "blood-testis" barrier in vitro. Toxicol. Appl. Pharmacol. 112, 51–57.

Janković, S., Radosavljević, V., 2007. Risk factors for bladder cancer. Tumori 93, 4–12.

Jarup, L., Alfven, T., Persson, B., Toss, G., Elinder, C.G., 1998. Cadmium may be a risk factor for osteoporosis. Occup. Environ. Med. 55, 435–439.

Jasani, B., Schmid, K.W., 1997. Significance of metallothionein overexpression in human tumours. Histopathology 31, 131–136.

Jebar, A.H., Hurst, C.D., Tomlinson, D.C., Johnston, C., Taylor, C.F., Knowles, M.A., 2005. FGFR3 and Ras gene mutations are mutually exclusive genetic events in urothelial cell carcinoma. Oncogene 24, 5218–5225.

Jeong, J., Eide, D.J., 2013. The SLC39 family of zinc transporters. Mol. Aspects Med. 34, 612–619.

Jin, R., Chow, V.T.-K., Tan, P.-H., Dheen, S.T., Duan, W., Bay, B.-H., 2002. Metallothionein 2A expression is associated with cell proliferation in breast cancer. Carcinogenesis 23, 81–86.

Jones, T.D., Wang, M., Eble, J.N., MacLennan, G.T., Lopez-Beltran, A., Zhang, S., Cocco, A., Cheng, L., 2005. Molecular evidence supporting field effect in urothelial carcinogenesis. Clin. Cancer Res. Off. J. Am. Assoc. Cancer Res. 11, 6512–6519.

Jost, S.P., 1986. Renewal of normal urothelium in adult mice. Virchows Arch. B Cell Pathol. Incl. Mol. Pathol. 51, 65–70.

Jost, S.P., Gosling, J.A., Dixon, J.S., 1989. The morphology of normal human bladder urothelium. J. Anat. 167, 103–115.

Kabata-Pendia, A., 2001. Trace Elements in Soils and Plants, 3rd ed. CRC Press, Florida.

Kadota, Y., Suzuki, S., Ideta, S., Fukinbara, Y., Kawakami, T., Imai, H., Nakagawa, Y., Sato, M., 2010. Enhanced metallothionein gene expression induced by mitochondrial oxidative stress is reduced in phospholipid hydroperoxide glutathione peroxidase-overexpressed cells. Eur. J. Pharmacol. 626, 166–170. doi:10.1016/j.ejphar.2009.09.060

Kägi, J.H., Kojima, Y., 1987. Chemistry and biochemistry of metallothionein. Experientia. Suppl. 52, 25–61.

Kägi, J.H., Kojima, Y., Kissling, M.M., Lerch, K., 1979. Metallothionein: an exceptional metal thiolate protein. Ciba Found. Symp. 72, 223–237.

Kägi, J.H., Schäffer, A., 1988. Biochemistry of metallothionein. Biochemistry (Mosc.) 27, 8509–8515.

Kanwal, R., Gupta, S., 2012. Epigenetic modifications in cancer. Clin. Genet. 81, 303–311.

Kao, C., Huang, J., Wu, S.Q., Hauser, P., Reznikoff, C.A., 1993. Role of SV40 T antigen binding to pRB and p53 in multistep transformation in vitro of human uroepithelial cells. Carcinogenesis 14, 2297–2302.

Karantza, V., 2011. Keratins in health and cancer: more than mere epithelial cell markers. Oncogene 30, 127–138. doi:10.1038/onc.2010.456

Karin, Eddy, R.L., Henry, W.M., Haley, L.L., Byers, M.G., Shows, T.B., 1984a. Human metallothionein genes are clustered on chromosome 16. Proc. Natl. Acad. Sci. U. S. A. 81, 5494–5498.

Karin, Haslinger, A., Holtgreve, H., Richards, R.I., Krauter, P., Westphal, H.M., Beato, M., 1984b. Characterization of DNA sequences through which cadmium and glucocorticoid hormones induce human metallothionein-IIA gene. Nature 308, 513–519.

Karin, M., Imbra, R.J., Heguy, A., Wong, G., 1985. Interleukin 1 regulates human metallothionein gene expression. Mol. Cell. Biol. 5, 2866–2869.

Keil, D.E., Berger-Ritchie, J., McMillin, G.A., 2011. Testing for Toxic Elements: A Focus on Arsenic, Cadmium, Lead, and Mercury. Lab. Med. 42, 735–742.

Kellen, E., Zeegers, M.P., Hond, E.D., Buntinx, F., 2007. Blood cadmium may be associated with bladder carcinogenesis: the Belgian case-control study on bladder cancer. Cancer Detect. Prev. 31, 77–82.

Kelly, E.J., Quaife, C.J., Froelick, G.J., Palmiter, R.D., 1996. Metallothionein I and II protect against zinc deficiency and zinc toxicity in mice. J. Nutr. 126, 1782–1790.

Kharchenko, P.V., Alekseyenko, A.A., Schwartz, Y.B., Minoda, A., Riddle, N.C., Ernst, J., Sabo, P.J., Larschan, E., Gorchakov, A.A., Gu, T., Linder-Basso, D., Plachetka, A., Shanower, G., Tolstorukov, M.Y., Luquette, L.J., Xi, R., Jung, Y.L., Park, R.W., Bishop, E.P., Canfield, T.K., Sandstrom, R., Thurman, R.E., MacAlpine, D.M., Stamatoyannopoulos, J.A., Kellis, M., Elgin, S.C.R., Kuroda, M.I., Pirrotta, V., Karpen, G.H., Park, P.J., 2011. Comprehensive analysis of the chromatin landscape in Drosophila melanogaster. Nature 471, 480–485.

Kheradmand, F., Nourmohammadi, I., Modarressi, M.H., Firoozrai, M., Ahmadi Faghih, M.A., 2010. Differential Gene-Expression of Metallothionein 1M and 1G in Response to Zinc in Sertoli TM4 Cells. Iran. Biomed. J. 14, 9–15.

Kikuchi, Y., Irie, M., Kasahara, T., Sawada, J., Terao, T., 1993. Induction of metallothionein in a human astrocytoma cell line by interleukin-1 and heavy metals. FEBS Lett. 317, 22–26.

Kim, H.G., Kim, J.Y., Han, E.H., Hwang, Y.P., Choi, J.H., Park, B.H., Jeong, H.G., 2011. Metallothionein-2A overexpression increases the expression of matrix metalloproteinase-9 and invasion of breast cancer cells. FEBS Lett. 585, 421–428. doi:10.1016/j.febslet.2010.12.030

Kim, J.-H., Wang, S.-Y., Kim, I.-C., Ki, J.-S., Raisuddin, S., Lee, J.-S., Han, K.-N., 2008. Cloning of a river pufferfish (Takifugu obscurus) metallothionein cDNA and study of its induction profile in cadmium-exposed fish. Chemosphere 71, 1251–1259.

Kimura, T., Itoh, N., Takehara, M., Oguro, I., Ishizaki, J.I., Nakanishi, T., Tanaka, K., 2001. Sensitivity of metallothionein-null mice to LPS/D-galactosamine-induced lethality. Biochem. Biophys. Res. Commun. 280, 358–362.

Kimura, T., Kambe, T., 2016. The Functions of Metallothionein and ZIP and ZnT Transporters: An Overview and Perspective. Int. J. Mol. Sci. 17, 336.

Klaassen, C.D., Choudhuri, S., McKim, J.M., Lehman-McKeeman, L.D., Kershaw, W.C., 1994. In vitro and in vivo studies on the degradation of metallothionein. Environ. Health Perspect. 102, 141–146.

Klaassen, C.D., Lehman-McKeeman, L.D., 1989. Regulation of the isoforms of metallothionein. Biol. Trace Elem. Res. 21, 119–129.

Knowles, M.A., Hurst, C.D., 2015. Molecular biology of bladder cancer: new insights into pathogenesis and clinical diversity. Nat. Rev. Cancer 15, 25–41.

Kobayashi, S., Kimura, M., 1980. Different inducibility of metallothionein in various mammalian cells in vitro. Toxicol. Lett. 5, 357–362.

Koizumi, S., Suzuki, K., Otsuka, F., 1992. A nuclear factor that recognizes the metal-responsive elements of human metallothionein IIA gene. J. Biol. Chem. 267, 18659–18664.

Krause, M., Rak-Raszewska, A., Pietilä, I., Quaggin, S.E., Vainio, S., 2015. Signaling during Kidney Development. Cells 4, 112–132.

Kreft, M.E., Hudoklin, S., Jezernik, K., Romih, R., 2010. Formation and maintenance of blood–urine barrier in urothelium. Protoplasma 246, 3–14.

Krezel, A., Maret, W., 2008. Thionein/metallothionein control Zn(II) availability and the activity of enzymes. J. Biol. Inorg. Chem. JBIC Publ. Soc. Biol. Inorg. Chem. 13, 401–409.

Krezel, A., Maret, W., 2006. Zinc-buffering capacity of a eukaryotic cell at physiological pZn. J. Biol. Inorg. Chem. JBIC Publ. Soc. Biol. Inorg. Chem. 11, 1049–1062.

Kriegmair, M., Baumgartner, R., Knuechel, R., Steinbach, P., Ehsan, A., Lumper, W., Hofstädter, F., Hofstetter, A., 1994. Fluorescence photodetection of neoplastic urothelial lesions following intravesical instillation of 5-aminolevulinic acid. Urology 44, 836–841.

Kundu, S., Sengupta, S., Bhattacharyya, A., 2011. EGFR upregulates inflammatory and proliferative responses in human lung adenocarcinoma cell line (A549), induced by lower dose of cadmium chloride. Inhal. Toxicol. 23, 339–348.

Kwon, J.Y., Weon, J.-I., Koedrith, P., Park, K.-S., Kim, I.S., Seo, Y.R., 2013. Identification of molecular candidates and interaction networks via integrative toxicogenomic analysis in a human cell line following low-dose exposure to the carcinogenic metals cadmium and nickel. Oncol. Rep. 30, 1185–1194.

Lacorte, L.M., Delella, F.K., Porto Amorim, E.M., Justulin, L.A., Godinho, A.F., Almeida, A.A., Felipe Pinheiro, P.F., Amorim, R.L., Felisbino, S.L., 2011. Early changes induced by short-term low-dose cadmium exposure in rat ventral and dorsolateral prostates. Microsc. Res. Tech. 74, 988–997.

Langmade, S.J., Ravindra, R., Daniels, P.J., Andrews, G.K., 2000. The transcription factor MTF-1 mediates metal regulation of the mouse ZnT1 gene. J. Biol. Chem. 275, 34803–34809.

Larson, J., Yasmin, T., Sens, D.A., Zhou, X.D., Sens, M.A., Garrett, S.H., Dunlevy, J.R., Cao, L., Somji, S., 2010. SPARC gene expression is repressed in human urothelial cells (UROtsa) exposed to or malignantly transformed by cadmium or arsenite. Toxicol. Lett. 199, 166–172.

Lazo, J.S., Kondo, Y., Dellapiazza, D., Michalska, A.E., Choo, K.H., Pitt, B.R., 1995. Enhanced sensitivity to oxidative stress in cultured embryonic cells from transgenic mice deficient in metallothionein I and II genes. J. Biol. Chem. 270, 5506–5510.

Lazzeri, M., 2006. The physiological function of the urothelium-more than a simple barrier. Urol. Int. 76, 289–295.

Lee, C.W., Stabile, E., Kinnaird, T., Shou, M., Devaney, J.M., Epstein, S.E., Burnett, M.S., 2004. Temporal patterns of gene expression after acute hindlimb ischemia in mice: insights into the genomic program for collateral vessel development. J. Am. Coll. Cardiol. 43, 474–482.

Lee, D.K., Geiser, J., Dufner-Beattie, J., Andrews, G.K., 2003. Pancreatic metallothionein-I may play a role in zinc homeostasis during maternal dietary zinc deficiency in mice. J. Nutr. 133, 45–50.

Lee, K.B., Parker, R.J., Reed, E., 1995. Effect of cadmium on human ovarian cancer cells with acquired cisplatin resistance. Cancer Lett. 88, 57–66.

Lehman-McKeeman, L.D., Andrews, G.K., Klaassen, C.D., 1988. Mechanisms of regulation of rat hepatic metallothionein-I and metallothionein-II levels following administration of zinc. Toxicol. Appl. Pharmacol. 92, 1–9.

Lei, Y.-X., Wei, L., Wang, M., Wu, G.-R., Li, M., 2008. Malignant transformation and abnormal expression of eukaryotic initiation factor in bronchial epithelial cells induced by cadmium chloride. Biomed. Environ. Sci. BES 21, 332–338.

Lerner, S.P., McConkey, D.J., Hoadley, K.A., Chan, K.S., Kim, W.Y., Radvanyi, F., Höglund, M., Real, F.X., 2016. Bladder Cancer Molecular Taxonomy: Summary from a Consensus Meeting. Bladder Cancer 2, 37–47.

Levadoux, M., Mahon, C., Beattie, J.H., Wallace, H.M., Hesketh, J.E., 1999. Nuclear import of metallothionein requires its mRNA to be associated with the perinuclear cytoskeleton. J. Biol. Chem. 274, 34961–34966.

Liang, Y., Li, H., Xiang, C., Lei, L., Jin, T., Nordberg, M., Nordberg, G.F., 2010. Increased Hepatic and Decreased Urinary Metallothionein in Rats after Cessation of Oral Cadmium Exposure. Basic Clin. Pharmacol. Toxicol. 106, 348–355.

Lim, D., Jocelyn, K.M.-X., Yip, G.W.-C., Bay, B.-H., 2009. Silencing the Metallothionein-2A gene inhibits cell cycle progression from G1- to S-phase involving ATM and cdc25A signaling in breast cancer cells. Cancer Lett. 276, 109–117. doi:10.1016/j.canlet.2008.10.038

Ling, S., Chang, X., Schultz, L., Lee, T.K., Chaux, A., Marchionni, L., Netto, G.J., Sidransky, D., Berman, D.M., 2011. An EGFR-ERK-SOX9 Signaling Cascade Links Urothelial Development and Regeneration to Cancer. Cancer Res. 71, 3812–3821. doi:10.1158/0008-5472.CAN-10-3072

Liu, J., Li, Y., Liao, Y., Mai, S., Zhang, Z., Liu, Z., Jiang, L., Zeng, Y., Zhou, F., Xie, D., 2013. High Expression of H3K27me3 Is an Independent Predictor of Worse Outcome in Patients with Urothelial Carcinoma of Bladder Treated with Radical Cystectomy. BioMed Res. Int. 2013, e390482. doi:10.1155/2013/390482

Liu, Z.-M., Hasselt, C.A. van, Song, F.-Z., Vlantis, A.C., Cherian, M.G., Koropatnick, J., Chen, G.G., 2009. Expression of functional metallothionein isoforms in papillary thyroid cancer. Mol. Cell. Endocrinol. 302, 92–98.

López-Knowles, E., Hernández, S., Malats, N., Kogevinas, M., Lloreta, J., Carrato, A., Tardón, A., Serra, C., Real, F.X., 2006. PIK3CA mutations are an early genetic alteration associated with FGFR3 mutations in superficial papillary bladder tumors. Cancer Res. 66, 7401–7404.

Luevano, J., Damodaran, C., 2014. A Review of Molecular Events of Cadmium-Induced Carcinogenesis. J. Environ. Pathol. Toxicol. Oncol. 33, 183–194.

Madejczyk, M.S., Baer, C.E., Dennis, W.E., Minarchick, V.C., Leonard, S.S., Jackson, D.A., Stallings, J.D., Lewis, J.A., 2015. Temporal Changes in Rat Liver Gene Expression after Acute Cadmium and Chromium Exposure. PLOS ONE 10, e0127327. doi:10.1371/journal.pone.0127327

Mahon, P., Partridge, K., Beattie, J.H., Glover, L.A., Hesketh, J.E., 1997. The 3′ untranslated region plays a role in the targeting of metallothionein-I mRNA to the perinuclear cytoplasm and cytoskeletal-bound polysomes. Biochim. Biophys. Acta BBA - Mol. Cell Res. 1358, 153–162. doi:10.1016/S0167-4889(97)00058-X

Malgieri, G., Zaccaro, L., Leone, M., Bucci, E., Esposito, S., Baglivo, I., Del Gatto, A., Russo, L., Scandurra, R., Pedone, P.V., Fattorusso, R., Isernia, C., 2011. Zinc to cadmium replacement in the A. thaliana SUPERMAN $Cys_2$ $His_2$ zinc finger induces structural rearrangements of typical DNA base determinant positions. Biopolymers 95, 801–810.

Marceau, N., 1990. Cell lineages and differentiation programs in epidermal, urothelial and hepatic tissues and their neoplasms. Lab. Investig. J. Tech. Methods Pathol. 63, 4–20.

Maret, W., 2011. Metals on the move: zinc ions in cellular regulation and in the coordination dynamics of zinc proteins. Biometals Int. J. Role Met. Ions Biol. Biochem. Med. 24, 411–418.

Maret, W., Li, Y., 2009. Coordination dynamics of zinc in proteins. Chem. Rev. 109, 4682–4707.

Margoshes, M., Vallee, B.L., 1957. A Cadmium Protein from Equine Kidney Cortex. J. Am. Chem. Soc. 79, 4813–4814.

Martin, J., Han, C., Gordon, L.A., Terry, A., Prabhakar, S., She, X., Xie, G., Hellsten, U., Chan, Y.M., Altherr, M., Couronne, O., Aerts, A., Bajorek, E., Black, S., Blumer, H., Branscomb, E., Brown, N.C., Bruno, W.J., Buckingham, J.M., Callen, D.F., Campbell, C.S., Campbell, M.L., Campbell, E.W., Caoile, C., Challacombe, J.F., Chasteen, L.A., Chertkov, O., Chi, H.C., Christensen, M., Clark, L.M., Cohn, J.D., Denys, M., Detter, J.C., Dickson, M., Dimitrijevic-Bussod, M., Escobar, J., Fawcett, J.J., Flowers, D., Fotopulos, D., Glavina, T., Gomez, M., Gonzales, E., Goodstein, D., Goodwin, L.A., Grady, D.L., Grigoriev, I., Groza, M., Hammon, N., Hawkins, T., Haydu, L., Hildebrand, C.E., Huang, W., Israni, S., Jett, J., Jewett, P.B., Kadner, K., Kimball, H., Kobayashi, A., Krawczyk, M.-C., Leyba, T., Longmire, J.L., Lopez, F., Lou, Y., Lowry, S., Ludeman, T., Manohar, C.F., Mark, G.A., McMurray, K.L., Meincke, L.J., Morgan, J., Moyzis, R.K., Mundt, M.O., Munk, A.C., Nandkeshwar, R.D., Pitluck, S., Pollard, M., Predki, P., Parson-Quintana, B., Ramirez, L., Rash, S., Retterer, J., Ricke, D.O., Robinson, D.L., Rodriguez, A., Salamov, A., Saunders, E.H., Scott, D., Shough, T., Stallings, R.L., Stalvey, M., Sutherland, R.D., Tapia, R., Tesmer, J.G., Thayer, N., Thompson, L.S., Tice, H.,

Torney, D.C., Tran-Gyamfi, M., Tsai, M., Ulanovsky, L.E., Ustaszewska, A., Vo, N., White, P.S., Williams, A.L., Wills, P.L., Wu, J.-R., Wu, K., Yang, J., Dejong, P., Bruce, D., Doggett, N.A., Deaven, L., Schmutz, J., Grimwood, J., Richardson, P., Rokhsar, D.S., Eichler, E.E., Gilna, P., Lucas, S.M., Myers, R.M., Rubin, E.M., Pennacchio, L.A., 2004. The sequence and analysis of duplication-rich human chromosome 16. Nature 432, 988–994.

Mason, A.Z., Jenkins, K.D., Sullivan, P.A., 1988. Mechanisms of trace metal accumulation in the polychaete Neanthes arenaceodentata. J. Mar. Biol. Assoc. U. K. 68, 61–80. doi:10.1017/S0025315400050104

Masters, J.R., Hepburn, P.J., Walker, L., Highman, W.J., Trejdosiewicz, L.K., Povey, S., Parkar, M., Hill, B.T., Riddle, P.R., Franks, L.M., 1986. Tissue culture model of transitional cell carcinoma: characterization of twenty-two human urothelial cell lines. Cancer Res. 46, 3630–3636.

Maxwell, P., Salnikow, K., 2004. HIF-1: an oxygen and metal responsive transcription factor. Cancer Biol. Ther. 3, 29–35.

Mayeux, R., 2004. Biomarkers: Potential Uses and Limitations. NeuroRx 1, 182–188.

McMahon, R.J., Cousins, R.J., 1998. Regulation of the zinc transporter ZnT-1 by dietary zinc. Proc. Natl. Acad. Sci. U. S. A. 95, 4841–4846.

Mehus, A.A., Muhonen, W.W., Garrett, S.H., Somji, S., Sens, D.A., Shabb, J.B., 2014. Quantitation of Human Metallothionein Isoforms: A Family of Small, Highly Conserved, Cysteine-rich Proteins. Mol. Cell. Proteomics 13, 1020–1033.

Méplan, C., Mann, K., Hainaut, P., 1999. Cadmium induces conformational modifications of wild-type p53 and suppresses p53 response to DNA damage in cultured cells. J. Biol. Chem. 274, 31663–31670.

Méplan, C., Richard, M.J., Hainaut, P., 2000. Metalloregulation of the tumor suppressor protein p53: zinc mediates the renaturation of p53 after exposure to metal chelators in vitro and in intact cells. Oncogene 19, 5227–5236.

Metts, M.C., Metts, J.C., Milito, S.J., Thomas, C.R., 2000. Bladder cancer: a review of diagnosis and management. J. Natl. Med. Assoc. 92, 285–294.

Michailidi, C., Hayashi, M., Datta, S., Sen, T., Zenner, K., Oladeru, O., Brait, M., Izumchenko, E., Baras, A., VandenBussche, C., Argos, M., Bivalacqua, T.J., Ahsan, H., Hahn, N.M., Netto, G.J., Sidransky, D., Hoque, M.O., 2015. Involvement of epigenetics and EMT related miRNA in arsenic induced neoplastic transformation and their potential clinical use. Cancer Prev. Res. (Phila. Pa.) 8, 208–221.

Miles, A.T., Hawksworth, G.M., Beattie, J.H., Rodilla, V., 2000. Induction, Regulation, Degradation, and Biological Significance of Mammalian Metallothioneins. Crit. Rev. Biochem. Mol. Biol. 35, 35–70.

Minsky, B.D., Chlapowski, F.J., 1978. Morphometric analysis of the translocation of lumenal membrane between cytoplasm and cell surface of transitional epithelial cells during the expansion-contraction cycles of mammalian urinary bladder. J. Cell Biol. 77, 685–697.

Mita, M., Satoh, M., Shimada, A., Okajima, M., Azuma, S., Suzuki, J.S., Sakabe, K., Hara, S., Himeno, S., 2008. Metallothionein is a crucial protective factor against

Helicobacter pylori-induced gastric erosive lesions in a mouse model. Am. J. Physiol. Gastrointest. Liver Physiol. 294, G877-884.

Miura, N., Koizumi, S., 2007. Heavy metal responses of the human metallothionein isoform genes. J. Pharm. Soc. Jpn. 127, 665–673.

Mohmand, J., Eqani, S.A.M.A.S., Fasola, M., Alamdar, A., Mustafa, I., Ali, N., Liu, L., Peng, S., Shen, H., 2015. Human exposure to toxic metals via contaminated dust: Bio-accumulation trends and their potential risk estimation. Chemosphere 132, 142–151.

Moleirinho, A., Carneiro, J., Matthiesen, R., Silva, R.M., Amorim, A., Azevedo, L., 2011. Gains, Losses and Changes of Function after Gene Duplication: Study of the Metallothionein Family. PLoS ONE 6, e18487.

Montironi, R., Cheng, L., Scarpelli, M., Lopez-Beltran, A., 2016. Pathology and Genetics: Tumours of the Urinary System and Male Genital System. Eur. Urol. 70, 120–123.

Morris, S., Huang, P.C., 1987. Transient response of amplified metallothionein genes in CHO cells to induction by alpha interferon. Mol. Cell. Biol. 7, 600–605.

Mowatt, G., N'Dow, J., Vale, L., Nabi, G., Boachie, C., Cook, J.A., Fraser, C., Griffiths, T.R.L., Aberdeen Technology Assessment Review (TAR) Group, 2011. Photodynamic diagnosis of bladder cancer compared with white light cystoscopy: Systematic review and meta-analysis. Int. J. Technol. Assess. Health Care 27, 3–10.

Mukherjee, J.J., Gupta, S.K., Kumar, S., 2008. Inhibition of benzopyrene diol epoxide-induced apoptosis by cadmium(II) is AP-1-independent: Role of extracelluler signal related kinase. Chem. Biol. Interact. 172, 72–80.

Mukherjee, J.J., Gupta, S.K., Kumar, S., Sikka, H.C., 2004. Effects of Cadmium(II) on (±)-anti-Benzo[a]pyrene-7,8-diol-9,10-epoxide-Induced DNA Damage Response in Human Fibroblasts and DNA Repair: A Possible Mechanism of Cadmium's Cogenotoxicity. Chem. Res. Toxicol. 17, 287–293.

Mysorekar, I.U., Mulvey, M.A., Hultgren, S.J., Gordon, J.I., 2002. Molecular Regulation of Urothelial Renewal and Host Defenses during Infection with Uropathogenic Escherichia coli. J. Biol. Chem. 277, 7412–7419. doi:10.1074/jbc.M110560200

Nakajima, M., Kobayashi, E., Suwazono, Y., Uetani, M., Oishi, M., Inaba, T., Kido, T., Shaikh, Z.A., Nogawa, K., 2005. Excretion of urinary cadmium, copper, and zinc in cadmium-exposed and nonexposed subjects, with special reference to urinary excretion of beta2-microglobulin and metallothionein. Biol. Trace Elem. Res. 108, 17–31.

Nasir, M.S., Fahrni, C.J., Suhy, D.A., Kolodsick, K.J., Singer, C.P., O'Halloran, T.V., 1999. The chemical cell biology of zinc: structure and intracellular fluorescence of a zinc-quinolinesulfonamide complex. J. Biol. Inorg. Chem. JBIC Publ. Soc. Biol. Inorg. Chem. 4, 775–783.

National Research Council (US) Subcommittee on Biologic Markers in Urinary Toxicology, 1995. Toxic Exposure of the Urinary Tract, in: Biologic Markers in Urinary Toxicology. National Academies Press (US), Washington DC.

Neff, J.M., 2002. Bioaccumulation Methods, in: Bioaccumulation in Marine Organisms: Effect of Contaminants from Oil Well Produced Water. Elsevier, p. 49.

Negrete, H.O., Lavelle, J.P., Berg, J., Lewis, S.A., Zeidel, M.L., 1996. Permeability properties of the intact mammalian bladder epithelium. Am. J. Physiol. 271, F886-894.

Nickerson, M.L., Witte, N., Im, K.M., Turan, S., Owens, C., Misner, K., Tsang, S.X., Cai, Z., Wu, S., Dean, M., Costello, J.C., Theodorescu, D., 2016. Molecular analysis of urothelial cancer cell lines for modeling tumor biology and drug response. Oncogene 36, 35–46.

Nielsen, A.E., Bohr, A., Penkowa, M., 2007. The Balance between Life and Death of Cells: Roles of Metallothioneins. Biomark. Insights 1, 99–111.

Nordberg, G., 2003. Cadmium and human health: A perspective based on recent studies in China. J. Trace Elem. Exp. Med. 16, 307–319.

Nriagu, J.O., 1996. A History of Global Metal Pollution. Science 272, 223–223.

Otsuka, F., 2001. Molecular Mechanism of the Metallothionein Gene Expression Mediated by Metal-Responsive Transcription Factor 1. J. Health Sci. 47, 513–519.

Otsuka, F., Okugaito, I., Ohsawa, M., Iwamatsu, A., Suzuki, K., Koizumi, S., 2000. Novel responses of ZRF, a variant of human MTF-1, to in vivo treatment with heavy metals. Biochim. Biophys. Acta 1492, 330–340.

Ouzzane, A., Rouprêt, M., Leon, P., Yates, D.R., Colin, P., 2014. Épidémiologie et facteurs de risque des tumeurs de la voie excrétrice urinaire supérieure : revue de la littérature pour le rapport annuel de l'Association française d'urologie. Prog. En Urol. 24, 966–976.

Ozaki, H., Karaki, H., 2002. Organ culture as a useful method for studying the biology of blood vessels and other smooth muscle tissues. Jpn. J. Pharmacol. 89, 93–100.

Palmiter, R.D., 1994. Regulation of metallothionein genes by heavy metals appears to be mediated by a zinc-sensitive inhibitor that interacts with a constitutively active transcription factor, MTF-1. Proc. Natl. Acad. Sci. U. S. A. 91, 1219–1223.

Palmiter, R.D., Findley, S.D., Whitmore, T.E., Durnam, D.M., 1992. MT-III, a brain-specific member of the metallothionein gene family. Proc. Natl. Acad. Sci. U. S. A. 89, 6333–6337.

Papafotiou, G., Paraskevopoulou, V., Vasilaki, E., Kanaki, Z., Paschalidis, N., Klinakis, A., 2016. KRT14 marks a subpopulation of bladder basal cells with pivotal role in regeneration and tumorigenesis. Nat. Commun. 7, 11914.

Park, S., Jee, S.H., Shin, H.-R., Park, E.H., Shin, A., Jung, K.-W., Hwang, S.-S., Cha, E.S., Yun, Y.H., Park, S.K., Boniol, M., Boffetta, P., 2014. Attributable fraction of tobacco smoking on cancer using population-based nationwide cancer incidence and mortality data in Korea. BMC Cancer 14, 406. doi:10.1186/1471-2407-14-406

Pedersen, M.Ø., Larsen, A., Stoltenberg, M., Penkowa, M., 2009. The role of metallothionein in oncogenesis and cancer prognosis. Prog. Histochem. Cytochem. 44, 29–64.

Penkowa, M., Cáceres, M., Borup, R., Nielsen, F.C., Poulsen, C.B., Quintana, A., Molinero, A., Carrasco, J., Florit, S., Giralt, M., Hidalgo, J., 2006. Novel roles

for metallothionein-I + II (MT-I + II) in defense responses, neurogenesis, and tissue restoration after traumatic brain injury: Insights from global gene expression profiling in wild-type and MT-I + II knockout mice. J. Neurosci. Res. 84, 1452–1474.

Penkowa, M., Carrasco, J., Giralt, M., Molinero, A., Hernández, J., Campbell, I.L., Hidalgo, J., 2000. Altered central nervous system cytokine-growth factor expression profiles and angiogenesis in metallothionein-I+II deficient mice. J. Cereb. Blood Flow Metab. 20, 1174–1189.

Person, R.J., Ngalame, N.N.O., Makia, N.L., Bell, M.W., Waalkes, M.P., Tokar, E.J., 2015. Chronic inorganic arsenic exposure in vitro induces a cancer cell phenotype in human peripheral lung epithelial cells. Toxicol. Appl. Pharmacol. 286, 36–43. doi:10.1016/j.taap.2015.03.014

Petzoldt, J.L., Leigh, I.M., Duffy, P.G., Sexton, C., Masters, J.R.W., 1995. Immortalisation of human urothelial cells. Urol. Res. 23, 377–380.

Pfister, C., Flaman, J.M., Dunet, F., Grise, P., Frebourg, T., 1999. p53 mutations in bladder tumors inactivate the transactivation of the p21 and Bax genes, and have a predictive value for the clinical outcome after bacillus Calmette-Guerin therapy. J. Urol. 162, 69–73. doi:10.1097/00005392-199907000-00017

Pilger, A., Rüdiger, H.W., 2006. 8-Hydroxy-2'-deoxyguanosine as a marker of oxidative DNA damage related to occupational and environmental exposures. Int. Arch. Occup. Environ. Health 80, 1–15.

Pinter, T.B.J., Stillman, M.J., 2015. Kinetics of Zinc and Cadmium Exchanges between Metallothionein and Carbonic Anhydrase. Biochemistry (Mosc.) 54, 6284–6293.

Potts, R.J., Bespalov, I.A., Wallace, S.S., Melamede, R.J., Hart, B.A., 2001. Inhibition of oxidative DNA repair in cadmium-adapted alveolar epithelial cells and the potential involvement of metallothionein. Toxicology 161, 25–38.

Prior, I.A., Lewis, P.D., Mattos, C., 2012. A comprehensive survey of Ras mutations in cancer. Cancer Res. 72, 2457–2467.

Prout, G.R., Barton, B.A., Griffin, P.P., Friedell, G.H., 1992. Treated history of noninvasive grade 1 transitional cell carcinoma. The National Bladder Cancer Group. J. Urol. 148, 1413–1419.

Puzio-Kuter, A.M., Castillo-Martin, M., Kinkade, C.W., Wang, X., Shen, T.H., Matos, T., Shen, M.M., Cordon-Cardo, C., Abate-Shen, C., 2009. Inactivation of p53 and Pten promotes invasive bladder cancer. Genes Dev. 23, 675–680.

Qu, W., Diwan, B.A., Liu, J., Goyer, R.A., Dawson, T., Horton, J.L., Cherian, M.G., Waalkes, M.P., 2002. The Metallothionein-Null Phenotype Is Associated with Heightened Sensitivity to Lead Toxicity and an Inability to Form Inclusion Bodies. Am. J. Pathol. 160, 1047–1056.

Qu, W., Tokar, E.J., Kim, A.J., Bell, M.W., Waalkes, M.P., 2012. Chronic Cadmium Exposure in Vitro Causes Acquisition of Multiple Tumor Cell Characteristics in Human Pancreatic Epithelial Cells. Environ. Health Perspect. 120, 1265–1271.

Quaife, C.J., Findley, S.D., Erickson, J.C., Froelick, G.J., Kelly, E.J., Zambrowicz, B.P., Palmiter, R.D., 1994. Induction of a new metallothionein isoform (MT-IV) occurs during differentiation of stratified squamous epithelia. Biochemistry (Mosc.) 33, 7250–7259.

Radtke, F., Georgiev, O., Müller, H.P., Brugnera, E., Schaffner, W., 1995. Functional domains of the heavy metal-responsive transcription regulator MTF-1. Nucleic Acids Res. 23, 2277–2286.

Radtke, F., Heuchel, R., Georgiev, O., Hergersberg, M., Gariglio, M., Dembic, Z., Schaffner, W., 1993. Cloned transcription factor MTF-1 activates the mouse metallothionein I promoter. EMBO J. 12, 1355–1362.

Raghavan, D., Shipley, W.U., Garnick, M.B., Russell, P.J., Richie, J.P., 1990. Biology and management of bladder cancer. N. Engl. J. Med. 322, 1129–1138.

Rahman, M.T., De Ley, M., 2001. Metallothionein isogene transcription in red blood cell precursors from human cord blood. Eur. J. Biochem. 268, 849–856. doi:10.1046/j.1432-1327.2001.01947.x

Raudenska, M., Gumulec, J., Podlaha, O., Sztalmachova, M., Babula, P., Eckschlager, T., Adam, V., Kizek, R., Masarik, M., 2013. Metallothionein polymorphisms in pathological processes. Metallomics 6, 55–68.

Rebouissou, S., Bernard-Pierrot, I., de Reyniès, A., Lepage, M.-L., Krucker, C., Chapeaublanc, E., Hérault, A., Kamoun, A., Caillault, A., Letouzé, E., Elarouci, N., Neuzillet, Y., Denoux, Y., Molinié, V., Vordos, D., Laplanche, A., Maillé, P., Soyeux, P., Ofualuka, K., Reyal, F., Biton, A., Sibony, M., Paoletti, X., Southgate, J., Benhamou, S., Lebret, T., Allory, Y., Radvanyi, F., 2014. EGFR as a potential therapeutic target for a subset of muscle-invasive bladder cancers presenting a basal-like phenotype. Sci. Transl. Med. 6, 244ra91.

Rebouissou, S., Hérault, A., Letouzé, E., Neuzillet, Y., Laplanche, A., Ofualuka, K., Maillé, P., Leroy, K., Riou, A., Lepage, M.-L., Vordos, D., de la Taille, A., Denoux, Y., Sibony, M., Guyon, F., Lebret, T., Benhamou, S., Allory, Y., Radvanyi, F., 2012. CDKN2A homozygous deletion is associated with muscle invasion in FGFR3-mutated urothelial bladder carcinoma. J. Pathol. 227, 315–324.

Reis-Filho, J.S., Simpson, P.T., Martins, A., Preto, A., Gärtner, F., Schmitt, F.C., 2003. Distribution of p63, cytokeratins 5/6 and cytokeratin 14 in 51 normal and 400 neoplastic human tissue samples using TARP-4 multi-tumor tissue microarray. Virchows Arch. Int. J. Pathol. 443, 122–132. doi:10.1007/s00428-003-0859-2

Resau, J.H., Sakamoto, K., Cottrell, J.R., Hudson, E.A., Meltzer, S.J., 1991. Explant organ culture: A review. Cytotechnology 7, 137–149.

Rhim, J.S., Webber, M.M., Bello, D., Lee, M.S., Arnstein, P., Chen, L.S., Jay, G., 1994. Stepwise immortalization and transformation of adult human prostate epithelial cells by a combination of HPV-18 and v-Ki-ras. Proc. Natl. Acad. Sci. U. S. A. 91, 11874–11878.

Richards, R.I., Heguy, A., Karin, M., 1984. Structural and functional analysis of the human metallothionein-IA gene: differential induction by metal ions and glucocorticoids. Cell 37, 263–272.

Rivlin, N., Brosh, R., Oren, M., Rotter, V., 2011. Mutations in the p53 Tumor Suppressor Gene. Genes Cancer 2, 466–474.

Roels, H.A., Hoet, P., Lison, D., 1999. Usefulness of biomarkers of exposure to inorganic mercury, lead, or cadmium in controlling occupational and environmental risks of nephrotoxicity. Ren. Fail. 21, 251–262.

Rushton, L., Hutchings, S.J., Fortunato, L., Young, C., Evans, G.S., Brown, T., Bevan, R., Slack, R., Holmes, P., Bagga, S., Cherrie, J.W., Van Tongeren, M., 2012. Occupational cancer burden in Great Britain. Br. J. Cancer 107, S3–S7.

Rusk, N., 2009. Reverse ChIP. Nat. Methods 6, 187. doi:10.1038/nmeth0309-187

Ruttkay-Nedecky, B., Nejdl, L., Gumulec, J., Zitka, O., Masarik, M., Eckschlager, T., Stiborova, M., Adam, V., Kizek, R., 2013. The Role of Metallothionein in Oxidative Stress. Int. J. Mol. Sci. 14, 6044–6066.

Ryter, S.W., Choi, A.M.K., 2005. Heme oxygenase-1: redox regulation of a stress protein in lung and cell culture models. Antioxid. Redox Signal. 7, 80–91.

Sadhu, C., Gedamu, L., 1988. Regulation of human metallothionein (MT) genes. Differential expression of MTI-F, MTI-G, and MTII-A genes in the hepatoblastoma cell line (HepG2). J. Biol. Chem. 263, 2679–2684.

Saga, Y., Hashimoto, H., Yachiku, S., Tokumitsu, M., Kaneko, S., 2002. Immunohistochemical expression of metallothionein in human bladder cancer: correlation with histopathological parameters and patient survival. J. Urol. 168, 2227–2231.

Said, N., 2016. Roles of SPARC in urothelial carcinogenesis, progression and metastasis. Oncotarget 7, 67574–67585.

Said, N., Frierson, H.F., Sanchez-Carbayo, M., Brekken, R.A., Theodorescu, D., 2013. Loss of SPARC in bladder cancer enhances carcinogenesis and progression. J. Clin. Invest. 123, 751–766.

Saito, S., Hunziker, P.E., 1996. Differential sensitivity of metallothionein-1 and -2 in liver of zinc-injected rat toward proteolysis. Biochim. Biophys. Acta 1289, 65–70.

Salnikow, K., An, W.G., Melillo, G., Blagosklonny, M.V., Costa, M., 1999. Nickel-induced transformation shifts the balance between HIF-1 and p53 transcription factors. Carcinogenesis 20, 1819–1823.

Salnikow, K., Davidson, T., Kluz, T., Chen, H., Zhou, D., Costa, M., 2003a. GeneChip analysis of signaling pathways effected by nickel. J. Environ. Monit. 5, 206–209.

Salnikow, K., Davidson, T., Zhang, Q., Chen, L.C., Su, W., Costa, M., 2003b. The Involvement of Hypoxia-inducible Transcription Factor-1-dependent Pathway in Nickel Carcinogenesis. Cancer Res. 63, 3524–3530.

Salnikow, K., Zhitkovich, A., 2008. Genetic and Epigenetic Mechanisms in Metal Carcinogenesis and Cocarcinogenesis: Nickel, Arsenic and Chromium. Chem. Res. Toxicol. 21, 28–44.

Sandbichler, A.M., Höckner, M., 2016. Cadmium Protection Strategies—A Hidden Trade-Off? Int. J. Mol. Sci. 17, 139.

Sangar, V.K., Ragavan, N., Matanhelia, S.S., Watson, M.W., Blades, R.A., 2005. The economic consequences of prostate and bladder cancer in the UK. BJU Int. 95, 59–63.

Sarkis, A.S., Dalbagni, G., Cordon-Cardo, C., Zhang, Z.F., Sheinfeld, J., Fair, W.R., Herr, H.W., Reuter, V.E., 1993. Nuclear overexpression of p53 protein in transitional cell bladder carcinoma: a marker for disease progression. J. Natl. Cancer Inst. 85, 53–59.

Sarma, S.N., Kim, Y.-J., Song, M., Ryu, J.-C., 2011. Induction of apoptosis in human leukemia cells through the production of reactive oxygen species and activation of HMOX1 and Noxa by benzene, toluene, and o-xylene. Toxicology 280, 109–117.

Satarug, S., Moore, M.R., 2004. Adverse Health Effects of Chronic Exposure to Low-Level Cadmium in Foodstuffs and Cigarette Smoke. Environ. Health Perspect. 112, 1099–1103.

Satoh, M., Kloth, D.M., Kadhim, S.A., Chin, J.L., Naganuma, A., Imura, N., Cherian, M.G., 1993. Modulation of Both Cisplatin Nephrotoxicity and Drug Resistance in Murine Bladder Tumor by Controlling Metallothionein Synthesis. Cancer Res. 53, 1829–1832.

Schulkens, I.A., Castricum, K.C.M., Weijers, E.M., Koolwijk, P., Griffioen, A.W., Thijssen, V.L., 2014. Expression, regulation and function of human metallothioneins in endothelial cells. J. Vasc. Res. 51, 231–238.

Scriven, S.D., Booth, C., Thomas, D.F.M., Trejdosiewicz, L.K., Southgate, J., 1997. Reconstitution of Human Urothelium From Monolayer Cultures. J. Urol. 158, 1147–1152.

Searle, P.F., 1990. Zinc dependent binding of a liver nuclear factor to metal response element MRE-a of the mouse metallothionein-I gene and variant sequences. Nucleic Acids Res. 18, 4683–4690.

Selvaraj, A., Balamurugan, K., Yepiskoposyan, H., Zhou, H., Egli, D., Georgiev, O., Thiele, D.J., Schaffner, W., 2005. Metal-responsive transcription factor (MTF-1) handles both extremes, copper load and copper starvation, by activating different genes. Genes Dev. 19, 891–896.

Sens, D.A., Park, S., Gurel, V., Sens, M.A., Garrett, S.H., Somji, S., 2004. Inorganic Cadmium- and Arsenite-Induced Malignant Transformation of Human Bladder Urothelial Cells. Toxicol. Sci. 79, 56–63.

Sens, M.A., Somji, S., Lamm, D.L., Garrett, S.H., Slovinsky, F., Todd, J.H., Sens, D.A., 2000. Metallothionein isoform 3 as a potential biomarker for human bladder cancer. Environ. Health Perspect. 108, 413–418.

Serén, N., Glaberman, S., Carretero, M.A., Chiari, Y., 2014. Molecular evolution and functional divergence of the metallothionein gene family in vertebrates. J. Mol. Evol. 78, 217–233.

Severson, P.L., Tokar, E.J., Vrba, L., Waalkes, M.P., Futscher, B., 2012. Agglomerates of aberrant DNA methylation are associated with toxicant-induced malignant transformation. Epigenetics 7, 1238–1248.

Shaikh, Z.A., Ellis, K.J., Subramanian, K.S., Greenberg, A., 1990. Biological monitoring for occupational cadmium exposure: the urinary metallothionein. Toxicology 63, 53–62.

Shaikh, Z.A., Tohyama, C., 1984. Urinary metallothionein as an indicator of cadmium body burden and of cadmium-induced nephrotoxicity. Environ. Health Perspect. 54, 171–174.

Shariati, F., Esaili Sari, A., Mashinchian, A., Pourkazemi, M., 2011. Metallothionein as potential biomarker of cadmium exposure in Persian sturgeon (Acipenser persicus). Biol. Trace Elem. Res. 143, 281–291.

Siegel, R.L., Miller, K.D., Jemal, A., 2016. Cancer statistics, 2016. CA. Cancer J. Clin. 66, 7–30.

Sievert, K.D., Amend, B., Nagele, U., Schilling, D., Bedke, J., Horstmann, M., Hennenlotter, J., Kruck, S., Stenzl, A., 2009. Economic aspects of bladder cancer: what are the benefits and costs? World J. Urol. 27, 295–300.

Sigel, A., Sigel, H., Sigel, R.K.O., 2009. Metallothioneins and Related Chelators, Metal Ions in Life Sciences. RSC Publishing, Cambridge.

Silbergeld, E., 2003. Facilitative mechanisms of lead as a carcinogen. Mutat. Res. Mol. Mech. Mutagen. 533, 121–133.

Sims, H.I., Chirn, G.-W., Marr, M.T., 2012. Single nucleotide in the MTF-1 binding site can determine metal-specific transcription activation. Proc. Natl. Acad. Sci. 109, 16516–16521.

Singh, K.P., Kumari, R., Pevey, C., Jackson, D., DuMond, J.W., 2009. Long duration exposure to cadmium leads to increased cell survival, decreased DNA repair capacity, and genomic instability in mouse testicular Leydig cells. Cancer Lett. 279, 84–92. doi:10.1016/j.canlet.2009.01.023

Singh, S.V., Srivastava, S.K., Choi, S., Lew, K.L., Antosiewicz, J., Xiao, D., Zeng, Y., Watkins, S.C., Johnson, C.S., Trump, D.L., Lee, Y.J., Xiao, H., Herman-Antosiewicz, A., 2005. Sulforaphane-induced Cell Death in Human Prostate Cancer Cells Is Initiated by Reactive Oxygen Species. J. Biol. Chem. 280, 19911–19924. doi:10.1074/jbc.M412443200

Siu, L.L., Banerjee, D., Khurana, R.J., Pan, X., Pflueger, R., Tannock, I.F., Moore, M.J., 1998. The prognostic role of p53, metallothionein, P-glycoprotein, and MIB-1 in muscle-invasive urothelial transitional cell carcinoma. Clin. Cancer Res. Off. J. Am. Assoc. Cancer Res. 4, 559–565.

Sjödahl, G., Lauss, M., Lövgren, K., Chebil, G., Gudjonsson, S., Veerla, S., Patschan, O., Aine, M., Fernö, M., Ringnér, M., Månsson, W., Liedberg, F., Lindgren, D., Höglund, M., 2012. A Molecular Taxonomy for Urothelial Carcinoma. Am. Assoc. Cancer Res. 18, 3377–3386.

Slusser-Nore, A., Larson-Casey, J.L., Zhang, R., Zhou, X.D., Somji, S., Garrett, S.H., Sens, D.A., Dunlevy, J.R., 2016. SPARC Expression Is Selectively Suppressed in Tumor Initiating Urospheres Isolated from As+3- and Cd+2-Transformed Human Urothelial Cells (UROtsa) Stably Transfected with SPARC. PLOS ONE 11, e0147362. doi:10.1371/journal.pone.0147362

Smaoui-Damak, W., Berthet, B., Hamza-Chaffai, A., 2009. In situ potential use of metallothionein as a biomarker of cadmium contamination in Ruditapes decussatus. Ecotoxicol. Environ. Saf. 72, 1489–1498.

Smeets, W., Pauwels, R., Laarakkers, L., Debruyne, F., Geraedts, J., 1987. Chromosomal analysis of bladder cancer. III. Nonrandom alterations. Cancer Genet. Cytogenet. 29, 29–41.

Smith, N.J., Hinley, J., Varley, C.L., Eardley, I., Trejdosiewicz, L.K., Southgate, J., 2015. The human urothelial tight junction: claudin 3 and the ZO-1α(+) switch. Bladder 2, e9.

Sobin, L.H., Gospodarowicz, M.K., Wittekind, C., 2009. TNM Classification of Malignant Tumours, 7th ed. Wiley-Blackwell, Singapore.

Somji, S., Bathula, C.S., Zhou, X.D., Sens, M.A., Sens, D.A., Garrett, S.H., 2008. Transformation of Human Urothelial Cells (UROtsa) by As3+ and Cd2+ Induces the Expression of Keratin 6a. Environ. Health Perspect. 116, 434–440.

Somji, S., Cao, L., Mehus, A., Zhou, X.D., Sens, M.A., Dunlevy, J.R., Garrett, S.H., Zheng, Y., Larson, J.L., Sens, D.A., 2011a. Comparison of expression patterns of keratin 6, 7, 16, 17, and 19 within multiple independent isolates of As(+3)- and Cd (+2)-induced bladder cancer : keratin 6, 7, 16, 17, and 19 in bladder cancer. Cell Biol. Toxicol. 27, 381–396.

Somji, S., Garrett, S.H., Toni, C., Zhou, X.D., Zheng, Y., Ajjimaporn, A., Sens, M.A., Sens, D.A., 2011b. Differences in the epigenetic regulation of MT-3 gene expression between parental and Cd+2 or As+3 transformed human urothelial cells. Cancer Cell Int. 11, 2.

Somji, S., Sens, M.A., Lamm, D.L., Garrett, S.H., Sens, D.A., 2001. Metallothionein isoform 1 and 2 gene expression in the human bladder: evidence for upregulation of MT-1X mRNA in bladder cancer. Cancer Detect. Prev. 25, 62–75.

Song, Y., Washington, M.K., Crawford, H.C., 2010. Loss of FOXA1/2 Is Essential for the Epithelial-to-Mesenchymal Transition in Pancreatic Cancer. Cancer Res. 70, 2115–2125. doi:10.1158/0008-5472.CAN-09-2979

Southgate, J., Hutton, K.A., Thomas, D.F., Trejdosiewicz, L.K., 1994. Normal human urothelial cells in vitro: proliferation and induction of stratification. Lab. Investig. J. Tech. Methods Pathol. 71, 583–594.

Southgate, J., Masters, J.R.W., Trejdosiewicz, L.K., 2002. Culture of Human Urothelium, in: Culture of Epithelial Cells. John Wiley & Sons, Inc., New York, pp. 381–399.

Southgate, J., Varley, C.L., Garthwaite, M.A., Hinley, J., Marsh, F., Stahlschmidt, J., Trejdosiewicz, L.K., Eardley, I., 2007. Differentiation Potential of Urothelium from Patients with Benign Bladder Dysfunction. BJU Int. 99, 1506–1516.

Starska, K., Krześlak, A., Forma, E., Olszewski, J., Morawiec-Sztandera, A., Aleksandrowicz, P., Lewy-Trenda, I., Bryś, M., 2014. The − 5 A/G single-nucleotide polymorphism in the core promoter region of MT2A and its effect on allele-specific gene expression and Cd, Zn and Cu levels in laryngeal cancer. Toxicol. Appl. Pharmacol. http://dx.doi.org/10.1016/j.taap.2014.08.016. doi:10.1016/j.taap.2014.08.016

Stav, K., Leibovici, D., Goren, E., Livshitz, A., Siegel, Y.I., Lindner, A., Zisman, A., 2004. Adverse effects of cystoscopy and its impact on patients' quality of life and sexual performance. Isr. Med. Assoc. J. IMAJ 6, 474–478.

Stoehr, R., Zietz, S., Burger, M., Filbeck, T., Denzinger, S., Obermann, E., Hammerschmied, C., Wieland, W., Knuechel, R., Hartmann, A., 2005. Deletions of Chromosomes 9 and 8p in Histologically Normal Urothelium of Patients with Bladder Cancer. Eur. Urol. 47, 58–63.

Stuart, G.W., Searle, P.F., Palmiter, R.D., 1985. Identification of multiple metal regulatory elements in mouse metallothionein-I promoter by assaying synthetic sequences. Nature 317, 828–831.

Studer, R., Vogt, C.P., Cavigelli, M., Hunziker, P.E., Kägi, J.H., 1997. Metallothionein accretion in human hepatic cells is linked to cellular proliferation. Biochem. J. 328, 63–67.

Sun, T.T., Liang, F.X., Wu, X.R., 1999. Uroplakins as markers of urothelial differentiation. Adv. Exp. Med. Biol. 462, 7–18.

Sun, X., Deng, Q., Liang, Z., Liu, Z., Geng, H., Zhao, L., Zhou, Q., Liu, J., Ma, J., Wang, D., Yu, D., Zhong, C., 2017. Cigarette smoke extract induces epithelial–mesenchymal transition of human bladder cancer T24 cells through activation of ERK1/2 pathway. Biomed. Pharmacother. 86, 457–465. doi:10.1016/j.biopha.2016.12.022

Suraneni, M.V., Badeaux, M.D., 2013. Tumor-Initiating Cells, Cancer Metastasis and Therapeutic Implications, in: Metastatic Cancer: Clinical and Biological Perspectives. Landes Bioscience, Austin.

Suwazono, Y., Kido, T., Nakagawa, H., Nishijo, M., Honda, R., Kobayashi, E., Dochi, M., Nogawa, K., 2009. Biological half-life of cadmium in the urine of inhabitants after cessation of cadmium exposure. Biomark. Biochem. Indic. Expo. Response Susceptibility Chem. 14, 77–81.

Suzuki, T., Nohara, K., 2012. Long-term arsenic exposure induces histone H3 Lys9 dimethylation without altering DNA methylation in the promoter region of p16(INK4a) and down-regulates its expression in the liver of mice. J. Appl. Toxicol. 33, 1–8.

Takiguchi, M., Achanzar, W.E., Qu, W., Li, G., Waalkes, M.P., 2003. Effects of cadmium on DNA-(Cytosine-5) methyltransferase activity and DNA methylation status during cadmium-induced cellular transformation. Exp. Cell Res. 286, 355–365.

Tang, L., Qiu, R., Tang, Y., Wang, S., 2014. Cadmium–zinc exchange and their binary relationship in the structure of Zn-related proteins: a mini review. Metallomics 6, 1313–1323.

Tang, W., Kido, T., Gross, W.A., Nogawa, K., Sabbioni, E., Shaikh, Z.A., 1999. Measurement of cadmium-induced metallothionein in urine by ELISA and prevention of overestimation due to polymerization. J. Anal. Toxicol. 23, 153–158.

Tanji, K., Irie, Y., Uchida, Y., Mori, F., Satoh, K., Mizushima, Y., Wakabayashi, K., 2003. Expression of metallothionein-III induced by hypoxia attenuates hypoxia-induced cell death in vitro. Brain Res. 976, 125–129.

Tchounwou, P.B., Yedjou, C.G., Patlolla, A.K., Sutton, D.J., 2012. Heavy Metals Toxicity and the Environment. EXS 101, 133–164.

Thirumoorthy, N., Manisenthil Kumar, K.-T., Shyam Sundar, A., Panayappan, L., Chatterjee, M., 2007. Metallothionein: an overview. World J. Gastroenterol. WJG 13, 993–996.

Tian, Q., Stepaniants, S.B., Mao, M., Weng, L., Feetham, M.C., Doyle, M.J., Yi, E.C., Dai, H., Thorsson, V., Eng, J., Goodlett, D., Berger, J.P., Gunter, B., Linseley, P.S., Stoughton, R.B., Aebersold, R., Collins, S.J., Hanlon, W.A., Hood, L.E., 2004. Integrated genomic and proteomic analyses of gene expression in Mammalian cells. Mol. Cell. Proteomics MCP 3, 960–969. doi:10.1074/mcp.M400055-MCP200

Tohyama, C., Shaikh, Z.A., Ellis, K.J., Cohn, S.H., 1981. Metallothionein excretion in urine upon cadmium exposure: its relationship with liver and kidney cadmium. Toxicology 22, 181–191.

Treas, J.N., Tyagi, T., Singh, K.P., 2012. Effects of chronic exposure to arsenic and estrogen on epigenetic regulatory genes expression and epigenetic code in human prostate epithelial cells. PloS One 7, e43880.

Ugajin, T., Nishida, K., Yamasaki, S., Suzuki, J., Mita, M., Kubo, M., Yokozeki, H., Hirano, T., 2015. Zinc-binding metallothioneins are key modulators of IL-4 production by basophils. Mol. Immunol. 66, 180–188.

Umeda, K., Ikenouchi, J., Katahira-Tayama, S., Furuse, K., Sasaki, H., Nakayama, M., Matsui, T., Tsukita, Sachiko, Furuse, M., Tsukita, Shoichiro, 2006. ZO-1 and ZO-2 independently determine where claudins are polymerized in tight-junction strand formation. Cell 126, 741–754.

Urani, C., Melchioretto, P., Bruschi, M., Fabbri, M., Sacco, M.G., Gribaldo, L., 2015. Impact of Cadmium on Intracellular Zinc Levels in HepG2 Cells: Quantitative Evaluations and Molecular Effects, Impact of Cadmium on Intracellular Zinc Levels in HepG2 Cells: Quantitative Evaluations and Molecular Effects. BioMed Res. Int. BioMed Res. Int. 2015, e949514.

Urani, C., Melchioretto, P., Canevali, C., Morazzoni, F., Gribaldo, L., 2007. Metallothionein and hsp70 expression in HepG2 cells after prolonged cadmium exposure. Toxicol. Vitro Int. J. Publ. Assoc. BIBRA 21, 314–319. doi:10.1016/j.tiv.2006.08.014

Urani, C., Melchioretto, P., Gribaldo, L., 2010. Regulation of metallothioneins and ZnT-1 transporter expression in human hepatoma cells HepG2 exposed to zinc and cadmium. Toxicol. In Vitro 24, 370–374.

Vale, C., 2003. Neoadjuvant chemotherapy in invasive bladder cancer: a systematic review and meta-analysis. The Lancet 361, 1927–1934.

Vallot, C., Stransky, N., Bernard-Pierrot, I., Hérault, A., Zucman-Rossi, J., Chapeaublanc, E., Vordos, D., Laplanche, A., Benhamou, S., Lebret, T., Southgate, J., Allory, Y., Radvanyi, F., 2011. A novel epigenetic phenotype associated with the most aggressive pathway of bladder tumor progression. J. Natl. Cancer Inst. 103, 47–60. doi:10.1093/jnci/djq470

Van Batavia, J., Yamany, T., Molotkov, A., Dan, H., Mansukhani, M., Batourina, E., Schneider, K., Oyon, D., Dunlop, M., Wu, X.-R., Cordon-Cardo, C., Mendelsohn, C., 2014. Bladder cancers arise from distinct urothelial sub-populations. Nat. Cell Biol. 16, 982–991.

Van Campenhout, K., Infante, H.G., Adams, F., Blust, R., 2004. Induction and binding of Cd, Cu, and Zn to metallothionein in carp (Cyprinus carpio) using HPLC-ICP-TOFMS. Toxicol. Sci. Off. J. Soc. Toxicol. 80, 276–287. doi:10.1093/toxsci/kfh149

van der Heijden, M.S., van Rhijn, B.W.G., 2014. The Molecular Background of Urothelial Cancer: Ready for Action? Eur. Urol. 67, 202–203.

Varley, C., Stahlschmidt, J., Smith, B., Stower, M., Southgate, J., 2004. Activation of peroxisome proliferator-activated receptor-gamma reverses squamous metaplasia and induces transitional differentiation in normal human urothelial cells. Am. J. Pathol. 164, 1789–1798.

Varley, C.L., Bacon, E.J., Holder, J.C., Southgate, J., 2009. FOXA1 and IRF-1 intermediary transcriptional regulators of PPARgamma-induced urothelial cytodifferentiation. Cell Death Differ. 16, 103–114. doi:10.1038/cdd.2008.116

Varley, C.L., Garthwaite, M.A.E., Cross, W., Hinley, J., Trejdosiewicz, L.K., Southgate, J., 2006. PPARgamma-regulated tight junction development during human urothelial cytodifferentiation. J. Cell. Physiol. 208, 407–417.

Varley, C.L., Southgate, J., 2011. Organotypic and 3D reconstructed cultures of the human bladder and urinary tract. Methods Mol. Biol. 695, 197–211.

Varley, C.L., Stahlschmidt, J., Lee, W.-C., Holder, J., Diggle, C., Selby, P.J., Trejdosiewicz, L.K., Southgate, J., 2004. Role of PPARgamma and EGFR signalling in the urothelial terminal differentiation programme. J. Cell Sci. 117, 2029–2036.

Varshney, U., Jahroudi, N., Foster, R., Gedamu, L., 1986. Structure, organization, and regulation of human metallothionein IF gene: differential and cell-type-specific expression in response to heavy metals and glucocorticoids. Mol. Cell. Biol. 6, 26–37.

Vašák, M., Meloni, G., 2011. Chemistry and biology of mammalian metallothioneins. J. Biol. Inorg. Chem. 16, 1067–1078.

Verkleji, J.A.., 1993. The effects of heavy metals stress on higher plants and their use as biomonitors, in: Plant as Bioindicators: Indicators of Heavy Metals in the Terrestrial Environment. VCH, New York, pp. 415–424.

Vermeulen, S.H., Hanum, N., Grotenhuis, A.J., Castaño-Vinyals, G., van der Heijden, A.G., Aben, K.K., Mysorekar, I.U., Kiemeney, L.A., 2015. Recurrent urinary tract infection and risk of bladder cancer in the Nijmegen bladder cancer study. Br. J. Cancer 112, 594–600.

Vogel, C., Abreu, R. de S., Ko, D., Le, S.-Y., Shapiro, B.A., Burns, S.C., Sandhu, D., Boutz, D.R., Marcotte, E.M., Penalva, L.O., 2010. Sequence signatures and mRNA concentration can explain two-thirds of protein abundance variation in a human cell line. Mol. Syst. Biol. 6, 400. doi:10.1038/msb.2010.59

Volkmer, J.-P., Sahoo, D., Chin, R.K., Ho, P.L., Tang, C., Kurtova, A.V., Willingham, S.B., Pazhanisamy, S.K., Contreras-Trujillo, H., Storm, T.A., Lotan, Y., Beck, A.H., Chung, B.I., Alizadeh, A.A., Godoy, G., Lerner, S.P., Rijn, M. van de, Shortliffe, L.D., Weissman, I.L., Chan, K.S., 2012. Three differentiation states risk-stratify bladder cancer into distinct subtypes. Proc. Natl. Acad. Sci. 109, 2078–2083.

von der Maase, H., Sengelov, L., Roberts, J.T., Ricci, S., Dogliotti, L., Oliver, T., Moore, M.J., Zimmermann, A., Arning, M., 2005. Long-term survival results of a randomized trial comparing gemcitabine plus cisplatin, with methotrexate, vinblastine, doxorubicin, plus cisplatin in patients with bladder cancer. J. Clin. Oncol. Off. J. Am. Soc. Clin. Oncol. 23, 4602–4608.

Waalkes, M.P., 2003. Cadmium carcinogenesis. Mutat. Res. 533, 107–120.

Waalkes, M.P., Hjelle, J.J., Klaassen, C.D., 1984. Transient induction of hepatic metallothionein following oral ethanol administration. Toxicol. Appl. Pharmacol. 74, 230–236. doi:10.1016/0041-008X(84)90147-9

Waalkes, M.P., Liu, J., Goyer, R.A., Diwan, B.A., 2004. Metallothionein-I/II Double Knockout Mice Are Hypersensitive to Lead-Induced Kidney Carcinogenesis Role of Inclusion Body Formation. Cancer Res. 64, 7766–7772.

Wang, R., Sens, D.A., Albrecht, A., Garrett, S., Somji, S., Sens, M.A., Lu, X., 2007. Simple Method for Identification of Metallothionein Isoforms in Cultured Human Prostate Cells by MALDI-TOF/TOF Mass Spectrometry. Anal. Chem. 79, 4433–4441.

Wang, Y., Fang, J., Leonard, S.S., Rao, K.M.K., 2004. Cadmium inhibits the electron transfer chain and induces reactive oxygen species. Free Radic. Biol. Med. 36, 1434–1443.

Wedel, W.R., Muirhead, D.E., Arnold, L.L., Dodmane, P.R., Lele, S.M., Maness-Harris, L., Hoyt, R., Cohen, S.M., 2013. Urothelial cell intracytoplasmic inclusions after treatment of promyelocytic leukemia with arsenic trioxide. Toxicol. Sci. Off. J. Soc. Toxicol. 134, 271–275.

Wei, H., Desouki, M.M., Lin, S., Xiao, D., Franklin, R.B., Feng, P., 2008. Differential expression of metallothioneins (MTs) 1, 2, and 3 in response to zinc treatment in human prostate normal and malignant cells and tissues. Mol. Cancer 7, 7.

West, A.K., Stallings, R., Hildebrand, C.E., Chiu, R., Karin, M., Richards, R.I., 1990. Human metallothionein genes: structure of the functional locus at 16q13. Genomics 8, 513–518.

Wezel, F., Pearson, J., Southgate, J., 2014. Plasticity of in vitro-generated urothelial cells for functional tissue formation. Tissue Eng. Part A 20, 1358–1368.

Whitfield, M.L., George, L.K., Grant, G.D., Perou, C.M., 2006. Common markers of proliferation. Nat. Rev. Cancer 6, 99–106. doi:10.1038/nrc1802

Wierzowiecka, B., Gomulkiewicz, A., Cwynar-Zajac, L., Olbromski, M., Grzegrzolka, J., Kobierzycki, C., Podhorska-Okolow, M., Dziegiel, P., 2016. Expression of Metallothionein and Vascular Endothelial Growth Factor Isoforms in Breast Cancer Cells. In Vivo 30, 271–278.

Witjes, J.A., Redorta, J.P., Jacqmin, D., Sofras, F., Malmström, P.-U., Riedl, C., Jocham, D., Conti, G., Montorsi, F., Arentsen, H.C., Zaak, D., Mostafid, A.H., Babjuk, M., 2010. Hexaminolevulinate-guided fluorescence cystoscopy in the diagnosis and follow-up of patients with non-muscle-invasive bladder cancer: review of the evidence and recommendations. Eur. Urol. 57, 607–614. doi:10.1016/j.eururo.2010.01.025

Wolf, C., Strenziok, R., Kyriakopoulos, A., 2009. Elevated metallothionein-bound cadmium concentrations in urine from bladder carcinoma patients, investigated by size exclusion chromatography-inductively coupled plasma mass spectrometry. Anal. Chim. Acta 631, 218–222.

Woodling, J.D., Brinkman, S.F., Horn, B.J., 2001. Nonuniform Accumulation of Cadmium and Copper in Kidneys of Wild Brown Trout (Salmo trutta) Populations. Arch. Environ. Contam. Toxicol. 40, 381–385. doi:10.1007/s002440010186

World Health Organisation, 2010. Exposure to Cadmium; a Major Public Health Concern, Preventing Disease Through Healthy Envrionments. WHO Document Production Services, Geneva.

World Health Organisation, 1996. Trace elements in human nutrition and health, Nutrition. WHO Document Production Services, Geneva.

Wu, X.-R., Kong, X.-P., Pellicer, A., Kreibich, G., Sun, T.-T., 2009. Uroplakins in Urothelial Biology, Function and Disease. Kidney Int. 75, 1153–1165.

Wülfing, C., van Ahlen, H., Eltze, E., Piechota, H., Hertle, L., Schmid, K.-W., 2007. Metallothionein in bladder cancer: correlation of overexpression with poor outcome after chemotherapy. World J. Urol. 25, 199–205.

Xiao, C., Liu, Y., Xie, C., Tu, W., Xia, Y., Costa, M., Zhou, X., 2015. Cadmium induces histone H3 lysine methylation by inhibiting histone demethylase activity. Toxicol. Sci.

Yadav, P.R., Tyagi, R., 2006. Three-dimensional Culture Techniques., in: Biotechnology of Animal Tissues. Discovery Publishing House, New Delhi, p. 101.

Yafi, F.A., North, S., Kassouf, W., 2011. First- and second-line therapy for metastatic urothelial carcinoma of the bladder. Curr. Oncol. 18, e25–e34.

Yamada, H., Koizumi, S., 2001. Lymphocyte metallothionein-mRNA as a sensitive biomarker of cadmium exposure. Ind. Health 39, 29–32.

Yamasaki, Y., Smith, C., Weisz, D., van Huizen, I., Xuan, J., Moussa, M., Stitt, L., Hideki, S., Cherian, M.G., Izawa, J.I., 2006. Metallothionein expression as prognostic factor for transitional cell carcinoma of bladder. Urology 67, 530–535.

Yang, L., Li, H., Yu, T., Zhao, H., Cherian, M.G., Cai, L., Liu, Y., 2008. Polymorphisms in metallothionein-1 and -2 genes associated with the risk of type 2 diabetes mellitus and its complications. Am. J. Physiol. - Endocrinol. Metab. 294, E987–E992. doi:10.1152/ajpendo.90234.2008

Yap, X., Tan, H.-Y., Huang, J., Lai, Y., Yip, G.W.-C., Tan, P.-H., Bay, B.-H., 2009. Over-expression of metallothionein predicts chemoresistance in breast cancer. J. Pathol. 217, 563–570.

Yutkin, V., Nisman, B., Pode, D., 2010. Can urinary biomarkers replace cystoscopic examination in bladder cancer surveillance? Expert Rev. Anticancer Ther. 10, 787–790.

Zeng, J., Heuchel, R., Schaffner, W., Kägi, J.H., 1991a. Thionein (apometallothionein) can modulate DNA binding and transcription activation by zinc finger containing factor Sp1. FEBS Lett. 279, 310–312.

Zeng, J., Vallee, B.L., Kägi, J.H., 1991b. Zinc transfer from transcription factor IIIA fingers to thionein clusters. Proc. Natl. Acad. Sci. 88, 9984–9988.

Zhou, T., Benda, C., Duzinger, S., Huang, Y., Li, X., Li, Y., Guo, X., Cao, G., Chen, S., Hao, L., Chan, Y.-C., Ng, K.-M., Ho, J.C., Wieser, M., Wu, J., Redl, H., Tse, H.-F., Grillari, J., Grillari-Voglauer, R., Pei, D., Esteban, M.A., 2011. Generation of Induced Pluripotent Stem Cells from Urine. J. Am. Soc. Nephrol. 22, 1221–1228.

Zhou, X.D., Sens, D.A., Sens, M.A., Namburi, V.B.R.K., Singh, R.K., Garrett, S.H., Somji, S., 2006a. Metallothionein-1 and -2 Expression in Cadmium- or Arsenic-Derived Human Malignant Urothelial Cells and Tumor Heterotransplants and as a Prognostic Indicator in Human Bladder Cancer. Toxicol. Sci. 91, 467–475.

Zhou, X.D., Sens, M.A., Garrett, S.H., Somji, S., Park, S., Gurel, V., Sens, D.A., 2006b. Enhanced expression of metallothionein isoform 3 protein in tumor heterotransplants derived from As+3- and Cd+2-transformed human urothelial cells. Toxicol. Sci. 93, 322–330.

Zhou, Z., Lei, Y., Wang, C., 2012. Analysis of aberrant methylation in DNA repair genes during malignant transformation of human bronchial epithelial cells induced by cadmium. Toxicol. Sci. 125, 412–417.